WHP P17E REVISIT IN 2017 DATA BOOK

Field Activity of JAMSTEC towards a Sustained Global Survey of the Ocean Interior

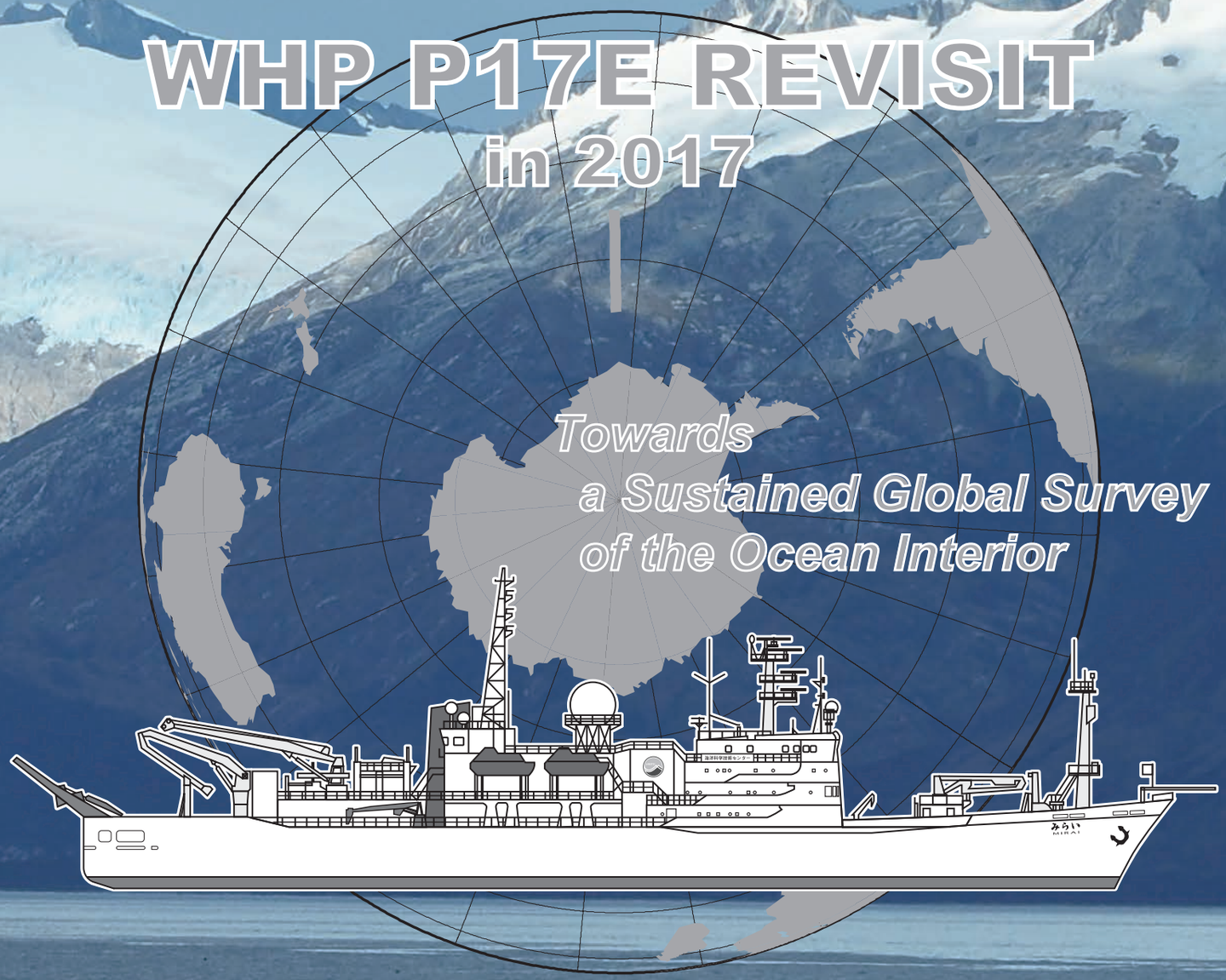

WHP P17E REVISIT IN 2017 DATA BOOK

Edited by
Hiroshi Uchida (JAMSTEC),
Akihiko Murata (JAMSTEC),
Naomi Harada (JAMSTEC),
Toshimasa Doi (JAMSTEC)

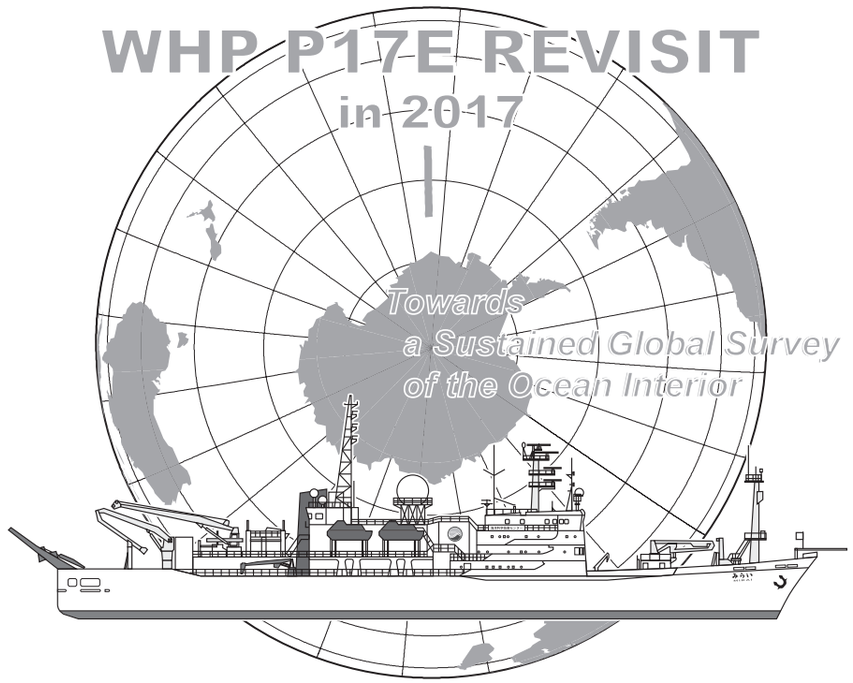

The photograph on the front and back cover of a glacier in the Strait of Magellan was taken by Mr. Toshio Kiuchi.

WHP P17E REVISIT IN 2017 DATA BOOK

March 22, 2019 Published

Edited by Hiroshi Uchida (JAMSTEC), Akihiko Murata (JAMSTEC), Naomi Harada (JAMSTEC) and Toshimasa Doi (JAMSTEC)

Published by © JAMSTEC, Yokosuka, Kanagawa, 2019

Japan Agency for Marine-Earth Science and Technology

2-15 Natsushima, Yokosuka, Kanagawa 237-0061, Japan

Phone +81-46-867-9474, Fax +81-46-867-9835

ISBN 978-4-901833-44-8

DOI: 10.17596/0000003

Printed by Aiwa Enterprise, Ltd.

3-22-4 Takanawa, Minato-ku, Tokyo 108-0074, Japan

Contents

Preface

Re-occupation of the P17E section of the World Ocean Circulation Experiment (WOCE) Hydrographic Program (WHP) was conducted towards the Global Ocean Ship-based Hydrographic Investigations Program (GO-SHIP) as a part of the R/V Mirai Trans South Pacific Project in FY2016. In this project, similar high-quality hydrographic measurements were made along the Chile coast. Although this coastal section is not assigned as the WHP section, the coastal hydrographic data is also included in this data book, because it must be useful for the oceanographic community.

In the WHP, the hydrographic observation along the P17E section was conducted by R/V Knorr in 1992. The P17E section along 126°W across the Amundsen Sea was revisited by R/V Mirai in 2017 for the first time in 24 years. The southernmost station in 2017 (station 1) is the same location as a station of the S04P section along 67°S conducted by RVIB N.B. Palmer in 2018 (station 84). The hydrographic observation at 26 stations was conducted within a limited shipboard time (7 days). At three stations (14, 17 and 19), XCTD casts up to 2000 m depths were conducted instead of conducting CTD/water sampling casts due to bad weather in the Southern Ocean. Five biogeochemical floats were deployed as a JAMSTEC contribution towards the SOCCOM (Southern Ocean Carbon and Climate Observations and Modeling) project. Water samples for pH, HPLC and POC analysis were collected at the five stations (2, 4, 8, 18 and 24) for the SOCCOM project and these data will be available from the project web page.

The Southern Ocean is the front lines of climate change. Recent high-quality hydrographic observations have revealed bottom water warming in the Southern Ocean (around 30 mK decade^{-1}) and Antarctic ice-sheet melting is freshening the bottom water around Antarctica. Such warming and freshening of the bottom water were also confirmed by this re-occupation of the P17E section. We hope that our efforts to obtain high-quality hydrographic data contribute to monitoring the drastic change of the global environment and elucidation of the role of the ocean on environmental changes.

You may find the contents of this data book, and links to other WHP revisit data books, on the web site http://www.jamstec.go.jp/iorgc/ocorp/data/post-woce.html. Updates and corrections will be found online. The data book published since 2018 is assigned a DOI (Digital Object Identifier), and all the previously published data books will also be assigned a DOI in the near future.

In the last February of the Heisei period in Japan

Hiroshi Uchida

Research and Development Center for Global Change (RCGC)

Japan Agency for Marine-Earth Science and Technology (JAMSTEC)

1 Cruise Narrative

Akihiko Murata (JAMSTEC)

Naomi Harada (JAMSTEC)

Natsue Abe (JAMSTEC)

Hiroshi Uchida (JAMSTEC)

1.1 Highlight

Cruise track: See Fig. 1.1.1

Cruise code: MR16-09

Expedition Designation: Leg 1, 49NZ20161227

Leg 2, 49NZ20170120

Leg 3, 49NZ20170208

Leg 4, 49NZ20170308

GHPO section designation: P17E

Ship name: R/V Mirai

Ports of Call: Leg 1, Suva, Fiji – Puerto Montt, Chile

Leg 2, Puerto Montt, Chile – Punta Arenas, Chile

Leg 3, Punta Arenas, Chile – Auckland, New Zealand

Leg 4, New Zealand – Sekinehama, Japan

Cruise Dates: Leg 1, 27 December 2016 – 17 January 2017

Leg 2, 20 January 2017 – 5 February 2017

Leg 3, 8 February 2017 – 5 March 2017

Leg 4, 8 March 2017 – 28 March 2017

Chief Scientist and Affiliation:

Leg 1, Akihiko Murata (murataa@jamstec.go.jp)

Leg 2, Naomi Harada (haradan@jamstec.go.jp)

Leg 3, Hiroshi Uchida (huchida@jamstec.go.jp)

Leg 4, Akihiko Murata (murataa@jamstec.go.jp)

Research and Development Center for Global Change (RCGC)

Japan Agency for Marine-Earth Science and Technology (JAMSTEC)

2-15 Natsushima, Yokosuka, Kanagawa, Japan 237-0061

Fax: +81-46-867-9835

Number of Stations: Leg 1, none

Leg 2, 9 stations

Leg 3, 23 stations

Leg 4, none

Floats and drifter deployed: 3 Argo floats, 2 Deep Argo floats, 5 BGC Argo floats (Leg 3)

2 pCO_2 drifting buoys (Leg 1), 5 pCO_2 drifting buoys (Leg 3)

Mooring recovery: none for legs 1, 3 and 4

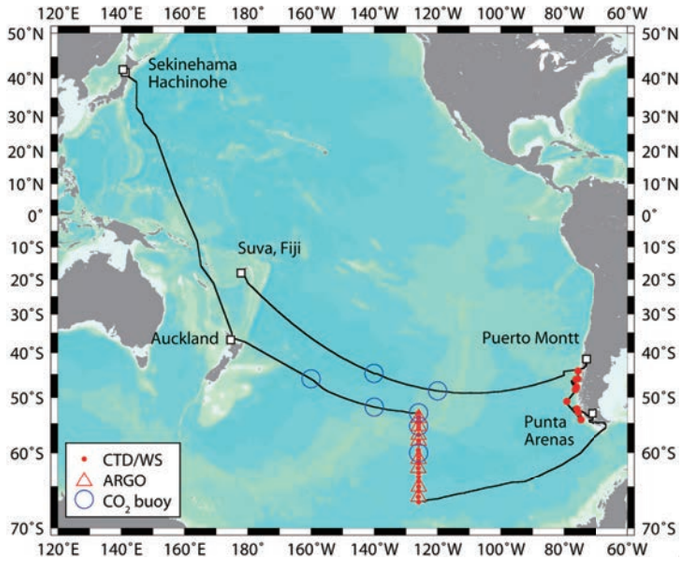

Fig. 1.1.1 MR16-09 cruise track.

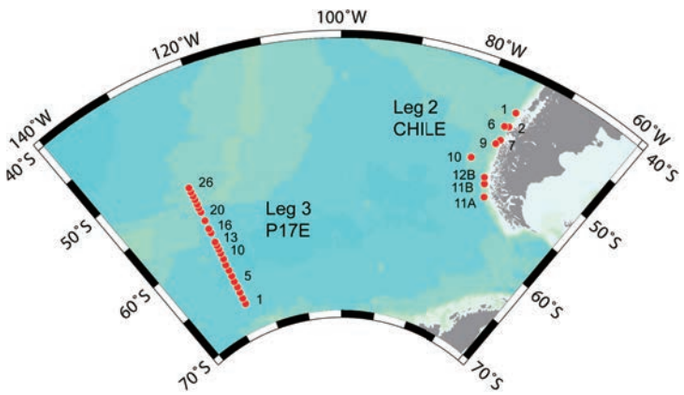

Fig. 1.1.2 CTD station locations for legs 2 and 3.

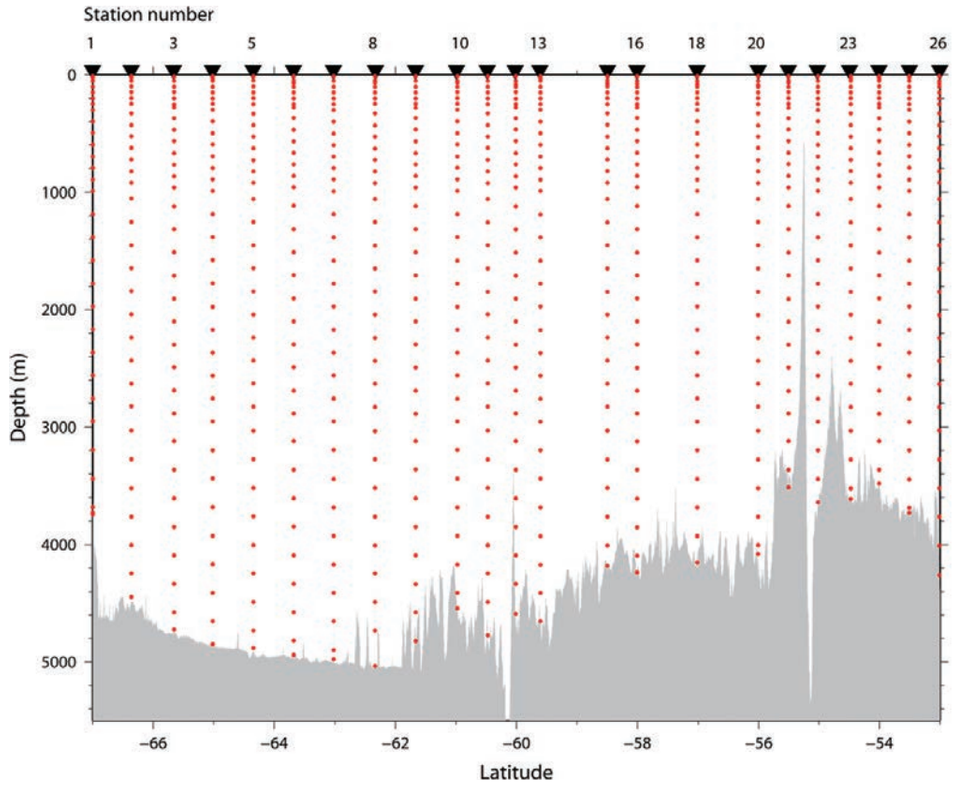

Fig. 1.1.3 Water sampling positions for leg 3 (P17E revisit).

1.2 Cruise Description

We are now at a transient stage moving from Holocene, which is characterized by a stable climate, to a new era: Anthropocene. Impacts due to human activities upon surface environment of the earth are appearing as catastrophic climate changes and the related collapse of ecosystem. In addition, as demonstrated by a series of great earthquakes occurred off Chilean coast, off Sumatra and off East Japan, and volcanic activities linked to the earthquakes, it can be said that we are now in the era, when the interior of the earth or crust is in an active phase. Therefore, the present cruise was aimed at clarifying what happened, in this Anthropocene,

era of great earth changes, in the fields on surface environment of the earth and those in the interior of it, focusing emergent and confronting issues: 1) Changes in heat and material transports by ocean circulation; 2) Detection of progressive ocean acidification and the response of marine biology, and relationship between biodiversity of marine organisms and changes in living environment; 3) Interaction among mantle, ocean ridge, and subduction system.

In the cruise, 8 science plans adopted by the *Mirai* science committee were also conducted together with the main mission: Trans South Pacific Project.

(1) Naomi Harada, Akihiko Murata and Natsue Abe: (JAMSTEC): Trans Pacific Project: Ocean Acidification, Marine Biodiversity, Pacific Meridional Overturning Circulation, Crustal Evolution;
(2) Fumikazu Taketani (JAMSTEC): Ship-borne measurements of aerosols in the marine atmosphere: Investigation of potential influence of marine aerosol particles on the climate;
(3) Shuhei Masuda (JAMSTEC): The monitoring of ocean climate change from surface to deep layer in the Southern Ocean by using Argo-type floats;
(4) Taichi Yokokawa (JAMSTEC): Geochemical and microbiological processes throughout water column of the Southern Ocean in the eastern Pacific sector;
(5) Toshiya Fujiwara (JAMSTEC): Regional distribution of seafloor displacement caused by the 2011 Tohoku-oki earthquake: What happened in the northern Japan Trench?
(6) Masaki Katsumata (JAMSTEC): Cumulus-scale air-sea interaction study by shipboard in-situ observations;
(7) Chisato Yoshikawa (JAMSTEC): Geochemical and microbiological investigation for sea surface to sea bottom along Chile margin;
(8) Kazuma Aoki (Toyama University): Aerosol optical characteristics measured by Ship-borne Sky radiometer;
(9) Takeshi Matsumoto (University of the Ryukyus): Cessation of active spreading axes at trenches.

1.3 Principal Investigators and personnel in charge onboard

The principal investigators (PI) and the persons responsible for major parameters are listed in Table 1.3.1.

Table 1.3.1. List of principal investigator and person in charge on the ship.

Item	Principal Investigator	Person in charge onboard
Underway		
Navigation	Akihiko Murata (JAMSTEC) *murataa@jamstec.go.jp*	Souichiro Sueyoshi (NME) (leg 1) Wataru Tokunaga (NME) (leg 2) Shinya Okumura (NME) (leg 3) Kazuho Yoshida (NME) (leg 4)
Bathymetry	Natsue Abe (JAMSTEC) *abenatsu@jamstec.go.jp*	Souichiro Sueyoshi (NME) (leg 1) Wataru Tokunaga (NME) (leg 2) Shinya Okumura (NME) (leg 3) Kazuho Yoshida (NME) (leg 4)
Magnetic Field	Natsue Abe (JAMSTEC) *abenatsu@jamstec.go.jp*	Souichiro Sueyoshi (NME) (leg 1) Wataru Tokunaga (NME) (leg 2) Shinya Okumura (NME) (leg 3) Kazuho Yoshida (NME) (leg 4)
Gravity	Natsue Abe (JAMSTEC) *abenatsu@jamstec.go.jp*	Souichiro Sueyoshi (NME) (leg 1) Wataru Tokunaga (NME) (leg 2) Shinya Okumura (NME) (leg 3) Kazuho Yoshida (NME) (leg 4)
Meteorology	Masaki Katsumata (JAMSTEC) *katsu@jamstec.go.jp*	Souichiro Sueyoshi (NME) (leg 1) Wataru Tokunaga (NME) (leg 2)

		Shinya Okumura (NME) (leg 3)
		Kazuho Yoshida (NME) (leg 4)
TSG	Hiroshi Uchida (JAMSTEC)	Hironori Sato (MWJ) (leg 1)
	huchida@jamtec.go.jp	Haruka Tamada (MWJ) (leg 2)
		Masanori Enoki (MWJ) (leg 3)
		Masahiro Orui (MWJ) (leg 4)
Underway pCO_2	Akihiko Murata (JAMSTEC)	Tomonori Watai (MWJ) (leg 1)
	murataa@jamstec.go.jp	Atsushi Ono (MWJ) (leg 2)
		Emi Deguchi (MWJ) (legs 3, 4)
Underway C_T	Akihiko Murata (JAMSTEC)	Nagisa Fujiki (MWJ)
	murataa@jamstec.go.jp	
ADCP	Shinya Kouketsu (JAMSTEC)	Souichiro Sueyoshi (NME) (leg 1)
	skouketsu@jamstec.go.jp	Wataru Tokunaga (NME) (lge 2)
		Shinya Okumura (NME) (leg 3)
		Kazuho Yoshida (NME) (leg 4)
Ceilometer	Masaki Katsumata (JAMSTEC)	Souichiro Sueyoshi (NME) (leg 1)
	katsu@jamstec.go.jp	Wataru Tokunaga (NME) (leg 2)
		Shinya Okumura (NME) (leg 3)
		Kazuho Yoshida (NME) (leg 4)
Marine Aerosols	Jun Noda (RGU)	Jun Noda (RGU) (leg 2)
	jnoda@rakuno.ac.jp	Taichi Yokokawa (JAMSTEC) (leg 3)
Sky Radiometer	Kazuma Aoki (Univ. of Toyama)	none
	kazuma@sci.u-toyama.ac.jp	
Doppler Radar	Masaki Katsumata (JAMSTEC)	Souichiro Sueyoshi (NME) (leg 1)
	katsu@jamstec.go.jp	Wataru Tokunaga (NME) (leg 2)
		Shinya Okumura (NME) (leg 3)
		Kazuho Yoshida (NME) (leg 4)

Lidar	Masaki Katsumata (JAMSTEC)	Masaki Katsumata (JAMSTEC) (leg 1)
	katsu@jamstec.go.jp	
Disdrometer	Masaki Katsumata (JAMSTEC)	Masaki Katsumata (JAMSTEC) (leg 1)
	katsu@jamstec.go.jp	
GNSS Precipitable Water		
	Masaki Katsumata (JAMSTEC)	Masaki Katsumata (JAMSTEC) (leg 1)
	katsu@jamstec.go.jp	
XCTD	Hiroshi Uchida (JAMSTEC)	Shinya Okumura (NME)
	huchida@jamstec.go.jp	
Radiosonde	Masaki Katsumata (JAMSTEC)	Souichiro Sueyoshi (NME)
	katsu@jamstec.go.jp	
Satellite Image	Masaki Katsumata (JAMSTEC)	Souichiro Sueyoshi (NME) (leg 1)
	katsu@jamstec.go.jp	Wataru Tokunaga (NME) (leg 2)
		Shinya Okumura (NME) (leg 3)
		Kazuho Yoshida (NME) (leg 4)
MAX-DOAS	Hisahiro Takashima (JAMSTEC)	Takuma Miyakawa (JAMSTEC) (leg 3)
	hisahiro@jamstec.go.jp	
Ozone and CO	Yugo Kanaya (JAMSTEC)	Takuma Miyakawa (JAMSTEC) (leg 3)
	yugo@jamstec.go.jp	
Black Carbon Particles	Fumikazu Taketani (JAMSTEC)	Takuma Miyakawa (JAMSTEC) (leg 3)
	taketani@jamstec.go.jp	
Fluorescent Aerosol Particles		
	Fumikazu Taketani (JAMSTEC)	Takuma Miyakawa (JAMSTEC) (leg 3)
	taketani@jamstec.go.jp	
Aerosol Particle Size Distribution		
	Takuma Miyakawa (JAMSTEC)	Takuma Miyakawa (JAMSTEC) (leg 3)
	miyakawat@jamstec.go.jp	

Aerosol Particle Sampling for post-analyses

Fumikazu Taketani (JAMSTEC) *taketani@jamstec.go.jp*

Takuma Miyakawa (JAMSTEC) (leg 3)

Station Observation

Single Channel Seismometer

Natsue Abe (JAMSTEC) *abenatsu@jamstec.go.jp*

Toshimasa Nasu (NME) (leg 2)

Sediment Core — Kana Nagashima (JAMSTEC) *nagashimak@jamstec.go.jp*; Yusuke Sato (MWJ) (leg 2)

Dredge — Natsue Abe (JAMSTEC) *abenatsu@jamstec.go.jp*; Yusuke Sato (MWJ) (leg 2)

Biological Sample — Leonardo Román Castro Cifuentes (UdeC) *lecastro@oceanografia.udec.cl*; Naomi Harada (JAMSTEC)

Suspended Particles — Humberto González (IDEAL) *hgonzale@uach.cl*; Naomi Harada (JAMSTEC)

FRRF — Jose Luis Iriarte (IDEAL) *jiriarte@uach.cl*; Naomi Harada (JAMSTEC)

CTD/O_2 — Hiroshi Uchida (JAMSTEC) *huchida@jamstec.go.jp*; Rei Ito (MWJ) (leg 2); Kenichi Katayama (MWJ) (leg 3)

Salinity — Hiroshi Uchida (JAMSTEC) *huchida@jamstec.go.jp*; Sonoka Tanihara (MWJ)

Oxygen — Yuichiro Kumamoto (JAMSTEC) *kumamoto@jamstec.go.jp*; Hironori Sato (MWJ) (leg 1); Haruka Tamada (MWJ) (legs 2, 3); Masahiro Orui (MWJ) (leg 4)

Nutrients — Michio Aoyama (Fukushima Univ.) *r706@ipc.fukushima-u.ac.jp*; Tomomi Sone (MWJ)

Density — Hiroshi Uchida (JAMSTEC) *huchida@jamstec.go.jp*; Takuhei Shiozaki (JAMSTEC) (leg 2); Hiroshi Uchida (JAMSTEC) (leg 3)

CFCs/SF_6/N_2O — Ken'ichi Sasaki (JAMSTEC) *ksasaki@jamstec.go.jp*; Ken'ichi Sasaki (JAMSTEC)

DIC — Akihiko Murata (JAMSTEC) *murataa@jamstec.go.jp*; Atsushi Ono (MWJ)

Alkalinity — Akihiko Murata (JAMSTEC) *murataa@jamstec.go.jp*; Atsushi Ono (MWJ) (leg 2); Tomonori Watai (MWJ) (leg 3)

Chlorophyll *a* — Kosei Sasaoka (JAMSTEC) *sasaoka@jamstec.go.jp*; Hironori Sato (MWJ) (leg 1); Takuhei Shiozaki (JAMSTEC) (leg 2); Kosei Sasaoka (JAMSTEC) (leg 3); Masahiro Orui (MWJ) (leg 4)

CDOM/Absorption Coefficients — Kosei Sasaoka (JAMSTEC) *sasaoka@jamstec.go.jp*; Kosei Sasaoka (JAMSTEC)

Calcium — Etsuro Ono (JAMSTEC) *et_ono@met.kishou.go.jp*; Etsuro Ono (JAMSTEC)

DOM — Masahiro Shigemitsu (JAMSTEC) *ma-shige@jamstec.go.jp*; Masahiro Shigemitsu (JAMSTEC)

$\Delta^{14}C/\delta^{13}C$ — Yuichiro Kumamoto (JAMSTEC) *kumamoto@jamstec.go.jp*; Yuichiro Kumamoto (JAMSTEC)

Beryllium isotopes — Yuichiro Kumamoto (JAMSTEC) *kumamoto@jamstec.go.jp*; Yuichiro Kumamoto (JAMSTEC)

$\delta^{18}O/\delta D$ — Hiroshi Uchida (JAMSTEC) *huchida@jamstec.go.jp*; Hiroshi Uchida (JAMSTEC)

N_2O/CH_4	Osamu Yoshida (RGU)	Kanta Chida (RGU) (leg 2)
	yoshida@rakuno.ac.jp	Noriko Iwamatsu (RGU) (leg 3)
Cell abundance	Michinari Sunamura (UT)	Hidetaka Nomaki (JAMSTEC) (leg 2)
	sunamura@eps.s.u-tokyo.ac.jp	Michinari Sunamura (UT) (leg 3)
Microbial diversity	Taichi Yokokawa (JAMSTEC)	Hidetaka Nomaki (JSMTEC) (leg 2)
	taichi.yokokawa@jamstec.go.jp	Taichi Yokokawa (JAMSTEC) (leg 3)
Microbial carbon uptake	Taichi Yokokawa (JAMSTEC)	Taichi Yokokawa (JAMSTEC) (leg 3)
	taichi.yokokawa@jamstec.go.jp	
$\delta^{13}C/CH_4$	Akiko Makabe (JAMSTEC)	Chisato Yoshikawa (JAMSTEC) (leg 2)
	makabea@jamstec.go.jp	Minami Koya (RGU) (leg 3)
$\delta^{15}N\ \delta^{18}O/N_2O$	Akiko Makabe (JAMSTEC)	Chisato Yoshikawa (JAMSTEC) (leg 2)
	makabea@jamstec.go.jp	Noriko Iwamatsu (RGU) (leg 3)
$\delta^{15}N\ \delta^{18}O/NO_3$	Chisato Yoshikawa (JAMSTEC)	Chisato Yoshikawa (JAMSTEC) (leg 2)
	yoshikawac@jamstec.go.jp	Minami Koya (RGU) (leg 3)
$\delta^{15}N$/chlorophyll	Chisato Yoshikawa (JAMSTEC)	Chisato Yoshikawa (JAMSTEC) (leg 2)
	yoshikawac@jamstec.go.jp	
LADCP	Shinya Kouketsu (JAMSTEC)	Katsuro Katsumata (JAMSTEC)
	skouketsu@jamstec.go.jp	
Micro-Rider	Shinya Kouketsu (JAMSTEC)	Katsuro Katsumata (JAMSTEC)
	skouketsu@jamstec.go.jp	
Sound Velocity	Hiroshi Uchida (JAMSTEC)	Rei Ito (MWJ) (leg 2)
	huchida@jamstec.go.jp	Hiroshi Uchida (JAMSTEC) (leg 3)
pH	Andrew Dickson (SIO)	Katsuro Katsumata (JAMSTEC)
	adickson@ucsd.edu	
POC	Susan Becker (SIO)	Kosei Sasaoka (JAMSTEC)
	sbecker@ucsd.edu	
HPLC	Susan Becker (SIO)	Kosei Sasaoka (JAMSTEC)
	sbecker@ucsd.edu	

Floats, Drifters, Moorings

ARGO Float	Shuhei Masuda (JAMSTEC)	Shungo Oshitani (MWJ)
	smasuda@jamstec.go.jp	
SOCCOM BGC Float	Stephen Riser (UW)	Katsuro Katsumata (JAMSTEC)
	riser@ocean.washington.edu	
CO_2 Buoy	Akihiko Murata (JAMSTEC)	Akihiko Murata (JAMSTEC) (leg 1)
	murataa@jamstec.go.jp	Kosei Sasaoka (JAMSTEC) (leg 3)

JAMSTEC	Japan Agency for Marine-Earth Science and Technology
NME	Nippon Marine Enterprises, Ltd.
MWJ	Marine Works Japan, Ltd.
RGU	Rakuno Gakuen University
TUS	Tokyo University of Science
UdeC	University of Conception
IDEAL	Centro de Investigación Dinámica de Ecosystemas Marinos de Altas Latitudes, Universidad Austral de Chile
SIO	Scripps Institute of Oceanography
UW	University of Washington
UT	The University of Tokyo

1.4 Cruise Participants

List of Participants for leg 1

Akihiko Murata	Chief scientist	JAMSTEC
Masaki Katsumata	Meteorology	JAMSTEC
Soichiro Sueyoshi	Chief technician, Meteorology/Geophysics/ADCP	NME
Yutaro Murakami	Meteorology/Geophysics/ADCP	NME
Tomonori Watai	Chief technician, CO2-system	MWJ
Sinichiro Yokogawa	Nutrients	MWJ
Hiroyasu Sato	DO/Thermosalinograph	MWJ
Nagisa Fujiki	CO2-system properties	MWJ

List of Participants for leg 2

Naomi Harada	Chief Scientist	JAMSTEC
Natsue Abe	Dredge, Single-channel Seismology	JAMSTEC
Kana Nagashima	Sediment	JAMSTEC
Takuhei Shiozaki	CTD/water sampling	JAMSTEC
Miyako Sato	CTD/water sampling, Sediment	JAMSTEC
Hidetaka Nomaki	Sediment	JAMSTEC
Chisato Yoshikawa	Water sampling	JAMSTEC
Shiki Machida	Dredge	JAMSTEC
Jun Noda	Aerosol, Water sampling	Rakuno Gakuen Univ.
Shinya Iwasaki	Sediment	National Institute of Advanced Industrial Science and Technology
Kanda Chida	Water sampling	Rakuno Gakuen Univ.
Ryo Anma	Dredge, Sediment	Univ of Tsukuba
Yuji Orihashi	Dredge	The Univ of Tokyo
Frank Lamy	Sediment	Alfred Wegener Institute
Helge Wolfgang Arz	Sediment	Leibniz-Institute for Baltic Sea Research Warnemünde
Leonardo Román Castro Cifuentes	Plankton Net	Univ of Concepcion
Wolfgang Schneider	CTD	Univ of Concepcion
Humberto González	Water sampling	Universidad Austral de Chile
Jose Luis Iriarte	FRRF	Universidad Austral de Chile
Eduardo Menschel A.	Water sampling	Universidad Austral de Chile
Marcelo Gutiérrez Astete	Aerosol, Water sampling	Univ of Concepcion
Alejandro Jose Avila Santis	Sediment	Univ of Concepcion
Victor Acuña	Sediment, Plankton Net	Univ of Concepcion
Wataru Tokunaga	Chief Technician, Meteorology/ Geophysics/ADCP	NME
Satsuki Iijima	Meteorology/Geophysics/ADCP	NME
Koichi Inagaki	Meteorology/Geophysics/ADCP	NME
Yutaro Murakami	Meteorology/Geophysics/ADCP	NME
Toshimasa Nasu	Single-channel Seismology	NME
Hiroyuki Hayashi	Single-channel Seismology	NME
Mitsuteru Kuno	Single-channel Seismology	NME
Yusuke Sato	Chief Technician, Sediment, Dredge	MWJ

Ei Hatakeyama	Sediment, Dredge	MWJ
Yuki Miyajima	Sediment, Dredge	MWJ
Mika Yamaguchi	Sediment, Dredge	MWJ
Yohei Katayama	Sediment, Dredge	MWJ
Kazuma Takahashi	Sediment, Dredge	MWJ
Rei Ito	CTD	MWJ
Sonoka Tanihara	Water sampling (Salinity)	MWJ
Atsushi Ono	CO2-system properties	MWJ
Tomomi Sone	Water sampling (Nutrients)	MWJ
Haruka Tamada	TSG, Water sampling (DO)	MWJ

List of Participants for leg 3

Hiroshi Uchida	Chief scientist/ Density/ Isotope of water/Sound Velocity	JAMSTEC
Yuichiro Kumamoto	DO/Water sampling/ Carbon isotopes/Beryllium isotopes	JAMSTEC
Katsuro Katsumata	SOCCOM project, LADCP/Micro rider	JAMSTEC
Kosei Sasaoka	Chlorophyll-a/Absorption coefficient/ CDOM/CO2 buoy/ SOCCOM project	JAMSTEC
Etsuro Ono	Calcium/Water sampling/CO2 buoy	JAMSTEC
Masahito Shigemitsu	DOM/Water sampling	JAMSTEC
Kenichi Sasaki	CFCs	JAMSTEC
Takuma Miyakawa	Aerosols	JAMSTEC
Taichi Yokokawa	Microbiology	JAMSTEC
Michinari Sunamura	Microbiology	The University of Tokyo
Momoka Yoshizue	Aerosols	Tokyo University of Science
Noriko Iwamatsu	Geochemistry and Microbiology	Rakuno Gakuen University
Minami Koya	Geochemistry and Microbiology	Rakuno Gakuen University
Shinya Okumura	Chief technician, Meteorology/ Geophysics/ADCP/XCTD	NME
Koichi Inagaki	Meteorology/Geophysics/ADCP/XCTD	NME
Ryo Kimura	Meteorology/Geophysics/ADCP/XCTD	NME
Satoshi Ozawa	Chief technician, Water sampling	MWJ
Kenichi Katayama	CTD	MWJ
Akira Watanabe	Water sampling/Salinity	MWJ
Shungo Oshitani	CTD/Argo	MWJ
Rio Kobayashi	CTD	MWJ
Shinichiro Yokogawa	Nutrients	MWJ
Tomonori Watai	Total alkalinity/Underway C_T	MWJ
Nagisa Fujiki	DIC/Underway C_T	MWJ
Ei Hatakeyama	DO/TSG/Chlorophyll-a	MWJ
Masanori Enoki	DO/TSG/Chlorophyll-a	MWJ
Hironori Sato	CFCs	MWJ
Hiroshi Hoshino	CFCs	MWJ
Misato Kuwahara	DO/TSG/Chlorophyll-a	MWJ
Koki Uda	Water sampling	MWJ
Yoshiaki Sato	Nutrients	MWJ
Rei Ito	CTD/Argo	MWJ

Sonoka Tanihara	Salinity	MWJ
Atsushi Ono	DIC/Underway C_T	MWJ
Tomomi Sone	Nutrients	MWJ
Haruka Tamada	DO/TSG/Chlorophyll-a	MWJ
Yoshiko Ishikawa	Nutrients	MWJ
Emi Deguchi	Total alkalinity	MWJ
Masahiro Orui	CFCs	MWJ

List of Participants for leg 4

Akihiko Murata	Chief scientist	JAMSTEC
Kazuho Yoshida	Chief technician, Meteorology/Geophysics/ADCP	NME
Ryo Kimura	Meteorology/Geophysics/ADCP	NME
Yoshiko Ishikawa	Chief technician	MWJ
Masahiro Orui	Thermosalinograph	MWJ
Emi Deguchi	CO2-system properties	MWJ

2 Underway Measurements

2.1 Navigation

(1) Personnel

Akihiko Murata	JAMSTEC: Principal investigator[*1]	- leg1,2,3,4 -
Souichiro Sueyoshi	Nippon Marine Enterprises Ltd., (NME)	- leg1 -
Yutaro Murakami	NME	- leg1,2 -
Wataru Tokunaga	NME	- leg2 -
Koichi Inagaki	NME	- leg2,3 -
Shinya Okumura	NME	- leg3 -
Kazuho Yoshida	NME	- leg4 -
Ryo Kimura	MIRAI crew / NME	- leg1,3,4 -
Masanori Murakami	MIRAI crew	- leg2,3,4 -

[*1] leg1,4: On-board, leg2,3: Not on-board

(2) System description

Ship's position and velocity were provided by Navigation System on R/V MIRAI. This system integrates GNSS position, Doppler sonar log speed, Gyro compass heading and other basic data for navigation. This system also distributed ship's standard time synchronized to GPS time server via Network Time Protocol. These data were logged on the network server as "SOJ" data every 5 seconds. Sensors for navigation data are listed below;

i) GNSS system:

R/V MIRAI has four GNSS systems, all GNSS positions were offset to radar-mast position, datum point. Anytime changeable manually switched as to GNSS receiving state.

a) StarPack-D & Multi-Fix (version 6), Differential GNSS system.

Antenna: Located on compass deck, starboard.

b) StarPack-D & Multi-Fix (version 6), Differential GNSS system.

Antenna: Located on compass deck, portside.

c) Standalone GPS system.

Receiver: Trimble SPS751

Antenna: Located on navigation deck, starboard.

d) Standalone GPS system.

Receiver: Trimble SPS751

Antenna: Located on navigation deck, portside.

ii) Doppler sonar log:

FURUNO DS-30, which use three acoustic beam for current measurement under the hull.

iii) Gyro compass:

TOKYO KEIKI TG-6000, sperry type mechanical gyrocompass.

iv) GPS time server:

SEIKO Precision TS-2540 Time Server, synchronizing to GPS satellites every 1 second.

(3) Data period (Time in UTC)

Leg1: 17:10, 26 Dec. 2016 to 11:00, 17 Jan. 2017

Leg2: 12:00, 20 Jan. 2017 to 13:00, 05 Feb. 2017

Leg3: 13:10, 08 Feb. 2017 to 21:00, 04 Mar. 2017

Leg4: 21:20, 08 Mar. 2017 to 00:00, 28 Mar. 2017

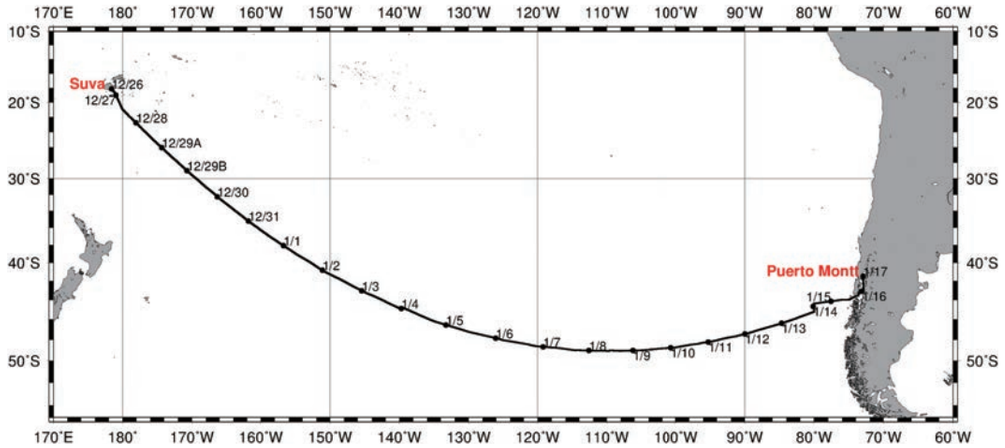

Fig. 2.1.1 Cruise track of MR16-09 Leg 1.

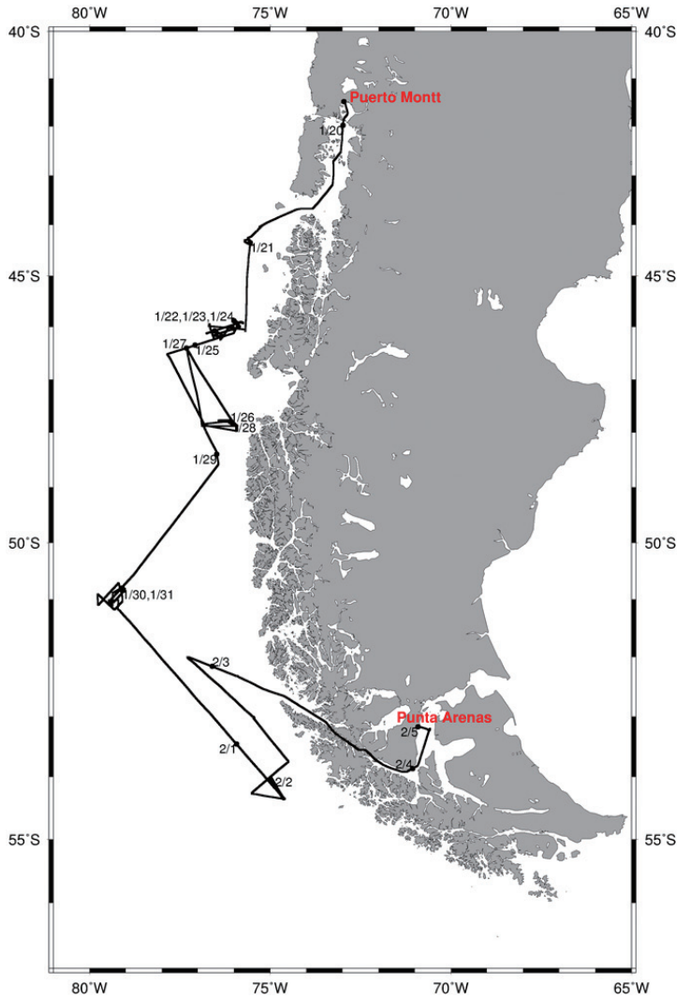

Fig. 2.1.2 Same as Fig. 2.1.1, but for Leg 2.

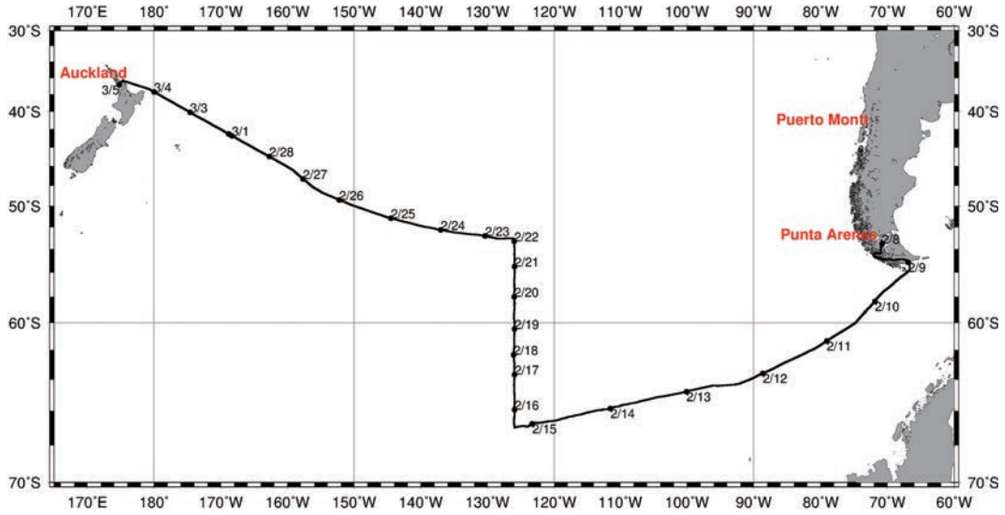

Fig. 2.1.3 Same as Fig. 2.1.1, but for Leg 3.

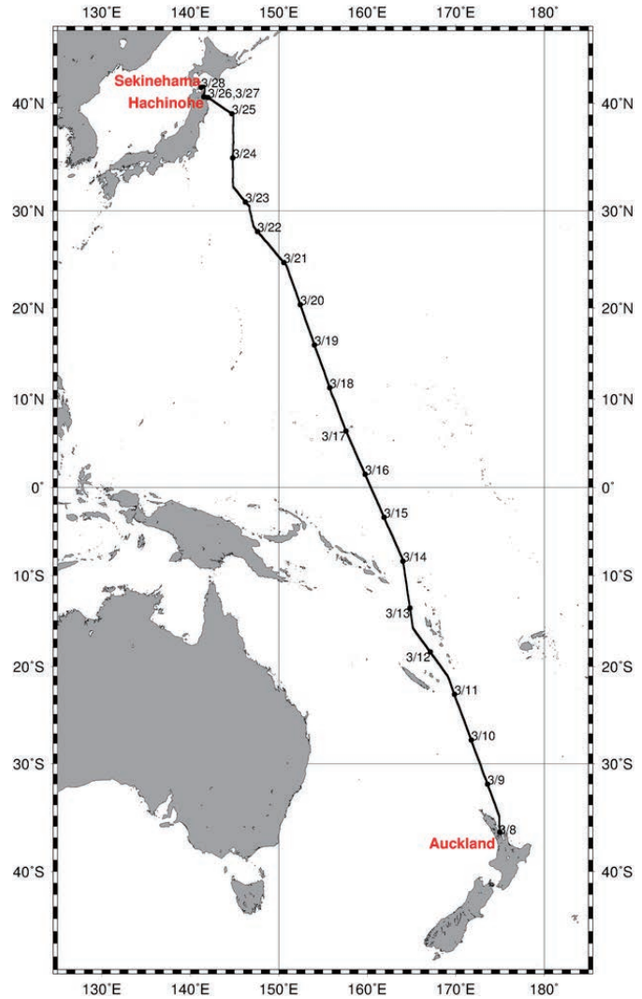

Fig. 2.1.4 Same as Fig. 2.1.1, but for Leg 4.

2.2 Swath Bathymetry

(1) Personnel

Natsue Abe	JAMSTEC: Principal investigator	- leg2 -
Takeshi Matsumoto	Univ. of the Ryukyus: Principal investigator (Not on board)	- leg1,2,3,4 -
Toshiya Fujiwara	JAMSTEC: Principal investigator (Not on board)	- leg4 -
Souichiro Sueyoshi	Nippon Marine Enterprises Ltd., (NME)	- leg1 -
Yutaro Murakami	NME	- leg1,2 -
Wataru Tokunaga	NME	- leg2 -
Koichi Inagaki	NME	- leg2,3 -
Shinya Okumura	NME	- leg3 -
Kazuho Yoshida	NME	- leg4 -
Ryo Kimura	MIRAI crew / NME	- leg1,3,4 -
Masanori Murakami	MIRAI crew	- leg2,3,4 -

(2) Introduction

R/V MIRAI is equipped with a Multi narrow Beam Echo Sounding system (MBES), SEABEAM 3012 (L3 Communications, ELAC Nautik). The objective of MBES is collecting continuous bathymetric data along ship's track to make a contribution to geological and geophysical investigations and global datasets.

(3) Data Acquisition

The "SEABEAM 3012" on R/V MIRAI was used for bathymetry mapping in the MR16-09 Leg1 to Leg4 cruises.

To get accurate sound velocity of water column for ray-path correction of acoustic multibeam, we used Surface Sound Velocimeter (SSV) data to get the sea surface sound velocity (at 6.62 m), and the deeper depth sound velocity profiles were calculated by temperature and salinity profiles from CTD and XCTD data by the equation in Del Grosso (1974) during these cruises. Table 2.2.1 shows system configuration and performance of SEABEAM 3012.

Table 2.2.1 SEABEAM 3012 system configuration and performance

Frequency:	12 kHz
Transmit beam width:	2.0 degree
Transmit power:	4 kW
Transmit pulse length:	2 to 20 msec.
Receive beam width:	1.6 degree
Depth range:	50 to 11,000 m
Number of beams:	301 beams
Beam spacing:	Equi-angle
Swath width:	60 to 150 degrees
Depth accuracy:	< 1 % of water depth (average across the swath)

(4) Data processing of MBES (leg 3)

i) Sound velocity correction

Bathymetry data were corrected with sound velocity profiles calculated from the nearest CTD or XCTD data in the distance. The equation of Del Grosso (1974) was used for calculating sound velocity. The data correction was carried out using the HIPS software version 9.1.4 (CARIS, Canada).

ii) Editing and Gridding

Editing for the bathymetry data was carried out using the HIPS. Firstly, the bathymetry data during ship's turning were basically deleted, and spike noise of swath data was removed. Then the bathymetry

data were checked by “BASE surface (resolution: 50 m averaged grid)”.

Finally, all accepted data were exported as XYZ ASCII data (longitude [degree], latitude [degree], depth [m]), and converted to 150 m grid data using “nearneighbor” utility of GMT (Generic Mapping Tool) software (Table 2.2.2).

Table 2.2.2 Parameters for gridding on “nearneighbor” in GMT

Gridding mesh size:	150 m
Search radius size:	150 m
Minimum number of neighbors for grid:	1

(5) Data Archives

These data obtained in this cruise will be submitted to the Data Management Group (DMG) in JAMSTEC, and will be opened to the public via “Data Research System for Whole Cruise Information in JAMSTEC (DARWIN)” in JAMSTEC web site (http://www.godac.jamstec.go.jp/darwin/e).

(6) Remarks (Time in UTC)

i) The following periods, the MBES observations were carried out.

Leg1: 18:46, 28 Dec. 2016 to 06:00, 15 Jan. 2017

Leg2: 12:11, 21 Jan. 2017 to 14:17, 21 Jan. 2017

14:32, 21 Jan. 2017 to 00:23, 04 Feb. 2017

Leg3: 21:00, 10 Feb. 2017 to 06:59, 03 Mar. 2017

Leg4: 07:03, 09 Mar. 2017 to 09:59, 10 Mar. 2017

10:00, 15 Mar. 2017 to 08:09, 16 Mar. 2017

01:50, 18 Mar. 2017 to 03:43, 26 Mar. 2017

ii) The following periods, data acquisition of MBES was suspended due to system trouble.

Leg4: 07:38, 09 Mar. 2017 to 07:47, 09 Mar. 2017

04:02, 25 Mar. 2017 to 04:11, 26 Mar. 2017

2.3 Surface Meteorological Observations

(1) Personnel

Masaki Katsumata	JAMSTEC: Principal investigator[*1]	- leg1,2,3,4 -
Souichiro Sueyoshi	Nippon Marine Enterprise Ltd., (NME)	- leg1 -
Yutaro Murakami	NME	- leg1,2 -
Wataru Tokunaga	NME	- leg2 -
Koichi Inagaki	NME	- leg2,3 -
Shinya Okumura	NME	- leg3 -
Kazuho Yoshida	NME	- leg4 -
Ryo Kimura	MIRAI crew / NME	- leg1,3,4 -
Masanori Murakami	MIRAI crew	- leg2,3,4 -

[*1] leg1:On-board, leg2,3,4:Not on-board

(2) Objectives

Surface meteorological parameters are observed as a basic dataset of the meteorology. These parameters provide the temporal variation of the meteorological condition surrounding the ship.

(3) Methods

Surface meteorological parameters were observed from the MR16-09 Leg1 cruise to Leg4 cruise. In these cruises, we used two systems for the observation.

i) MIRAI Surface Meteorological observation (SMet) system

Instruments of SMet system are listed in Table 2.3.1 and measured parameters are listed in Table 2.3.2. Data were collected and processed by KOAC-7800 weather data processor made by Koshin-Denki, Japan. The data set consists of 6-second averaged data.

ii) Shipboard Oceanographic and Atmospheric Radiation (SOAR) measurement system

SOAR system designed by BNL (Brookhaven National Laboratory, USA) consists of major five parts.

a) Portable Radiation Package (PRP) designed by BNL – short and long wave downward radiation.
b) Analog meteorological data sampling with CR1000 logger manufactured by Campbell Inc. Canada – wind, pressure, and rainfall (by a capacitive rain gauge) measurement.
c) Digital meteorological data sampling from individual sensors - air temperature, relative humidity and rainfall (by ORG (optical rain gauge)) measurement.
d) Photosynthetically Available Radiation (PAR) sensor manufactured by Biospherical Instruments Inc. (USA) - PAR measurement.
e) Scientific Computer System (SCS) developed by NOAA (National Oceanic and Atmospheric Administration, USA) – centralized data acquisition and logging of all data sets.

SCS recorded PRP, CR1000 data, air temperature and relative humidity data, ORG data. SCS composed Event data (JamMet) from these data and ship's navigation data every 6 seconds. Instruments and their locations are listed in Table 2.3.3 and measured parameters are listed in Table 2.3.4.

For the quality control as post processing, we checked the following sensors, before and after the cruise.

i. Young rain gauge (SMet and SOAR)
   Inspect of the linearity of output value from the rain gauge sensor to change input value by adding fixed quantity of test water.
ii. Barometer (SMet and SOAR)
   Comparison with the portable barometer value, PTB220, VAISALA
iii. Thermometer (air temperature and relative humidity) (SMet and SOAR)
   Comparison with the portable thermometer value, HM70, VAISALA

(4) Preliminary results

Fig. 2.3.1 to Fig. 2.3.4 show the time series of the following parameters;

Wind (SOAR)

Air temperature (SMet)

Relative humidity (SMet)

Precipitation (SOAR, ORG)

Short/long wave radiation (SOAR)

Pressure (SMet)

Sea surface temperature (SMet)

Significant wave height (SMet)

(5) Data archives

These data obtained in these cruises will be submitted to the Data Management Group of JAMSTEC, and will be opened to the public via "Data Research System for Whole Cruise Information in JAMSTEC (DARWIN)" in JAMSTEC web site (http://www.godac.jamstec.go.jp/darwin/e).

(6) Remarks (Times in UTC)

i) The following periods, the observation were carried out.

Leg1: 18:45, 28 Dec. 2016 to 06:13, 15 Jan. 2017

Leg2: 12:11, 21 Jan. 2017 to 14:17, 21 Jan. 2017

14:32, 21 Jan. 2017 to 00:23, 04 Feb. 2017

Leg3: 21:00, 10 Feb. 2017 to 06:59, 03 Mar. 2017

Leg4: 07:03, 09 Mar. 2017 to 09:59, 10 Mar. 2017

10:00, 15 Mar. 2017 to 08:09, 16 Mar. 2017

01:50, 18 Mar. 2017 to 00:00, 29 Mar. 2017

ii) The following periods, sea surface temperature of SMet data was available.

Leg1: 18:45, 28 Dec. 2016 to 06:13, 15 Jan. 2017

Leg2: 12:11, 21 Jan. 2017 to 14:17, 21 Jan. 2017

14:32, 21 Jan. 2017 to 00:23, 04 Feb. 2017

Leg3: 21:00, 10 Feb. 2017 to 06:59, 03 Mar. 2017

Leg4: 07:03, 09 Mar. 2017 to 09:59, 10 Mar. 2017

10:00, 15 Mar. 2017 to 08:09, 16 Mar. 2017

01:50, 18 Mar. 2017 to 05:30, 26 Mar. 2017

iii) The following period, downwelling shortwave radiation amount of SOAR was invalid due to a PSP sensor failure.

about 13:00, 02 Jan. 2017 to 16:11, 07 Jan. 2017

iv) PSP senor of PRP was replaced to a spare due to a sensor failure at 06:11, 07 Jan. 2017.

v) The following period, FRSR data acquisition was stopped due to a trouble of heater in the FRSR sensor.

08:14, 27 Feb. 2017 to 07:00, 03 Mar. 2017

vi) The following period, FRSR data acquisition was suspended to prevent the shadow-band from freezing.

21:25, 12 Feb. 2017 to 23:28, 22 Feb. 2017

vii) The following periods, downwelling shortwave radiation amount and longwave radiation amount data of SOAR were invalid due to PRP system maintenance.

21:15, 06 Jan. 2017 to 21:51, 06 Jan. 2017

15:55, 07 Jan. 2017 to 16:15, 07 Jan. 2017

viii) The following periods, downwelling shortwave radiation amount and longwave radiation amount data of SOAR were not acquired due to PRP system maintenance.

21:23, 12 Feb. 2017 to 21:24, 12 Feb. 2017

23:24, 22 Feb. 2017 to 23:28, 22 Feb. 2017

07:56, 27 Feb. 2017 to 08:13, 27 Feb. 2017

17:33, 27 Feb. 2017 to 17:50, 27 Feb. 2017

23:22, 27 Feb. 2017 to 23:26, 27 Feb. 2017

ix) The following time, increasing of SMet capacitive rain gauge data were invalid due to transmitting for MF/HF or VHF radio.

21:27, 06 Jan. 2017

20:17, 03 Feb. 2017

20:21, 03 Feb. 2017

23:20, 18 Mar. 2017

15:01, 23 Mar. 2017

15:04, 23 Mar. 2017

x) The following time, increasing of SMet optical rain gauge data were invalid due to maintenance.

02:50, 25 Feb. 2017

20:29, 01 Mar. 2017

20:30, 01 Mar. 2017

06:21, 23 Mar. 2017

Table 2.3.1 Instruments and installation locations of MIRAI Surface Meteorological observation system

Sensors	Type	Manufacturer	Location (attitude from surface)
Anemometer	KE-500	Koshin Denki, Japan	Foremast (24 m)
Tair/RH	HMP155	Vaisala, Finland	
with 43408 Gill aspirated radiation shield		R.M. Young, USA	Compass deck (21 m)
			starboard and portside
Thermometer: SST	RFN2-0	Koshin Denki, Japan	4th deck (-1m, inlet -5m)
Barometer	Model-370	Setra System, USA	Captain deck (13 m)
			weather observation room
Capacitive rain gauge	50202	R. M. Young, USA	Compass deck (19 m)
Optical rain gauge	ORG-815DS	Osi, USA	Compass deck (19 m)
Radiometer (short wave)	MS-802	Eko Seiki, Japan	Radar mast (28 m)
Radiometer (long wave)	MS-202	Eko Seiki, Japan	Radar mast (28 m)
Wave height meter	WM-2	Tsurumi-seiki, Japan	Bow (10 m)
			Stern (8m)

Table 2.3.2 Parameters of MIRAI Surface Meteorological observation system

Parameter		Units	Remarks
1	Latitude	degree	
2	Longitude	degree	
3	Ship's speed	knot	MIRAI log DS-30, Furuno
4	Ship's heading	degree	MIRAI gyro, TG-6000, TOKYO-KEIKI
5	Relative wind speed	m/s	6sec./10min. averaged
6	Relative wind direction	degree	6sec./10min. averaged
7	True wind speed	m/s	6sec./10min. averaged
8	True wind direction	degree	6sec./10min. averaged
9	Barometric pressure	hPa	adjusted to sea surface level 6sec. averaged
10	Air temperature (starboard side)	degC	6sec. averaged
11	Air temperature (port side)	degC	6sec. averaged
12	Dewpoint temperature (starboard side)	degC	6sec. averaged
13	Dewpoint temperature (port side)	degC	6sec. averaged
14	Relative humidity (starboard side)	%	6sec. averaged
15	Relative humidity (port side)	%	6sec. averaged
16	Sea surface temperature	degC	6sec. averaged
17	Rain rate (optical rain gauge)	mm/hr	hourly accumulation
18	Rain rate (capacitive rain gauge)	mm/hr	hourly accumulation
19	Down welling shortwave radiation	W/m^2	6sec. averaged
20	Down welling infra-red radiation	W/m^2	6sec. averaged
21	Significant wave height (bow)	m	hourly
22	Significant wave height (aft)	m	hourly
23	Significant wave period (bow)	second	hourly
24	Significant wave period (aft)	second	hourly

Table 2.3.3 Instruments and installation locations of SOAR system

Sensors (Meteorological)	Type	Manufacturer	Location (altitude from surface)
Anemometer	05106	R.M. Young, USA	Foremast (25 m)
Barometer	PTB210	Vaisala, Finland	
with 61002 Gill pressure port		R.M. Young, USA	Foremast (23 m)
Capacitive rain gauge	50202	R.M. Young, USA	Foremast (24 m)
Tair/RH	HMP155	Vaisala, Finland	
with 43408 Gill aspirated radiation shield		R.M. Young, USA	Foremast (23 m)
Optical rain gauge	ORG-815DR	Osi, USA	Foremast (24 m)

Sensors (PRP)	Type	Manufacturer	Location (altitude from surface)
Radiometer (short wave)	PSP	Epply Labs, USA	Foremast (25 m)
Radiometer (long wave)	PIR	Epply Labs, USA	Foremast (25 m)
Fast rotating shadowband radiometer		Yankee, USA	Foremast (25 m)

Sensor (PAR)	Type	Manufacturer	Location (altitude from surface)
PAR sensor	PUV-510	Biospherical Instru ments Inc., USA	Navigation deck (18m)

Table 2.3.4 Parameters of SOAR system (JamMet)

Parameter	Units	Remarks
1 Latitude	degree	
2 Longitude	degree	
3 SOG	knot	
4 COG	degree	
5 Relative wind speed	m/s	
6 Relative wind direction	degree	
7 Barometric pressure	hPa	
8 Air temperature	degC	
9 Relative humidity	%	
10 Rain rate (optical rain gauge)	mm/hr	
11 Precipitation (capacitive rain gauge)	mm	reset at 50 mm
12 Down welling shortwave radiation	W/m^2	
13 Down welling infra-red radiation	W/m^2	
14 Defuse irradiance	W/m^2	
15 PAR	$microE/cm^2/sec$	

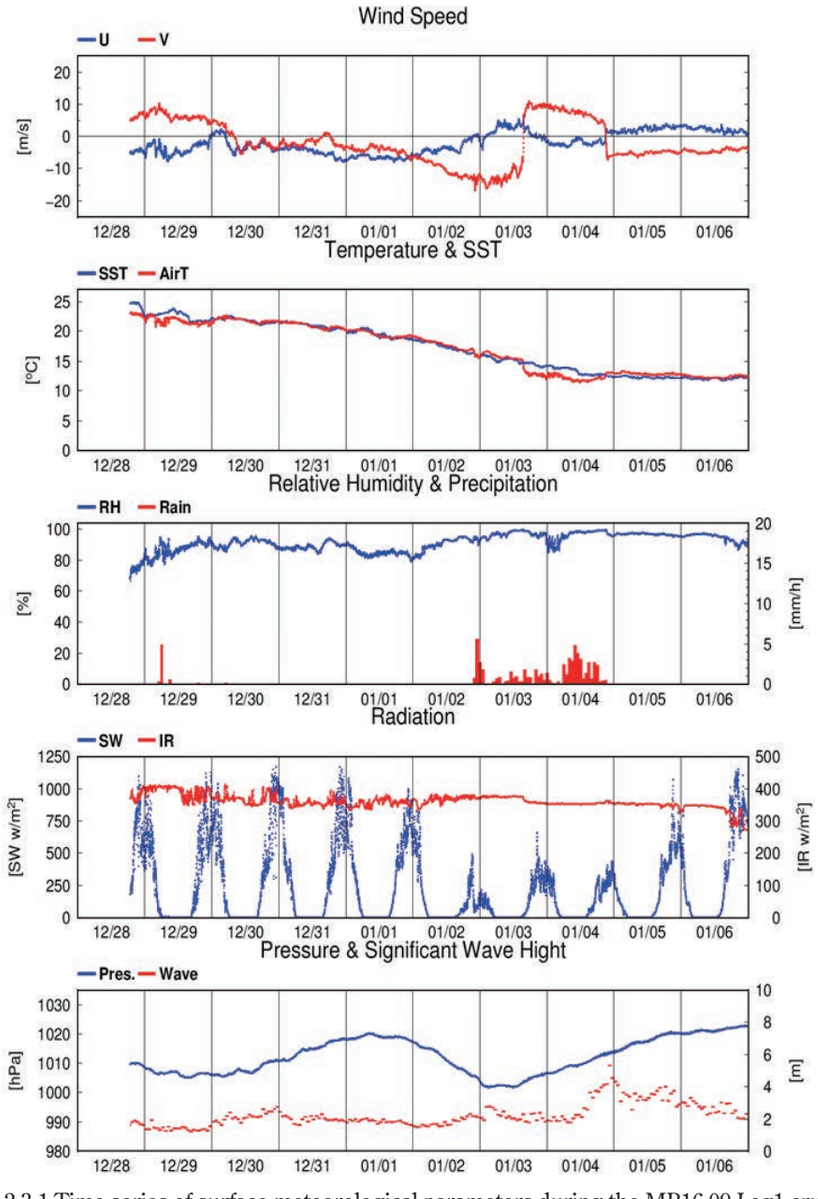

Fig. 2.3.1 Time series of surface meteorological parameters during the MR16-09 Leg1 cruise.

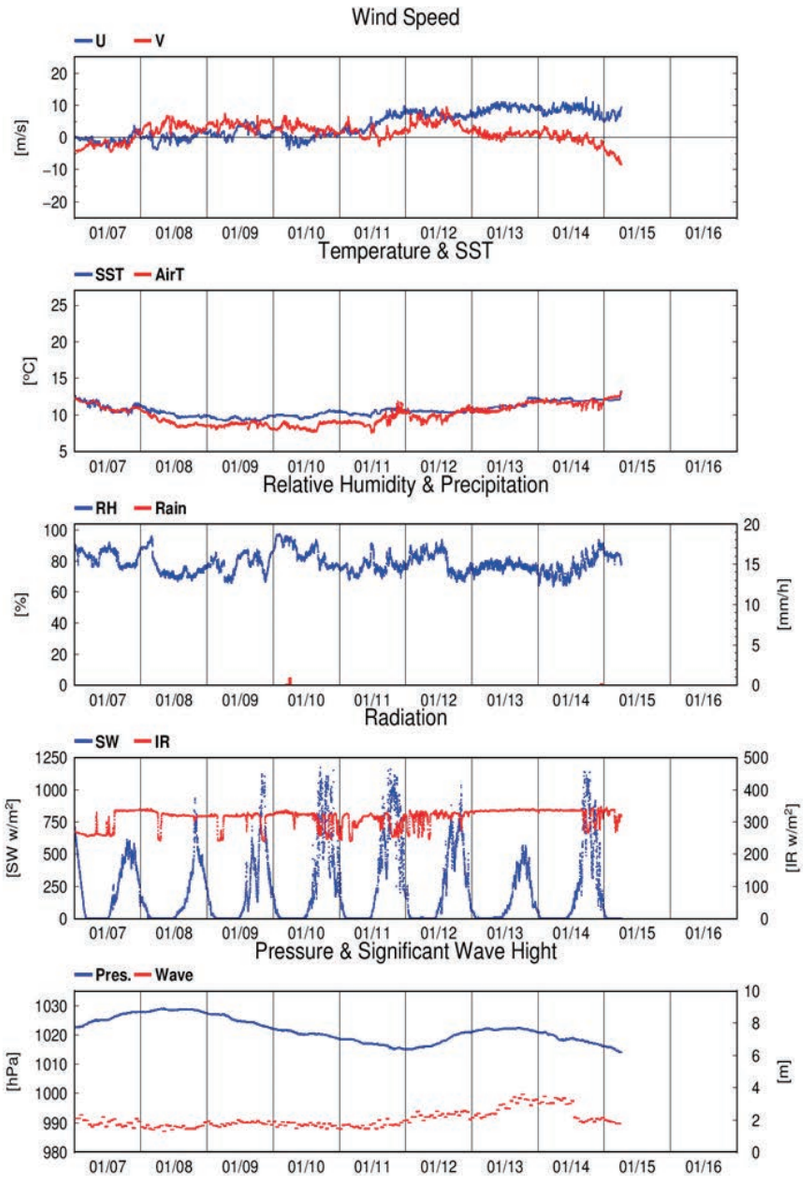

Fig. 2.3.1 (Continued)

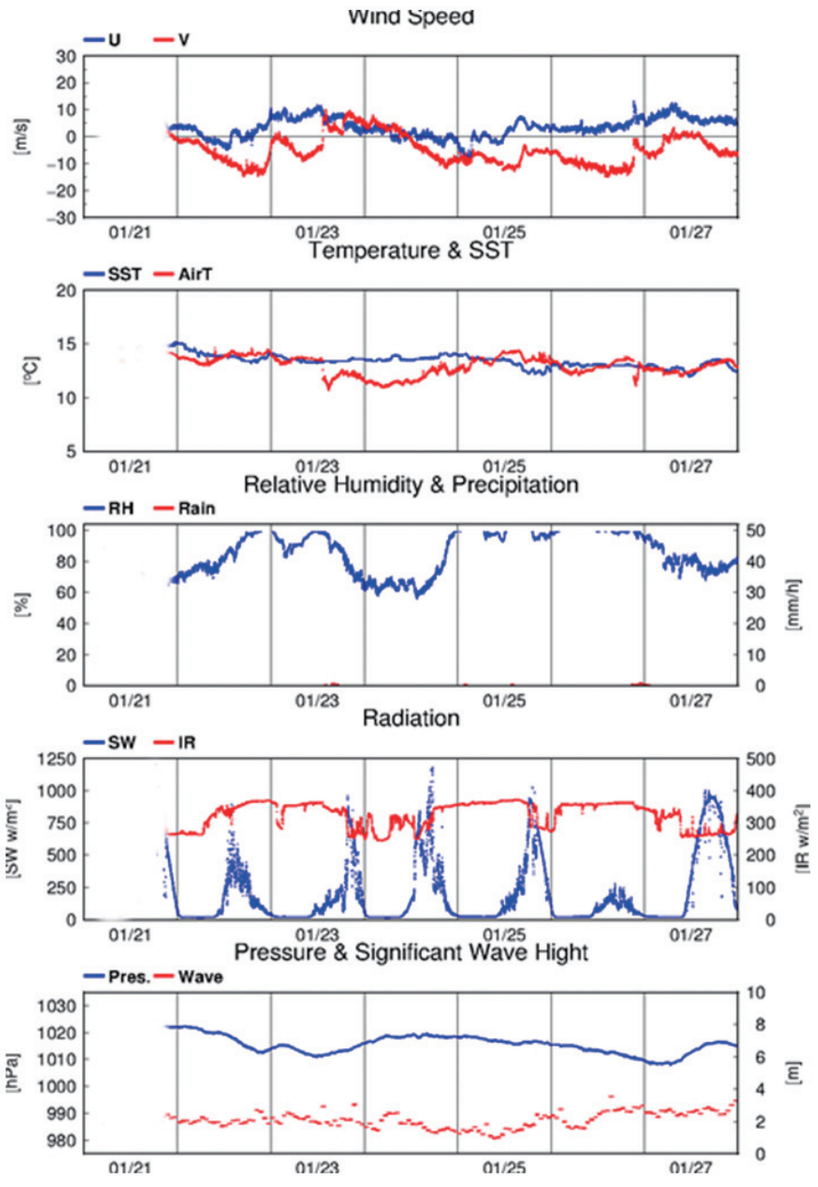

Fig. 2.3.2 Time series of surface meteorological parameters during the MR16-09 Leg2 cruise

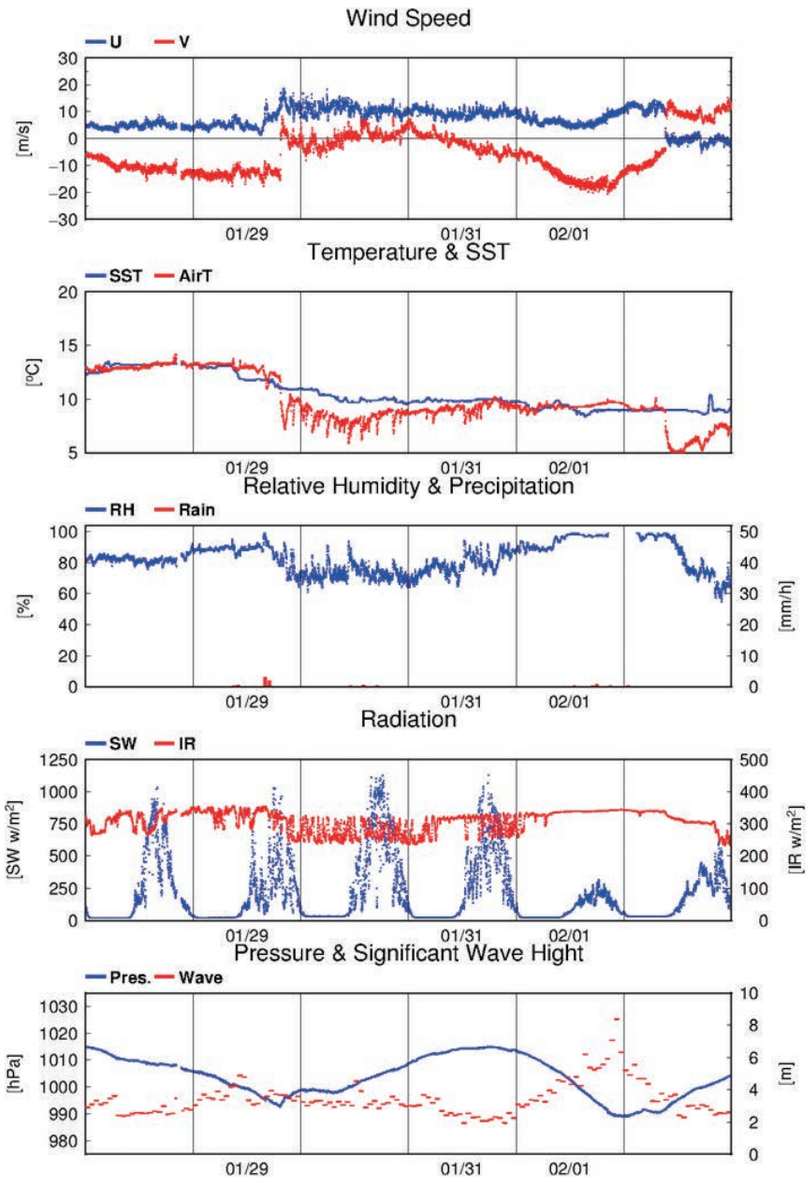

Fig. 2.3.2 (Continued)

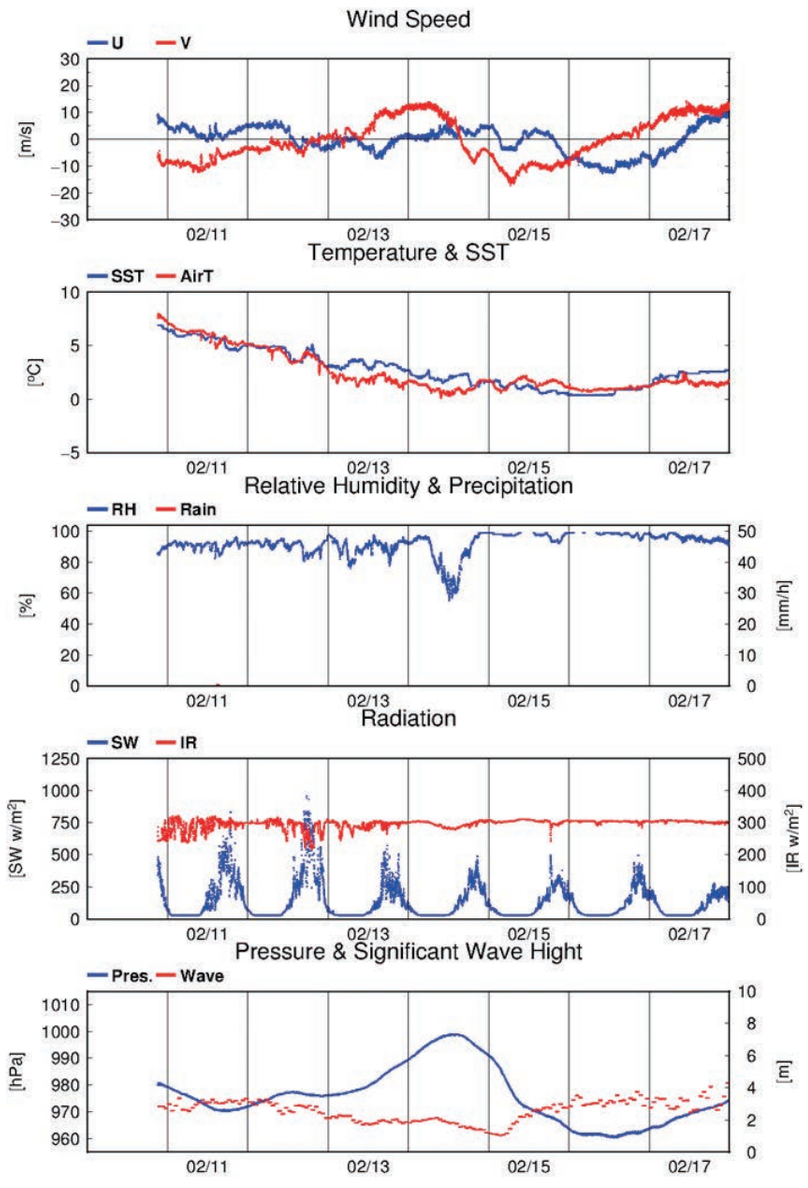

Fig. 2.3.3 Time series of surface meteorological parameters during the MR16-09 Leg3 cruise

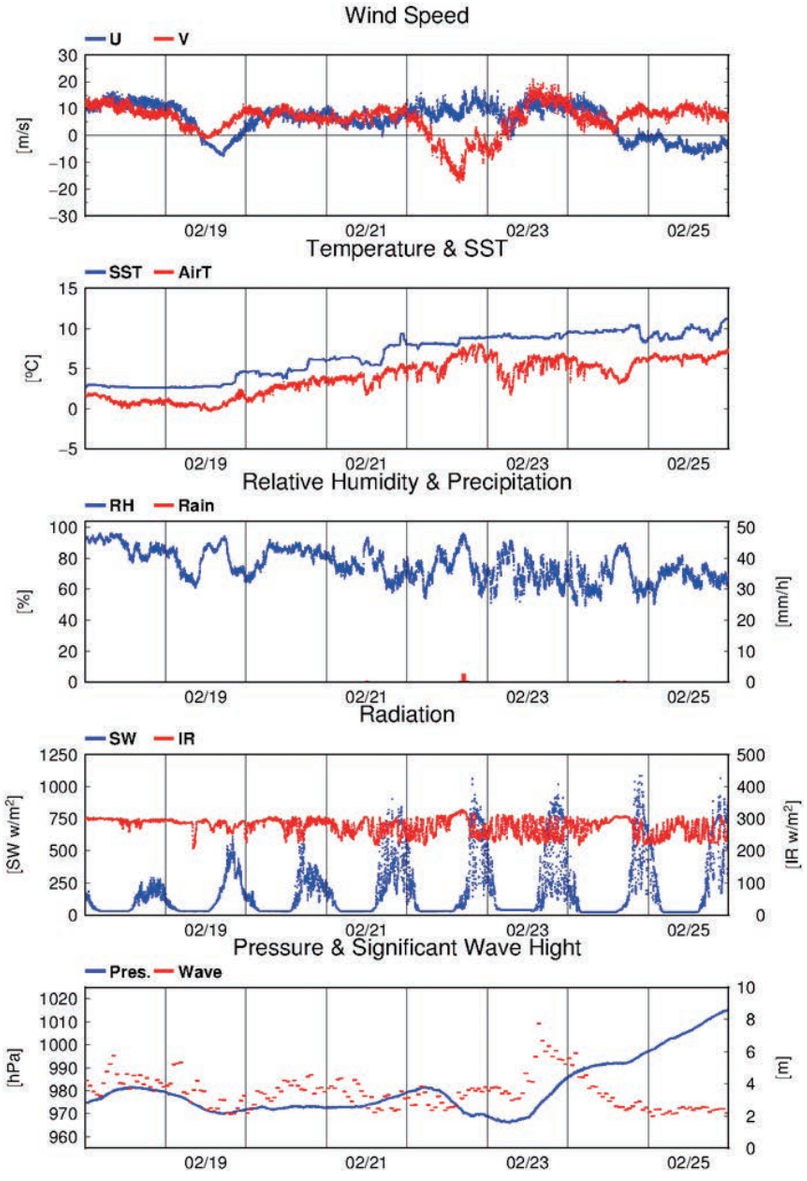

Fig. 2.3.3 (Continued)

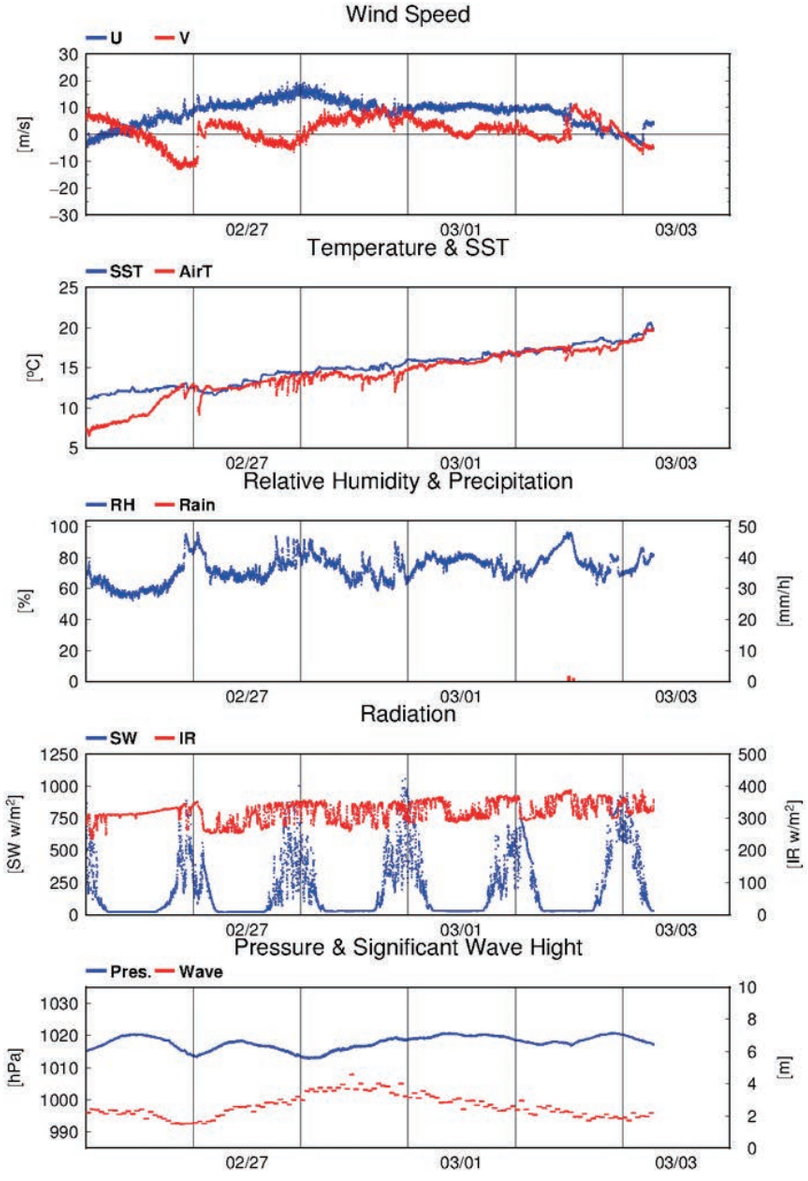

Fig. 2.3.3 (Continued)

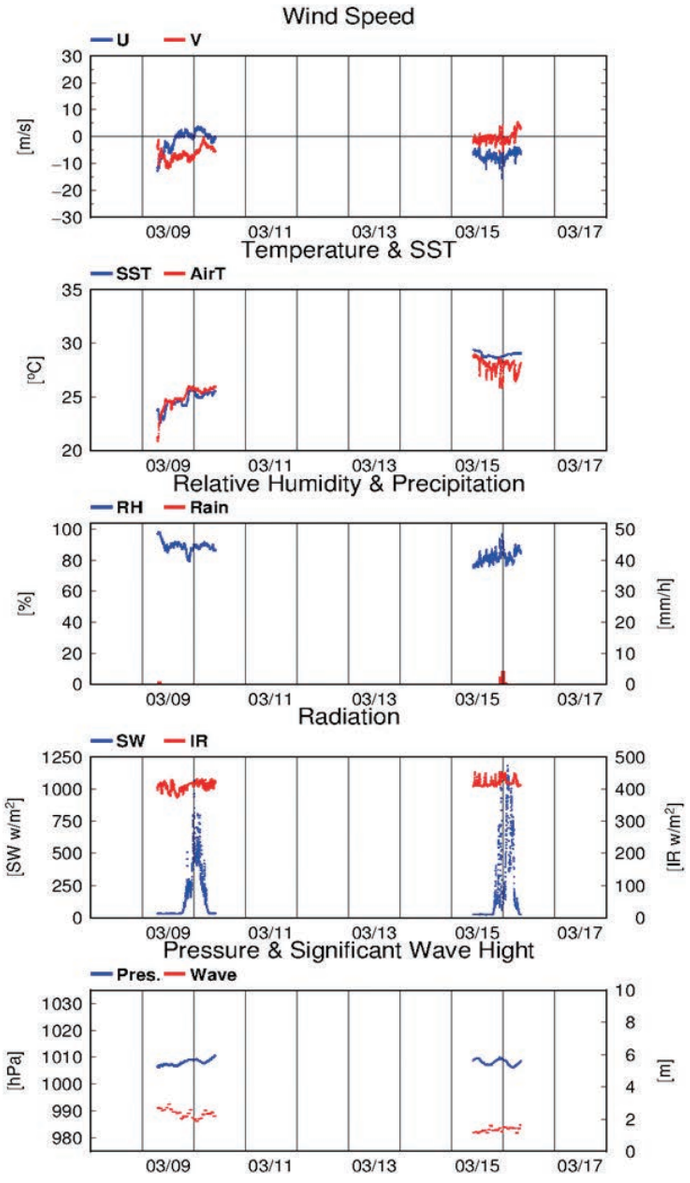

Fig. 2.3.4 Time series of surface meteorological parameters during the MR16-09 Leg4 cruise

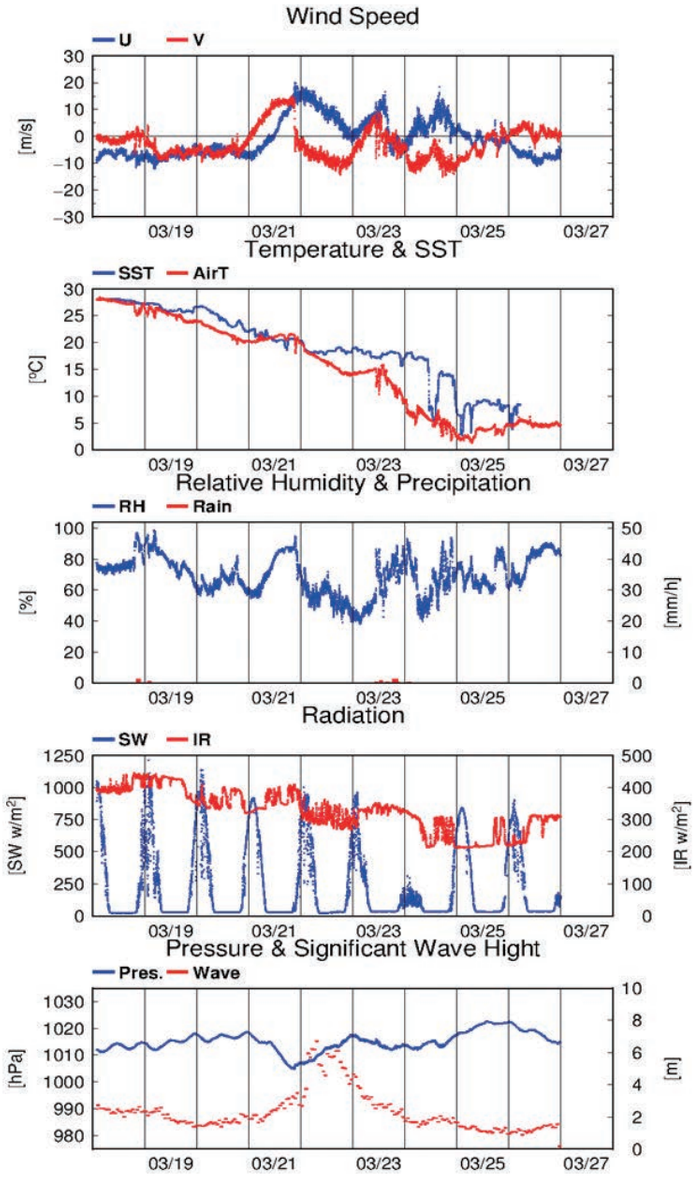

Fig. 2.3.4 (Continued)

2.4 Thermo-Salinograph and Related Measurements

May 17, 2017

(1) Personnel

Hiroshi Uchida (JAMSTEC)

Takuhei Shiozaki (JAMSTEC)

Kosei Sasaoka (JAMSTEC)

Hironori Sato (MWJ)

Haruka Tamada (MWJ)

Masanori Enoki (MWJ)

Misato Kuwahara (MWJ)

Masahiro Orui (MWJ)

(2) Objectives

The objective is to collect sea surface salinity, temperature, dissolved oxygen, fluorescence and turbidity data continuously along the cruise track.

(3) Materials and methods

The Continuous Sea Surface Water Monitoring System (Marine Works Japan Co, Ltd.) has seven sensors and automatically measures salinity, temperature, dissolved oxygen, fluorescence, and turbidity in sea surface water every 1 minute. This system is located in the sea surface monitoring laboratory and bottom of the ship and connected to shipboard LAN system. Measured data along with time and location of the ship were displayed on a monitor and stored in a desktop computer. The sea surface water was continuously pumped up to the laboratory from about 5 m water depth and flowed into the system through a vinyl-chloride pipe. One thermometer is located just before the sea water pump at bottom of the ship. The flow rate of the surface seawater was controlled to be about 1.2 L/min. Periods of measurement, maintenance and problems are listed in Table 2.4.1.

Software and sensors used in this system are listed below.

i. Software

Seamoni-kun Ver.1.50

ii. Sensors

Temperature and conductivity sensor

Model:	SBE 45, Sea-Bird Electronics, Inc.
Serial number:	4557820-0319
Pre-cruise calibration:	19 May 2016, Sea-Bird Electronics, Inc.

Bottom of ship thermometer

Model:	SBE 38, Sea-Bird Electronics, Inc.
Serial number:	3852788-0457
Pre-cruise calibration:	8 March 2016, Sea-Bird Electronics, Inc.

Dissolved oxygen sensor

Model:	RINKO-II, JFE Adantech Co. Ltd.
Serial number:	0013
Pre-cruise calibration:	24 April 2016, JAMSTEC

Model:	OPTODE 3835, Aanderaa Data Instruments, AS.
Serial number:	1915
Pre-cruise calibration:	13 May 2015, JAMSTEC

Fluorometer and turbidity sensor

Model:	C3, Turner Designs, Inc.
Serial number:	2300384

Table 2.4.1. Events of the Continuous Sea Surface Water Monitoring System operation.

System Date [UTC]	System Time [UTC]	Event
Leg 1		
2016/12/28	18:46	Logging start
2017/01/06	00:11~00:57	Logging stop for filter cleaning
2017/01/15	06:12	Logging stop
Leg 2		
2017/01/21	14:32	Logging start
2017/01/28	11:01~11:43	Logging stop for filter cleaning
2017/01/28	12:02~12:03	C3 data unavailable
2017/01/28	19:14~19:15	All data unavailable
2017/01/28	19:15~19:18	C3 data unavailable
2017/01/28	20:15~21:21	Logging stop for entering into Chilean territorial waters
2017/01/31	08:50~08:55	Flow rate for RINKO/Optode was zero
2017/02/03	23:59	Logging stop
Leg 3		
2017/02/10	21:15	Logging start
2017/02/16	03:17~04:10	Logging stop for filter cleaning
2017/02/16	08:16~15:46	Flow rate for RINKO/Optode might be small
2017/02/16	20:55~	Flow rate for SBE 45 was unstable
2017/02/17	~12:07	
2017/02/17	12:08~13:25	Logging stop for filter cleaning
2017/03/03	07:00	Logging stop
Leg 4		
2017/03/09	07:03	Logging start
2017/03/10	10:00~	Logging stop for entering into foreign EEZs
2017/03/15	~09:59	
2017/03/16	08:10~	Logging stop for entering into foreign EEZs
2017/03/18	~01:49	
2017/03/25	23:00	Logging stop

(4) Pre-cruise calibration

Pre-cruise sensor calibrations for the SBE 45 and SBE 38 were performed at Sea-Bird Electronics, Inc.

Pre-cruise sensor calibrations for the oxygen sensors were performed at JAMSTEC. The oxygen sensors were immersed in fresh water in a 1-L semi-closed glass vessel, which was immersed in a temperature-controlled water bath. Temperature of the water bath was set to 1, 10, 20 and 29°C. Temperature of the fresh water in the vessel was measured by a thermistor thermometer (expanded uncertainty of smaller than 0.01°C, ARO-PR, JFE Advantech, Co., Ltd.). At each temperature, the fresh water in the vessel was bubbled with standard gases (4, 10, 17 and 25% oxygen consisted of the oxygen-nitrogen mixture, whose relative expanded uncertainty is 0.5%) for more than 30 minutes to insure saturation. Absolute pressure of the vessel headspace was measured by a reference quartz crystal barometer (expanded uncertainty of 0.01% of reading) and ranged from about 1040 to 1070 hPa. The data were averaged over 5 minutes at each calibration point (a matrix of 24 points). As a reference, oxygen concentration of the fresh water in the calibration vessel was calculated from the oxygen concentration of the gases, temperature and absolute pressure at the water depth (about 8 cm) of the sensor's sensing foil as follows:

$$O_2\ (\mu mol/L) = \{1000 \times c(T) \times (A_p - pH_2O)\} / \{0.20946 \times 22.3916 \times (1013.25 - pH_2O)\}$$

where $c(T)$ is the oxygen solubility, A_p is absolute pressure [in hPa], and pH_2O is the water vapor pressure [in hPa].

The RINKO was calibrated by the modified Stern-Volmer equation slightly modified from a method by Uchida et al. (2010):

$$O_2\ (\mu mol/L) = [(V_0 / V)^E - 1] / K_{sv}$$

where V is raw phase difference, V_0 is raw phase difference in the absence of oxygen, K_{sv} is Stern-Volmer constant. The coefficient E corrects nonlinearity of the Stern-Volmer equation. The V_0 and the K_{sv} are assumed to be functions of temperature as follows.

$$K_{sv} = C_0 + C_1 \times T + C_2 \times T^2$$

$$V_0 = 1 + C_3 \times T$$

$$V = C_4 + C_5 \times V_b$$

where T is CTD temperature (°C) and V_b is raw output. The oxygen concentration is calculated using accurate temperature data from the SBE 45 instead of temperature data from the RINKO. The calibration coefficients were as follows:

C_0 = 5.123682697760924e–3

C_1 = 2.216599487021134e–4

C_2 = 4.123214071344090e–6

C_3 = –6.672929550710492e–4

C_4 = 2.395966849477748e–2

C_5 = 0.1951644347447042

E = 1.5

(5) Data processing and post-cruise calibration

Data from the Continuous Sea Surface Water Monitoring System were obtained at 1-minute intervals. These data were processed as follows. Spikes in the temperature and salinity data were removed using a median filter with a window of 3 scans (3 minutes) when difference between the original data and the median filtered data was larger than 0.1°C for temperature and 0.5 for salinity. Data gaps were linearly interpolated when the gap was ≤ 13 minutes. Fluorometer and turbidity data were low-pass filtered using a median filter with a window of 3 scans (3 minutes) to remove spikes. Raw data from the RINKO oxygen sensor, fluorometer and turbidity data were low-pass filtered using a Hamming filter with a window of 15 scans (15 minutes).

Salinity (S [PSU]), dissolved oxygen (O [µmol/kg]), and fluorescence (Fl [RFU]) data were corrected using the water sampled data. Details of the measurement methods are described in Sections 3.2, 3.4 and 3.10 for salinity, dissolved oxygen, and chlorophyll-a, respectively. Corrected salinity (S_{cor}), dissolved oxygen (O_{cor}), and estimated chlorophyll *a* (Chl-*a*) were calculated from following equations

S_{cor} [PSU] = $c_0 + c_1 S + c_2 t$

O_{cor} [µmol/kg] = $c_0 + c_1 O + c_2 T + c_3 t$

Chl-*a* [µg/L] = $c_0 + c_1 Fl$

where S is practical salinity, t is days from a reference time (2016/12/28 18:46 [UTC]), T is temperature in °C. The best fit sets of calibration coefficients (c_0~c_3) were determined by a least square technique to minimize the deviation from the water sampled data. The calibration coefficients were listed in Table 2.4.2. Comparisons between the Continuous Sea Surface Water Monitoring System data and water sampled data are shown in Figs. 2.4.1, 2.4.2 and 2.4.3. The calibration coefficients were basically determined for each leg.

For leg 3, salinity data were shifted at routine maintenance (2017/02/16 03:17~04:10). Therefore, the coefficient c_0 was changed before and after the maintenance.

For fluorometer data, water sampled data obtained at night [PAR (Photosynthetically Available Radiation) < 50 µE/(m^2 sec)] were used for the calibration, since sensitivity of the fluorometer to chlorophyll *a* is different at nighttime and daytime (Section 2.4 in Uchida et al., 2015). Sensitivity of the fluorometer to chlorophyll *a* may also has regional differences. Therefore, the calibration coefficients were change in leg 2.

For leg 2, chlorophyll *a* data obtained at 10 m depths of CTD/water sampling casts were also used to calibrate the fluorometer data.

(6) References

Uchida, H., G. C. Johnson, and K. E. McTaggart (2010): CTD oxygen sensor calibration procedures, The GO-SHIP Repeat Hydrography Manual: A collection of expert reports and guidelines, IOCCP Rep., No. 14, ICPO Pub. Ser. No. 134.

Uchida, H., K. Katsumata, and T. Doi (2015): WHP P14S, S04I Revisit Data Book, JASTEC, Yokosuka, 187 pp.

Table 2.4.2. Calibration coefficients for the salinity, dissolved oxygen, and chlorophyll *a*.

	c_0	c_1	c_2	c_3
Salinity				
Leg 1	4.130002e–2	0.9988262	3.781427e–4	
Leg 2	–7.173855e–3	0.9997166	4.655501e–4	
Leg 3	–5.867472e–5	0.9992261	4.396308e–4	(for ~ 2017/02/16 04:00)
	–5.160587e–3	0.9992261	4.396308e–4	(for 2017/02/16 04:00 ~)
Leg 4	–9.554012e–3	0.9994091	2.991207e–4	
Dissolved oxygen				
Leg 1	–10.49821	0.9774294	0.4408163	7.269963e–2
Leg 2	–8.846670	0.9636318	0.4452296	0.1050298
Leg 3	3.415634	0.9044650	–5.714148e–3	0.2063646
Leg 4	53.65725	0.8189659	–0.3604695	–0.1434302
Chlorophyll a				
Leg 1	0.0	2.615018e–2	(for Fl < 8)	
	–0.1071907	3.954902e–2	(for Fl >= 8)	
Leg 2 (for ~ 2017/01/25 19:50 or 2017/01/29 19:50 ~)				
	0.0	6.722433e–2	(for Fl < 7)	
	–0.3219685	0.1132198	(for Fl >= 7)	
(for 2017/01/25 19:50 ~ 2017/01/29 19:50)				
	0.0	0.1164691	(for Fl < 8)	
	–3.496350	0.5535129	(for Fl >= 8 and Fl < 12)	
	2.689773	3.800260e–2	(for Fl >= 12)	
Leg 3	0.0	5.766692e–2	(for Fl < 8)	
	–0.1513446	7.658499e–2	(for Fl >= 8)	
Leg 4	0.0	0.1164691	(for Fl < 8)	
	–3.496350	0.5535129	(for Fl >= 8 and Fl < 12)	
	2.689773	3.800260e–2	(for Fl >= 12)	

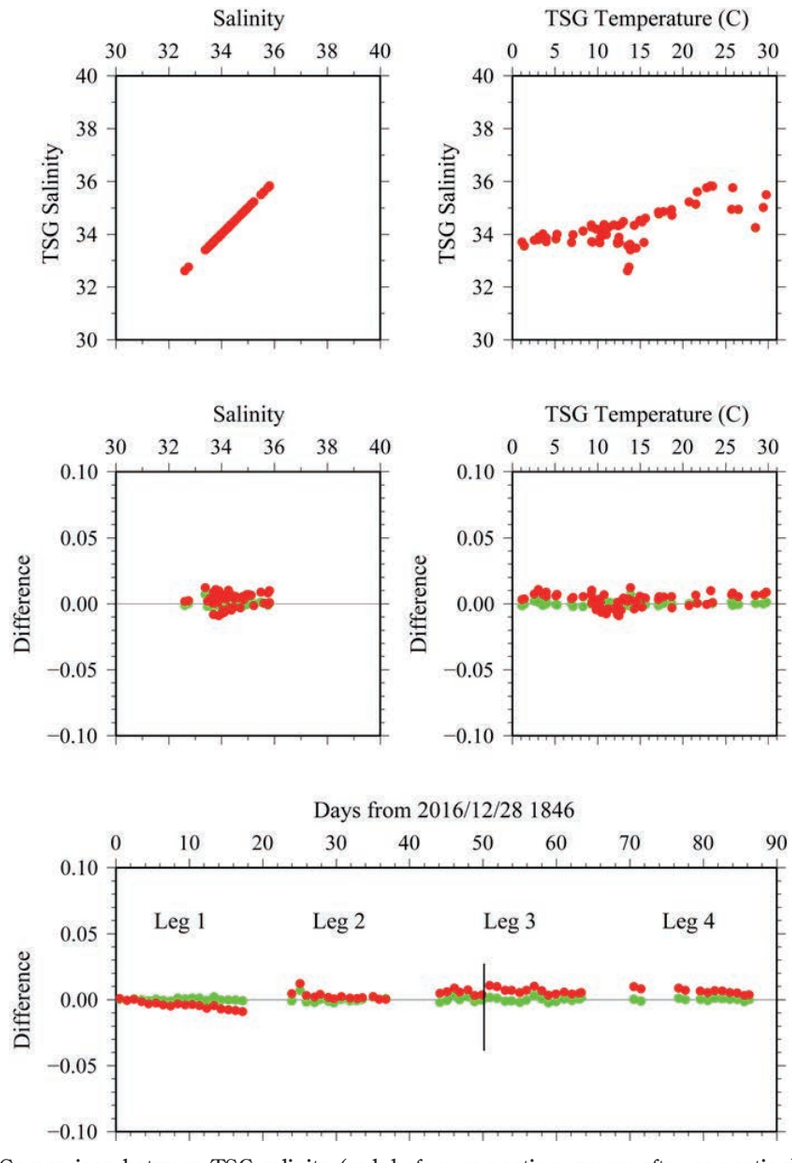

Figure 2.4.1. Comparison between TSG salinity (red: before correction, green: after correction) and sampled salinity.

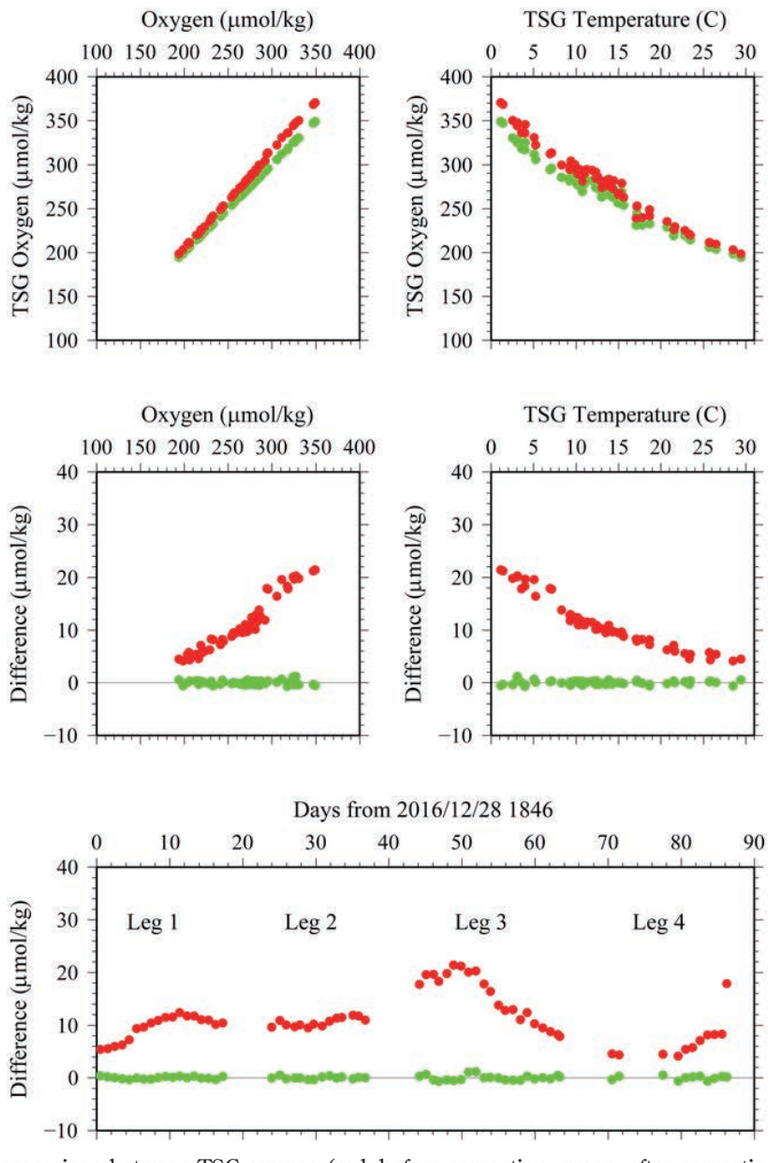

Figure 2.4.2. Comparison between TSG oxygen (red: before correction, green: after correction) and sampled oxygen.

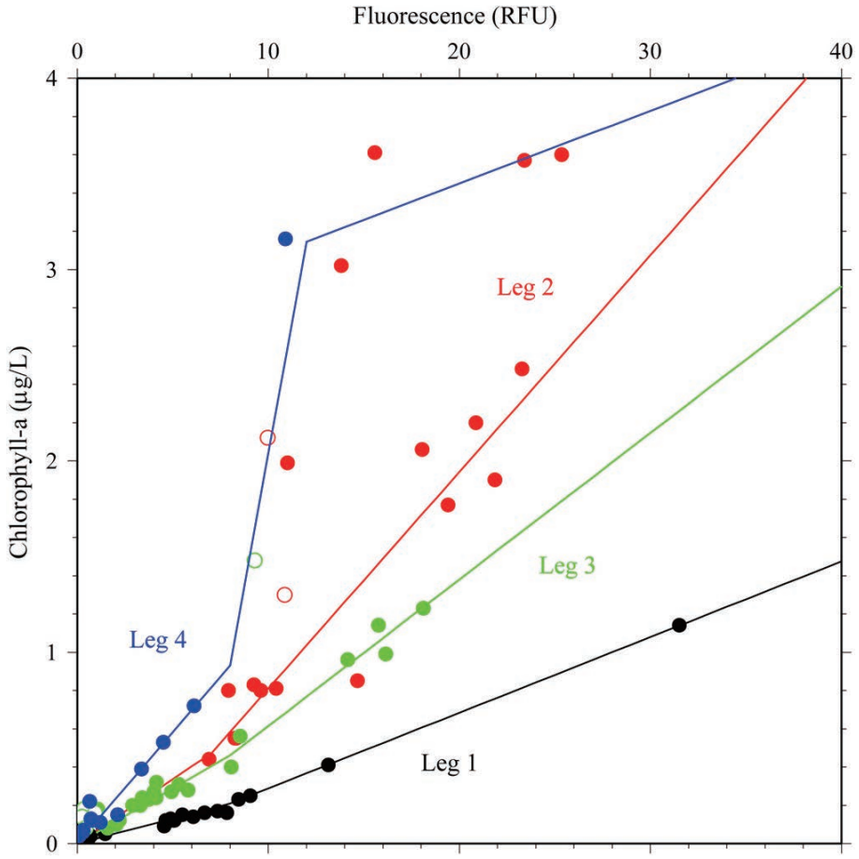

Figure 2.4.3. Comparison between TSG fluorescence and sampled chlorophyll-*a*. Open dots show that PAR data were greater than 50 µE/(m^2 sec). Calibration functions are also shown as lines.

2.5 Underway pCO_2

23 November 2018

Personnel

Akihiko Murata (JAMSTEC)

Tomonori Watai (MWJ)

Atsushi Ono (MWJ)

Emi Deguchi (MWJ)

Nagisa Fujiki (MWJ)

Introduction

Concentrations of CO_2 in the atmosphere are now increasing at a rate of about 2.0 ppmv yr^{-1} owing to human activities such as burning of fossil fuels, deforestation, and cement production. It is an urgent task to estimate as accurately as possible the absorption capacity of the oceans against the increased atmospheric CO_2, and to clarify the mechanism of the CO_2 absorption, because the magnitude of the anticipated global warming depends on the levels of CO_2 in the atmosphere, and because the ocean currently absorbs 1/3 of the 6 Gt of carbon emitted into the atmosphere each year by human activities.

In this cruise, we were aimed at quantifying how much anthropogenic CO_2 absorbed in the surface ocean in the Pacific. For the purpose, we measured pCO_2 (partial pressure of CO_2) in the atmosphere and surface seawater along the cruise track including WHP P17E line.

Apparatus and shipboard measurement

Continuous underway measurements of atmospheric and surface seawater pCO_2 were made with the CO_2 measuring system (Nihon ANS, Inc.) installed in the R/V *Mirai* of JAMSTEC. The system comprises of a non-dispersive infrared gas analyzer (Li-COR LI-7000, modified by Nihon ANS, Inc.), an air-circulation module and a showerhead-type equilibrator. To measure concentrations (mole fraction) of CO_2 in dry air (xCO_2a), air sampled from the bow of the ship (approx. 13 m above the sea level) was introduced into the NDIR through a dehydrating route with an electric dehumidifier (kept at ~2 °C), a Perma Pure dryer (GL Sciences Inc.), and a chemical desiccant ($Mg(ClO_4)_2$). The flow rate of the air was approx. 500 ml min^{-1}. To measure surface seawater concentrations of CO_2 in dry air (xCO_2s), the air equilibrated with seawater within the equilibrator was introduced into the NDIR through the same flow route as the dehydrated air used in measuring xCO_2a. The flow rate of the equilibrated air was 600 – 800 ml min^{-1}. The seawater was taken by a pump from the intake placed at the approx. 4.5 m below the sea surface. The flow rate of seawater in the equilibrator was 4000 – 5000 ml min^{-1}.

The CO_2 measuring system was set to repeat the measurement cycle such as 4 kinds of CO_2 standard gases (Table 2.5.1), xCO_2a (twice), xCO_2s (7 times). This measuring system was run automatically throughout the cruise by a PC control.

Quality control

Concentrations of CO_2 of the standard gases are listed in Table 2.5.1, which were calibrated after cruise by the JAMSTEC primary standard gases. The CO_2 concentrations of the primary standard gases were calibrated by the Japan Meteorological Agency, and traceable to the WMO 2007 scale.

In actual shipboard observations, the signals of NDIR usually reveal a trend. The trends were adjusted linearly using the signals of the standard gases analyzed before and after the sample measurements.

Effects of water temperature increased between the inlet of surface seawater and the equilibrator on xCO_2s were adjusted based on Takahashi *et al.* (1993), although the temperature increases were slight, being usually <0.1 °C.

We checked values of xCO_2a and xCO_2s by examining signals of the NDIR by plotting the xCO_2a and xCO_2s as a function of sequential day, longitude, sea surface temperature and sea surface salinity.

Reference

Takahashi, T., J. Olafsson, J. G. Goddard, D. W. Chipman, and S. C. Southerland (1993) Seasonal variation of CO_2 and nutrients in the high-latitude surface oceans: a comparative study, *Global Biogeochem. Cycles*, 7, 843–878.

Table 2.5.1. Concentrations of CO_2 standard gases used during the Pacific cruise.

Cylinder no.	Concentrations (ppmv)
CQC00046	229.932
CQC00047	290.137
CQC00048	370.093
CQC00049	430.156

2.6 Underway C_T

23 November 2018

Personnel

Akihiko Murata (JAMSTEC)

Tomonori Watai (MWJ)

Atsushi Ono (MWJ)

Emi Deguchi (MWJ)

Nagisa Fujiki (MWJ)

Introduction

Concentrations of CO_2 in the atmosphere are now increasing at a rate of about 2.0 ppmv yr^{-1} owing to human activities such as burning of fossil fuels, deforestation, and cement production. It is an urgent task to estimate as accurately as possible the absorption capacity of the oceans against the increased atmospheric CO_2, and to clarify the mechanism of the CO_2 absorption, because the magnitude of the anticipated global warming depends on the levels of CO_2 in the atmosphere, and because the ocean currently absorbs 1/3 of the 6 Gt of carbon emitted into the atmosphere each year by human activities.

In this cruise, we were aimed at quantifying how much anthropogenic CO_2 absorbed in the surface ocean in the Pacific. For the purpose, we measured dissolved inorganic carbon in surface seawater continuously along the cruise track of MR16-09 leg 3 including WHP P17E line.

Apparatus and shipboard measurement

Continuous underway measurements of surface seawater C_T were made with the C_T measuring system (Nihon ANS, Inc.) installed in the R/V *Mirai* of JAMSTEC. The system is almost the same as those used for discrete samples of C_T in water columns (see section 3.7), except for underway water sampling device.

The underway water sampling device collects surface seawater in a ~300 ml borosilicate glass bottle automatically after overflow of the 3 times volume. Before measurement, water samples are kept at 20°C. The seawater is then transferred into a pipette (~15 ml), which is kept at 20°C by a water jacket, in which water from a water bath set at 20°C is circulated. CO_2 dissolved in a seawater sample is extracted in a stripping chamber of the CO_2 extraction system by adding phosphoric acid (~10 % v/v) of about 2 ml. The stripping chamber is approx. 25 cm long and has a fine frit at the bottom. The acid is added to the stripping chamber from the bottom of the chamber by pressurizing an acid bottle for a given time to push out the right amount of acid. The pressurizing is made with nitrogen gas (99.9999 %). After the acid is transferred to the stripping chamber, a seawater sample kept in a pipette is introduced to the stripping chamber by the same method as in adding an acid. The seawater reacted with phosphoric acid is stripped of CO_2 by bubbling the nitrogen gas through a fine frit at the bottom of the stripping chamber. The CO_2 stripped in the chamber is carried by the nitrogen gas (flow rates is 140 ml min^{-1}) to the coulometer through a dehydrating module. The module consists of two electric dehumidifiers (kept at ~2°C) and a chemical desiccant ($Mg(ClO_4)_2$).

The measurement sequence such as ~1.5 % CO_2 gas in a nitrogen base, system blank (phosphoric acid blank), sea water samples (6) is programmed to repeat. The measurement of ~1.5 % CO_2 gas is made to monitor response of coulometer solutions purchased from UIC.

Quality control

For calibration of the C_T measuring system, blank and 5 kinds of Na_2CO_3 solutions were used. The calibration factor obtained by Na_2CO_3 solutions was re-calibrated based on Dickson CRM (batch 112, certified value: 2011.09 ± 0.36 µmol kg^{-1}). Due to malfunction of the water sampling system installed on the R/V *Mirai*, it was found that water supply to the system was not sufficient. The data from insufficient water volume were deleted from the final dataset.

The repeatability of measurements was estimated to be 2.8 µmol kg^{-1}, which was calculated from 11 measurements of the CRM.

2.7 ADCP

(1) Personnel

Shinya Kouketsu	JAMSTEC: Principal Investigator (Not on board)	- leg1,2,3,4 -
Wolfgang Schneider	Univ. of Concepcion: Principal Investigator	- leg2 -
Souichiro Sueyoshi	Nippon Marine Enterprises Ltd., (NME)	- leg1 -
Yutaro Murakami	NME	- leg1,2 -
Wataru Tokunaga	NME	- leg2 -
Koichi Inagaki	NME	- leg2,3 -
Shinya Okumura	NME	- leg3 -
Kazuho Yoshida	NME	- leg4 -
Ryo Kimura	MIRAI crew / NME	- leg1,3,4 -
Masanori Murakami	MIRAI crew	- leg2,3,4 -

(2) Objective

To obtain continuous measurement of the current profile along the ship's track.

(3) Methods

Upper ocean current measurements were made in the MR16-09 Leg1 to Leg4 cruises, using the hull-mounted Acoustic Doppler Current Profiler (ADCP) system. For most of its operation the instrument was configured for water-tracking mode. Bottom-tracking mode, interleaved bottom-ping with water-ping, was made to get the calibration data for evaluating transducer misalignment angle in the shallow water. The system consists of following components;

1) R/V MIRAI has installed vessel-mount ADCP (acoustic frequency 76.8 kHz "Ocean Surveyor", Teledyne RD Instruments). It has a phased-array transducer with single ceramic assembly and creates 4 acoustic beams electronically. We mounted the transducer head rotated to a ship-relative angle of 45 degrees azimuth from the keel.
2) For heading source, we use ship's gyro compass (TOKYO KEIKI, Japan), continuously providing heading to the ADCP system directory. Also we have Inertial Navigation System (PHINS, IXBLUE) which provide high-precision heading and attitude information are stored in ".N2R" data files.
3) Differential GNSS system (Multi-Fix, Fugro, Netherlands) providing precise ship's position fixes.
4) We used VmDas version 1.46.5 (TRDI) for data acquisition.
5) To synchronize time stamp of pinging with GPS time, the clock of the logging computer is adjusted to GPS time every 8 minutes.
6) The sound speed at the transducer does affect the vertical bin mapping and vertical velocity measurement, is calculated from temperature, salinity (constant value; 35.0 psu) and depth (6.5 m; transducer depth) by equation in Medwin (1975).

Data was configured for 8-m intervals starting 23-m below the surface. Every ping was recorded as raw ensemble data (.ENR). Major parameters for the measurement (Direct Command) are shown in Table 2.7.1.

(4) Data process

ADCP-coordinate velocities were converted to the earth-coordinate velocities using ship attitude data from INU, and then the 5-minute mean current velocities were obtained by subtracting ship velocities based on GPS from the ADCP-coordinate velocities with misalignment and scale corrections for ADCP measurements. Corrections of misalignment (0.002 radian) and scale factors (0.99) were made using the bottom track data. In the processing, we remove weak echo intensity data (< 40 counts). After the processing, we screened out the velocities with relatively large estimation errors (> 0.5 m/s) regarded as unreliable.

(5) Data archive

These data obtained in these cruises will be submitted to the Data Management Group of JAMSTEC, and will be opened to the public via "Data Research System for Whole Cruise Information in JAMSTEC

(DARWIN)" in JAMSTEC web site (http://www.godac.jamstec.go.jp/darwin/e).

(6) Remarks (Time in UTC)

i) The following periods, the observations were carried out.

Leg1: 18:46, 28 Dec. 2016 to 06:00, 15 Jan. 2017

Leg2: 14:32, 21 Jan. 2017 to 20:14, 28 Jan. 2017

21:22, 28 Jan. 2017 to 23:56, 03 Feb. 2017

Leg3: 21:00, 10 Feb. 2017 to 06:59, 03 Mar. 2017

Leg4: 07:03, 09 Mar. 2017 to 09:59, 10 Mar. 2017

10:00, 15 Mar. 2017 to 08:09, 16 Mar. 2017

01:50, 18 Mar. 2017 to 00:00, 28 Mar. 2017

ii) The following period, Temperature and Sound Velocity data were constant (0.0°C and 1449m/s) due to system trouble.

02:55, 16 Feb. 2017 to 02:19, 19 Feb. 2017

Table 2.7.1 Major parameters

Bottom-Track Commands	
BP = 001	Pings per Ensemble (almost less than 1300m depth)
	Leg1: None
	Leg2: 22:19, 21 Jan. 2017 to 06:00, 22, Jan. 2017
	21:43, 26 Jan. 2017 to 23:19, 26 Jan. 2017
	23:02, 28 Jan. 2017 to 01:25, 29 Jan. 2017
	22:55, 03 Feb. 2017 to 23:56, 03 Feb. 2017
	Leg3: None
	Leg4: 07:58, 09 Mar. 2017 to 18:34, 09 Mar. 2017
	22:19, 25 Mar. 2017 to 00:00, 28 Mar. 2017
Environmental Sensor Commands	
EA = +04500	Heading Alignment (1/100 deg)
EB = +00000	Heading Bias (1/100 deg)
ED = 00065	Transducer Depth (0 - 65535 dm)
EF = +001	Pitch/Roll Divisor/Multiplier (pos/neg) [1/99 - 99]
EH = 00000	Heading (1/100 deg)
ES = 35	Salinity (0-40 pp thousand)
EX = 00000	Coord Transform (Xform:Type; Tilts; 3Bm; Map)
EZ = 10200010	Sensor Source (C; D; H; P; R; S; T; U)
	C (1): Sound velocity calculates using ED, ES, ET (temp.)
	D (0): Manual ED
	H (2): External synchro
	P (0), R (0): Manual EP, ER (0 degree)

S (0): Manual ES

T (1): Internal transducer sensor

U (0): Manual EU

Timing Commands

TE = 00:00:02.00	Time per Ensemble (hrs:min:sec.sec/100)
TP = 00:02.00	Time per Ping (min:sec.sec/100)

Water-Track Commands

WA = 255	False Target Threshold (Max) (0-255 count)
WB = 1	Mode 1 Bandwidth Control (0=Wid, 1=Med, 2=Nar)
WC = 120	Low Correlation Threshold (0-255)
WD = 111 100 000	Data Out (V; C; A; PG; St; Vsum; Vsum^2;#G;P0)
WE = 1000	Error Velocity Threshold (0-5000 mm/s)
WF = 0800	Blank After Transmit (cm)
WG = 001	Percent Good Minimum (0-100%)
WI = 0	Clip Data Past Bottom (0 = OFF, 1 = ON)
WJ = 1	Rcvr Gain Select (0 = Low, 1 = High)
WM = 1	Profiling Mode (1-8)
WN = 100	Number of depth cells (1-128)
WP = 00001	Pings per Ensemble (0-16384)
WS= 0800	Depth Cell Size (cm)
WT = 000	Transmit Length (cm) [0 = Bin Length]
WV = 0390	Mode 1 Ambiguity Velocity (cm/s radial)

3 Hydrographic Measurements

3.1 $CTDO_2$ Measurements

May 14, 2017

(1) Personnel

Hiroshi Uchida (JAMSTEC)

Rei Ito (MWJ)

Sonoka Tanihara (MWJ)

Kenichi Katayama (MWJ)

Shungo Oshitani (MWJ)

Rio Kobayashi (MWJ)

Michinari Sunamura (The University of Tokyo) (CDOM measurement)

(2) Winch arrangements

The CTD package was deployed by using 4.5 Ton Traction Winch System (Dynacon, Inc., Bryan, Texas, USA), which was renewed on the R/V *Mirai* in April 2014 (e.g. Fukasawa et al., 2004). Primary system components include a complete CTD Traction Winch System with up to 9000 m of 9.53 mm armored cable (Rochester Wire & Cable, LLC, Culpeper, Virginia, USA).

(3) Overview of the equipment

The CTD system was SBE 911plus system (Sea-Bird Electronics, Inc., Bellevue, Washington, USA). The SBE 911plus system controls 36-position SBE 32 Carousel Water Sampler. The Carousel accepts 12-litre Niskin-X water sample bottles (General Oceanics, Inc., Miami, Florida, USA). The SBE 9plus was mounted horizontally in a 36-position carousel frame. SBE's temperature (SBE 3) and conductivity (SBE 4) sensor modules were used with the SBE 9plus underwater unit. The pressure sensor is mounted in the main housing of the underwater unit and is ported to outside through the oil-filled plastic capillary tube. A modular unit of underwater housing pump (SBE 5T) flushes water through sensor tubing at a constant rate independent of the CTD's motion, and pumping rate (3000 rpm) remain nearly constant over the entire input voltage range of 12-18 volts DC. Flow speed of pumped water in standard TC duct is about 2.4 m/s. Two sets of temperature and conductivity modules were used. An SBE's dissolved oxygen sensor (SBE 43) was placed between the primary conductivity sensor and the pump module. Auxiliary sensors, a Deep Ocean Standards Thermometer (SBE 35), an altimeter (PSA-916T; Teledyne Benthos, Inc., North Falmous, Massachusetts, USA), an oxygen optodes (RINKO-III; JFE Advantech Co., Ltd, Kobe Hyogo, Japan), a fluorometers (Seapoint sensors, Inc., Kingston, New Hampshire, USA), a transmissometer (C-Star Transmissometer; WET Labs, Inc., Philomath, Oregon, USA), a turbidity meter (Seapoint Sensors, Inc., Exeter, New Hampshire, USA), a Photosynthetically Active Radiation (PAR) sensor (Satlantic, LP, Halifax, Nova Scotia, Canada), and a colored dissolved organic matter (ECO FL CDOM, WET Labs, Inc., Philomath, Oregon, USA) were also used with the SBE 9plus underwater unit. To minimize rotation of the CTD package, a heavy stainless frame (total weight of the CTD package without sea water in the bottles is about 1000 kg) was used with an aluminum plate (54 × 90 cm).

Summary of the system used in this cruise

36-position Carousel system

Deck unit:

SBE 11plus, S/N 11P54451-0872

Under water unit:

SBE 9plus, S/N 09P21746-0575 (79492)

Temperature sensor:

SBE 3, S/N 031525 (primary)

SBE 3plus, S/N 03P4421 (secondary)

Conductivity sensor:

SBE 4, S/N 042435 (primary)

SBE 4, S/N 041088 (secondary)

Oxygen sensor:

SBE 43, S/N 432471

JFE Advantech RINKO-III, S/N 0024 (foil batch no. 144002A)

Pump:

SBE 5T, S/N 054595 (primary)

SBE 5T, S/N 053293 (secondary)

Altimeter:

PSA-916T, S/N 1157

Deep Ocean Standards Thermometer:

SBE 35, S/N 0045

Fluorometer:

Seapoint Sensors, Inc., S/N 3618 (measurement range: 0-15 µg/L) (Gain: 10X)

Turbidity meter:

Seapoint Sensors, Inc., S/N 14953 (measurement range: 0-500 FTU) (Gain: 5X) for leg 2

(measurement range: 0-25 FTU) (Gain: 100X) for leg 3

Transmissometer:

C-Star, S/N CST-1726DR

PAR:

Satlantic LP, S/N 1025

CDOM:

ECO FL CDOM, S/N FLCDRTD-2014 (measurement range: 0-500 ppb)

Carousel Water Sampler:

SBE 32, S/N 3254451-0826

Water sample bottle:

12-litre Niskin-X model 1010X (no TEFLON coating)

General Oceanics, Inc., Miami, Florida, USA,

(4) Pre-cruise calibration

i. Pressure

The Paroscientific series 4000 Digiquartz high pressure transducer (Model 415K: Paroscientific, Inc., Redmond, Washington, USA) uses a quartz crystal resonator whose frequency of oscillation varies with pressure induced stress with 0.01 per million of resolution over the absolute pressure range of 0 to 15000 psia (0 to 10332 dbar). Also, a quartz crystal temperature signal is used to compensate for a wide range of temperature changes at the time of an observation. The pressure sensor has a nominal accuracy of 0.015 % FS (1.5 dbar), typical stability of 0.0015 % FS/month (0.15 dbar/month), and resolution of 0.001 % FS (0.1 dbar). Since the pressure sensor measures the absolute value, it inherently includes atmospheric pressure (about 14.7 psi). SEASOFT subtracts 14.7 psi from computed pressure automatically.

Pre-cruise sensor calibrations for linearization were performed at SBE, Inc. The time drift of the pressure sensor is adjusted by periodic recertification corrections against an electronic dead-weight tester (Model E-DWT-H, S/N 181, Fluke Co, Phoenix, Arizona, USA, Calibrated on 3 April 2016 at Ohte Giken, Inc., Tsukuba, Ibaraki, Japan). The corrections are performed at JAMSTEC, Yokosuka, Kanagawa, Japan by Marine Works Japan Ltd. (MWJ), Yokohama, Kanagawa, Japan, usually once in a year in order to monitor sensor time drift and linearity.

S/N 0575, 13 April 2016

slope = 0.99982448

offset = 2.98685

ii. Temperature (SBE 3)

The temperature sensing element is a glass-coated thermistor bead in a stainless steel tube, providing a pressure-free measurement at depths up to 10500 (6800) m by titanium (aluminum) housing. The SBE 3 thermometer has a nominal accuracy of 1 mK, typical stability of 0.2 mK/month, and resolution of 0.2 mK at 24 samples per second. The premium temperature sensor, SBE 3plus, is a more rigorously tested and calibrated version of standard temperature sensor (SBE 3).

Pre-cruise sensor calibrations were performed at SBE, Inc.

S/N 031525, 7 May 2016

S/N 03P4421, 7 May 2016

iii. Conductivity (SBE 4)

The flow-through conductivity sensing element is a glass tube (cell) with three platinum electrodes to provide in-situ measurements at depths up to 10500 (6800) m by titanium (aluminum) housing. The SBE 4 has a nominal accuracy of 0.0003 S/m, typical stability of 0.0003 S/m/month, and resolution of 0.00004 S/m at 24 samples per second. The conductivity cells have been replaced to newer style cells for deep ocean measurements.

Pre-cruise sensor calibrations were performed at SBE, Inc.

S/N 042435, 12 May 2016

S/N 041088, 12 May 2016

The value of conductivity at salinity of 35, temperature of 15 °C (IPTS-68) and pressure of 0 dbar is 4.2914 S/m.

iv. Oxygen (SBE 43)

The SBE 43 oxygen sensor uses a Clark polarographic element to provide in-situ measurements at depths up to 7000 m. The range for dissolved oxygen is 120 % of surface saturation in all natural waters, nominal accuracy is 2 % of saturation, and typical stability is 2 % per 1000 hours.

Pre-cruise sensor calibration was performed at SBE, Inc.

S/N 432471, 10 May 2016

v. Deep Ocean Standards Thermometer

Deep Ocean Standards Thermometer (SBE 35) is an accurate, ocean-range temperature sensor that can be standardized against Triple Point of Water and Gallium Melt Point cells and is also capable of measuring temperature in the ocean to depths of 6800 m. The SBE 35 was used to calibrate the SBE 3 temperature sensors in situ (Uchida et al., 2007).

Pre-cruise sensor linearization was performed at SBE, Inc.

S/N 0045, 27 September 2002

Then the SBE 35 is certified by measurements in thermodynamic fixed-point cells of the TPW (0.01 °C) and GaMP (29.7646 °C). The slow time drift of the SBE 35 is adjusted by periodic recertification corrections. Pre-cruise sensor calibration was performed at SBE, Inc. Since 2014, fixed-point cells traceable to NIST temperature standards is directly used in the manufacturer's calibration of the SBE 35 (Uchida et al., 2015). Since 2016, pre-cruise sensor calibration was performed at RCGC/JAMSTEC by using fixed-point cells traceable to NMIJ temperature standards (Fig. 3.1.1).

S/N 0045, 30 June 2016 (slope and offset correction)

Slope = 1.000023

Offset = –0.001053

The time required per sample = 1.1 × NCYCLES + 2.7 seconds. The 1.1 seconds is total time per an acquisition cycle. NCYCLES is the number of acquisition cycles per sample and was set to 4. The 2.7 seconds is required for converting the measured values to temperature and storing average in EEPROM.

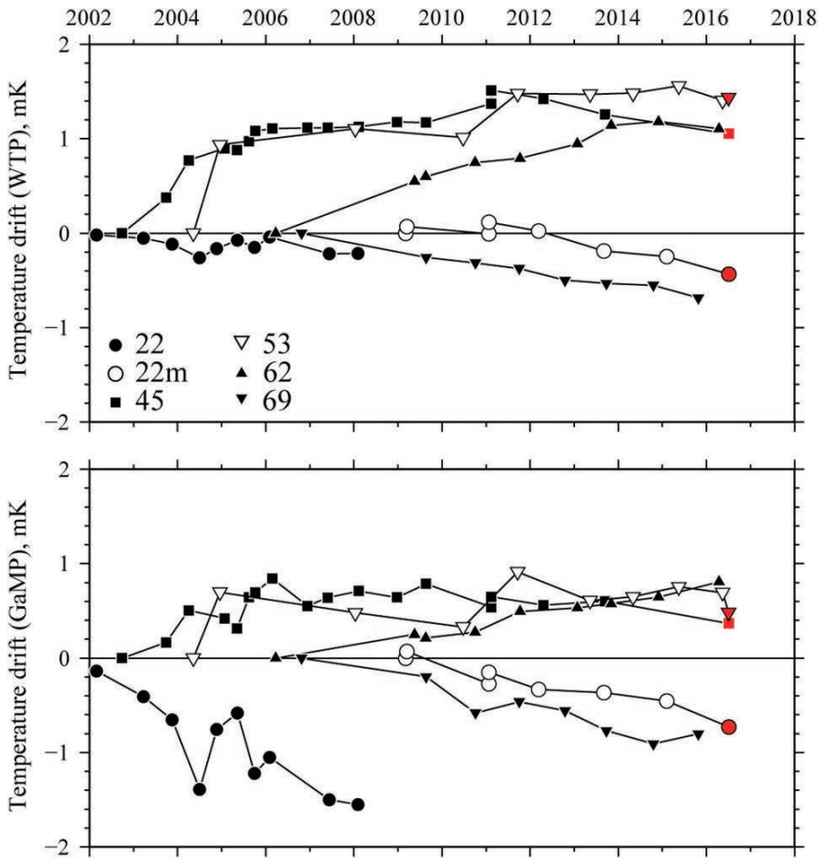

Fig. 3.1.1. Time drifts (temperature offsets relative to the first calibration) of six reference thermometers (SBE 35) based on laboratory calibrations in fixed-point cells. Results performed at JAMSTEC are shown in red marks.

vi. Altimeter

Benthos PSA-916T Sonar Altimeter (Teledyne Benthos, Inc.) determines the distance of the target from the unit by generating a narrow beam acoustic pulse and measuring the travel time for the pulse to bounce back from the target surface. It is rated for operation in water depths up to 10000 m. The PSA-916T uses the nominal speed of sound of 1500 m/s.

vii. Oxygen optode (RINKO)

RINKO (JFE Alec Co., Ltd.) is based on the ability of selected substances to act as dynamic fluorescence quenchers. RINKO model III is designed to use with a CTD system which accept an auxiliary analog sensor, and is designed to operate down to 7000 m.

Data from the RINKO can be corrected for the time-dependent, pressure-induced effect by means of the same method as that developed for the SBE 43 (Edwards et al., 2010). The calibration coefficients, H1 (amplitude of hysteresis correction), H2 (curvature function for hysteresis), and H3 (time constant for hysteresis) were determined empirically as follows.

H1 = 0.0055 (for S/N 0024)

H2 = 5000 dbar

H3 = 2000 seconds

Outputs from RINKO are the raw phase shift data. The RINKO can be calibrated by the modified Stern-Volmer equation slightly modified from a method by Uchida et al. (2010):

$$O_2\ (\mu mol/l) = [(V_0 / V)^E - 1] / K_{sv}$$

where V is voltage, V_0 is voltage in the absence of oxygen, K_{sv} is Stern-Volmer constant. The coefficient E corrects nonlinearity of the Stern-Volmer equation. The V_0 and the K_{sv} are assumed to be functions of temperature as follows.

$$K_{sv} = C_0 + C_1 \times T + C_2 \times T^2$$

$$V_0 = 1 + C_3 \times T$$

$$V = C_4 + C_5 \times V_b$$

where T is CTD temperature (°C) and V_b is raw output (volts). V_0 and V are normalized by the output in the absence of oxygen at 0°C. The oxygen concentration is calculated using accurate temperature data from the CTD temperature sensor instead of temperature data from the RINKO. The pressure-compensated oxygen concentration O_{2c} can be calculated as follows.

$$O_{2c} = O_2 (1 + C_p p / 1000)$$

where p is CTD pressure (dbar) and C_p is the compensation coefficient. Since the sensing foil of the optode is permeable only to gas and not to water, the optode oxygen must be corrected for salinity. The salinity-compensated oxygen can be calculated by multiplying the factor of the effect of salt on the oxygen solubility (Garcia and Gordon, 1992).

Pre-cruise sensor calibrations were performed at RCGC/JAMSTEC.

S/N 0024, 10 May 2015

viii. Fluorometer

The Seapoint Chlorophyll Fluorometer (Seapoint Sensors, Inc., Kingston, New Hampshire, USA) provides in-situ measurements of chlorophyll-a at depths up to 6000 m. The instrument uses modulated blue LED lamps and a blue excitation filter to excite chlorophyll-a. The fluorescent light emitted by the chlorophyll-a passes through a red emission filter and is detected by a silicon photodiode. The low level signal is then processed using synchronous demodulation circuitry, which generates an output voltage proportional to chlorophyll-a concentration.

ix. Transmissometer

The C-Star Transmissometer (WET Labs, Inc., Philomath, Oregon, USA) measures light transmittance at a single wavelength (650 nm) over a know path (25 cm). In general, losses of light propagating through water can be attributed to two primary causes: scattering and absorption. By projecting a collimated beam of light through the water and placing a focused receiver at a known distance away, one can quantify these losses. The ratio of light gathered by the receiver to the amount originating at the source is known as the beam transmittance. Suspended particles, phytoplankton, bacteria and dissolved organic matter contribute to the losses sensed by the instrument. Thus, the instrument provides information both for an indication of the total concentrations of matter in the water as well as for a value of the water clarity.

Light transmission T_r (in %) and beam attenuation coefficient c_p are calculated from the sensor output (V in volt) as follows.

$$T_r = (c_0 + c_1 V) \times 100$$

$$c_p = - (1 / 0.25) \ln(T_r / 100)$$

Pre-cruise sensor calibration was performed at WET Labs.

S/N CST-1726DR, 26 May 2015

x. Turbidity meter

The Seapoint turbidity meter (Seapoint Sensors, Inc., Kingston, New Hampshire, USA) detects light scattered by particles suspended in water at depths up to 6000 m. The sensor generates an output voltage proportional to turbidity or suspended solids. The unique optical design confines the sensing volume to within 5 cm of the sensor.

xi. PAR

Photosynthetically Active Radiation (PAR) sensors (Satlantic, LP, Halifax, Nova Scotia, Canada) provide highly accurate measurements of PAR (400 – 700 nm) for a wide range of aquatic and terrestrial applications. The ideal spectral response for a PAR sensor is one that gives equal emphasis to all photons between 400 – 700 nm. Satlantic PAR sensors use a high quality filtered silicon photodiode to provide a near equal spectral response across the entire wavelength range of the measurement.

Pre-cruise sensor calibration was performed at Satlantic, LP.

S/N 1025, 6 July 2015

xii. CDOM

The Environmental Characterization Optics (ECO) miniature fluorometer (WET Labs, Inc., Philomath, Oregon, USA) allows the user to measure relative Colored Dissolved Organic Matter (CDOM) concentrations by directly measuring the amount of fluorescence emission in a sample volume of water. The CDOM fluorometer uses an UV LED to provide the excitation source. An interference filter is used to reject the small amount of out-of-band light emitted by the LED. The light from the source enters the water volume at an angle of approximately 55-60 degrees with respect to the end face of the unit. Fluoresced light is received by a detector positioned where the acceptance angle forms a 140-degree intersection with the source beam. An interference filter is used to discriminate against the scattered excitation light.

CDOM (Quinine Dihydrate Equivalent) concentration expressed in ppb can be derived using the equation as follows.

CDOM = Scale Factor * (Output – Dark Counts)

Pre-cruise sensor calibration was performed at WET Labs.

S/N FLCDRTD-2014, 1 September 2015

Dark Counts: 0.025 V

Scale Factor: 106 ppb/V

(5) Data collection and processing

i. Data collection

CTD system was powered on at least 20 minutes in advance of the data acquisition to stabilize the pressure sensor and was powered off at least two minutes after the operation in order to acquire pressure data on the ship's deck.

The package was lowered into the water from the starboard side and held 10 m beneath the surface in order to activate the pump. After the pump was activated, the package was lifted to the surface and lowered at a rate of 1.0 m/s to 200 m (or 300 m when significant wave height was high) then the package was stopped to operate the heave compensator of the crane. The package was lowered again at a rate of 1.2 m/s to the bottom. For the up cast, the package was lifted at a rate of 1.1 m/s except for bottle firing stops. As a rule, the bottle was fired after waiting from the stop for more than 20 seconds and the package was stayed at least 5 seconds for measurement of the SBE 35 at each bottle firing stops. For depths where vertical gradient of water properties were expected to be large (from surface to thermocline), the bottle was exceptionally fired after waiting from the stop for 60 seconds to enhance exchanging the water between inside and outside of the bottle. At 200 m (or 300 m) from the surface, the package was stopped to stop the heave compensator of the crane.

Water samples were collected using a 36-bottle SBE 32 Carousel Water Sampler with 12-litre Niskin-X bottles. Before a cast taken water for CFCs, the bottle frame and Niskin-X bottles were wiped with acetone.

Data acquisition software

SEASAVE-Win32, version 7.23.2

ii. Data collection problems

(a) Miss trip, miss fire, and remarkable leak

Miss trip, miss fire and remarkable leak occurred during the cruise were listed below.

Miss trip	Miss fire	Leak
none	none	007_1 #20 end closure: O-ring of the end closure replaced
		010_1 #21 end closure: O-ring of the end closure replaced
		022_1 #22 end closure: O-ring of the end closure checked
		024_1 #4 end closure: O-ring of the end closure checked

(b) Slight leaks

Slight leaks were observed from the root of stopcocks during drawing of the samples at station leg3_011_1 (#2, #4, #5, #7, #11, #12), leg3_015_1 (#25, #26, #27, #29), leg3_016_1 (#25, #27), leg3_018_1 (#3), and leg3_026_1 (#36). The bottle flags for those bottles were set to 2 since the bottle data (salinity and oxygen) were normal and there was no leak for those bottles at the leak check before the drawing of the samples.

(c) Noise in down cast data

Transmissometer data were noisy at station leg2_006_1 (504~506, 519~521, 820~826, 833~838, 939~947, 968~970, 1063~1067, 1255~1259 dbar), leg2_007_1 (117~118, 1022~1025 dbar), leg2_12B_1 (736~741, 1035~1037 dbar), leg2_11B_1 (131~133 dbar), leg3_009_1 (1071-1076 dbar), leg3_015_1 (821~826 dbar), leg3_016_1 (1497~1541, 1574~1578 dbar), leg3_021_1 (400~527 dbar), leg3_023_1 (992~998 dbar), leg3_024_1 (2248~2253 dbar) and leg3_025_1 (64~65, 473~475 dbar), and the data were removed and linearly interpolated.

iii. Data processing

SEASOFT consists of modular menu driven routines for acquisition, display, processing, and archiving of oceanographic data acquired with SBE equipment. Raw data are acquired from instruments and are stored as unmodified data. The conversion module DATCNV uses instrument configuration and calibration coefficients to create a converted engineering unit data file that is operated on by all SEASOFT post processing modules. The following are the SEASOFT and original software data processing module sequence and specifications used in the reduction of CTD data in this cruise.

Data processing software

SBEDataProcessing-Win32, version 7.23.2

DATCNV converted the raw data to engineering unit data. DATCNV also extracted bottle information where scans were marked with the bottle confirm bit during acquisition. The duration was set to 4.4 seconds, and the offset was set to 0.0 second. The hysteresis correction for the SBE 43 data (voltage) was applied for both profile and bottle information data.

RINKOCOR (original module, version 1.0) corrected the time-dependent, pressure-induced effect (hysteresis) of the RINKO for both profile data.

RINKOCORROS (original module, version 1.0) corrected the time-dependent, pressure-induced effect (hysteresis) of the RINKO for bottle information data by using the hysteresis-corrected profile data.

BOTTLESUM created a summary of the bottle data. The data were averaged over 4.4 seconds.

ALIGNCTD converted the time-sequence of sensor outputs into the pressure sequence to ensure that all calculations were made using measurements from the same parcel of water. For a SBE 9plus CTD with the ducted temperature and conductivity sensors and a 3000-rpm pump, the typical net advance of the conductivity relative to the temperature is 0.073 seconds. So, the SBE 11plus deck unit was set to advance the primary and the secondary conductivity for 1.73 scans (1.75/24 = 0.073 seconds). Oxygen data are also systematically delayed with respect to depth mainly because of the long time constant of the oxygen sensor and of an additional delay from the transit time of water in the pumped plumbing line. This delay was compensated by 5 seconds advancing the SBE 43 oxygen sensor output (voltage) relative to the temperature data. Delay of the RINKO data was also compensated by 1 second advancing sensor output (voltage) relative to the temperature data. Delay of the transmissometer data was also compensated by 2 seconds advancing sensor output (voltage) relative to the temperature data.

WILDEDIT marked extreme outliers in the data files. The first pass of WILDEDIT obtained an accurate estimate of the true standard deviation of the data. The data were read in blocks of 1000 scans. Data greater than 10 standard deviations were flagged. The second pass computed a standard deviation over the same 1000 scans excluding the flagged values. Values greater than 20 standard deviations were marked bad. This process was applied to pressure, temperature, conductivity, and SBE 43 output.

CELLTM used a recursive filter to remove conductivity cell thermal mass effects from the measured conductivity. Typical values used were thermal anomaly amplitude alpha = 0.03 and the time constant 1/beta = 7.0.

FILTER performed a low pass filter on pressure with a time constant of 0.15 seconds. In order to produce zero phase lag (no time shift) the filter runs forward first then backwards.

WFILTER performed as a median filter to remove spikes in fluorometer, turbidity meter, transmissometer, and CDOM data. A median value was determined by 49 scans of the window. For CDOM data, an additional box-car filter with a window of 361 scans was applied to remove noise.

SECTIONU (original module, version 1.1) selected a time span of data based on scan number in order to reduce a file size. The minimum number was set to be the start time when the CTD package was beneath the sea-surface after activation of the pump. The maximum number was set to be the end time when the

depth of the package was 1 dbar below the surface. The minimum and maximum numbers were automatically calculated in the module.

LOOPEDIT marked scans where the CTD was moving less than the minimum velocity of 0.0 m/s (traveling backwards due to ship roll).

DESPIKE (original module, version 1.0) removed spikes of the data. A median and mean absolute deviation was calculated in 1-dbar pressure bins for both down- and up-cast, excluding the flagged values. Values greater than 4 mean absolute deviations from the median were marked bad for each bin. This process was performed 2 times for temperature, conductivity, SBE 43, and RINKO output.

DERIVE was used to compute oxygen (SBE 43).

BINAVG averaged the data into 1-dbar pressure bins. The center value of the first bin was set equal to the bin size. The bin minimum and maximum values are the center value plus and minus half the bin size. Scans with pressures greater than the minimum and less than or equal to the maximum were averaged. Scans were interpolated so that a data record exist every dbar.

BOTTOMCUT (original module, version 0.1) deleted the deepest pressure bin when the averaged scan number of the deepest bin was smaller than the average scan number of the bin just above.

DERIVE was re-used to compute salinity, potential temperature, and density (σ_θ).

SPLIT was used to split data into the down cast and the up cast.

Remaining spikes in the CTD data were manually eliminated from the 1-dbar-averaged data. The data gaps resulting from the elimination were linearly interpolated with a quality flag of 6.

(6) Post-cruise calibration

i. Pressure

The CTD pressure sensor offset in the period of the cruise was estimated from the pressure readings on the ship deck. For best results the Paroscientific sensor was powered on for at least 20 minutes before the operation. In order to get the calibration data for the pre- and post-cast pressure sensor drift, the CTD deck pressure was averaged over first and last one minute, respectively. Then the atmospheric pressure deviation from a standard atmospheric pressure (14.7 psi) was subtracted from the CTD deck pressure to check the pressure sensor time drift. The atmospheric pressure was measured at the captain deck (20 m high from the base line) and sub-sampled one-minute interval as a meteorological data.

Time series of the CTD deck pressure is shown in Figs. 3.1.2 and 3.1.3. The CTD pressure sensor offset was estimated from the deck pressure. Mean of the pre- and the post-casts data over the whole period gave an estimation of the pressure sensor offset (0.66 dbar) from the pre-cruise calibration. The post-cruise correction of the pressure data was carried out by subtracting 0.66 dbar from the pressure data. Figs. 3.1.2 and 3.1.3 show the pressure data after the post-cruise correction.

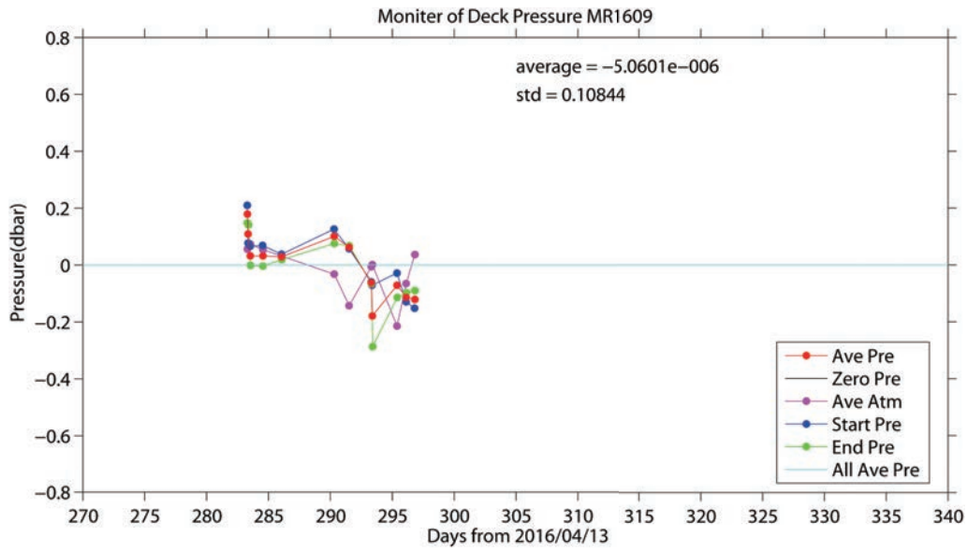

Fig. 3.1.2 Time series of the CTD deck pressure for leg 2. Atmospheric pressure deviation (magenta dots) from a standard atmospheric pressure was subtracted from the CTD deck pressure. Blue and green dots indicate pre- and post-cast deck pressures, respectively. Red dots indicate averages of the pre- and the post-cast deck pressures.

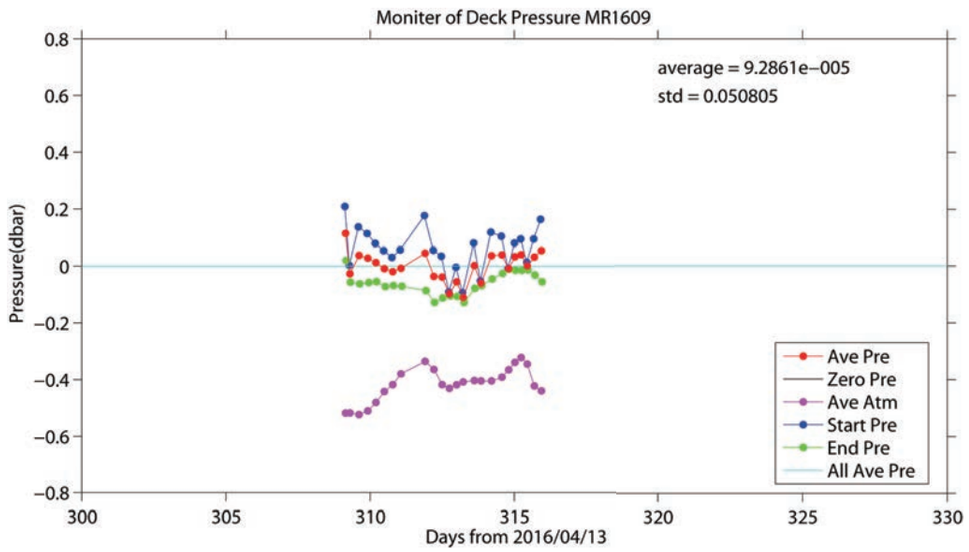

Fig. 3.1.3 Same as Fig. 3.1.2, but for leg 3.

ii. Temperature

The CTD temperature sensors (SBE 3) were calibrated with the SBE 35 under the assumption that discrepancies between SBE 3 and SBE 35 data were due to pressure sensitivity, the viscous heating effect, and time drift of the SBE 3, according to a method by Uchida et al. (2007).

Post-cruise sensor calibration for the SBE 35 will be performed at JAMSTEC in 2017

The CTD temperature was preliminary calibrated as

$$\text{Calibrated temperature} = T - (c_0 \times P + c_1 \times t + c_2)$$

where T is CTD temperature in °C, P is pressure in dbar, t is time in days from pre-cruise calibration date of the CTD temperature and c_0, c_1, and c_2 are calibration coefficients. The coefficients were determined using the data for the depths deeper than 1950 dbar. The coefficient c_1 was set to zero for this cruise.

The primary temperature data were basically used for the post-cruise calibration. The secondary temperature sensor was also calibrated and used instead of the primary temperature data when the data quality of the primary temperature data was bad. The calibration coefficients are listed in Table 3.1.1. The results of the post-cruise calibration for the CTD temperature are summarized in Table 3.1.2 and shown in Figs. 3.1.4 and 3.1.5.

Table 3.1.1 Calibration coefficients for the CTD temperature sensors.

Serial number	c_0 (°C/dbar)	c_1 (°C/day)	c_2 (°C)
031525	−1.713992e−8	0.0	0.00029

Table 3.1.2 Difference between the CTD temperature and the SBE 35 after the post-cruise calibration. Mean and standard deviation (Sdev) are calculated for the data below and above 1950 dbar. Number of data used is also shown.

Serial number	Pressure ≥ 1950 dbar			Pressure < 1950 dbar		
	Number	Mean (mK)	Sdev (mK)	Number	Mean (mK)	Sdev (mK)
031525	326	0.0	0.2	616	−0.3	2.7

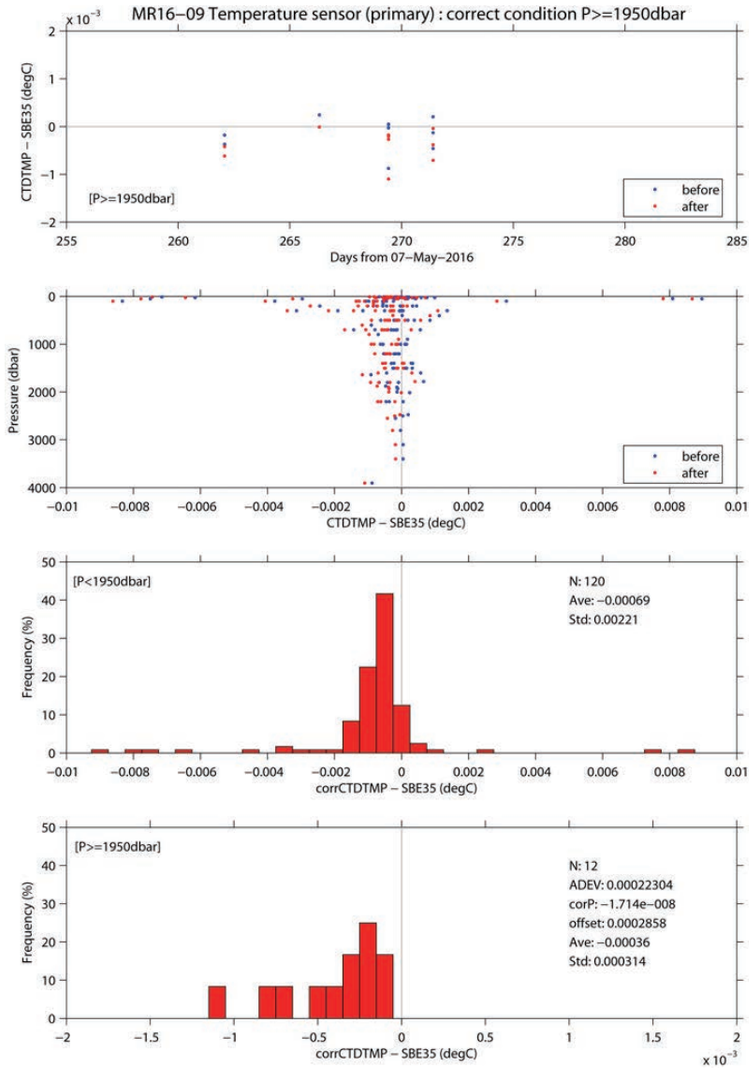

Fig. 3.1.4 Difference between the CTD temperature (primary) and the SBE 35 for leg 2. Blue and red dots indicate before and after the post-cruise calibration using the SBE 35 data, respectively. Lower two panels show histogram of the difference after the calibration.

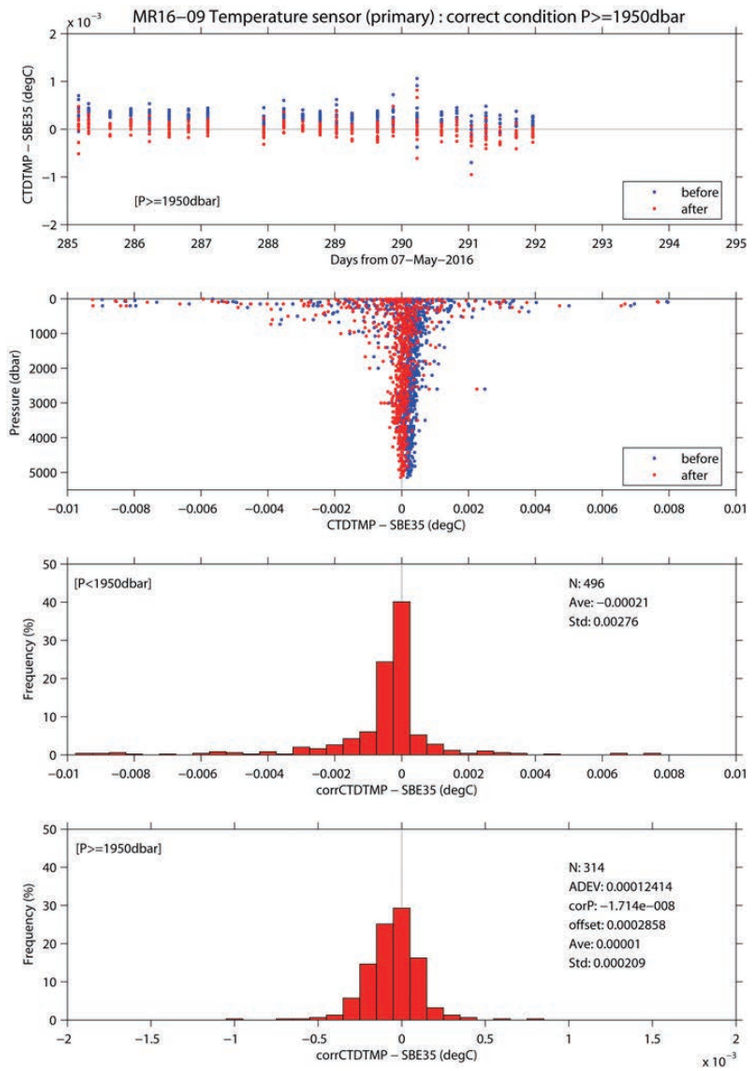

Fig. 3.1.5 Same as Fig. 3.1.4, but for leg 3.

iii. Salinity

The discrepancy between the CTD conductivity and the conductivity calculated from the bottle salinity data with the CTD temperature and pressure data is considered to be a function of conductivity, pressure and time. The CTD conductivity was calibrated as

Calibrated conductivity =

$$C - (c_0 \times C + c_1 \times P + c_2 \times C \times P + c_3 \times P^2 + c_4 \times P^2 \times C + c_5 \times P^2 \times C^2 + c_6)$$

where C is CTD conductivity in S/m, P is pressure in dbar, and c_0, c_1, c_2, c_3, c_4, c_5 and c_6 are calibration coefficients. The best fit sets of coefficients were determined by a least square technique to minimize the deviation from the conductivity calculated from the bottle salinity data.

The primary conductivity data created by the software module ROSSUM were used after the post-cruise calibration for the temperature data. The calibration coefficients are listed in Table 3.1.3. The results of the post-cruise calibration for the CTD salinity are summarized in Table 3.1.4 and shown in Figs 3.1.6 and 3.1.7.

Table 3.1.3 Calibration coefficients for the CTD conductivity sensors.

Coefficient	S/N 042435
c_0	7.2645896049e–6
c_1	2.9691992467e–7
c_2	–7.2958281688e–8
c_3	1.9466613572e–10
c_4	–1.6842918454e–10
c_5	3.3411307753e–11
c_6	–9.7770147557e–5

Table 3.1.4 Difference between the CTD salinity and the bottle salinity after the post-cruise calibration. Mean and standard deviation (Sdev) (in 10^{-3}) are calculated for the data below and above 950 dbar. Number of data used is also shown.

Serial number	Pressure ≥ 950 dbar			Pressure < 950 dbar		
	Number	Mean	Sdev	Number	Mean	Sdev
042435	465	–0.1	0.6	390	0.1	3.1

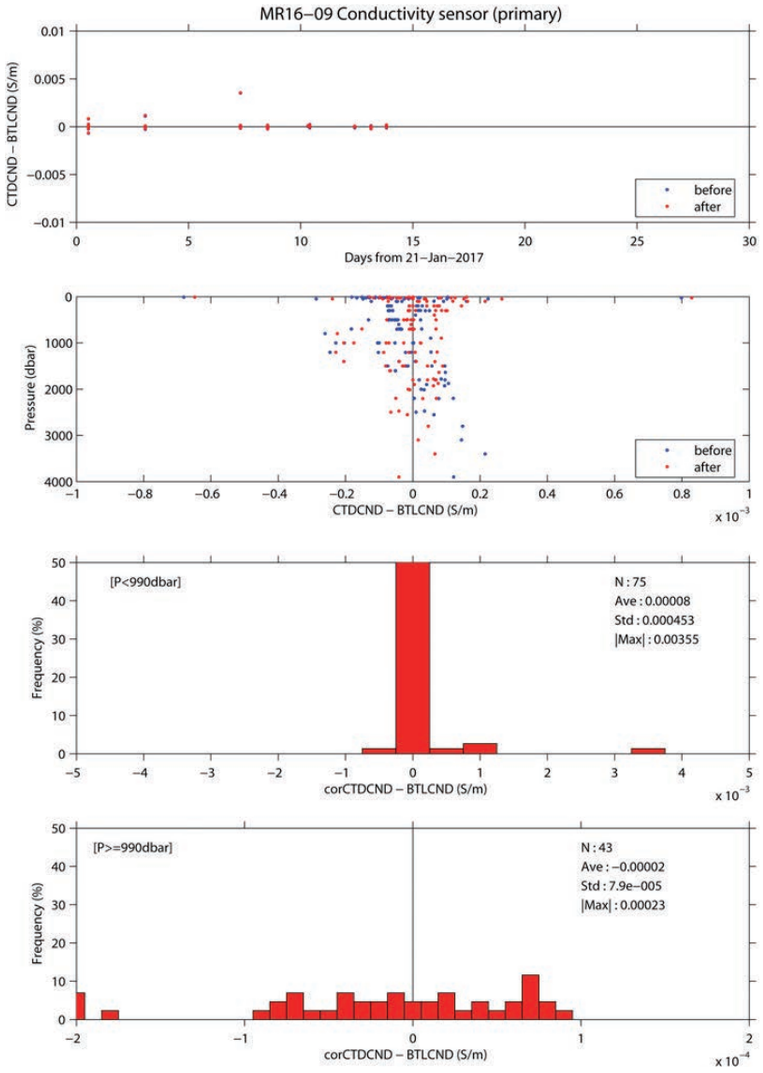

Fig. 3.1.6 Difference between the CTD salinity (primary) and the bottle salinity for leg 2. Blue and red dots indicate before and after the post-cruise calibration, respectively. Lower two panels show histogram of the difference after the calibration.

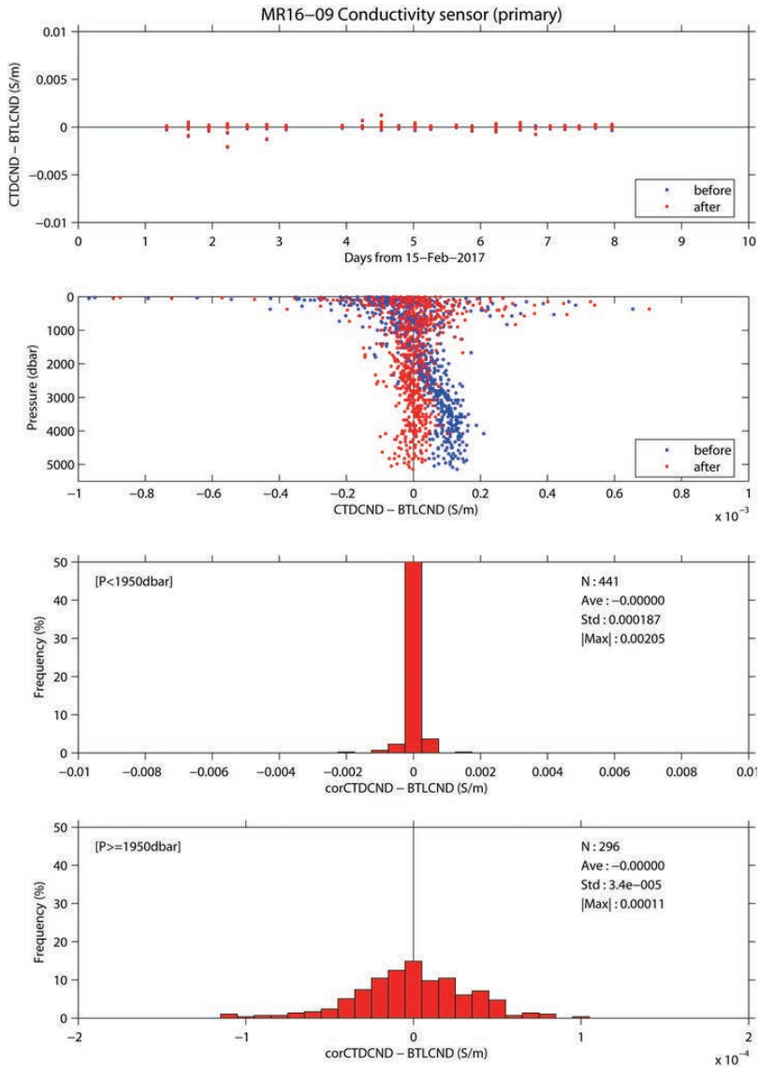

Fig. 3.1.7 Same as Fig. 3.1.6, but for leg 3.

iv. Oxygen

The RINKO oxygen optode (S/N 0024) was calibrated and used as the CTD oxygen data, since the RINKO has a fast time response. The pressure-hysteresis corrected RINKO data was calibrated by the modified Stern-Volmer equation, basically according to a method by Uchida et al. (2010) with slight modification:

$$[O_2]\ (\mu mol/l) = [(V_0 / V)^{1.5} - 1] / K_{sv}$$

and

$$K_{sv} = C_0 + C_1 \times T + C_2 \times T^2$$

$$V_0 = 1 + C_3 \times T$$

$$V = C_4 + C_5 \times V_b + C_6 \times t + C_7 \times t \times V_b$$

where V_b is the RINKO output (voltage), V_0 is voltage in the absence of oxygen, T is temperature in °C, and t is working time (days) integrated from the first CTD cast. Time drift of the RINKO output was corrected. The calibration coefficients were determined by minimizing the sum of absolute deviation with a weight from the bottle oxygen data. The revised quasi-Newton method (DMINF1) was used to determine the sets.

The post-cruise calibrated temperature and salinity data were used for the calibration. The calibration coefficients are listed in Table 3.1.5. The results of the post-cruise calibration for the RINKO oxygen are summarized in Table 3.1.6 and shown in Figs. 3.1.8 and 3.1.9.

Table 3.1.5 Calibration coefficients for the RINKO oxygen sensors.

Coefficient	S/N 0024
c_0	5.942125838095365e–3
c_1	2.112922682529651e–4
c_2	2.453149432631086e–6
c_3	–2.858906729587995e–3
c_4	–3.724762205027561e–2
c_5	0.3277293704143511
c_6	6.221125143791855e–4
c_7	–5.158472610105331e–4
C_p	0.014

Table 3.1.6 Difference between the RINKO oxygen and the bottle ooxygen after the post-cruise calibration. Mean and standard deviation (Sdev) are calculated for the data below and above 950 dbar. Number of data used is also shown.

Serial number	Pressure ≥ 950 dbar			Pressure < 950 dbar		
	Number	Mean [µmol/kg]	Sdev	Number	Mean [µmol/kg]	Sdev
0024	465	0.00	0.27	391	–0.10	0.88

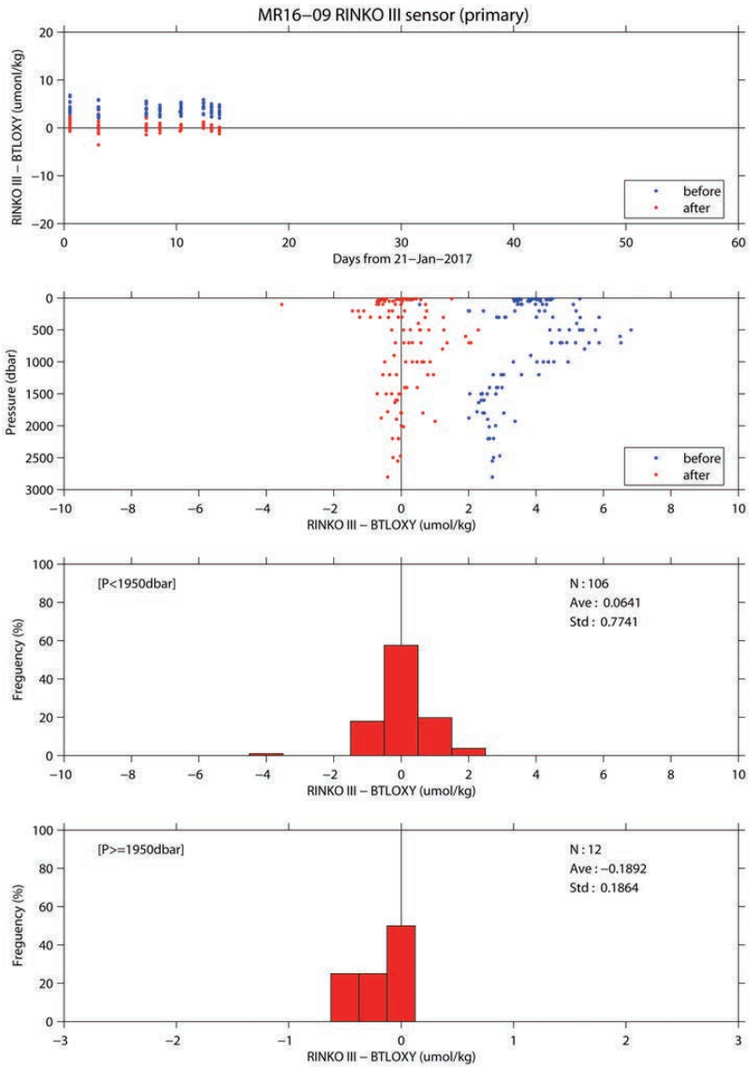

Fig. 3.1.8 Difference between the CTD oxygen and the bottle oxygen for leg 2. Blue and red dots indicate before and after the post-cruise calibration, respectively. Lower two panels show histogram of the difference after the calibration.

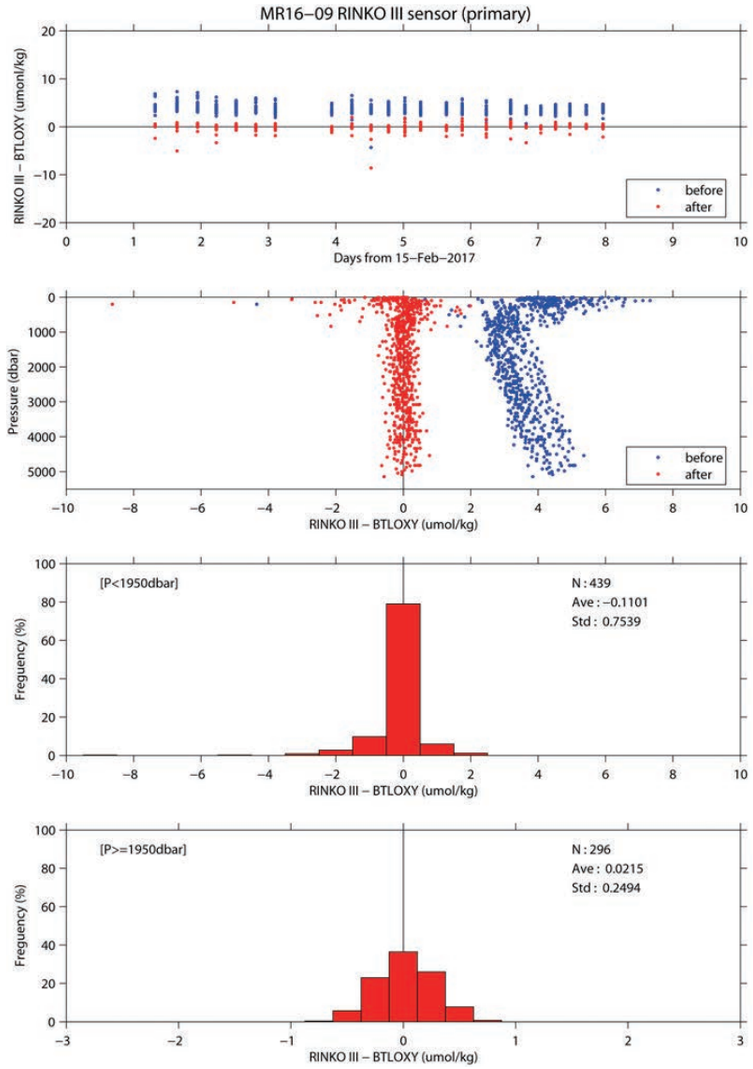

Fig. 3.1.9 Same as Fig. 3.1.8, but for leg 3.

v. Fluorometer

The CTD fluorometer (FLUOR in µg/L) was calibrated by comparing with the bottle sampled chlorophyll-a as

$$FLUORc = c_0 + c_1 \times FLUOR$$

where c_0 and c_1 are calibration coefficients. The CTD fluorometer data is slightly noisy so that the up cast profile data which was averaged over one decibar agree with the bottle sampled data better than the discrete CTD fluorometer data obtained at bottle-firing stop. Therefore, the CTD fluorometer data at water sampling depths extracted from the up cast profile data were compared with the bottle sampled chlorophyll-*a* data. The bottle sampled data obtained at dark condition [PAR (Photosynthetically Available Radiation) < 50 µE/(m^2 sec)] were used for the calibration, since sensitivity of the fluorometer to chlorophyll *a* is different at nighttime and daytime (Section 2.4 in Uchida et al., 2015).

Firstly, bias of sensor output ($-c_0/c_1$) was determined from the minimum of the sensor output as 0.022. Then the calibration coefficients were determined under this condition ($-c_0/c_1 = 0.022$) for three groups: station 007 of leg 2, stations of leg 2 except for 007, and stations of leg 3. The calibration coefficients are listed in Table 3.1.7. The results of the post-cruise calibration for the fluorometer are summarized in Table 3.1.8 and shown in Fig. 3.1.10.

Table 3.1.7. Calibration coefficients for the CTD fluorometer.

c_0	c_1	Note
–3.415403161178421e-02	1.552455920202864	for stn. 007 of leg 2
–1.070073772820049e-02	0.4863967142398999	for leg 2 except for stn. 007
–6.244323339035114e-03	0.2839634259958261	for leg 3

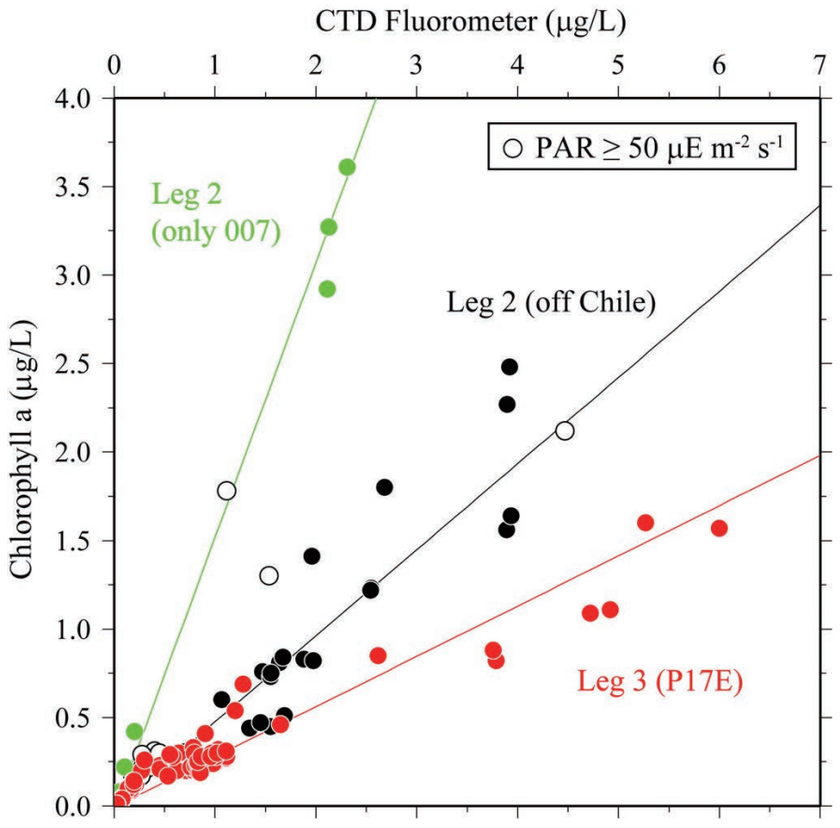

Fig. 3.1.10. Comparison of the CTD fluorometer and the bottle sampled chlorophyll-*a*. The regression lines are also shown.

Table 3.1.8. Difference between the CTD fluorometer and the bottle chlorophyll-*a* after the post-cruise calibration. Mean, standard deviation (Sdev), and number of data used are shown. Data obtained at daytime are also used in this calculation.

Number	Mean	Sdev
306	0.00 µg/L	0.12 µg/L

vi. Transmissometer

The transmissometer (T_r in %) is calibrated as

$$T_r = (V - V_d) / (V_r - V_d) \times 100$$

wehre V is the measured signal (voltage), V_d is the dark offset for the instrument, and V_r is the signal for clear water. V_d can be obtained by blocking the light path. V_d and V_{air}, which is the signal for air, were measured on deck before each cast after wiping the optical windows with ethanol. V_d was constant (0.0024) during the cruise. V_r is estimated from the measured maximum signal in the deep ocean at each cast. Since the transmissometer drifted in time (Fig. 3.1.11), V_r is expressed as

$$V_r = c_0 + c_1 \times t + c_2 \times t^2$$

where t is working time (in days) of the transmissometer integrated from the first CTD cast., and c_0, c_1, and c_2 are calibration coefficients.

Maximum signal was extracted for each cast. Data for leg 2 were not used to estimate V_r (open dots in Fig. 3.1.11). The calibration coefficients are listed in Table 3.1.9.

Table 3.1.9. Calibration coefficients for the CTD transmissometer.

Coefficient	
c_0	4.749551191426855
c_1	–7.943810401172799e–3
c_2	9.065035348634040e–4
V_d	0.0024

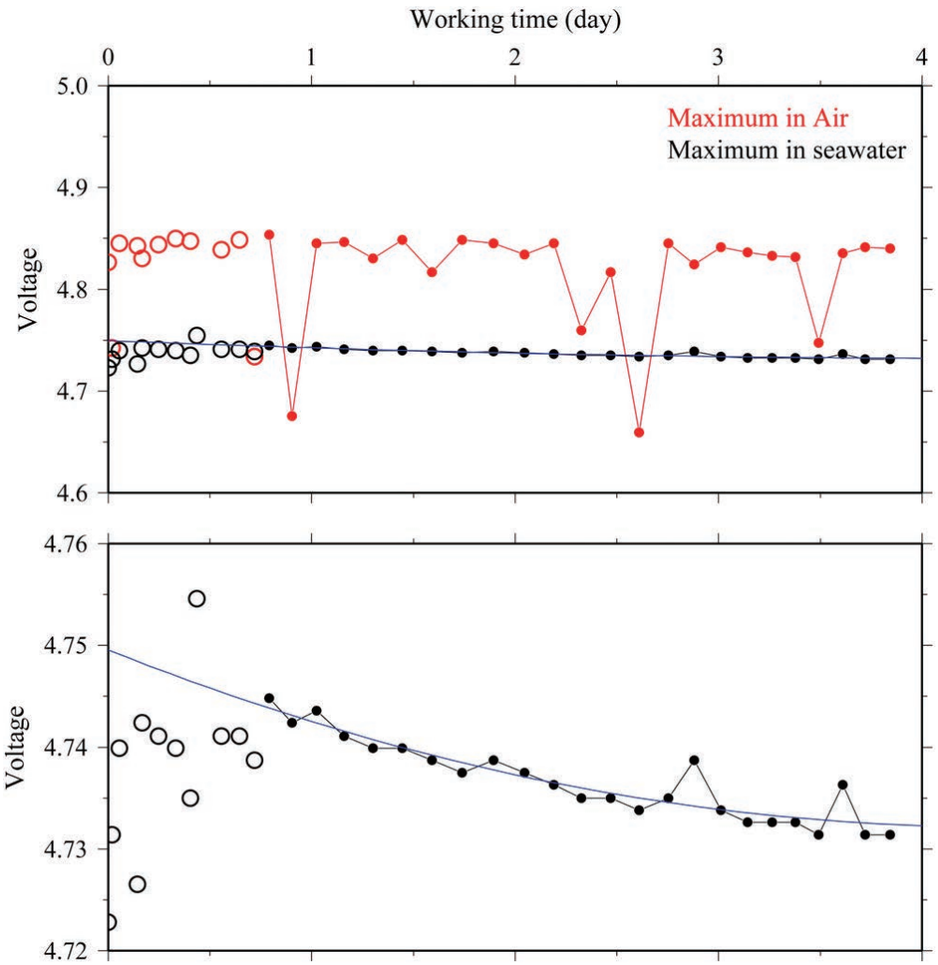

Fig. 3.1.11. Time series of an output signal (voltage) from transmissometer at deep ocean (Vdeep). Data in air are also shown in red dots. The black solid line indicates the modeled signal in the deep clear ocean. Open dots were not used to estimate the final calibration coefficients.

vii. Turbidity meter

Turbidity data obtained in leg 2 were not available, because measurement range of the sensor was inadequate (0-500 FTU) to resolve actual turbidity signal. Post-cruise correction for the turbidity meter data wasn't carried out. The turbidity data are well correlated with beam attenuation coefficient data obtained from transmissometer (Fig. 3.1.12).

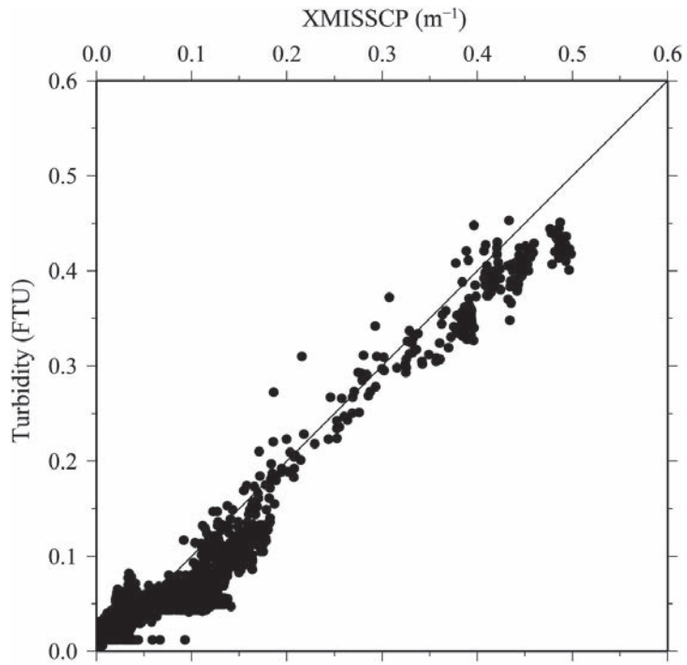

Fig. 3.1.12. Comparison between turbidity data and beam attenuation coefficient data (XMISSCP) from transmissometer.

viii. PAR

The PAR sensor was calibrated with an offset correction. The offset was estimated from the data measured in the deep ocean during the cruise. The corrected data (PARc) is calculated from the raw data (PAR) as follows:

$$PARc\ [\mu E\ m^{-2}\ s^{-1}] = PAR - 0.104.$$

ix. CDOM

Post-cruise correction for the CDOM sensor wasn't carried out. The data were low-pass filtered by a running mean with a window of 15 seconds (about 13 m) in the data processing mentioned above, since the data was noisy. Moreover, CDOM data were flagged as 4 (bad measurement) for depths deeper than about 4000 m due to large shift of the data caused by unknown reason.

(7) References

Edwards, B., D. Murphy, C. Janzen and N. Larson (2010): Calibration, response, and hysteresis in deep-sea dissolved oxygen measurements, *J. Atmos. Oceanic Technol.*, 27, 920–931.

Fukasawa, M., T. Kawano and H. Uchida (2004): Blue Earth Global Expedition collects CTD data aboard Mirai, BEAGLE 2003 conducted using a Dynacon CTD traction winch and motion-compensated crane, *Sea Technology*, 45, 14–18.

García, H. E. and L. I. Gordon (1992): Oxygen solubility in seawater: Better fitting equations. *Limnol. Oceanogr.*, 37 (6), 1307–1312.

Uchida, H., G. C. Johnson, and K. E. McTaggart (2010): CTD oxygen sensor calibration procedures, The GO-SHIP Repeat Hydrography Manual: A collection of expert reports and guidelines, IOCCP Rep., No. 14, ICPO Pub. Ser. No. 134.

Uchida, H., K. Katsumata, and T. Doi (2015): WHP P14S, S04I Revisit Data Book, JASTEC, Yokosuka, 187 pp.

Uchida, H., T. Nakano, J. Tamba, J. V. Widiatmo, K. Yamazawa, S. Ozawa and T. Kawano (2015): Deep ocean temperature measurement with an uncertainty of 0.7 mK, J. Atmos. Oceanic Technol., 32, 2199–2210.

Uchida, H., K. Ohyama, S. Ozawa, and M. Fukasawa (2007): In situ calibration of the Sea-Bird 9plus CTD thermometer, *J. Atmos. Oceanic Technol.*, 24, 1961–1967.

3.2 Bottle Salinity

May 14, 2017

(1) Personnel

Hiroshi Uchida (JAMSTEC)

Sonoka Tanihara (MWJ)

Akira Watanabe (MWJ)

(2) Objectives

Bottle salinities were measured to calibrate CTD salinity data.

(3) Instrument and Method

Salinity measurement was conducted basically based on a method by Kawano (2010).

i. Salinity Sample Collection

The bottles in which the salinity samples were collected and stored were 250 ml brown borosilicate glass bottles with screw caps (PTFE packing). Each bottle was rinsed three times with sample water and was filled to the shoulder of the bottle. The caps were also thoroughly rinsed. Salinity samples were stored more than 24 hours in the same laboratory as the salinity measurement was made.

For the salinity samples for correction of the thermo-salinograph, a polyethylene inner plug was used for the sample bottle to store a few weeks.

ii. Instruments and Methods

Salinity of water samples was measured with a salinometer (Autosal model 8400B; Guildline Instruments Ltd., Ontario, Canada; S/N 62556 for legs 1~3 and S/N 71758 for leg 4), which was modified by adding a peristaltic-type intake pump (Ocean Scientific International Ltd., Hampshire, UK) and two platinum resistance thermometers (Guildline Instruments Ltd., model 9450). One thermometer monitored an ambient temperature and the other monitored a salinometer's bath temperature. The resolution of the thermometers was 0.001 °C. The measurement system was almost same as Aoyama et al. (2002). The salinometer was operated in the air-conditioned laboratory of the ship at a bath temperature of 24 °C.

The ambient temperature varied from approximately 22.3 to 24.3 °C, while the bath temperature was stable and varied within ±0.006 °C. A measure of a double conductivity ratio of a sample was taken as a median of 31 readings. Data collection was started after 10 seconds and it took about 10 seconds to collect 31 readings by a personal computer. Data were sampled for the sixth and seventh filling of the cell. In case where the difference between the double conductivity ratio of these two fillings was smaller than 0.00002, the average value of the two double conductivity ratios was used to calculate the bottle salinity with the algorithm for practical salinity scale, 1978 (UNESCO, 1981). When the difference was greater than or equal to the 0.00003, we measured another additional filling of the cell. In case where the double conductivity ratio of the additional filling did not satisfy the criteria above, we measured other additional fillings of the cell within 10 fillings in total. In case where the number of fillings was 10 and those fillings did not satisfy the criteria above, the median of the double conductivity ratios of five fillings were used to calculate the bottle salinity.

The measurement was conducted about from 2 to 19 hours per day and the cell was cleaned with soap (50 times diluted solution of S-CLEAN WO-23 [Neutral], Sasaki Chemical Co. Ltd., Kyoto, Japan) after the measurement for each day. A total of 1672 water samples for legs 1~3 were measured during the cruise, and a total of 12 water samples for leg 4 were measured after the cruise (5 April 2017) in a laboratory at JAMSTEC, Yokosuka.

(4) Results

i. Standard Seawater

Standardization control was set to 702. The value of STANDBY was 5206±0001 and that of ZERO was 0.00000 or ±0.00001. We used IAPSO Standard Seawater batch P159 whose conductivity ratio is 0.99988 (double conductivity ratio is 1.99976) as the standard for salinity measurement. We measured 66 bottles of

the Standard Seawater during the cruise and measured three bottles after the cruise for the samples for leg 4. History of double conductivity ratio measurement of the Standard Seawater for legs 1~3 is shown in Fig. 3.2.1.

Time drift of the salinometer was corrected by using the Standard Seawater measurements. Linear time drift of the salinometer was estimated from the Standard Seawater measurement excluding the shifted data (–0.00006 in double conductivity ratio) in the middle of the measurements by using the least square method (thin black line in Fig. 3.2.1). Additional offset (0.00006) correction was applied to the measurement during shift. The average of double conductivity ratio after the corrections was 1.99976 and the standard deviation was 0.00001, which is equivalent to 0.0002 in salinity.

For leg 4, there was no remarkable drift for the Standard Seawater measurements and the average of double conductivity ratio was adjusted to 1.99976 and the standard deviation was 0.00002, which is equivalent to 0.0004 in salinity.

ii. Sub-Standard Seawater

We also used sub-standard seawater which was deep-sea water filtered by pore size of 0.45 μm and stored in a 20-liter cubitainer made of polyethylene and stirred for at least 24 hours before measuring. It was measured every 6-8 samples to check the possible sudden drift of the salinometer. During the whole measurements, there was no detectable sudden drift of the salinometer.

iii. Replicate Samples

We took 149 pairs of replicate samples collected from the same Niskin bottle in leg 2 and 3. Histogram of the absolute difference between replicate samples is shown in Fig. 3.2.2. The root-mean-square for 148 pairs of replicate samples which are acceptable-quality data was 0.0003.

iv. Duplicate Samples

In this cruise, four to six Niskin bottles were closed at same depth (deeper than 1700 dbar) of station leg3_003_1 (#1, #2, #3, #4, #5), leg3_005_1 (#6, #7, #8, #9, #10), leg3_007_1 (#11, #12, #13, #14), leg3_009_1 (#15, #16, #17, #18, #19), leg3_011_1 (#20, #21, #22, #23, #24), leg3_015_1 (#3, #4, #5, #6, #7, #8 [originally #25, #26, #27, #28, #29, #30]), and leg3_018_1 (#4, #5, #6, #7, #8, #9 [originally #31, #32, #33, #34, #35, #36]) for duplicate samples. The standard deviation for each group was 0.0002 in salinity on average (from 0.0000 to 0.0004) when excluding the result for Niskin bottle #16. For the Niskin bottle #16, salinity measurement was largely deviated (0.0015) from the mean, though oxygen measurement was not deviated (0.02 μmol/kg) from the mean.

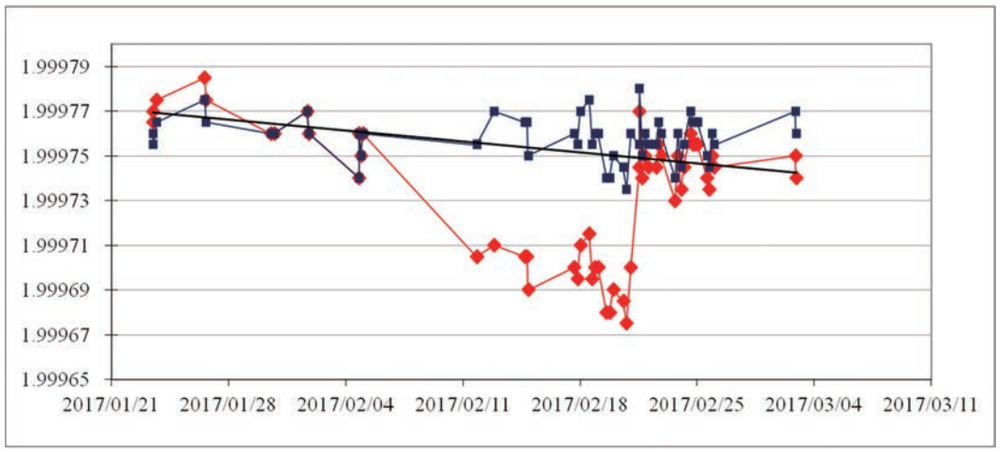

Fig. 3.2.1. History of double conductivity ratio measurement of the Standard Seawater (P159). Horizontal and vertical axes represent date and double conductivity ratio, respectively. Red dots indicate raw data and blue dots indicate corrected data.

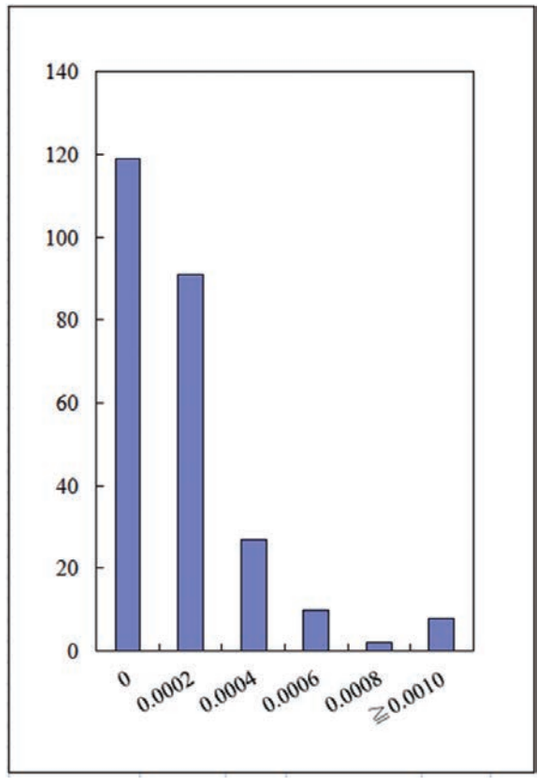

Fig. 3.2.2. Histogram of the absolute difference between replicate samples. Horizontal axis is absolute difference in salinity and vertical axis is frequency.

(5) References

Aoyama, M., T. Joyce, T. Kawano and Y. Takatsuki (2002): Standard seawater comparison up to P129. Deep-Sea Research, I, Vol. 49, 1103-1114.

Kawano (2010): Salinity. The GO-SHIP Repeat Hydrography Manual: A collection of Expert Reports and Guidelines, IOCCP Report No. 14, ICPO Publication Series No. 134, Version 1.

UNESCO (1981): Tenth report of the Joint Panel on Oceanographic Tables and Standards. UNESCO Tech. Papers in Mar. Sci., 36, 25 pp.

3.3 Density

January 9, 2018

(1) Personnel

Hiroshi Uchida (JAMSTEC)

Takuhei Shiozaki (JAMSTEC)

(2) Objectives

The objective of this study is to collect absolute salinity (also called "density salinity") data, and to evaluate an algorithm to estimate absolute salinity provided along with TEOS-10 (the International Thermodynamic Equation of Seawater 2010) (IOC et al., 2010).

(3) Materials and methods

Seawater densities were measured during the cruise with an oscillation-type density meter (DMA 5000M, serial no. 80570578, Anton-Paar GmbH, Graz, Austria) with a sample changer (Xsample 122, serial no. 80548492, Anton-Paar GmbH). The sample changer was used to load samples automatically from up to ninety-six 12-mL glass vials.

The water samples were collected in 100-mL aluminum bottles (Mini Bottle Can, Daiwa Can Company, Japan). The bottles were stored at room temperature (~23 °C) upside down usually for 12 to 24 hours to make the temperature of the sample equal to the room temperature. The water sample was filled in a 12-mL glass vial and the glass vial was sealed with Parafilm M (Pechiney Plastic Packaging, Inc., Menasha, Wisconsin, USA) immediately after filling. Densities of the samples were measured at 20 °C by the density meter two times for each bottle and averaged to estimate the density. When the difference between the two measurements was greater than 0.002 kg/m^3, additional measurements were conducted until two samples satisfying the above criteria were obtained.

Time drift of the density meter was monitored by periodically measuring the density of ultra-pure water (Milli-Q water, Millipore, Billerica, Massachusetts, USA) prepared from Yokosuka (Japan) tap water in October 2012. The true density at 20 °C of the Milli-Q water was estimated to be 998.2042 kg m^{-3} from the isotopic composition (δD = –8.76 ‰, $\delta^{18}O$ = –56.86 ‰) and International Association for the Properties of Water and Steam (IAPWS)-95 standard. An offset correction was applied to the measured density by using the Milli-Q water measurements ($\rho_{Milli\text{-}Q}$) with a slight modification of the density dependency (Uchida et al., 2011). The offset (ρ_{offset}) of the measured density (ρ) was reevaluated for the serial no. 80570578 in November 2014 as follows:

$$\rho_{offset} = (\rho_{Milli\text{-}Q} - 998.2042) - (\rho - 998.2042) \times 0.000411 \ [kg\ m^{-3}].$$

The offset correction was verified by measuring Reference Material for Density in Seawater (prototype Dn-RM1 and PRE18) developing with Marine Works Japan, Ltd., Kanagawa, Japan, and produced by Kanso Technos Co., Ltd., Osaka, Japan, along with the Milli-Q water.

Density salinity can be back calculated from measured density and temperature (20 °C) with TEOS-10.

(4) Results

Results of density measurements of the Reference Material for Density in Seawater (Dn-RM1 and PRE18) were shown in Table 3.3.1.

A total of 37 pairs of replicate samples were measured. The root-mean square of the absolute difference of replicate samples was 0.0015 g/kg.

The measured density salinity anomalies (δS_A) are shown in Fig. 3.3.1. The measured δS_A were slightly smaller than calculated δS_A from Pawlowicz et al. (2011) which exploits the correlation between δS_A and nutrient concentrations and carbonate system parameters based on mathematical investigation using a model relating composition, conductivity and density of arbitrary seawaters.

(5) References

IOC, SCOR and IAPSO (2010): The international thermodynamic equation of seawater – 2010: Calculation and use of thermodynamic properties. Intergovernmental Oceanographic Commission, Manuals and Guides

No. 56, United Nations Educational, Scientific and Cultural Organization (English), 196 pp.

Pawlowicz, R., D. G. Wright and F. J. Millero (2011): The effects of biogeochemical processes on ocean conductivity/salinity/density relationships and the characterization of real seawater. *Ocean Science*, 7, 363–387.

Uchida, H., T. Kawano, M. Aoyama and A. Murata (2011): Absolute salinity measurements of standard seawaters for conductivity and nutrients. *La mer*, 49, 237–244.

Table 3.3.1. Result of density measurements of the Reference Material for Density in Seawater (prototype Dn-RM1 and PRE18). Number in parentheses shows number of measurements.

Date	Stations	Mean density of Dn-RM1 (kg/m^3)	Mean density of PRE18 (kg/m^3)
2017/02/10-11	all of leg 2	1024.2627 (3)	1024.2223 (18)
2017/02/17-19	1,2,4	1024.2596 (3)	1024.2210 (12)
2017/02/20-21	6,8,12	1024.2608 (3)	1024.2206 (15)
2017/02/24-26	16,20,22,23,24,26	1024.2616 (3)	1024.2214 (13)
			1024.2209 (8)
	Average:	1024.2612 ± 0.0013	1024.2212 ± 0.0007

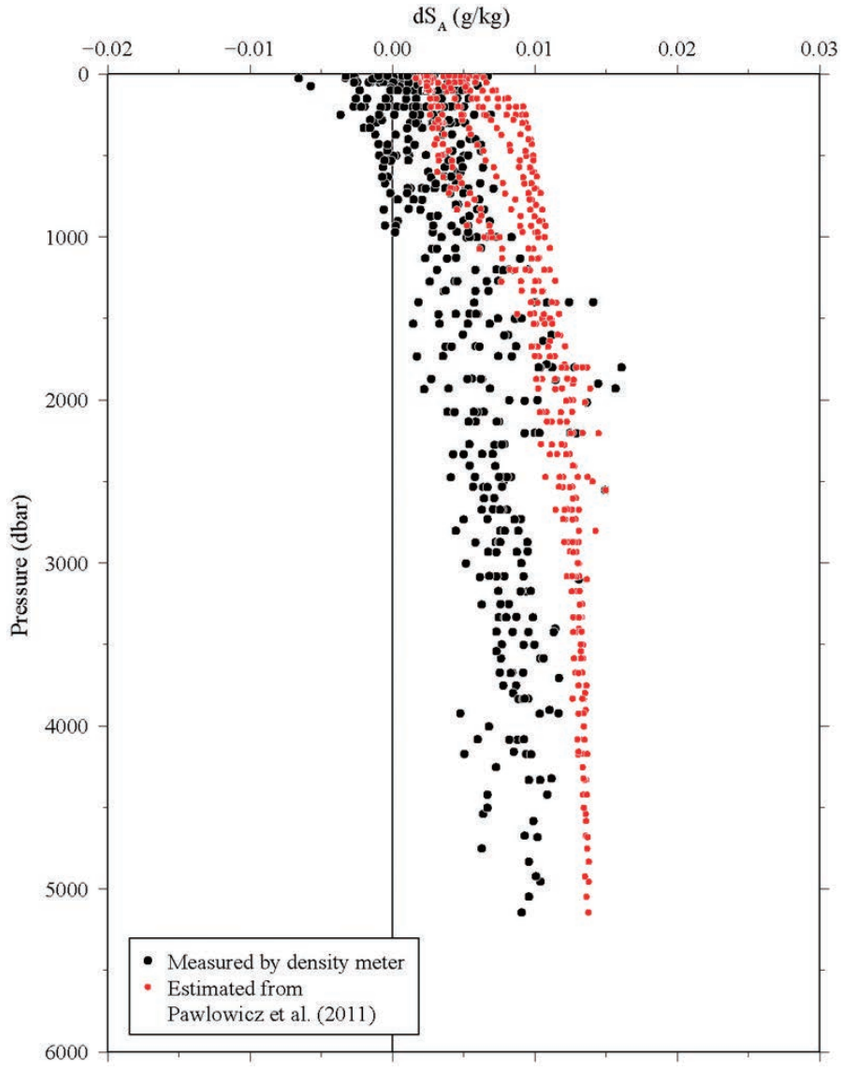

Figure 3.3.1. Vertical distribution of density salinity anomaly measured by the density meter. Absolute Salinity anomaly estimated from nutrients and carbonate parameters (Pawlowicz et al., 2011) are also shown for comparison.

3.4 Oxygen

October 30, 2018

(1) Personnel

Yuichiro Kumamoto

Japan Agency for Marine-Earth Science and Technology

(2) Objectives

Dissolved oxygen is one of good tracers for the ocean circulation. Climate models predict a decline in dissolved oxygen concentration and a consequent expansion of oxygen minimum layer under the global warming condition, which results mainly from decreased interior advection and ongoing oxygen consumption by remineralization. The mechanism of the decrease, however, is still unknown. During MR16-09 Leg-2 and Leg-3 cruise, we measured dissolved oxygen concentration from surface to bottom layer at all the hydrocast stations in the South Pacific Ocean and Southern Ocean. Our purpose is to evaluate temporal change in dissolved oxygen concentration in these oceans during the past decades. In addition, dissolved oxygen in surface seawater, which was pumped up from about 4 m depth, was measured for calibration of oxygen sensors for the surface water during all the legs (Leg-1, 2, 3, and 4).

(3) Reagents

Pickling Reagent I: Manganous chloride solution (3M)

Pickling Reagent II: Sodium hydroxide (8M) / sodium iodide solution (4M)

Sulfuric acid solution (5M)

Sodium thiosulfate (0.025M)

Potassium iodate (0.001667M): National Metrology Institute of Japan (NMIJ), Certified Reference Material (CRM), 3006-a No.045, Mass fraction: 99.973 ± 0.018 % (expanded uncertainty)

CSK standard of potassium iodate: Lot KPG6393, Wako Pure Chemical Industries Ltd., 0.0100N

(4) Instruments

Burette for sodium thiosulfate and potassium iodate;

APB-620 and APB-510 manufactured by Kyoto Electronic Co. Ltd. / 10 cm^3 of titration vessel

Detector;

Automatic photometric titrator, DOT-01X manufactured by Kimoto Electronic Co. Ltd.

(5) Seawater sampling

During the Leg-2 and 3, seawater samples were collected from 12-liter Niskin sample bottles attached to the CTD-system. During Leg-2, surface seawater was collected using a bucket. The pumped-up surface seawater was collected from a tap on conduit once a day approximately. Seawater for bottle oxygen measurement was transferred to a volume calibrated glass flask (ca. 100 cm^3) through a plastic tube. Three times volume of the flask of seawater was overflowed. Sample temperature was measured during the water sampling using a thermometer. Then two reagent solutions (Reagent I, II) of 1.0 cm^3 each were added immediately into the sample flask and the stopper was inserted carefully into the flask. The sample flask was then shaken vigorously to mix the contents and to disperse the precipitate finely throughout. After the precipitate has settled at least halfway down the flask, the flask was shaken again to disperse the precipitate. The sample flasks containing pickled samples were stored in an air-conditioned laboratory until they were titrated. These procedure is based on a determination method in the WHP Operations Manual (Dickson, 1996).

(6) Sample measurement

At least two hours after the re-shaking, the pickled samples were measured on board. A magnetic stirrer bar and 1 cm^3 sulfuric acid solution were added into the sample flask and stirring began. Samples were titrated by sodium thiosulfate solution whose molarity was determined by potassium iodate solution. Temperature of sodium thiosulfate during titration was recorded by a thermometer. We measured dissolved oxygen concentration using three sets of the titration apparatus system, named DOT-6, DOT-7, and DOT-8. Dissolved oxygen concentration (μmol kg^{-1}) was calculated by the sample temperature during the sampling,

salinity, flask volume, and titrated volume of the sodium thiosulfate solution.

(7) Standardization

Concentration of sodium thiosulfate titrant (ca. 0.025M) was determined by potassium iodate solution. The NMIJ-CRM potassium iodate was dried in an oven at 130°C. 1.7835 g potassium iodate weighed out accurately was dissolved in deionized water and diluted to final volume of 5 dm^3 in a calibrated volumetric flask (0.001667M). 10 cm^3 of the standard potassium iodate solution was added to a flask using a volume-calibrated dispenser. Then 90 cm^3 of deionized water, 1 cm^3 of sulfuric acid solution, and 1.0 cm^3 of pickling reagent solution II and I were added into the flask in order. Amount of titrated volume of sodium thiosulfate (usually 5 times measurements average) gave the molarity of the sodium thiosulfate titrant. Table 3.4.1-4 show results of the standardization during this cruise. Coefficient of variation (C.V.) for the standardizations for Leg-1, 2, 3, and 4 were 0.025 ± 0.015 % (standard deviation, n = 5), 0.016 ± 0.005 % (n = 10), 0.018 ± 0.007 % (n = 17), and 0.017 ± 0.006 % (n = 4), respectively.

(8) Determination of the blank

The oxygen in the pickling reagents I (1.0 cm^3) and II (1.0 cm^3) was assumed to be 7.6×10^{-8} mol (Murray *et al.*, 1968). The blank from the presence of redox species apart from oxygen in the reagents (the pickling reagents I, II, and the sulfuric acid solution) was determined as follows. 1 and 2 cm^3 of the standard potassium iodate solution were added to two flasks respectively. Then 100 cm^3 of deionized water, 1 cm^3 of sulfuric acid solution, and 1.0 cm^3 of pickling reagent solution II and I each were added into the two flasks in order. The blank was determined by difference between the two times of the first (1 cm^3 of KIO_3) titrated volume of the sodium thiosulfate and the second (2 cm^3 of KIO_3) one. The results of 3 times blank determinations were averaged (Table 3.4.1-4).

Table 3.4.1 Standardization (End point, E.P.) and blank determinations (cm^3) during Leg-1.

Date (UTC)	KIO_3 No.	$Na_2S_2O_3$ No.	DOT-8		Samples
			E.P.	blank	
2016/12/28	K1605C01	T1606E	3.966	0.004	TSG01-03
2017/01/01	K1605C02	T1606E	3.964	0.005	TSG04-07
2017/01/05	K1605C03	T1606E	3.964	0.006	TSG08-12
2017/01/09	K1605C04	T1606E	3.963	0.004	TSG13-18

Table 3.4.2 Same as Table 3.4.1 but for Leg-2.

Date (UTC)	KIO_3 No.	$Na_2S_2O_3$ No.	DOT-7		DOT-8		Samples
			E.P.	blank	E.P.	blank	
2017/01/22	K1605D01	T1606F	3.959	0.002	3.965	0.004	Stn.01,06,TSG01-05
2017/01/27	K1605D02	T1606F	3.958	0.003	3.962	0.005	Stn.07,09,10,TSG06-12
2017/02/01	K1605D03	T1606F	3.963	0.007	3.963	0.005	Stn.12B,11A,11B,TSG13-15

Table 3.4.3 Same as Table 3.4.1 but for Leg-3.

Date (UTC)	KIO_3 No.	$Na_2S_2O_3$ No.	DOT-6		DOT-8		Stations
			E.P.	blank	E.P.	blank	
2017/02/11	K1606E01	T1606F	3.966	0.006	3.963	0.003	TSG01-05
2017/02/18	K1606E03	T1606G	3.965	0.007	3.963	0.003	Stn.01-13,15,16,18,TSG06-11
2017/02/21	K1606E05	T1606H	3.965	0.005	3.965	0.004	Stn.20-26,TSG12-13
2017/02/24	K1606E06	T1606H	3.964	0.007	3.965	0.006	TSG14-21

Table 3.4.4 Same as Table 3.4.1 but for Leg-4.

Date (UTC)	KIO_3 No.	$Na_2S_2O_3$ No.	DOT-6		Samples
			E.P.	blank	
2017/03/10	K1606F01	T1606H	3.966	0.005	TSG01-02
2017/03/16	K1606F02	T1606H	3.968	0.007	TSG03-08
2017/03/22	K1606F03	T1606H	3.966	0.004	TSG09-12

(9) Replicate sample measurement

At all the hydrocast stations during Leg-2 and 3, a pair of replicate samples was collected at a few depths. The standard deviations of the replicate measurement during Leg-2 and 3 were 0.09 (n = 16) and 0.08 μmol kg^{-1} (n = 92), respectively. The difference between the pair of replicate measurement did not depend on the concentration (Fig. 3.4.1).

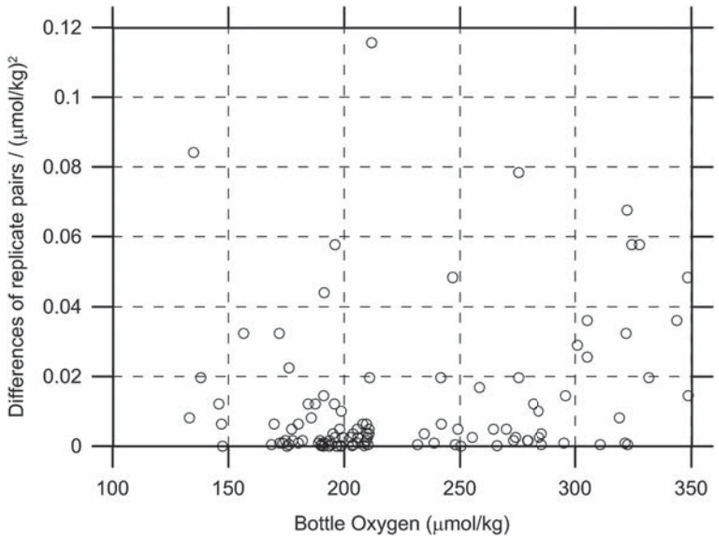

Figure 3.4.1 Oxygen difference between measurements of a replicate pair against oxygen concentration.

(10) Duplicate sample measurement

During Leg-3 duplicate sampling was taken for all the Niskin bottles (36 bottles, Table 3.4.5). The standard deviation of the duplicate measurements were calculated to be 0.09 μmol kg^{-1}, which were equivalent with that of the replicate measurements (0.08 μmol kg^{-1}, see section 9).

(11) CSK standard measurements

The CSK standard is a commercial potassium iodate solution (0.0100 N) for analysis of dissolved oxygen. We titrated the CSK standard solution (Lot KPG6393) against our KIO_3 standards as samples during this cruise (Table 3.4.6). A good agreement among them confirms that there was no systematic shift in our oxygen analyses on board.

Table 3.4.5 Results of duplicate sample measurements.

No.	Leg	Station	Sampling Pres. (db)	Niskin position #	Niskin bottle #	Dissolved oxygen (μmol/kg)
1	3	3	4849	1	X12J01	215.09
				2	X12J02	215.27
				3	X12J03	215.25
				4	X12J04	215.11
				5	X12J05	215.11
2	3	5	4985	6	X12J06	211.20
				7	X12J07	211.16
				8	X12J08	211.10
				9	X12J09	210.85
				10	X12J10	211.16
3	3	7	5099	11	X12J11	203.95
				12	X12J12	203.91
				13	X12J13	203.83
				14	X12J14	203.84

No.	Leg	Station	Sampling Pres. (db)	Niskin position #	Niskin bottle #	Dissolved oxygen (μmol/kg)
4	3	9	4880	15	X12J15	193.33
				16	X12J16	193.46
				17	X12J17	193.42
				18	X12J18	193.50
				19	X12J19	193.49
5	3	11	4718	20	X12J20	212.81
				21	X12J21	212.66
				22	X12J22	212.69
				23	X12J23	212.66
				24	X12J24	212.63
6	3	15*	4260	3	X12J25	202.81
				4	X12J26	202.96
				5	X12J27	203.01
				6	X12J28	202.96
				7	X12J29	202.96
				8	X12J30	202.92
7	3	18*	4190	4	X12J31	204.90
				5	X12J32	204.91
				6	X12J33	205.11
				7	X12J34	204.83
				8	X12J35	204.92
				9	X12J36	204.83

*At stations 15 and 18 position of Niskin bottle was changed for the duplicate sampling.

Table 3.4.6 Results of the CSK standard (Lot KPG6393) measurements.

Date (UTC)	KIO_3 ID No.	Conc. (N)	error (N)	Conc. (N)	error (N)	Remarks
		DOT-7		DOT-8		
2016/12/28	K1605C01			0.010004	0.000003	Leg-1
2017/01/15	K1605C05			0.010016	0.000005	Leg-1
		DOT-7		DOT-8		
2017/01/22	K1605D01	0.010003	0.000002	0.010001	0.000002	Leg-2
		DOT-6		DOT-8		
2017/02/11	K1606E01	0.010003	0.000004	0.010006	0.000004	Leg-3
		DOT-6				
2017/03/10	K1606F01	0.010009	0.000003			Leg-4

(12) Quality control flag assignment

Quality flag values for oxygen data from Niskin bottles were assigned according to the code defined in Table 4.9 of WHP Office Report WHPO 90-1 Rev.2 section 4.5.2 (Joyce *et al.*, 1994). Measurement flags of 2 (good), 3 (questionable), 4 (bad), and 5 (missing) have been assigned (Table 3.4.7). For the choice between 2, 3, or 4, we basically followed a flagging procedure as listed below:

a. Bottle oxygen concentration at the sampling layer was plotted against sampling pressure. Any points not lying on a generally smooth trend were noted.

b. Difference between bottle oxygen and oxygen sensor was then plotted against sampling pressure. If a datum deviated from a group of plots, it was flagged 3.

c. Vertical sections against pressure and potential density were drawn. If a datum was anomalous on the section plots, datum flag was degraded from 2 to 3, or from 3 to 4.

d. If there was problem in the measurement, the datum was flagged 4.

e. If the bottle flag was 4 (did not trip correctly), a datum was flagged 4 (bad). In case of the bottle flag 3 (leaking) or 5 (unknown problem), a datum was flagged based on steps a, b, c, and d.

Quality flag values for oxygen data from pumped-up surface seawater were assigned according to a flagging procedure as listed below:

f. Bottle oxygen data was plotted against that from oxygen sensors. If a datum deviated from a group of plots, it was flagged 3.

g. If there was problem in the measurement, the datum was flagged 4.

Table 3.4.7 Summary of assigned quality control flags.

Flag	Definition	Number*
2	Good	922
3	Questionable	0
4	Bad	0
5	Not report (missing)	0
	Total	922

*Replicate samples (n = 108) were not included.

References

Dickson, A. (1996) Determination of dissolved oxygen in sea water by Winkler titration, in WHPO Pub. 91-1 Rev. 1, November 1994, Woods Hole, Mass., USA.

Joyce, T., and C. Corry, eds., C. Corry, A. Dessier, A. Dickson, T. Joyce, M. Kenny, R. Key, D. Legler, R. Millard, R. Onken, P. Saunders, M. Stalcup (1994) Requirements for WOCE Hydrographic Programme Data Reporting, WHPO Pub. 90-1 Rev. 2, May 1994 Woods Hole, Mass., USA.

Murray, C.N., J.P. Riley, and T.R.S. Wilson (1968) The solubility of oxygen in Winkler reagents used for determination of dissolved oxygen, Deep-Sea Res., 15, 237-238.

3.5 Nutrients

27 April 2017 ver.2.1

(1) Personnel

Michio AOYAMA (JAMSTEC/Fukushima Univ., Principal Investigator)

LEG 2

Tomomi SONE (Department of Marine & Earth Science, Marine Works Japan Ltd.)

Atsushi ONO (Department of Marine & Earth Science, Marine Works Japan Ltd.)

LEG 3

Tomomi SONE (Department of Marine & Earth Science, Marine Works Japan Ltd.)

Shinichiro YOKOGAWA (Department of Marine & Earth Science, Marine Works Japan Ltd.)

Yoshiko ISHIKAWA (Department of Marine & Earth Science, Marine Works Japan Ltd.)

Yoshiaki SATO (Department of Marine & Earth Science, Marine Works Japan Ltd.)

(2) Objectives

The objectives of nutrients analyses during the R/V *Mirai* MR1609 cruise, cruise in Chilean coastal area (Leg2) and GO-SHIP P17E repeat cruise in 2017, in the South Pacific Ocean (Leg3) are as follows;

Leg2

- Understand the progress in ocean acidification Chilean coastal area and marine organism's responses in the modern ocean and reconstruction of the past climate change recorded in sediments.
- Investigate marine biodiversity and relationship with changes in surrounding environment.

Leg3

- Describe the present status of nutrients concentration with excellent comparability.
- The determinants are nitrate, nitrite, silicate, phosphate and ammonium.
- Study the temporal and spatial variation of nutrients concentration based on a part of the previous high quality experiments data of WOCE previous P17E cruises in 1992.
- Study of temporal and spatial variation of nitrate: phosphate ratio, so called Redfield ratio.
- Obtain more accurate estimation of total amount of nitrate, silicate, phosphate and ammonium in the interested area.
- Provide more accurate nutrients data for physical oceanographers to use as tracers of water mass movement.

(3) Summary of nutrients analysis

We made 8 QuAAtro 2-HR runs for the samples collected by 9 casts at 8 stations in Leg2 and 23 runs for the samples collected by 23 casts at 23 stations in Leg3. The total amount of layers of the seawater sample reached to 270 in Leg2 and 1460 in Leg3. We made duplicate measurement at all layers at all stations. We made basically duplicate measurement. The station locations for nutrients measurement is shown in Figure 3.5.1, Figure 3.5.2, Table 3.5.1 and Table 3.5.2.

We also measured the samples as listed below. 99 pore water samples, 6 sea samples collected from just above the sea bottom, 24 salinity standard samples and 36 underway samples.

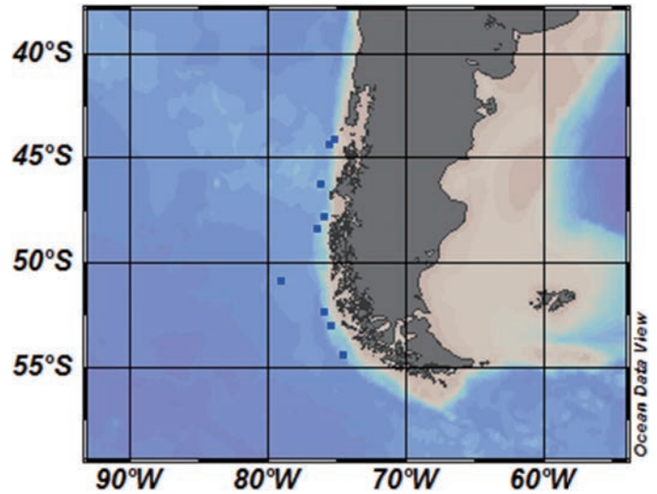

Figure 3.5.1 Sampling positions of nutrients sample in MR1609Leg2.

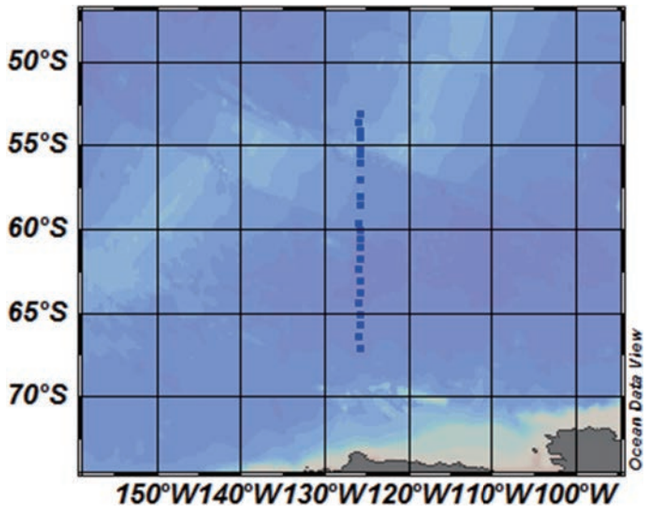

Figure 3.5.2 Sampling positions of nutrients sample in MR1609Leg3.

Table 3.5.1 List of stations of MR1609Leg2

Station	Cast	Station serial	Date (UTC)	Position*		Depth (dbar)
			(mmddyy)	Latitude	Longitude	
001	1	1	012117	44-17.72S	75-35.53W	1,920
006	1	2	012417	46-10.81S	76-17.64W	2,522
007	1	3	012817	47-47.96S	76-01.99W	1,992
009	1	4	012917	48-23.16S	76-28.09W	1,639
010	1	5	013117	50-48.41S	79-06.80W	3,852
010	2	5	013117	50-48.46S	79-07.15W	3,852
012B	1	6	020217	54-20.20S	74-38.03W	2,462
011B	1	7	020317	53-00.08S	75-29.35W	1,767
011A	1	8	020317	52-19.08S	75-56.71W	1,822

Table 3.5.2 List of stations of MR1609Leg3

Station	Cast	Station serial	Date (UTC)	Position*		Depth (dbar)
			(mmddyy)	Latitude	Longitude	
001	2	1	021617	66-59.99S	125-58.58W	3,709
002	1	2	021617	66-21.56S	126-03.77W	4,470
003	1	3	021617	65-39.45S	125-57.43W	4,745
004	1	4	021717	65-01.00S	125-57.59W	4,866
005	1	5	021717	64-20.81S	126-01.84W	4,891
006	1	6	021717	63-41.01S	125-59.57W	4,955
007	1	7	021817	63-01.25S	125-59.78W	4,994
008	1	8	021817	62-20.12S	126-06.64W	5,047
009	1	9	021917	61-39.83S	125-59.62W	4,833
010	1	10	021917	60-58.71S	126-00.43W	4,590
011	1	11	021917	60-28.63S	125-58.51W	4,833
012	1	12	022017	60-00.83S	125-58.53W	4,634
013	1	13	022017	59-36.44S	126-03.24W	4,637
015	1	14	022017	58-29.95S	125-59.05W	4,209
016	1	15	022017	58-00.63S	125-59.75W	4,274
018	1	16	022117	57-01.00S	125-59.23W	4,168
020	1	17	022117	56-00.65S	125-57.34W	4,169
021	1	18	022117	55-30.21S	125-58.63W	3,502
022	1	19	022217	55-01.09S	125-58.60W	3,654
023	1	20	022217	54-28.36S	125-59.12W	3,629
024	1	21	022217	54-00.38S	125-58.60W	3,586
025	1	22	022217	53-30.49S	126-01.35W	3,742
026	1	23	022217	53-00.73S	126-00.05W	4,229

(4) Instrument and Method

(4.1) Analytical detail using QuAAtro 2-HR systems (BL TEC K.K.)

We applied two units of QuAAtro in this cruise. Unit 1 and Unit 2 were put for R/V *Mirai* equipment. Configurations of all units are completely same for five parameters, Nitrate, Nitrite, Silicate, Phosphate, and Ammonium.

Nitrate + nitrite and nitrite were analyzed according to the modification method of Grasshoff (1970). The sample nitrate was reduced to nitrite in a cadmium tube inside of which was coated with metallic copper. The sample streamed with its equivalent nitrite was treated with an acidic, sulfanilamide reagent and the nitrite forms nitrous acid which reacted with the sulfanilamide to produce a diazonium ion. N-1-Naphthylethylene-diamine added to the sample stream then coupled with the diazonium ion to produce a red, azo dye. With reduction of the nitrate to nitrite, both nitrate and nitrite reacted and were measured; without reduction, only nitrite reacted. Thus, for the nitrite analysis, no reduction was performed and the alkaline buffer was not necessary. Nitrate was computed by difference.

The silicate method was analogous to that described for phosphate. The method used was essentially that of Grasshoff et al. (1983), wherein silicomolybdic acid was first formed from the silicate in the sample and added molybdic acid; then the silicomolybdic acid was reduced to silicomolybdous acid, or "molybdenum blue" using ascorbic acid as the reductant. The analytical methods of the nutrients, nitrate, nitrite, silicate and phosphate, during this cruise were same as the methods used in (Kawano et al. 2009).

The phosphate analysis was a modification of the procedure of Murphy and Riley (1962). Molybdic acid was added to the seawater sample to form phosphomolybdic acid which was in turn reduced to phosphomolybdous acid using L-ascorbic acid as the reductant.

The details of modification of analytical methods for four parameters, Nitrate, Nitrite, Silicate and Phosphate, used in this cruise are also compatible with the methods described in nutrients section in GO-SHIP repeat hydrography manual (Hydes et al., 2010), while an analytical method of ammonium is compatible with Determination of ammonia in seawater using a vaporization membrane permeability method (Kimura, 2000). The flow diagrams and reagents for each parameter are shown in Figures 3.5.3 to 3.5.7.

(4.2) Nitrate Reagents

Imidazole (buffer), 0.06 M (0.4 % w/v)

Dissolve 4 g imidazole (CAS No. 288-32-4), in 1000 ml DIW, add 2 ml Hydrogen chloride (CAS No. 7647-01-0). After mixing, 1 ml Triton™ X-100 (50 % solution in ethanol) is added.

Sulfanilamide, 0.06 M (1 % w/v) in 1.2 M HCl

Dissolve 10 g 4-Aminobenzenesulfonamide (CAS No. 63-74-1), in 900 ml of DIW, add 100 ml Hydrogen chloride (CAS No. 7647-01-0). After mixing, 2 ml Triton™ X-100 (50 %f solution in ethanol) is added.

NED, 0.004 M (0.1 %f w/v)

Dissolve 1 g N-(1-Naphthalenyl)-1,2-ethanediamine, dihydrochloride (CAS No. 1465-25-4), in 1000 ml of DIW and add 10 ml Hydrogen chloride (CAS No. 7647-01-0). After mixing, 1 ml Triton™ X-100 (50 %f solution in ethanol) is added.

Stored in a dark bottle.

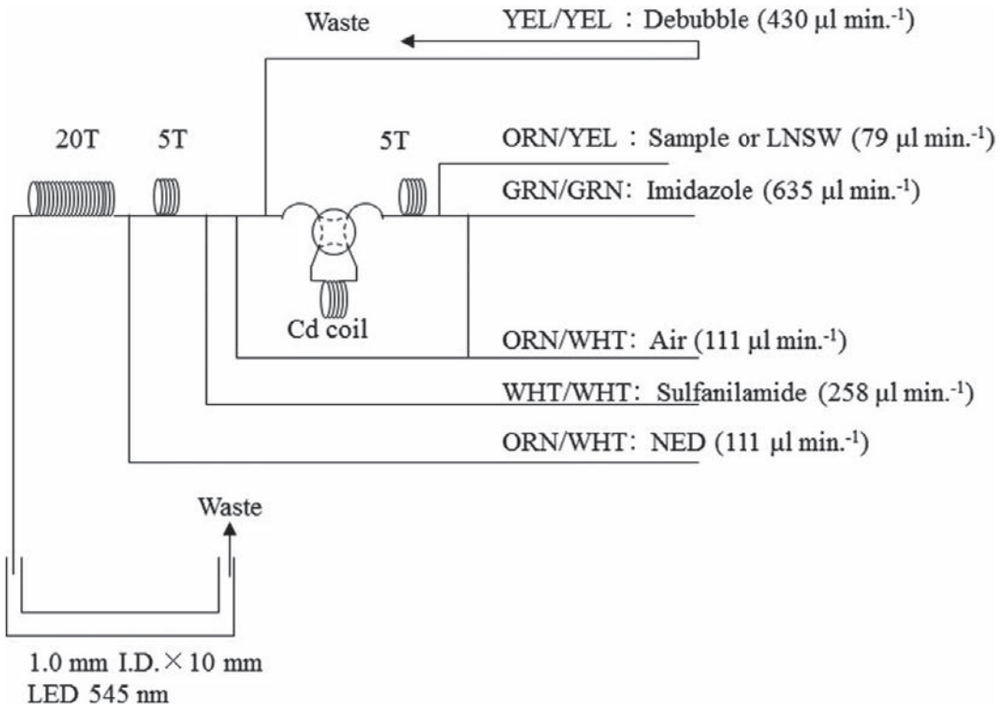

Figure 3.5.3 NO_3+NO_2 (1ch.) Flow diagram.

(4.3) Nitrite Reagents

Sulfanilamide, 0.06 M (1% w/v) in 1.2 M HCl

Dissolve 10 g 4-Aminobenzenesulfonamide (CAS No. 63-74-1), in 900 ml of DIW, add 100 ml Hydrogen chloride (CAS No. 7647-01-0). After mixing, 2 ml Triton™ X-100 (50% solution in ethanol) is added.

NED, 0.004 M (0.1% w/v)

Dissolve 1 g N-(1-Naphthalenyl)-1,2-ethanediamine, dihydrochloride (CAS No. 1465-25-4), in 1000 ml of DIW and add 10 ml Hydrogen chloride (CAS No. 7647-01-0). After mixing, 1 ml Triton™ X-100 (50% solution in ethanol) is added. This reagent was stored in a dark bottle.

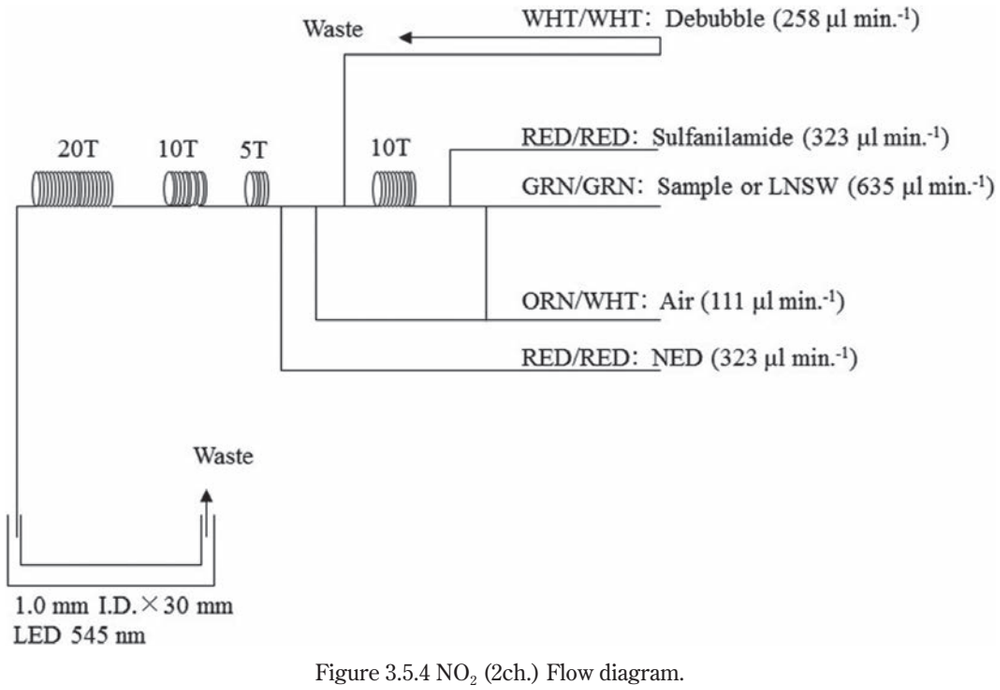

Figure 3.5.4 NO_2 (2ch.) Flow diagram.

(4.4) Silicate Reagents

Molybdic acid, 0.06 M (2% w/v)

Dissolve 15 g Sodium molybdate (CAS No. 7631-95-0), in 980 ml DIW, add 8 ml Sulfuric acid (CAS No. 7664-93-9). After mixing, 20 ml Sodium dodecyl sulfate (CAS No. 151-21-3), (15% solution in water) is added.

Oxalic acid, 0.6 M (5% w/v)

Dissolve 50 g Oxalic Acid (CAS No. 144-62-7), in 950 ml of DIW.

Ascorbic acid, 0.01 M (3% w/v)

Dissolve 2.5g L-Ascorbic acid (CAS No. 50-81-7), in 100 ml of DIW. This reagent was freshly prepared at every day.

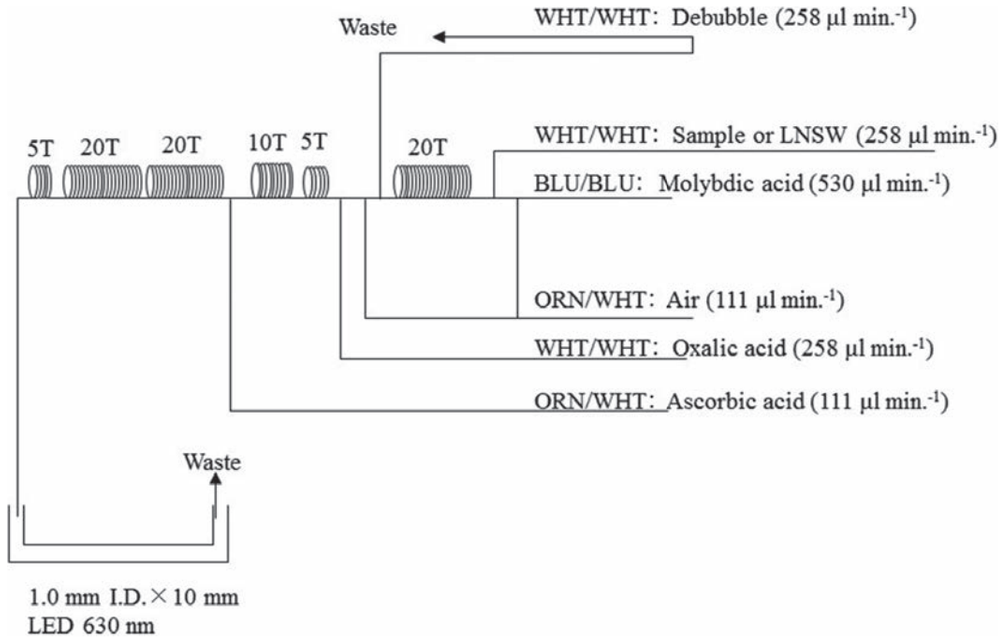

Figure 3.5.5 SiO_2 (3ch.) Flow diagram.

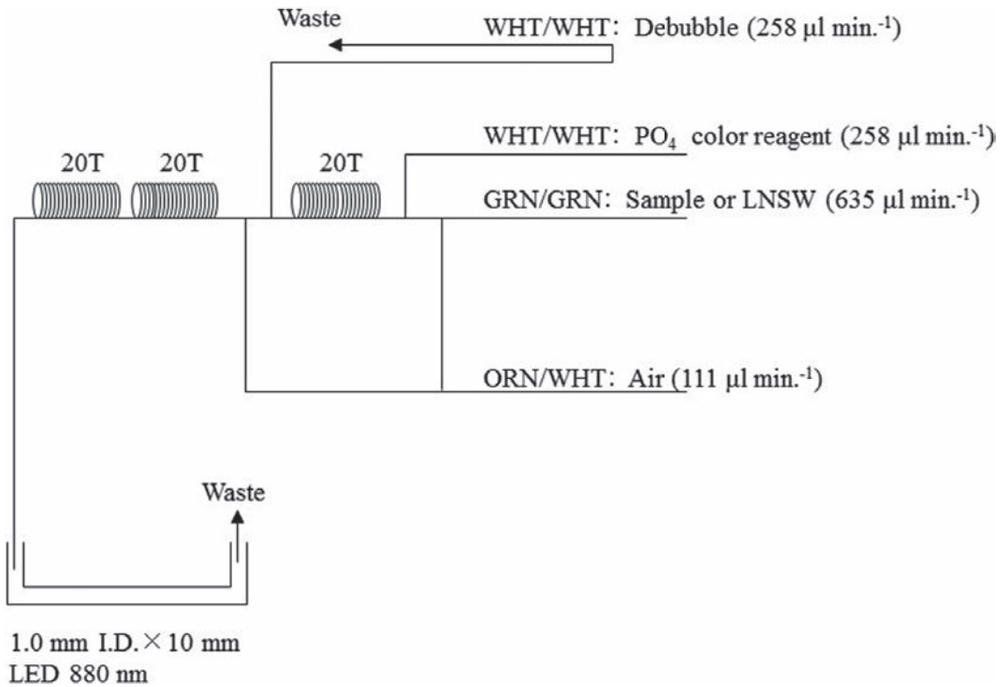

Figure 3.5.6 PO_4 (4ch.) Flow diagram.

(4.5) Phosphate Reagents

Stock molybdate solution, 0.03 M (0.8% w/v)

Dissolve 8 g Sodium molybdate (CAS No. 7631-95-0), and 0.17 g Antimony potassium tartrate trihydrate (CAS No. 28300-74-5), in 950 ml of DIW and added 50 ml Sulfuric acid (CAS No. 7664-93-9).

Mixed Reagent

Dissolve 1.2 g L-Ascorbic acid (CAS No. 50-81-7), in 150 ml of stock molybdate solution. After mixing, 3 ml Sodium dodecyl sulfate (CAS No. 151-21-3), (15% solution in water) was added. This reagent was freshly prepared before every measurement.

(4.6) Ammonium Reagents

EDTA

Dissolve 41 g Tetrasodium EDTA tetrahydrate (CAS No. 13235-36-4), and 2 g Boric acid (CAS No. 10043-35-3), in 200 ml of DIW. After mixing, 1 ml Triton™ X-100 (30% solution in DIW) is added. This reagent is prepared at a week about.

NaOH

Dissolve 5 g Sodium hydroxide (CAS No. 1310-73-2), and 16 g Tetrasodium EDTA tetrahydrate (CAS No. 13235-36-4) in 100 ml of DIW. This reagent is prepared at a week about.

Stock Nitroprusside

Dissolve 0.25 g Sodium nitroferricyanide dehydrate (CAS No. 13755-38-9) in 100 ml of DIW and add 0.2 ml 1M H_2SO_4. Stored in a dark bottle and prepared at a month about.

Nitroprusside solution

Mixed 4 ml stock nitroprusside and 5 ml 1M H_2SO_4 in 500 ml of DIW. After mixing, 2 ml Triton™ X-100 (30% solution in DIW) is added. This reagent is stored in a dark bottle and prepared at every 2 or 3 days.

Alkaline phenol

Dissolve 10 g Phenol (CAS No. 108-95-2), 5 g Sodium hydroxide (CAS No. 1310-73-2) and 2g Sodium citrate dehydrate (CAS No. 6132-04-3), in 200 ml DIW. Stored in a dark bottle and prepared at a week about.

NaClO solution

Mix 3 ml sodium hypochlorite solution, Sodium hypochlorite (CAS No. 7681-52-9), in 47 ml DIW. Stored in a dark bottle and fleshly prepared before every measurement. This reagent is prepared 0.3% available chlorine.

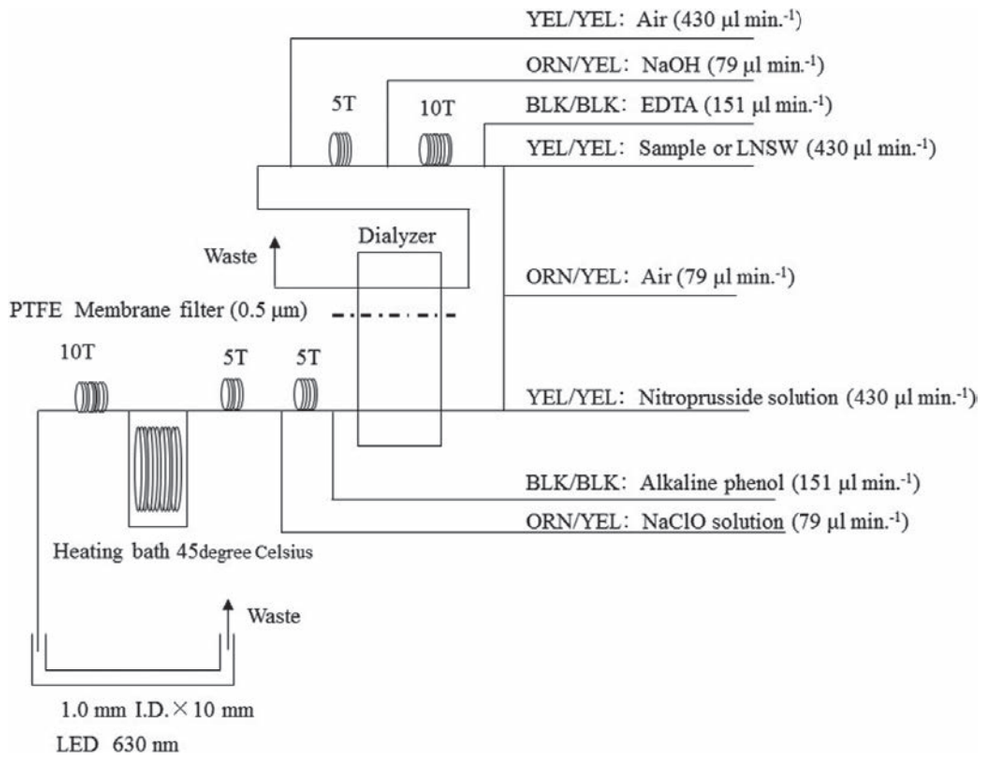

Figure 3.5.7 NH_4 (5ch.) Flow diagram.

(4.7) Sampling procedures

Sampling of nutrients followed that oxygen, salinity and trace gases. Samples were drawn into two of virgin 10 mL polyacrylates vials without sample drawing tubes. These were rinsed three times before filling and then vials were capped immediately after the drawing. The vials were put into water bath adjusted to ambient temperature, 22 ± 1 deg. C, in about 30 minutes before use to stabilize the temperature of samples in MR1609.

No transfer was made and the vials were set an auto sampler tray directly. Samples were analyzed after collection basically within 24 hours in principal.

(4.8) Data processing

Raw data from QuAAtro 2-HR was treated as follows:

- Checked baseline shift.
- Checked the shape of each peak and positions of peak values taken, and then changed the positions of peak values taken if necessary.
- Carry-over correction and baseline drift correction were applied to peak heights of each samples followed by sensitivity correction.
- Baseline correction and sensitivity correction were done basically using liner regression.
- Loaded pressure and salinity from CTD data to calculate density of seawater. In case of bucket sample, we generally used bottle salinity from AUTOSAL.
- Calibration curves to get nutrients concentration were assumed second order equations.

(5) Certified Reference Material of nutrients in seawater

KANSO CRMs (Lot: BY, CD, CA, BW, CC, CB, BZ) were used to ensure the comparability and traceability of nutrient measurements during this cruise. The details of CRMs are shown below.

Production

KANSO CRMs are certified reference material (CRM) for inorganic nutrients in seawater. These were produced by KANSO Co.,Ltd. This certified reference material has been produced using autoclaved natural seawater on the basis of quality control system under IS0 Guide 34 (JIS Q 0034).

KANSO Co.,Ltd. has been accredited under the Accreditation System of National Institute of Technology and Evaluation (ASNITE) as a CRM producer since 2011. (Accreditation No.: ASNITE 0052 R)

Property value assignment

The certified values are arithmetic means of the results of 30 bottles from each batch (measured in duplicates) analysed by KANSO Co.,Ltd. and Japan Agency for Marine-Earth Science and Technology (JAMSTEC) using the colorimetric method (continuous flow analysis, CFA, method). The salinity of calibration solutions were adjusted to the salinity of this CRM ±0.5 psu.

Metrological Traceability

Each certified value of nitrate, nitrite, and phosphate of KANSO CRMs were calibrated versus one of Japan Calibration Service System (JCSS) standard solutions for each nitrate ions, nitrite ions, and phosphate ions. JCSS standard solutions are calibrated versus the secondary solution of JCSS for each of these ions. The secondary solution of JCSS is calibrated versus the specified primary solution produced by Chemicals Evaluation and Research Institute (CERI), Japan. CERI specified primary solutionsare calibrated versus the National Metrology Institute of Japan (NMIJ) primary standards solution of nitrate ions, nitrite ions and phosphate ions, respectively.

For a certified value of silicate of KANSO CRM was determined by one of Merck KGaA silicon standard solution 1000 mg/L Si traceable to National Institute of Standards and Technology (NIST) SRM of silicon standard solution (SRM3150).

The certified values of nitrate, nitrite, and phosphate of KASNO CRM are thus traceable to the International System of Units (SI) through an unbroken chain of calibrations, JCSS, CERI and NMIJ solutions as stated above, each having stated uncertainties. The certified values of silicate of KANSO CRM are traceable to the International System of Units (SI) through an unbroken chain of calibrations, Merck KGaA and NIST SRM3150 solutions, each having stated uncertainties.

As stated in the certificate of NMIJ CRMs each certified value of dissolved silica, nitrate ions, and nitrite ions was determined by more than one method using one of NIST (National Institute of Standards and Technology) SRM of silicon standard solution and NMIJ primary standards solution of nitrate ions and nitrite ions. The concentration of phosphate ions as stated information value in the certificate was determined NMIJ primary standards solution of phosphate ions. Those values in the certificate of NMIJ CRMs are traceable to the International System of Units (SI).

One of analytical methods used for certification of NMIJ CRM for nitrate ions, nitrite ions, phosphate ions

and dissolved silica was colorimetric method (continuous mode and batch one). The colorimetric method is same as the analytical method (continuous mode only) used for certification of KANSO CRM. For certification of dissolved silica, exclusion chromatography/isotope dilution-inductively coupled plasma mass spectrometry and Ion exclusion chromatography with post-column detection were used. For certification of nitrate ions, Ion chromatography by direct analysis and Ion chromatography after halogen-ion separation were used. For certification of nitrite ions, Ion chromatography by direct analysis was used.

NMIJ CRMs were analysed at the time of certification process for CRM and the results were confirmed within expanded uncertainty stated in the certificate of NMIJ CRMs.

(5.1) CRMs for this cruise

5 lot of CRMs were used as calibration standards together with the C-6. These bottles were stored at a room in the ship, REAGENT STORE, where the temperature was maintained around 20- 24 deg. C. The concentrations for CRM lots BY, CD, CA, BW, CB, BZ, and CC are shown in Table 3.5.3.

Table 3.5.3 Certified concentration and uncertainty (k=2) of CRMs.

unit: μmol kg^{-1}

Lot	Nitrate	Nitrite	Silicate	Phosphate	Ammonia*
BY	0.02 ± 0.02	0.02 ± 0.01	1.76 ± 0.06	0.039 ± 0.010	0.89
CD	5.50 ± 0.05	0.02 ± 0.01	13.93 ± 0.10	0.446 ± 0.008	1.11
CA	19.66 ± 0.15	0.06 ± 0.01	36.58 ± 0.22	1.407 ± 0.014	0.67
BW	24.59 ± 0.20	0.07 ± 0.01	60.01 ± 0.42	1.541 ± 0.014	0.93
CB	35.79 ± 0.27	0.12 ± 0.01	109.2 ± 0.62	2.520 ± 0.022	0.77
BZ	43.35 ± 0.33	0.22 ± 0.01	161.0 ± 0.93	3.056 ± 0.033	0.43
CC	30.88 ± 0.24	0.12 ± 0.01	86.16 ± 0.48	2.080 ± 0.019	1.05

*For ammonia values are references

(6) Nutrients standards

(6.1) Volumetric laboratory ware of in-house standards

All volumetric glass ware and polymethylpentene (PMP) ware used were gravimetrically calibrated. Plastic volumetric flasks were gravimetrically calibrated at the temperature of use within 3 K.

Volumetric flasks

Volumetric flasks of Class quality (Class A) are used because their nominal tolerances are 0.05 % or less over the size ranges likely to be used in this work. Class A flasks are made of borosilicate glass, and the standard solutions were transferred to plastic bottles as quickly as possible after they are made up to volume and well mixed in order to prevent excessive dissolution of silicate from the glass. PMP volumetric flasks were gravimetrically calibrated and used only within 3 K of the calibration temperature.

The computation of volume contained by glass flasks at various temperatures other than the calibration temperatures were done by using the coefficient of linear expansion of borosilicate crown glass.

Because of their larger temperature coefficients of cubical expansion and lack of tables constructed for these materials, the plastic volumetric flasks were gravimetrically calibrated over the temperature range of intended use and used at the temperature of calibration within 3 K. The weights obtained in the calibration weightings were corrected for the density of water and air buoyancy.

Pipettes and pipettors

All pipettes were gravimetrically calibrated in order to verify and improve upon the nominal tolerance.

(6.2) Reagents, general considerations

Specifications

For nitrate standard, “potassium nitrate 99.995 suprapur®” provided by Merck, Lot. B0771365211, CAS No.: 7757-91-1, was used.

For nitrite standard solution, we used “nitrous acid iron standard solution (NO_2^- 1000) provided by Wako,

Lot ECF5432 (Leg2) and ECP4122 (Leg3), Code. No. 140-06451." This standard solution was certified by Wako using Ion chromatograph method. Calibration result is 999 mg L^{-1} at 20 degree Celsius. Expanded uncertainty of calibration (k=2) is 0.7 % for the calibration result.

For phosphate standard, "potassium dihydrogen phosphate anhydrous 99.995 suprapur®" provided by Merck, Lot. B1144508528, CAS No.: 7778-77-0, was used.

For the silicate standard, we use "Silicon standard solution SiO_2 in NaOH 0.5 mol/l CertiPUR®" provided by Merck, CAS No.: 1310-73-2, of which lot number is HC54715536 are used. The silicate concentration is certified by NIST-SRM3150 with the uncertainty of 0.7 %. HC54715536 is certified as 1005 mg L^{-1}.

For ammonia standard, "ammonium Chloride" provided by NMIJ. We used NMIJ CRM 3011-a. The purity of this standard was greater than 99.9 %. Expanded uncertainty of calibration (k=2) is 0.065 %.

Treatment of silicate standard due to high alkalinity

Since the silicon standard solution Merck CertiPUR® is in NaOH 0.5 mol/l, we need to dilute and neutralize to avoid make precipitation of $MgOH_2$ etc. When we make B standard, silicon standard solution is diluted by factor 12 with pure water and neutralized by HCl 1.0 mol L^{-1} to be about 7. After that B standard solution is used to prepare C standards.

Ultra pure water

Ultra pure water (MilliQ water) freshly drawn was used for preparation of reagents, standard solutions and for measurement of reagent and system blanks.

Low-Nutrient Seawater (LNSW)

Surface water having low nutrient concentration was taken and filtered using 0.20 μm pore capsule cartridge filter at MR1505 cruise on January, 2016. This water is stored in 20 liter cubitainer with paper box.

LNSW concentrations were assigned in August 2016 during MR1606 cruise.

(6.3) Concentrations of nutrient for A, B and C standards

Concentrations of nutrients for A, B, C and D standards are set as shown in Table 3.5.4 and Table 3.5.6. The C standard is prepared according recipes as shown in Table 3.5.5. and Table 3.5.7. All volumetric laboratory tools were calibrated prior the cruise as stated in chapter (6.1). Then the actual concentration of nutrients in each fresh standard was calculated based on the ambient, solution temperature and determined factors of volumetric laboratory wares.

The calibration curves for each run were obtained using 6 levels, C-1, C-2, C-3, C-4, C-5 and C-6. C-1, C-2, C-3, C-4 and C-5 were the certified reference material of nutrients in seawater (hereafter CRM) and C-6 was in-house standard.

Table 3.5.4 Nominal concentrations of nutrients for A, B and C standards in Leg2.

	A	B	D	C-1	C-2	C-3	C-4	C-5	C-6	C-7	C-8
NO_3(μM)	22500	900	900	BY	CD	BW	CC	CB	45	-	-
NO_2(μM)	21800	26	875	BY	CD	BW	CC	CB	1.0	-	-
SiO_2(μM)	35800	2860		BY	CD	BW	CC	CB	144	-	-
PO_4(μM)	3000	60		BY	CD	BW	CC	CB	3.0	-	-
NH_4(μM)	4000	200		-	-	-	-	-	6.0	2.0	0

Table 3.5.5 Working calibration standard recipes in Leg2.

C std.	B-1 std.	B-2 std.	B-3 std
C-6	25 mL	20 mL	15 mL
C-7	-	-	5 mL
C-8	-	-	0 mL

Table 3.5.6 Nominal concentrations of nutrients for A, B and C standards in Leg3.

	A	B	D	C-1	C-2	C-3	C-4	C-5	C-6	C-7	C-8
NO_3(μM)	22500	900	900	BY	CD	CA	BW	BZ	36	-	-
NO_2(μM)	21800	26	875	BY	CD	CA	BW	BZ	1.0	-	-
SiO_2(μM)	35800	2860		BY	CD	CA	BW	BZ	115	-	-
PO_4(μM)	3000	60		BY	CD	CA	BW	BZ	2.4	-	-
NH_4(μM)	4000	200		-	-	-	-	-	6.0	2.0	0

Table 3.5.7 Working calibration standard recipes in Leg3.

C std.	B-1 std.	B-2 std.	B-3 std
C-6	20 mL	20 mL	15 mL
C-7	-	-	5 mL
C-8	-	-	0 mL

B-1 std.: Mixture of nitrate, silicate and phosphate
B-2 std.: Nitrite
B-3 std: Ammonium

(6.4) Renewal of in-house standard solutions.

In-house standard solutions as stated in paragraph (5.2) were renewed as shown in Table 3.5.8 (a) to (c).

Table 3.5.8(a) Timing of renewal of in-house standards.

NO_3, NO_2, SiO_2, PO_4, NH_4	Renewal
A-1 std. (NO_3)	maximum a month
A-2 std. (NO_2)	commercial prepared solution
A-3 std. (SiO_2)	commercial prepared solution
A-4 std. (PO_4)	maximum a month
A-5 std. (NH_4)	maximum a month
B-1 std. (mixture of A-1, A-3 and A-4 std.)	maximum 8 days
B-2 std. (dilute D-2 std.)	maximum 8 days
B-3 std. (dilute A-5 std.)	maximum 8 days

Table 3.5.8(b) Timing of renewal of in-house standards.

Working standards	Renewal
C-6 std. (mixture of B-1, B-2 and B-3 std.)	
C-7 std. (dilute B-3 std.)	every 24 hours
C-8 (LNSW)	

Table 3.5.8(c) Timing of renewal of in-house standards for reduction estimation.

Reduction estimation	Renewal
D-1 std. (900 μM NO_3)	maximum 8 days
D-2 std. (875 μM NO_2)	maximum 8 days
36 μM NO_3	when C Std. renewed
35 μM NO_2	when C Std. renewed

(7) Quality control

(7.1) Precision of nutrients analyses during this cruise

Precision of nutrients analyses during this cruise was evaluated based on the 7 to 11 measurements, which are measured every 8 to 13 samples, during a run at the concentration of C-6 std. Summary of precisions are shown as Table 3.5.9, Table 3.5.10 and Figures 3.5.8 to 3.5.13, the precisions for each parameter are generally good considering the analytical precisions during the R/V Mirai cruses conducted in 2009 - 2015. Analytical precisions in Leg2 were 0.15% for nitrate, 0.13% for phosphate and 0.07% for silicate in terms of median of precision, respectively. Analytical precisions in Leg3 were 0.18% for nitrate, 0.15% for phosphate and 0.12% for silicate in terms of median of precision, respectively.

Table 3.5.9 Summary of precision based on the replicate analyses for unit 1 in Leg2.

	Nitrate CV%	Nitrite CV%	Silicate CV%	Phosphate CV %	Ammonium CV %
Median	0.15	0.13	0.07	0.14	0.24
Mean	0.15	0.13	0.07	0.13	0.27
Maximum	0.26	0.26	0.17	0.19	0.40
Minimum	0.06	0.04	0.03	0.08	0.16
N	8	8	8	8	8

Table 3.5.10 Summary of precision based on the replicate analyses for all unit in Leg3.

	Nitrate CV%	Nitrite CV%	Silicate CV%	Phosphate CV%	Ammonium CV%
Median	0.17	0.21	0.12	0.14	0.25
Mean	0.18	0.25	0.12	0.15	0.28
Maximum	0.42	0.56	0.25	0.27	0.51
Minimum	0.07	0.10	0.04	0.06	0.09
N	23	23	23	23	23

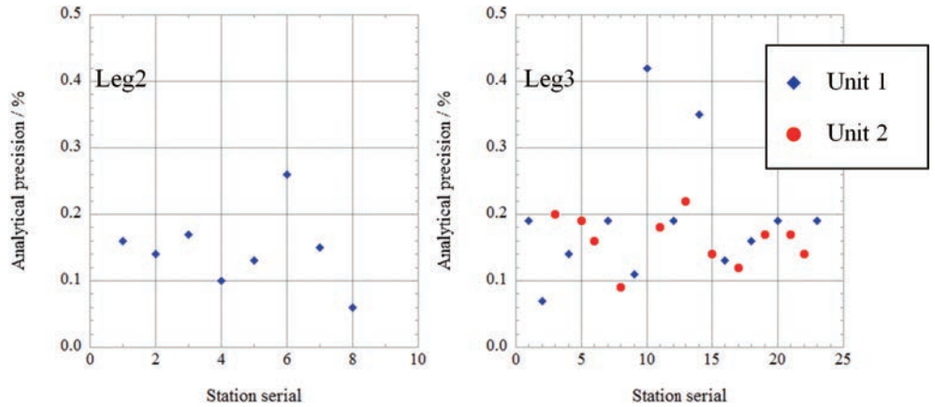

Figure 3.5.8 Time series of precision of nitrate in MR1609Leg2 and Leg3.

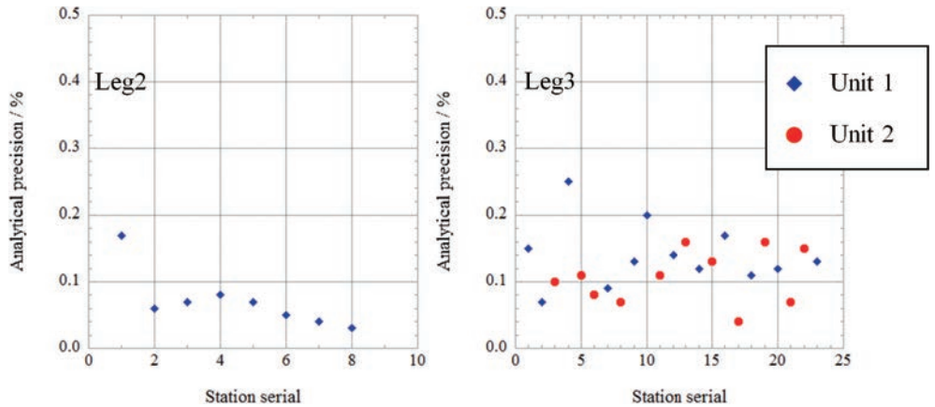

Figure 3.5.9 Time series of precision of silicate in MR1609Leg2 and Leg3.

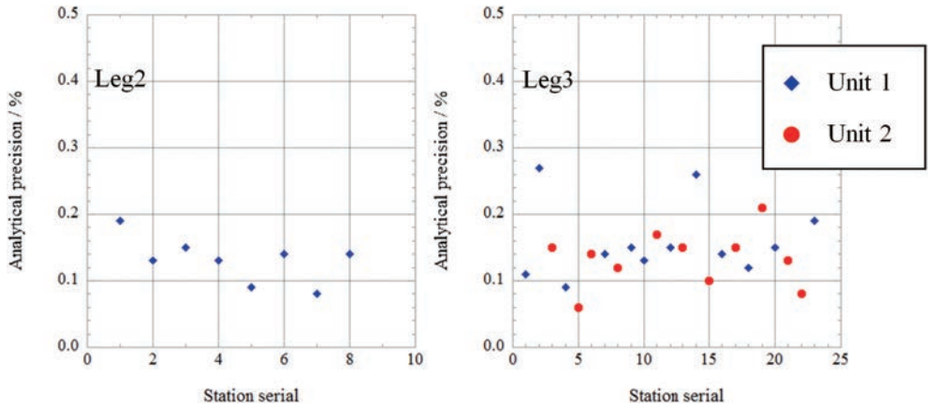

Figure 3.5.10 Time series of precision of phosphate in MR1609Leg2 and Leg3.

(7.2) CRM lot. CC measurement during this cruise

CRM lot. CC was measured every run to monitor the comparability among runs. The results of lot. BV during this cruise are shown as Figures 3.5.11 to 3.5.16. Error bars represent analytical precision in Figures 3.5.8 to 3.5.13.

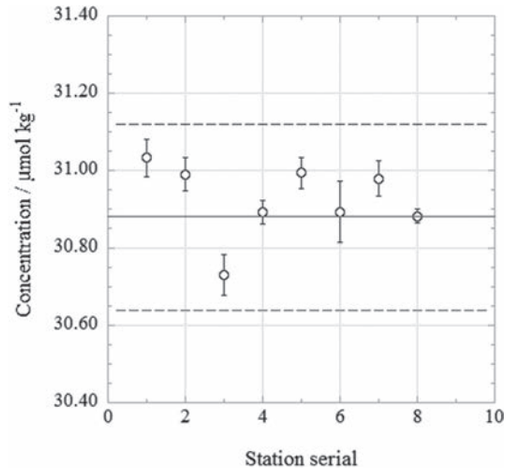

Figure 3.5.11 Time series of CRM-CC of nitrate in MR1609Leg2.

Solid line : certified value, broken line : uncertainty of certified value (k=2)

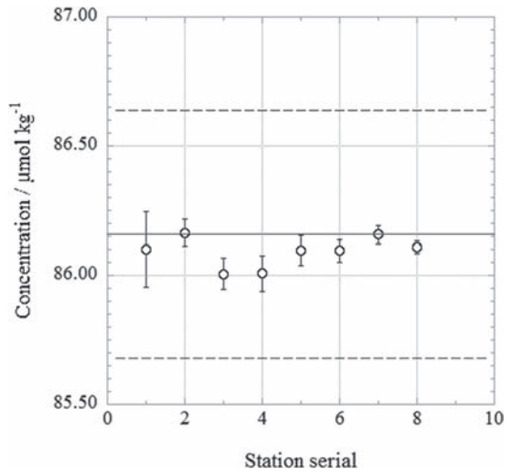

Figure 3.5.12 Time series of CRM-CC of silicate in MR1609Leg2.

Solid line : certified value, broken line : uncertainty of certified value (k=2)

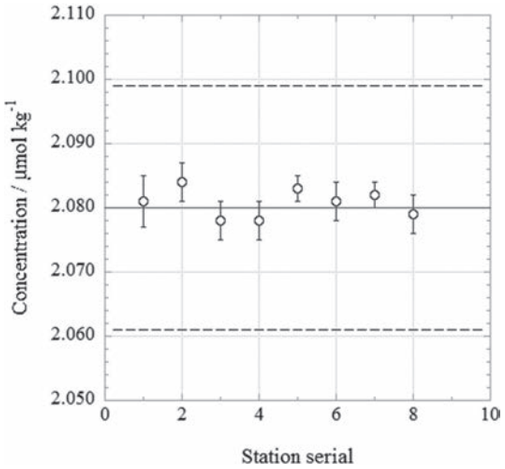

Figure 3.5.13 Time series of CRM-CC of phosphate in MR1609Leg2.

Solid line : certified value, broken line : uncertainty of certified value (k=2)

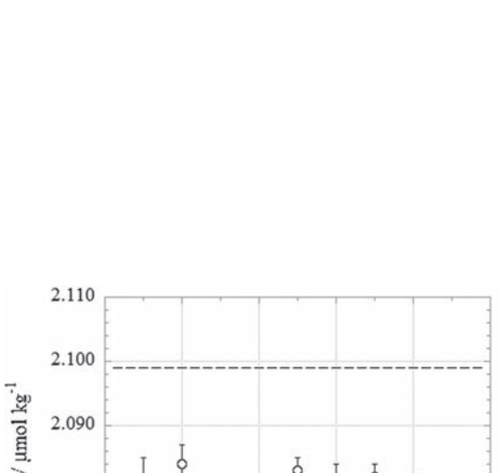

Figure 3.5.14 Time series of CRM-CC of nitrate in MR1609Leg3.

Solid line : certified value, broken line : uncertainty of certified value (k=2)

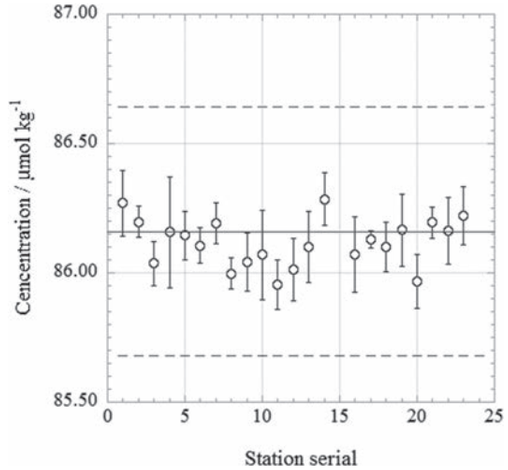

Figure 3.5.15 Time series of CRM-CC of silicate in MR1609Leg3.

Solid line : certified value, broken line : uncertainty of certified value (k=2)

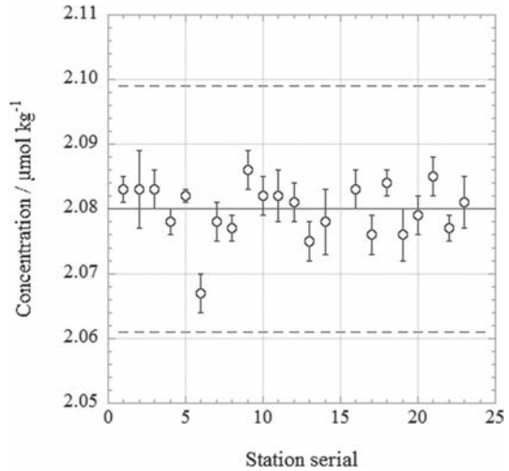

Figure 3.5.16 Time series of CRM-CC of phosphate in MR1609Leg3.

Solid line : certified value, broken line : uncertainty of certified value (k=2)

(7.3) Carryover

We can also summarize the magnitudes of carryover throughout the cruise. These are small enough within acceptable levels as shown in Table 3.5.11, Table 3.5.12 and Figures 3.5.17 to 3.5.19. The carryover in silicate and phosphate had a bias by equipments. It was 0.09% and 0.14%, mean value, at Unit 2. The other hand, it was 0.17% and 0.29 %, mean value, at Unit 1.

Table 3.5.11 Summary of carry over throughout Leg2.

	Nitrate CV%	Nitrite CV%	Silicate CV%	Phosphate CV%	Ammonium CV%
Median	0.19	0.16	0.20	0.16	0.66
Mean	0.19	0.16	0.20	0.16	0.63
Maximum	0.22	0.35	0.22	0.19	0.95
Minimum	0.15	0.00	0.18	0.12	0.19
N	8	8	8	8	8

Table 3.5.12 Summary of carry over throughout Leg3.

	Nitrate CV%	Nitrite CV%	Silicate CV%	Phosphate CV%	Ammonium CV%
Median	0.18	0.14	0.11	0.17	0.77
Mean	0.18	0.15	0.13	0.22	0.74
Maximum	0.26	0.48	0.24	0.43	1.34
Minimum	0.11	0.00	0.00	0.04	0.14
N	23	23	23	23	23

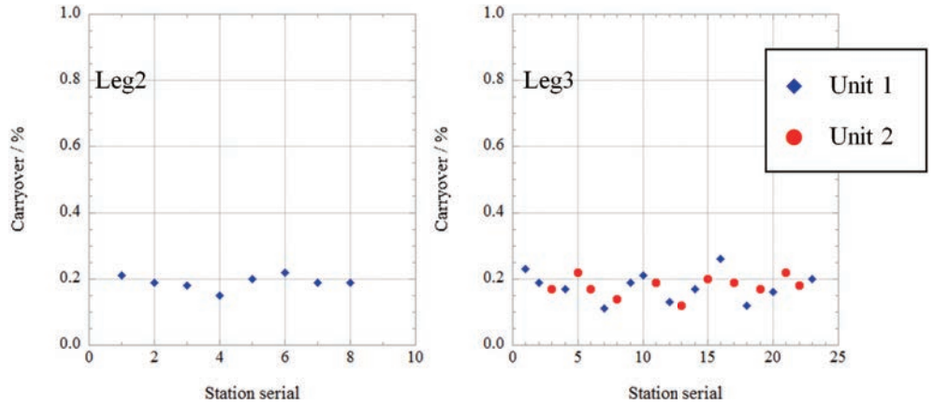

Figure 3.5.17 Time series of carryover of nitrate in MR1609Leg2 and Leg3.

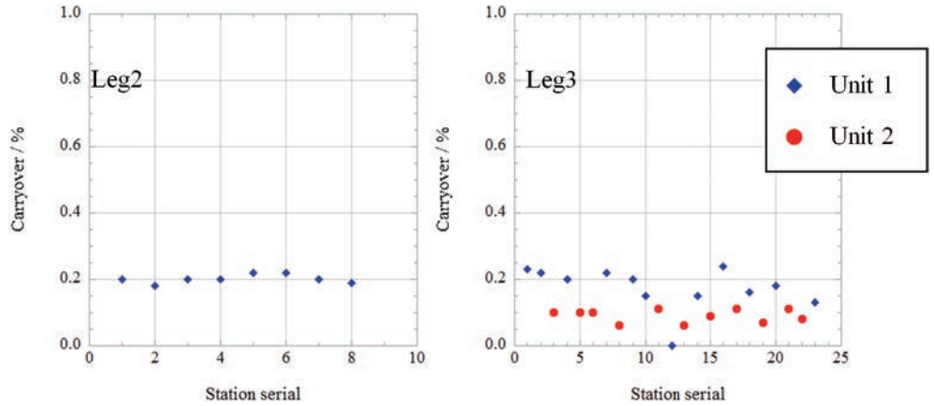

Figure 3.5.18 Time series of carryover of silicate in MR1609Leg2 and Leg3.

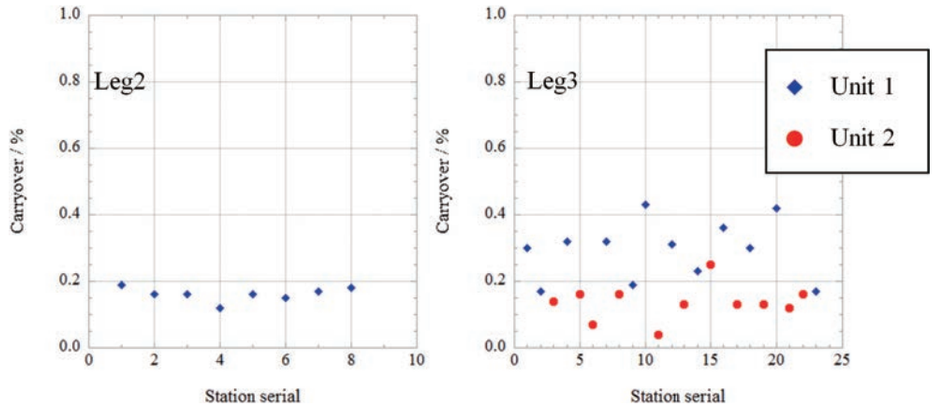

Figure 3.5.19 Time series of carryover of phosphate in MR1609Leg2 and Leg3.

(7.4) Estimation of uncertainty of phosphate, nitrate and silicate concentrations

We estimate the uncertainty of measurement of nutrient by merging data from both Leg2 and Leg3 because the numbers of the run in each leg were small, 8 runs and 23 runs, respectively.

Empirical equations, eq. (1), (2), and (3) to estimate uncertainty of measurement of phosphate, nitrate and silicate are used based on measurements of 31 sets of CRMs during this cruise. Empirical equations, eq. (4), (5) are used to estimate uncertainty of measurement of nitrite and ammonium based on duplicate measurements of the samples. These empirical equations and graphic presentation of equations are as follows, respectively.

Phosphate Concentration Cp in μmol kg^{-1}:

Uncertainty of measurement of phosphate (%) =

$0.051 + 0.256 * (1 / Cp)$ — (1)

where Cp is phosphate concentration of sample.

Nitrate Concentration Cno_3 in μmol kg^{-1}:

Uncertainty of measurement of nitrate (%) =

$0.13 + 1.46 * (1 / Cno_3)$ — (2)

where Cno_3 is nitrate concentration of sample.

Silicate Concentration Cs in μmol kg^{-1}:

Uncertainty of measurement of silicate (%) =

$0.08 + 2.19 * (1 / Cs)$ — (3)

where Cs is silicate concentration of sample.

Nitrite Concentration Cno_2 in μmol kg^{-1}:

Uncertainty of measurement of nitrite (%) =

$-0.23 + 0.25 * (1 / Cno_2) - 0.000014 * (1 / Cno_2) * (1 / Cno_2)$ — (4)

where Ca is ammonium concentration of sample.

Ammonium Concentration Ca in μmol kg^{-1}:

Uncertainty of measurement of ammonium (%) =

$0.58 + 1.50 * (1 / Ca) - 0.00046 * (1 / Ca) * (1 / Ca)$ — (5)

where Ca is ammonium concentration of sample.

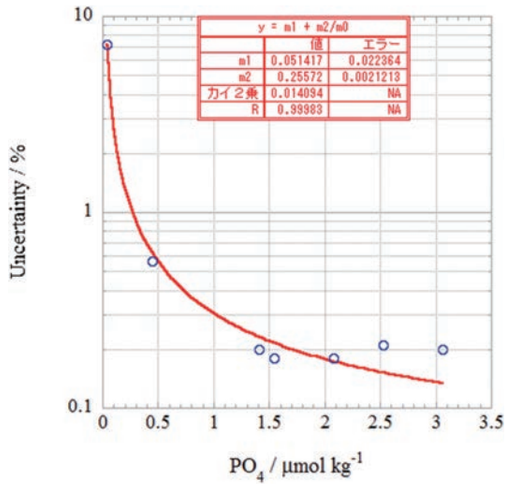

Figure 3.5.20 Estimation of uncertainty for phosphate in MR1609.

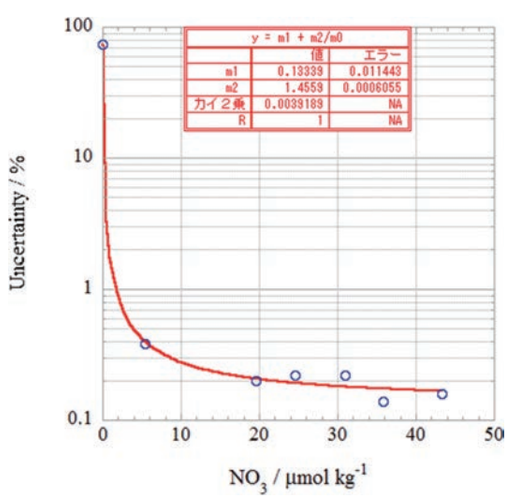

Figure 3.5.21 Estimation of uncertainty for nitrate in MR1609.

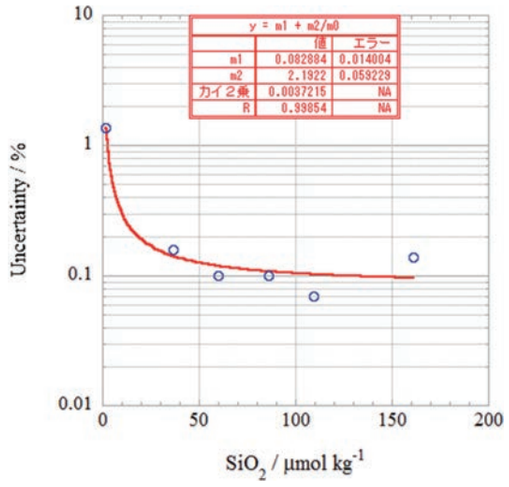

Figure 3.5.22 Estimation of uncertainty for silicate in MR1609.

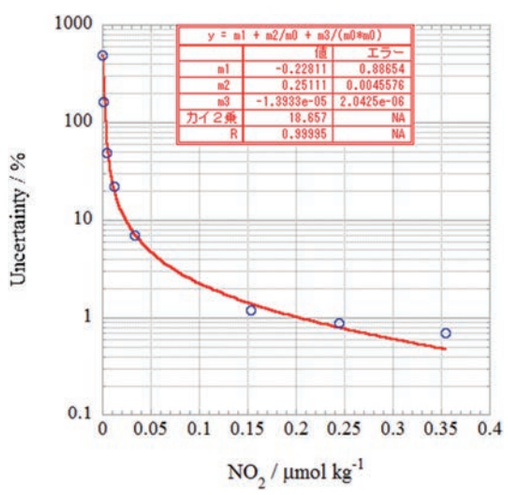

Figure 3.5.23 Estimation of uncertainty for nitrite in MR1609.

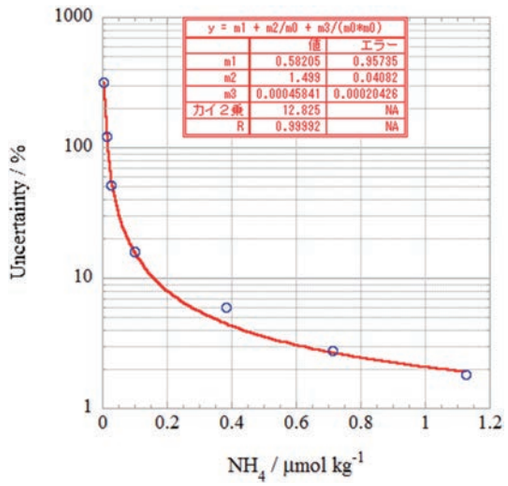

Figure 3.5.24 Estimation of uncertainty for ammonium in MR1609.

(8) Problems / improvements occurred and solutions

(8.1) Centrifuged samples

When we found the value of transparency of the sample was less than 100% or doubtful for the particles in the sample, we carried out centrifuging for the samples by using the centrifuge (type : CN-820, AZONE). The centrifuged sample list for nutrients is shown in Table 3.5.13 and Table 3.5.14.

Table 3.5.13 Centrifugation sample list of MR1609Leg2

Station	Cast	Bottle	Depth (dbar)	Trans (%)
6	1	0	0	-
		32	10.6	86.591
		35	25.7	86.667
		29	25.7	86.612
10	2	0	0	-
		34	10.8	96.177
		33	25.6	96.200
		32	51	96.283
12	B	35	27	95.235
		30	26.6	95.270
		27	50.4	95.305
		24	102	99.468
11	B	0	0	-
		32	11.4	96.237
		35	25.8	96.217
		29	26.1	96.247
		26	50.7	96.273
11	A	0	0	-
		32	11	92.910
		29	25.1	92.765
		26	50	95.334
		23	101.4	99.720

Table3.5.14 Centrifugation sample list of MR1609Leg3

Station	Cast	Bottle	Depth(dbar)	Trans(%)
2	1	0	0	-
		36	11.2	89.205
		2	21.2	89.464
		35	51.6	95.998
		34	99.8	99.994
3	1	0	0	-
		36	12.6	90.649
		35	50.8	91.419
		34	101	99.875
4	1	0	0	-
		36	11.8	92.014
		2	31.3	92.152
		35	51.4	95.637
		34	101.5	99.606
5	1	0	0	-
		36	10.6	96.588
		35	50.6	96.441
		34	100.2	99.501
		33	150.9	99.992
6	1	0	0	-
		36	10.1	96.804
		35	50.6	96.816
		2	69.9	97.251
		34	102.4	98.945
		33	150.9	99.946
7	1	0	0	-
		36	11.7	96.804
		35	51.7	96.844
		34	101.2	99.672
		33	150.8	99.858
8	1	0	0	-
		36	11.2	97.279
		35	50.3	97.292
		2	67.6	98.584
		34	101.8	99.388
		33	151.6	99.699
9	1	0	0	-
		36	12	97.035
		35	52.1	97.04
		34	101.5	99.548
		33	151.6	99.773
10	1	0	0	-
		36	10.2	97.433
		35	52	97.424
		2	67.3	97.449
		34	102.3	99.107
		33	150.3	99.836
11	1	0	0	-
		36	10.5	97.242
		35	51.3	97.503
		34	102	99.117
		33	152.4	99.578
		32	201.6	99.885
		31	250.9	99.997

Station	Cast	Bottle	Depth (dbar)	Trans (%)
12	1	0	0	-
		36	11.4	98.067
		35	52.5	98.286
		2	80.4	98.402
		34	101.7	99.367
		33	150.6	99.908
13	1	0	0	-
		36	11.9	97.178
		2	31.7	97.077
		35	52.2	97.258
		34	101.7	98.83
		33	150.8	99.519
15	1	0	0	-
		36	10	97.758
		35	50.3	97.774
		2	75.9	97.812
		34	100.5	98.683
		33	152.1	99.706
		32	200.4	99.956
16	1	0	0	-
		36	12.1	98.011
		35	53	98.083
		2	77.3	98.242
		34	104.1	99.211
18	1	0	0	-
		36	11.5	98.226
		35	51	98.232
		2	82.5	98.503
		34	101.6	99.776

Station	Cast	Bottle	Depth (dbar)	Trans (%)
20	1	0	0	-
		36	10.7	98.364
		35	51.2	98.386
		2	86	98.525
		34	101.9	99.12
		33	151.6	99.875
21	1	0	0	-
		36	11.2	97.343
		35	50.7	97.489
		2	66.5	97.987
		34	101.9	99.987
22	1	0	0	-
		36	11.3	97.419
		35	51.3	97.556
		34	101.8	99.961
23	1	0	0	-
		36	11.8	97.86
		2	32.5	97.804
		35	51.9	97.875
		34	101.2	98.583
24	1	0	0	-
		36	10.8	97.95
		2	30.9	97.937
		35	50.2	98.013
		34	100.2	98.279
25	1	0	0	-
		36	10.9	97.569
		2	21.4	97.588
		35	52.1	97.62
		34	102	99.851

Station	Cast	Bottle	Depth(dbar)	Trans(%)
26	1	0	0	-
		36	11	97.177
		35	51	97.28
		2	75.9	97.536
		34	100.8	99.342

(8.2) Bad peak shape at NO_3+NO_2 channel

We found that peak shape at NO_3+NO_2 channel became bad in the middle of run for stn. 10 and stn. 11 in Leg3. The bad peak shape was probably due to clogging of Cd coil. We speculated that at stations 1, 2 and 4, the chlorophyll concentration exceeded 1 micro g l^{-1} and transparency of samples were around 90 %, then the magnitude of centrifugation of these samples might not enough and a part of the particles remains. The cause of the damage of the Cd coil might come from the remained particles.

We analysed again all samples of stn. 10 and stn. 11. We accepted NO_3 data of first run for all samples except for 10_1_9 that both primary and secondary peak shape was bad at the first run. NO_3 data of second run was accepted for 10_1_9.

We should re-examine the condition of centrifugation of such samples of which chlorophyll contents is high and transparency is low.

(9) Data archive

All data will be submitted to JAMSTEC Data Management Office (DMO) and is currently under its control.

(10) List of reagent

List of reagent is shown in Table 3.5.15.

Table 3.5.15 List of reagent in MR1609.

IUPAC name	CAS Number	Formula	Compound Name	Manufacture	Grade
Hydrogen chloride	7647-01-0	HCl	Hydrochloric acid	Wako Pure Chemical Industries, Ltd.	JIS Special Grade
Sulfuric acid	7664-93-9	H_2SO_4	Sulfuric Acid	Wako Pure Chemical Industries, Ltd.	JIS Special Grade
Imidazole	288-32-4	$C_3H_4N_2$	Imidazole	Wako Pure Chemical Industries, Ltd.	JIS Special Grade
4-Aminobenzenesulfonamide	63-74-1	$C_6H_8N_2O_2S$	sulfanilamide	Wako Pure Chemical Industries, Ltd.	JIS Special Grade
N-(1-Naphthalenyl)-1,2-ethanediamine, dihydrochloride	1465-25-4	$C_{12}H_{16}C_{l2}N_2$	N-1-Naphthylethylenediamine Dihydrochloride	Wako Pure Chemical Industries, Ltd.	for Nitrogen Oxides Analysis
Oxalic Acid	144-62-7	$C_2H_2O_4$	Oxalic Acid	Wako Pure Chemical Industries, Ltd.	Wako Special Grade
L-Ascorbic acid	50-81-7	$C_6H_8O_6$	L-ascorbic acid	Wako Pure Chemical Industries, Ltd.	JIS Special Grade
Sodium molybdate	7631-95-0	Na_2MoO_4	Disodium Molybdate(VI) Dihydrate	Wako Pure Chemical Industries, Ltd.	JIS Special Grade
Sodium dodecyl sulfate	151-21-3	$C_{12}H_{25}NaO_4S$	Sodium Dodecyl Sulfate	Wako Pure Chemical Industries, Ltd.	for Biochemistry
Antimony potassium tartrate trihydrate	28300-74-5	$K_2(SbC_4H_2O_6)\cdot 3H_2O$	Bis[(+)-tartrato]diantimonate(III) Dipotassium Trihydrate	Wako Pure Chemical Industries, Ltd.	JIS Special Grade
Boric acid	10043-35-3	H_3BO_3	Boric Acid	Wako Pure Chemical Industries, Ltd.	JIS Special Grade
Phenol	108-95-2	C_6H_6O	Phenol	Wako Pure Chemical Industries, Ltd.	JIS Special Grade
Sodium citrate dihydrate	6132-04-3	$Na_3C_6H_5O_7\cdot 2H_2O$	Trisodium Citrate Dihydrate	Wako Pure Chemical Industries, Ltd.	JIS Special Grade
Sodium hydroxide	1310-73-2	NaOH	Sodium Hydroxide for Nitrogen Compounds Analysis	Wako Pure Chemical Industries, Ltd.	for Nitrogen Analysis
Sodium hypochlorite	7681-52-9	NaClO	Sodium hypochlorite solution	Kanto Chemical co., Inc.	Extra pure
Sodium nitroferricyanide dihydrate	13755-38-9	$Na_2[Fe(CN)_5NO]\cdot 2H_2O$	Sodium Pentacyanonitrosylferrate(III) Dihydrate	Wako Pure Chemical Industries, Ltd.	JIS Special Grade
tetrasodium;2-[2-[bis(carboxylatomethyl)amino]ethyl-(carboxylatomethyl)amino]acetate;tetrahydrate	13235-36-4	$C_{10}H_{20}N_2Na_4O_{12}$	Ethylenediamine-N,N,N',N'-tetraacetic Acid Tetrasodium Salt Tetrahydrate (4NA)	Dojindo Molecular Technologies, Inc.	-

References

Aminot, A. and Kerouel, R. 1991. Autoclaved seawater as a reference material for the determination of nitrate and phosphate in seawater. Anal. Chim. Acta, 248: 277-283.

Aminot, A. and Kirkwood, D.S. 1995. Report on the results of the fifth ICES intercomparison exercise for nutrients in sea water, ICES coop. Res. Rep. Ser., 213.

Aminot, A. and Kerouel, R. 1995. Reference material for nutrients in seawater: stability of nitrate, nitrite,

ammonia and phosphate in autoclaved samples. Mar. Chem., 49: 221-232.

Aoyama M., and Joyce T.M. 1996, WHP property comparisons from crossing lines in North Pacific. In Abstracts, 1996 WOCE Pacific Workshop, Newport Beach, California.

Aoyama, M., 2006: 2003 Intercomparison Exercise for Reference Material for Nutrients in Seawater in a Seawater Matrix, Technical Reports of the Meteorological Research Institute No.50, 91pp, Tsukuba, Japan.

Aoyama, M., Susan B., Minhan, D., Hideshi, D., Louis, I. G., Kasai, H., Roger, K., Nurit, K., Doug, M., Murata, A., Nagai, N., Ogawa, H., Ota, H., Saito, H., Saito, K., Shimizu, T., Takano, H., Tsuda, A., Yokouchi, K., and Agnes, Y. 2007. Recent Comparability of Oceanographic Nutrients Data: Results of a 2003 Intercomparison Exercise Using Reference Materials. Analytical Sciences, 23: 1151-1154.

Aoyama M., J. Barwell-Clarke, S. Becker, M. Blum, Braga E. S., S. C. Coverly,E. Czobik, I. Dahllof, M. H. Dai, G. O. Donnell, C. Engelke, G. C. Gong, Gi-Hoon Hong, D. J. Hydes, M. M. Jin, H. Kasai, R. Kerouel, Y. Kiyomono, M. Knockaert, N. Kress, K. A. Krogslund, M. Kumagai, S. Leterme, Yarong Li, S. Masuda, T. Miyao, T. Moutin, A. Murata, N. Nagai, G.Nausch, M. K. Ngirchechol, A. Nybakk, H. Ogawa, J. van Ooijen, H. Ota, J. M. Pan, C. Payne, O. Pierre-Duplessix, M. Pujo-Pay, T. Raabe, K. Saito, K. Sato, C. Schmidt, M. Schuett, T. M. Shammon, J. Sun, T. Tanhua, L. White, E.M.S. Woodward, P. Worsfold, P. Yeats, T. Yoshimura, A.Youenou, J. Z. Zhang, 2008: 2006 Intercomparison Exercise for Reference Material for Nutrients in Seawater in a Seawater Matrix, Technical Reports of the Meteorological Research Institute No. 58, 104pp.

Aoyama, M., Nishino, S., Nishijima, K., Matsushita, J., Takano, A., Sato, K., 2010a. Nutrients, In: R/V Mirai Cruise Report MR10-05. JAMSTEC, Yokosuka, pp. 103-122.

Aoyama, M., Matsushita, J., Takano, A., 2010b. Nutrients, In: MR10-06 preliminary cruise report. JAMSTEC, Yokosuka, pp. 69-83

Gouretski, V.V. and Jancke, K. 2001. Systematic errors as the cause for an apparent deep water property variability: global analysis of the WOCE and historical hydrographic data·REVIEW ARTICLE, Progress In Oceanography, 48: Issue 4, 337-402.

Grasshoff, K., Ehrhardt, M., Kremling K. et al. 1983. Methods of seawater anylysis. 2nd rev. Weinheim: Verlag Chemie, Germany, West.

Hydes, D.J., Aoyama, M., Aminot, A., Bakker, K., Becker, S., Coverly, S., Daniel, A., Dickson, A.G., Grosso, O., Kerouel, R., Ooijen, J. van, Sato, K., Tanhua, T., Woodward, E.M.S., Zhang, J.Z., 2010. Determination of Dissolved Nutrients (N, P, Si) in Seawater with High Precision and Inter-Comparability Using Gas-Segmented Continuous Flow Analysers, In: GO-SHIP Repeat Hydrography Manual: A Collection of Expert Reports and Guidelines. IOCCP Report No. 14, ICPO Publication Series No 134.

Joyce, T. and Corry, C. 1994. Requirements for WOCE hydrographic programmed data reporting. WHPO Publication, 90-1, Revision 2, WOCE Report No. 67/91.

Kawano, T., Uchida, H. and Doi, T. WHP P01, P14 REVISIT DATA BOOK, (Ryoin Co., Ltd., Yokohama, 2009).

Kimura, 2000. Determination of ammonia in seawater using a vaporization membrane permeability method. 7th auto analyzer Study Group, 39-41.

Kirkwood, D.S. 1992. Stability of solutions of nutrient salts during storage. Mar. Chem., 38 : 151-164.

Kirkwood, D.S. Aminot, A. and Perttila, M. 1991. Report on the results of the ICES fourth intercomparison exercise for nutrients in sea water. ICES coop. Res. Rep. Ser., 174.

Mordy, C.W., Aoyama, M., Gordon, L.I., Johnson, G.C., Key, R.M., Ross, A.A., Jennings, J.C. and Wilson. J. 2000. Deep water comparison studies of the Pacific WOCE nutrient data set. Eos Trans-American Geophysical Union. 80 (supplement), OS43.

Murphy, J., and Riley, J.P. 1962. Analyticachim. Acta 27, 31-36.

Sato, K., Aoyama, M., Becker, S., 2010. CRM as Calibration Standard Solution to Keep Comparability for Several Cruises in the World Ocean in 2000s. In: Aoyama, M., Dickson, A.G., Hydes, D.J., Murata, A., Oh, J.R., Roose, P., Woodward, E.M.S., (Eds.), Comparability of nutrients in the world's ocean. Tsukuba, JAPAN: MOTHER TANK, pp 43-56.

Uchida, H. &Fukasawa, M. WHP P6, A10, I3/I4 REVISIT DATA BOOK Blue Earth Global Expedition 2003 1, 2, (Aiwa Printing Co., Ltd., Tokyo, 2005).

3.6 Chlorofluorocarbons and Sulfur hexafluoride

January 19, 2019

(1) Personnel

Ken'ichi Sasaki (JAMSTEC)

Hironori Sato (MWJ)

Hiroshi Hoshino (MWJ)

Masahiro Ohrui (MWJ)

(2) Objectives

Chlorofluorocarbons (CFCs) and sulfur hexafluoride (SF_6) are man-made stable gases. These atmospheric gases can slightly dissolve in sea surface water by air-sea gas exchange and then are spread into the ocean interior. So, these dissolved gases could be used as chemical tracers for the ocean circulation. We measured concentrations of three chemical species of CFCs, CFC-11 (CCl_3F), CFC-12 (CCl_2F_2), and CFC-113 ($C_2Cl_3F_3$), and SF_6 in seawater on board. We tried to detect nitrous oxide (N_2O) that was separated during the measurement process of CFCs and SF_6.

(3) Apparatus

We used three measurement systems. One of them was CFCs analyzing system (call as system D). Other two were SF_6 – CFCs simultaneous analyzing systems (called as system A and B). Trial analysis of N_2O was made on latter systems. Both systems are based on purging and trapping – electron capture detector (ECD) – gas chromatography. The instruments are summarized in table 3.6.1 and 3.6.2.

Table 3.6.1 Instruments and analytical columns for the system A and B.

Gas Chromatograph:	GC-14B (Shimadzu Ltd.)
Detector 1&2:	ECD-14 (Shimadzu Ltd.)
Analytical Columns:	
Pre-column 1:	Silica Plot capillary column [i.d.: 0.53 mm, length: 6 m, film thickness: 6 µm]
Pre-column 2:	Molesive 5A Plot capillary column [i.d.: 0.53 mm, length: 5 m, film thickness: 15 µm]
Main column 1:	Connected two capillary columns (Pora Bond-Q [i.d.: 0.53 mm, length: 9 m, film thickness: 10 µm] followed by Silica Plot [i.d.: 0.53 mm, length: 18 m, film thickness: 6 µm])
Main column 2:	Connected two capillary columns (Molesive 5A Plot [i.d.: 0.53 mm, length: 3 m, film thickness: 15 µm] followed by Pora Bond-Q [i.d.: 0.53 mm, length: 9 m, film thickness: 10 µm])
Purging & trapping:	Developed in JAMSTEC. Cold trap columns are 30 cm length stainless steel tubing packed the section of 5 cm with 80/100 mesh Porapak Q and followed by the section of 5 cm of 100/120 mesh Carboxen 1000. Outer diameters of the main and focus trap columns are 1/8" and 1/16", respectively.

Table 3.6.2 Instruments and analytical columns for system D.

Gas Chromatograph:	GC-14B (Shimadzu Ltd.)
Detector:	ECD-14 (Shimadzu Ltd.)
Analytical Columns:	
Pre-column:	Silica Plot capillary column [i.d.: 0.53 mm, length: 6 m, film thickness: 6 µm]
Main column:	Connected two capillary columns (Pora Bond-Q [i.d.: 0.53 mm, length: 9 m, film thickness: 10 µm] followed by Silica Plot [i.d.: 0.53 mm, length: 18 m, film thickness: 6 µm])
Purging & trapping:	Developed in JAMSTEC. Cold trap columns are 1/16" SUS tubing packed the section of 5 cm with 100/120 mesh Porapak T.

(4) Shipboard measurement

(4.1) Sampling

Seawater sub-samples were collected from 12 liter Niskin bottles to 450 ml of glass bottles developed in JAMSTEC. The glass bottles were filled by CFC free gas (pure nitrogen gas) before sampling. Two times of the bottle volume of seawater sample were overflowed. The seawater samples in the bottle were kept in water bath controlled at 7 °C until analysis. The samples were analyzed as soon as possible after sampling (usually within 12 hours).

In order to confirm stabilities of standard gas composition and also to check saturation levels of the components in sea surface water, mixing ratios of the compounds in background air were measured in almost every station. The end of 10 mm OD Dekaron tubing was put on a head of the compass deck and another end was connected onto the air pump in the laboratory. Air samples were continuously led into laboratory by the pump. The tubing was relayed by a T-type union which had a small stop cock. Air sample was collected from the flowing air into a 200 ml glass cylinder attached on the cock. The Air samples were analyzed as soon as possible after sampling (usually within 10 minutes).

(4.2) Analysis

i. SF_6 – CFCs (– N_2O) simultaneous analyzing system (System A and B)

Constant volume of sample water (200 ml) was taken into a sample loop. The sample was sent into a stripping chamber and dissolved SF_6, CFCs and N_2O were de-gassed by N_2 gas purging for 8 minutes. The gas sample was dried by magnesium perchlorate desiccant and concentrated on a main trap column cooled down to -80 °C. Stripping efficiencies were frequently confirmed by re-stripping of surface layer samples. More than 99 % of dissolved SF6 and CFC12, 97 % of CFC-11 and 95 % of N_2O were extracted on the first purge. Following purging & trapping, the main trap column was isolated and electrically heated to 180 °C. After 1 minute, the desorbed gases were sent onto focus trap cooled down to -80 °C for 30 seconds. Gaseous sample on the focus trap were desorbed by same manner as that on the main trap, and lead onto the pre-column 1 (PC 1). Sample gases were roughly separated on the PC 1. Eluting SF_6, CFCs and N_2O onto pre-column 2 (PC 2), PC 1 was connected to cleaning line and high boiling point compounds on the PC 1 were flushed by counter flow of pure nitrogen gas. SF_6 and CFCs were rapidly eluted from PC 2 onto main-column 1 (MC 1) and N_2O was retained on PC 2. Then PC 2 was connected back-flush carrier gas line and N_2O was sent onto main-column 2 (MC 2). SF_6 and CFCs were further separated on MC 1 and detected by ECD 1. N_2O on MC 2 was sent into ECD 2. Nitrogen gases used in these systems was filtered by gas purifier column packed with Molecular Sieve 13X (MS-13X). Measurements were calibrated using gas phase mixture standard prepared by gravimetric method.

Analytical conditions for the systems are listed in table 3.6.3. Standard gas cylinders used in this cruise are listed in table 3.6.4.

Table 3.6.3 Measurement conditions for system A and B.

Temperature	
Analytical Column:	95 °C
Detector (ECD):	300 °C
Trap column:	-80 °C (at adsorbing) & 180 °C (at desorbing)
Mass flow rates of nitrogen gas (99.99995%)	
Carrier gas 1:	10 ml min^{-1}
Carrier gas 2:	10 ml min^{-1}
Detector make-up gas 1:	27 ml min^{-1}
Detector make-up gas 2:	27 ml min^{-1}
Back flush gas:	10 ml min^{-1}
Sample purge gas:	220 ml min^{-1}

Table 3.6.4 Standard gases List (supplied by Japan Fine Products co. Ltd.).

Cylinder No.	Base gas	CFC-11	CFC-12	CFC113	SF_6	N_2O	remarks
		ppt	ppt	ppt	ppt	ppm	
CPB20725	N_2	873	472	81.5	9.83	14.6	for system A&B
CPB21090	N_2	891	472	81.9	9.77	15.0	for system A&B
CPB09873	N_2	301	160	30.2	0.0	0.0	for system D
CPB16993	N_2	300	160	29.9	0.0	0.0	Reference

ii. CFCs analyzing system (System D)

Constant volume of sample water (50 ml) was taken into a sample loop. The sample was send into stripping chamber and dissolved CFCs were de-gassed by N_2 gas purging for 8 minutes. The gas sample was dried by magnesium perchlorate desiccant and concentrated on a trap column cooled down to -50 °C. Stripping efficiencies were frequently confirmed by re-stripping of surface layer samples and more than 99.5 % of dissolved CFCs were extracted on the first purge. Following purging & trapping, the trap column was isolated and electrically heated to 140 °C. The desorbed gases were lead onto the pre-column. Sample gases were roughly separated in the pre-column. When CFC-113 completely eluted from pre-column onto main column, the pre-column was connected onto another line and other compounds were flushed by counter flow of pure nitrogen gas. CFCs sent on main-column were further separated and detected by ECD. Nitrogen gases used in this system was also filtered by MS-13X gas purifier column.

Measurement conditions for this system are listed in table 3.6.5.

Table 3.6.5 Measurement conditions for system D.

Temperature

Analytical Column:	95 °C
Detector (ECD):	240 °C
Trap column:	-50 °C (at adsorbing) & 140 °C (at desorbing)

Mass flow rates of nitrogen gas (99.99995%)

Carrier gas:	10 ml min^{-1}
Detector make-up gas:	27 ml min^{-1}
Back flush gas:	10 ml min^{-1}
Sample purge gas:	130 ml min^{-1}

(5) Major problems in analyses

i. CFC-113

Analyzing surface water by system D, interfering components may overlap the chromatogram peak of CFC-113 in some cases. In this cruise, such a case was found at station 25 and flag 4 was given to that data. In systems A and B, such interference was not observed, possibly due to differences in analytical columns.

ii. N_2O

In the detection of N_2O, it seemed that there was a difference in detector sensitivity between analyses of seawater and gas samples. We are currently exploring the cause of this difference. Here we report the N_2O value as preliminary data (flag 1). It may recalculate in the future if correction becomes possible.

(6) Quality control

i. Blanks

In order to make the blank water, deep water (~5 L) was degassed for several days with a nitrogen flow of 200 ml min^{-1} in a glass bottle. The blank water was sub-sampled into the same bottle as the seawater sample. Estimated blank values were 0.043 fmol kg^{-1} for SF_6 (1 fmol = 1 x 10^{-15} mol), 0.017 pmol kg^{-1} for CFC-11 (1 pmol = 1 x 10^{-12} mol), 0.006 pmol kg^{-1} for CFC-12, and 0.005 pmol kg^{-1} for CFC-113. The blanks were subtracted from all data.

ii. Background air

Background air samples were analyzed for almost all stations. Average mixing ratios of the compounds were calculated to be 230.4 +/- 3.7 ppt for CFC-11 (n = 22), 518.7 +/- 5.3 ppt for CFC-12 (n = 22), 71.0 +/- 3.2 ppt for CFC-113 (n = 22), and 9.25 +/-0.06 ppt for SF_6 (n =13) in this cruise.

iii. Precisions

The precisions of measurements were calculated from replicate measurements. The estimated values are +/-0.014 pmol kg^{-1} or 1 % (which ever grater) for CFC-11, +/-0.006 pmol kg-1 or 1 % (which ever grater) for CFC-12, +/-0.005 pmol kg^{-1} or 5 % (which ever grater) for CFC-113, and +/-0.021 fmol kg^{-1} or 3 % (which ever grater) for SF_6.

3.7 Carbon Items (C_T and A_T)

23 November, 2018

(1) Personnel

Akihiko Murata (JAMSTEC)

Tomonori Watai (MWJ)

Atsushi Ono (MWJ)

Emi Deguchi (MWJ)

Nagisa Fujiki (MWJ)

(2) Objectives

Concentrations of CO_2 in the atmosphere are now increasing at a rate of about 2.0 ppmv y^{-1} owing to human activities such as burning of fossil fuels, deforestation, and cement production. It is an urgent task to estimate as accurately as possible the absorption capacity of the oceans against the increased atmospheric CO_2, and to clarify the mechanism of the CO_2 absorption, because the magnitude of the anticipated global warming depends on the levels of CO_2 in the atmosphere, and because the ocean currently absorbs 1/3 of the 6 Gt of carbon emitted into the atmosphere each year by human activities.

In this cruise, we were aimed at quantifying how much anthropogenic CO_2 was absorbed in the South Pacific. For the purpose, we measured CO_2-system parameters such as dissolved inorganic carbon (C_T) and total alkalinity (A_T) along the WHP P17E section in the region.

(3) Apparatus

i. C_T

Measurement of C_T was made with a total CO_2 measuring system (called as System D, Nippon ANS, Inc.). The system comprised of a seawater dispensing system, a CO_2 extraction system and a coulometer. In this cruise, we used a coulometer Model 3000, which was constructed by Nippon ANS. The systems had a specification as follows:

The seawater dispensing system has an auto-sampler (6 ports), which dispenses seawater from a 300 ml borosilicate glass bottle into a pipette of about 15 ml volume by PC control. The pipette is kept at 20°C by a water jacket, in which water from a water bath set at 20°C is circulated. CO_2 dissolved in a seawater sample is extracted in a stripping chamber of the CO_2 extraction system by adding phosphoric acid (~10 % v/v) of about 2 ml. The stripping chamber is approx. 25 cm long and has a fine frit at the bottom. The acid is added to the stripping chamber from the bottom of the chamber by pressurizing an acid bottle for a given time to push out the right amount of acid. The pressurizing is made with nitrogen gas (99.9999 %). After the acid is transferred to the stripping chamber, a seawater sample kept in a pipette is introduced to the stripping chamber by the same method as in adding an acid. The seawater reacted with phosphoric acid is stripped of CO_2 by bubbling the nitrogen gas through a fine frit at the bottom of the stripping chamber. The CO_2 stripped in the chamber is carried by the nitrogen gas (flow rates is 140 ml min-1) to the coulometer through a dehydrating module. The module consists of two electric dehumidifiers (kept at ~2 °C) and a chemical desiccant ($Mg(ClO_4)_2$).

The measurement sequence such as system blank (phosphoric acid blank), ~1.5 % CO_2 gas in a nitrogen base, sea water samples (6) is programmed to repeat. The measurement of ~1.5 % CO_2 gas is made to monitor response of coulometer solutions purchased from UIC.

ii. A_T

Measurement of A_T was made based on spectrophotometry using a custom-made system (Nippon ANS, Inc.). The system comprises of a water dispensing unit, a HCl titration unit (Hamilton No.2), and a detection unit of a spectrophotometer (TM-UV/VIS C10082CAH, Hamamatsu Photonics, Japan) and an optical source (Mikropack, Germany). The system was automatically controlled by a PC. The water dispensing unit had a water-jacketed pipette and a water-jacketed glass titration cell.

A seawater of approx. 42 ml was transferred from a sample bottle (borosilicate glass bottle; maximum = ~130 ml) into the water-jacketed (25°C) pipette by pressurizing the sample bottle (nitrogen gas), and was introduced into the water-jacketed (25°C) glass titration cell. The introduced seawater was used to rinse the

titration cell. After dumping the seawater used for rinse, Milli-Q water was introduced into the titration cell to rinse it. The rinse by Milli-Q water is repeated twice. Then, a seawater of approx. 42 ml was weighted again by the pipette, and was transferred into the titration cell. Then, for seawater blank, absorbances were measured at three wavelengths (730, 616 and 444 nm). After the measurement, an acid titrant, which was a mixture of approx. 0.05 M HCl in 0.65 M NaCl and bromocresol green (BCG), was added into the titration cell. The volume of acid titrant solution was changed according to expected values of A_T from approx. 2.0 ml to 2.2 ml. The seawater and acid titrant were mixed for 5 minutes by a stirring tip and bubbling by nitrogen gas in the titration cell. Then, absorbances at the three wavelengths were measured again.

Calculation of A_T was made by the following equation:

$$A_T = (-[H^+]_T V_{SA} + M_A V_A) / V_S,$$

where M_A is the molarity of the acid titrant added to the seawater sample, $[H^+]_T$ is the total excess hydrogen ion concentration in the seawater, and V_S, V_A and V_{SA} are the initial seawater volume, the added acid titrant volume, and the combined seawater plus acid titrant volume, respectively. $[H^+]_T$ is calculated from the measured absorbances based on the following equation (Yao and Byrne, 1998):

$$pH_T = -\log[H^+]_T = 4.2699 + 0.002578(35 - S) + \log((R - 0.00131)/(2.3148 - 0.1299R)) - \log(1 - 0.001005S),$$

where S is the sample salinity, and R is the absorbance ratio calculated as:

$$R = (A_{616} - A_{750})/(A_{444} - A_{750}),$$

where A_i is the absorbance at wavelength i nm.

The HCl in the acid titrant was standardized on land (0.049992 mol L-1). The concentrations of BCG were estimated to be approx. 2.0×10^{-6} mol L^{-1} in the sample seawater, respectively.

(4) Shipboard measurement

(4.1) Sampling

i. C_T

All seawater samples were collected from depth with 12 liter Niskin bottles basically at every other stations. The seawater samples for C_T were taken with a plastic drawing tube (PFA tubing connected to silicone rubber tubing) into a 250 ml DURAN® glass bottle. The glass bottle was filled with seawater smoothly from the bottom following a rinse with a seawater of 2 full, bottle volumes. The glass bottle was closed by an inner cap loosely, which was fitted tightly to the bottle mouth after mercuric chloride was added.

At a chemical laboratory on ship, a volume of about 3mL seawater was removed with a plastic pipette from sampling bottles to have a headspace of approx. 1% of the bottle volume. A saturated mercuric chloride of 100 µl was added to poison seawater samples. The seawater samples were kept at 5°C in a refrigerator until analysis. A few hours just before analysis, the seawater samples were kept at 20°C in a water bath.

ii. A_T

All seawater samples were collected from depth using 12 liter Niskin bottles at the same stations as for C_T. The seawater samples for A_T were taken with a plastic drawing tube (PFA tubing connected to silicone rubber tubing) into a 100 ml DURAN® glass bottle. The glass bottle was filled with seawater smoothly from the bottom after rinsing it with a seawater of 2 full, bottle volume.

The samples were stored at about 5°C in a refrigerator. A few hours before analysis, the seawater samples were kept at 25 °C in a water bath.

(4.2) Analysis

i. C_T

At the start of each leg, we calibrated the measuring systems by blank and 5 kinds of Na_2CO_3 solutions

(nominally 500, 1000 1500, 2000, 2500 μmol L^{-1}). As it was empirically known that coulometers do not show a stable signal (low repeatability) with fresh (low absorption of carbon) coulometer solutions. Therefore, we measured ~1.5% CO_2 gas repeatedly until the measurements became stable. Then we started the calibration.

The measurement sequence such as system blank (phosphoric acid blank), ~1.5% CO_2 gas in a nitrogen base, seawater samples (6) was programmed to repeat. The measurement of ~1.5% CO_2 gas was made to monitor response of coulometer solutions (from UIC, Inc. or in-house made). For every renewal of coulometer solutions, certified reference materials (CRMs, batch 149, certified value = 2011.67 ± 0.24 μmol kg^{-1}) provided by Prof. A. G. Dickson of Scripps Institution of Oceanography were analyzed. In addition, in-house reference materials (RM) (batch Q34) were measured at the initial, intermediate and end times of a coulometer solution's lifetime.

The preliminary values were reported in a data sheet on the ship. Repeatability and vertical profiles of C_T based on raw data for each station helped us check performances of the measuring systems.

In the cruise, we finished all the analyses for C_T on board the ship.

ii. A_T

We analyzed reference materials (RM, QM34), which were produced for C_T measurement by JAMSTEC, but were efficient also for the monitor of A_T measurement. In addition, certified reference materials (CRM, batches 149, certified value = 2224.69±0.18 μmol kg^{-1}) were analyzed periodically to monitor systematic differences of measured A_T. The reported values of A_T were set to be comparable to the certified value of the batch 149.

The preliminary values were reported in a data sheet on ship. Repeatability calculated from replicate samples and vertical profiles of A_T based on raw data for each station helped us check performance of the measuring system.

In the cruise, we finished all the analyses for A_T on board the ship.

(5) Quality control

i. C_T

We conducted quality control of the data after return to a laboratory on land. With calibration factors, which had been determined on board a ship based on blank and 5 kinds of Na_2CO_3 solutions, we calculated C_T of CRM (batches 149), and plotted the values as a function of sequential day, separating legs and the systems used. There were no statistically-significant trends of CRM measurements.

The repeatability of sample measurements was estimated to be 1.23 μmol kg^{-1}, which was calculated from 56 differences of replicate measurements.

ii. A_T

Temporal changes of A_T, which originate from analytical problems, were monitored by measuring A_T of CRM. We found no abnormal measurements during the cruises.

The repeatability of measurements was estimated to be 1.1 μmol kg^{-1}, which was calculated from 52 differences of replicate measurements.

References

Dickson, A. G., C. L. Sabine and J. R. Christian eds. (2007) *Guide to best practices for ocean CO_2 measurements*, PICES Special Publication 3, 191 pp.

Yao, W. and R. B. Byrne (1998) Simplified seawater alkalinity analysis: Use of linear array spectrometers. Deep-Sea Research 45, 1383-1392.

3.8 Calcium

(1) Personnel

Etsuro Ono (JAMSTEC)

(2) Objectives

Calcium is one of the major dissolved components in the sea water. Many corals and marine organisms consume calcium to produce calcium carbonate ($CaCO_3$) as their shells and skeletons.

According to the recent IPCC report, ocean acidification is progressing, because about 30% of the anthropogenic carbon dioxide has been absorbed into the ocean. Ocean acidification is characterized by an increase of H^+ (i.e., a decrease of pH) and a concurrent decrease of carbonate ion concentration (CO_3^{2-}). The decrease of CO_3^{2-} promotes dissolution of $CaCO_3$, which is unfavorable to marine calcifying organisms.

In this cruise, to evaluate dissolution and precipitation of calcium carbonate, we measured directly the concentration of calcium in the sea water in a subantarctic region of the Southern Pacific Ocean and the Antarctic Ocean.

(3) Instruments

The analysis system consisted of a modified Dissolved Oxygen Titrator (DOT-01: Kimoto Electronic Co. Ltd.) which had a band-pass filter centered at 620 nm, a xenon light source, a photodiode detector, and Auto-Burette system with control unit (Kimoto Electronic Co. Ltd.).

(4) Sampling and analytical methods

The samples from niskin sampler were collected to 60 ml of HDPE bottles from niskins. After sampling, the samples were stored at a cool and dark place for about 7 days before measurement.

The measurement method of calcium was based on a photometric method suggested by Culkin and Cox (1966).

The reagents and the procedure of the measurement in this cruise were as follows:

- Reagents

  Titrant : 0.02 mol/l EGTA (Ethylene Glycol Tetraacetic Acid)

  Buffer : Mixture solution of 0.4 mol/l NH_4Cl and 0.4 mol/l NH_3

  Indicator : 4 mmol/l Zincon® solution

  Zinc source : Mixuture solution of 8 mmol/l $ZnSO_4$ and 8 mmol/l EGTA

- Pretreatment of sea samples

  10 ml of seawater was transferred into a tall beaker by a volumetric pipet.

  A stirrer tip was put into the sample.

  1 ml of buffer solution was added to keep the solution at pH 9.5.

  1 ml of Zincon indicator was added which stained the sample red.

  1 ml of Zinc source was added which turned the sample blue.

  Mille-Q water was added such that the overall solution was approx. 80 ml.

  (When measuring the acidic standard solution, the solution was neutralized by the solution of sodium hydroxide (NaOH) before buffer solution was added.)

(5) Preparation of standard solution

The in-house Ca-standard was prepared for determination of the concentration of EGTA titrant. The concentration of the standard solution was 10 mmol/l, which was calculated by the gravimetric method. For preparation of the standard solution, pure $CaCO_3$ produced by NMIJ (CRM 3013-a) was used as Ca-source.

Pure $CaCO_3$ was in advance dried in an oven at 110°C for 2 hours and accurately weighed at 1.0009 g, then 50 ml of 0.5M HCl solution was added to $CaCO_3$ until $CaCO_3$ was dissolved completely and degas CO_2 from the solution. After bubbles in the degassing solution calmed down, the solution was transferred to a 1000 ml volumetric flask, with pure water added until 1000 ml, and the weight of the whole solution was measured. The acidity of the standard solution was about pH = 2.0.

The density of the Ca-standard solution was necessary to calculate the concentration of the standard

solution. The method is described in Section 3.3 (Density).

(6) Calibration of EGTA titrant

In this cruise, two standard solutions were measured for monitoring the concentration of titrant. One is the in-house Ca-standard and the other is 1000 mg/L Calcium Standard Solution produced by Wako Pure Chemical Industries, Ltd. Volume of the standard solution for the monitoring measurement was 10 ml for the in-house Ca-standard and 4 ml for the Wako standard, so that calcium level was close to that of the sea samples.

Figure 3.8.1 shows the end point values (ml) of titration and their trends. The end point values tend to decrease. Also, the trend of the value in the in-house Ca-standard measurement is similar to that in the Wako standard. Thus, it's assumed that the concentration of EGTA titrant was increasing during the sample measurements because of evaporation of solvent caused by the headspace in the bottle of titrant. The variation of the concentration was not negligible, because the magnitude of that was more than 0.1% c.v. Therefore, the calibration of EGTA titrant was carried out by fitting a linear function calculated from the in-house Ca-standard.

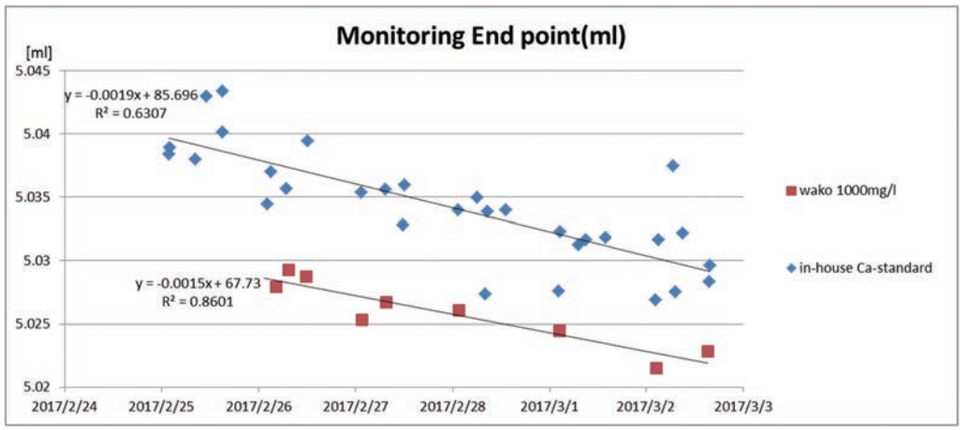

Fig. 3.8.1 Plots of the end point of standard measurements.

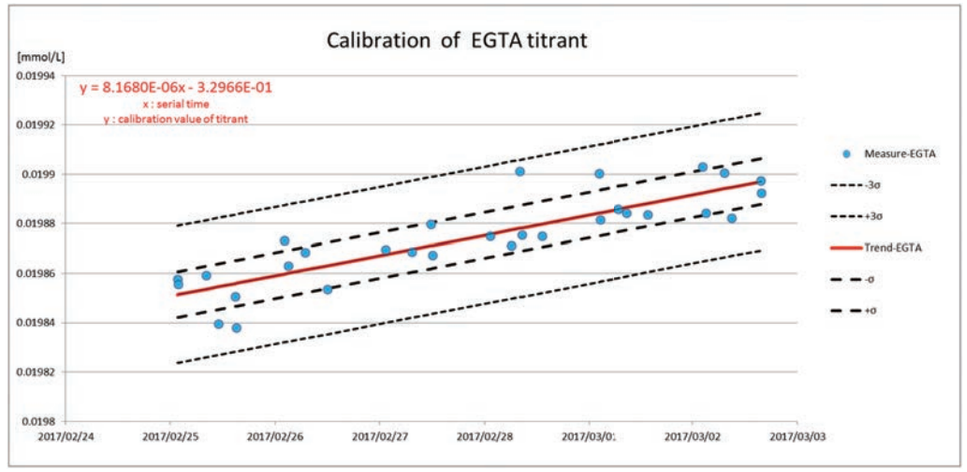

Fig. 3.8.2 Plots and calibration line for EGTA titrant.

(7) Interference to titrations by magnesium

A previous work (Culkin and Cox, 1966) points out that magnesium (Mg) and strontium (Sr) cause positive bias to the titrated volume of Ca because of their interference with the reaction between EGTA and Ca; the bias caused by Mg was 0.729% and by Sr was 0.388%.

Also, in our preparation before the cruise, when Ca-standard with Mg source in same proportion as sea water was measured, it was suggested that the end point of that was increased by 0.745% as compared with the sample without Mg. This result agreed with the previous work.

Although Mg interferes the titration of Ca in this titrating condition, no correction was given to the data submitted in this cruise.

Table 3.8.1 Results of interference by Mg.

	Average end point [ml]	2σ	N
No Mg	5.1136	0.0076	9
Add Mg	5.1517	0.0046	9

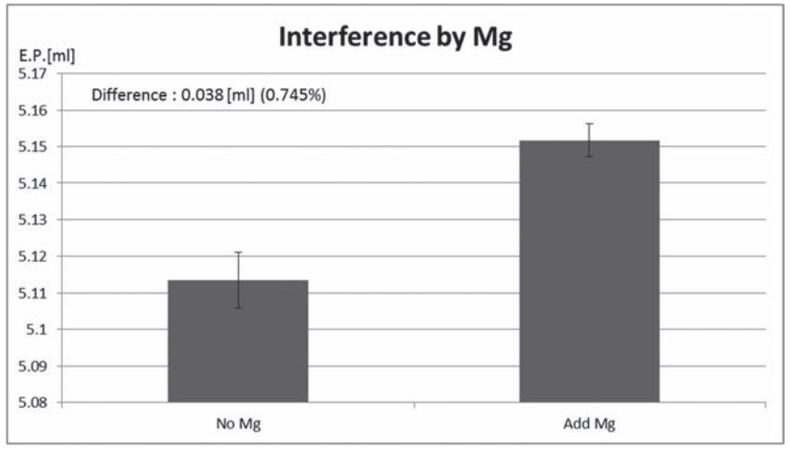

Fig. 3.8.3 Comparison of the end point for Ca-standard added Mg and not containing Mg.

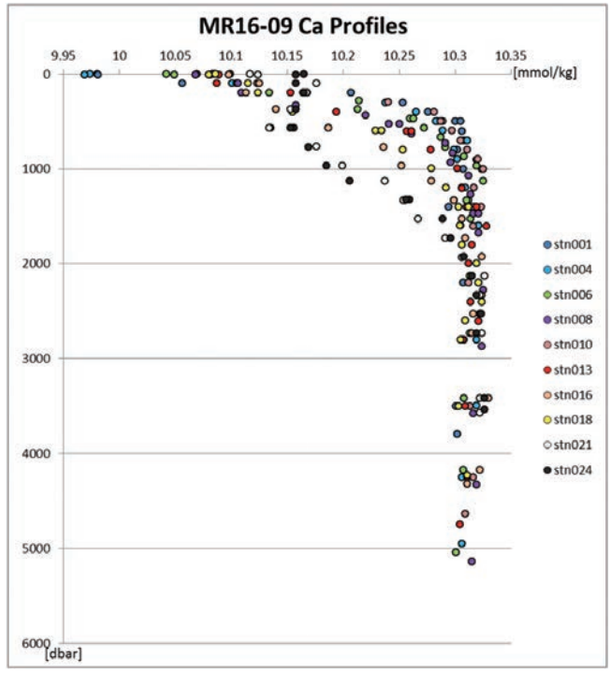

Fig. 3.8.4 Vertical profiles of calcium.

(8) Performance

The replicate samples were collected from 2 layers at each station to examine repeatability. The precision of replicate samples was estimated at 0.0052 mmol kg^{-1} (n=20 pairs). We used the SOP23 method to estimate the repeatability.

There were no major troubles with the analysis during the cruise.

References

F. Culkin, and R. A. Cox (1966) Sodium, potassium, magnesium, calcium and strontium in sea water. Deep-Sea Res., 13, 789-804.

3.9 Dissolved Organic Carbon

(1) Personnel

Masahito Shigemitsu (JAMSTEC): Principal investigator

Masahide Wakita (JAMSTEC)

Akihiko Murata (JAMSTEC)

(2) Objective

Dissolved organic matter (DOM) in the ocean is affected by advection and mixing, and DOM has refractory fractions which resist biological degradation. Such a characteristic of DOM plays an important role in the ocean biogeochemistry, and DOM contributes to the biological pump, which makes the marine dissolved organic carbon (DOC) the largest ocean reservoir of reduced carbon.

In this cruise, we aim to gain insights into the behavior of DOC in the Southern Ocean which is considered to be a key region for the oceanic carbon cycle.

(3) Sampling

Seawater samples were obtained from Niskin bottles on a CTD-rosette system at 10 stations (Figure 3.9.1). Each sample taken in the upper 250 m was filtered using a pre-combusted (450 °C for 4 hours) 47-mm Whatman GF/F filter. The filtration was carried out by connecting a spigot of the Niskin bottle through silicone tube to an inline plastic filter holder. Filtrates were collected in acid-washed 60 mL High Density Polyethylene (HDPE) bottles, and were immediately stored frozen until analysis. Other samples taken below 250 m were unfiltered and stored in the same way.

(4) DOC concentrations

The frozen samples were thawed at room temperature, and acidified to pH < 2 with hydrochloric acid. Then, concentrations of DOC were measured by using a Shimadzu TOC-L system. The instrument conditions were as follows:

Combustion temperature	720 °C
Carrier gas	G1 Air
Carrier flow rate	150 ml/min
Sample sparge time	~10 min
Minimum number of injections	4
Maximum number of injections	6
CV maximum	2.0%
Injection volume	100 µL

Standardization was achieved using glucose. All DOC analyses were referenced against the reference material provided by Hansell Laboratory, University of Miami. The precision of DOC measurements, based on the standard deviation of the references analyzed throughout all the runs, was less than 0.5 µmol kg^{-1} and the repeatability was calculated to be ~1.0 µmol kg^{-1} by using a statistical procedure (SOP23) in DOC (1994).

(5) Reference

DOE (1994) Handbook of methods for the analysis of the various parameters of the carbon dioxide system in sea water; version 2. A. G. Dickson and C. Goyet (eds), ORNL/CDIAC-74.

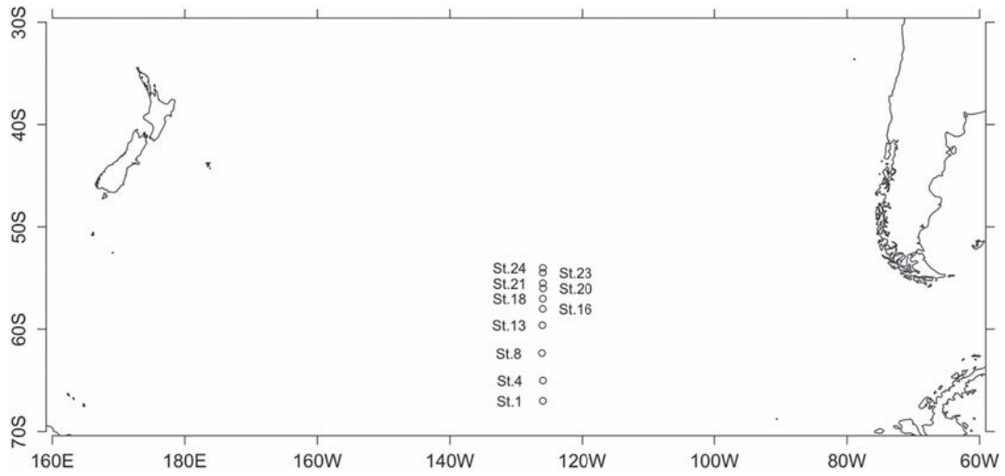

Figure 3.9.1 Map showing sampling sites

3.10 Chlorophyll *a*

(1) Personnel

Kosei Sasaoka (JAMSTEC) (Leg 3)

Takuhei Shiozaki (JAMSTEC) (Leg 2)

Hironori Sato (MWJ) (Leg 1)

Masanori Enoki (MWJ) (Leg 3)

Misato Kuwahara (MWJ) (Leg 3)

Haruka Tamada (MWJ) (Leg 3)

Ei Hatakeyama (MWJ) (Leg 3)

(2) Objectives

Chlorophyll *a* is one of the most convenient indicators of phytoplankton stock, and has been used extensively for the estimation of phytoplankton abundance in various aquatic environments. In this study, we investigated horizontal and vertical distribution of phytoplankton around the Chilean coast (Leg 2) and along the P17E section (Leg 3) in the Southern Ocean. The chlorophyll *a* data is also utilized for calibration of fluorometers, which were installed in the surface water monitoring and CTD profiler system.

(3) Instrument and Method

Seawater samples were collected in 280 mL (Leg 2) and 500 mL (Leg 3) brown Nalgene bottles without head-space, and samples from the surface (0 m) were collected using a bucket. The whole samples were gently filtrated by low vacuum pressure (<0.02 MPa) through Whatman GF/F filter (diameter 25 mm) in the dark room. Whole volume of each sampling bottle was precisely measured in advance. After filtration, phytoplankton pigments were immediately extracted in 7 ml of N,N-dimethylformamide (DMF), and samples were stored at –20°C under the dark condition to extract chlorophyll *a* more than 24 hours. Chlorophyll *a* concentrations were measured by the Turner fluorometer (10-AU-005, TURNER DESIGNS), which was previously calibrated against a pure chlorophyll *a* (Sigma-Aldrich Co., LLC) (Figure 3.10.1). To estimate the chlorophyll *a* concentrations, we applied to the fluorometric "Non-acidification method" (Welschmeyer, 1994).

(4) Results

Vertical profiles of chlorophyll *a* concentrations around the Chilean coast (Leg 2) and along the P17E section (Leg 3) during the cruise are shown in Figure 3.10.2 and Figure 3.10.3, respectively. Cross section of chlorophyll *a* concentrations along the P17E line (Leg 3) is shown in Figure 3.10.4. To estimate the measurement precision, 34-pairs of replicate samples were obtained from hydrographic casts (Leg 3). All pairs of the replicate samples were collected in 500 ml bottles. Although the absolute values of the difference between 34-pairs replicate samples were 0- 0.07 μg/L, those standard deviation were approximately 0.013.

(5) Reference

Welschmeyer, N. A. (1994): Fluorometric analysis of chlorophyll a in the presence of chlorophyll b and pheopigments. Limnor. Oceanogr., 39, 1985-1992.

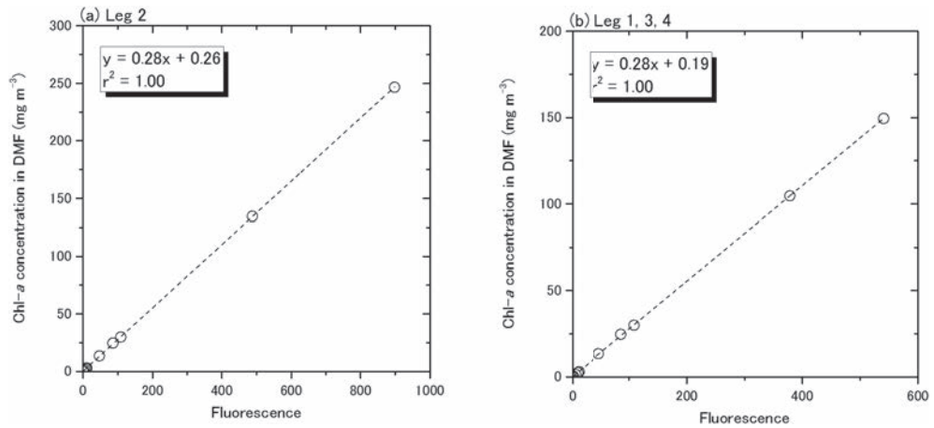

Figure 3.10.1 Relationships between pure chlorophyll *a* concentrations and fluorescence light intensity ((a) Leg 2, (b) Leg 1, 3, 4).

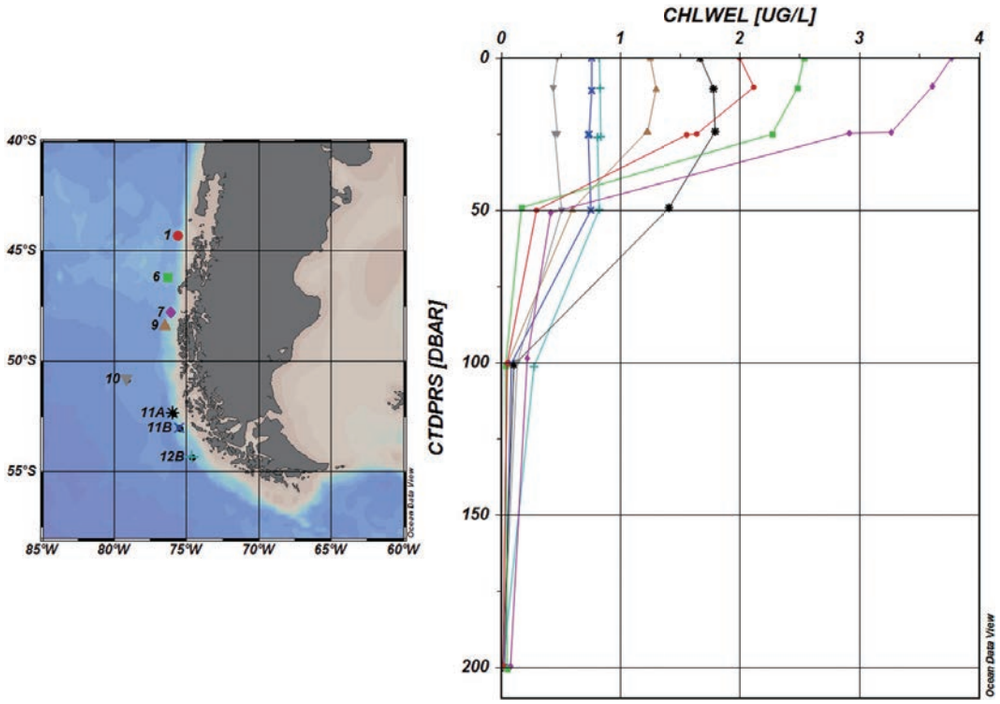

Figure 3.10.2 Vertical profiles of chlorophyll *a* concentrations around the Chilean coast (Leg 2) obtained from hydrographic casts.

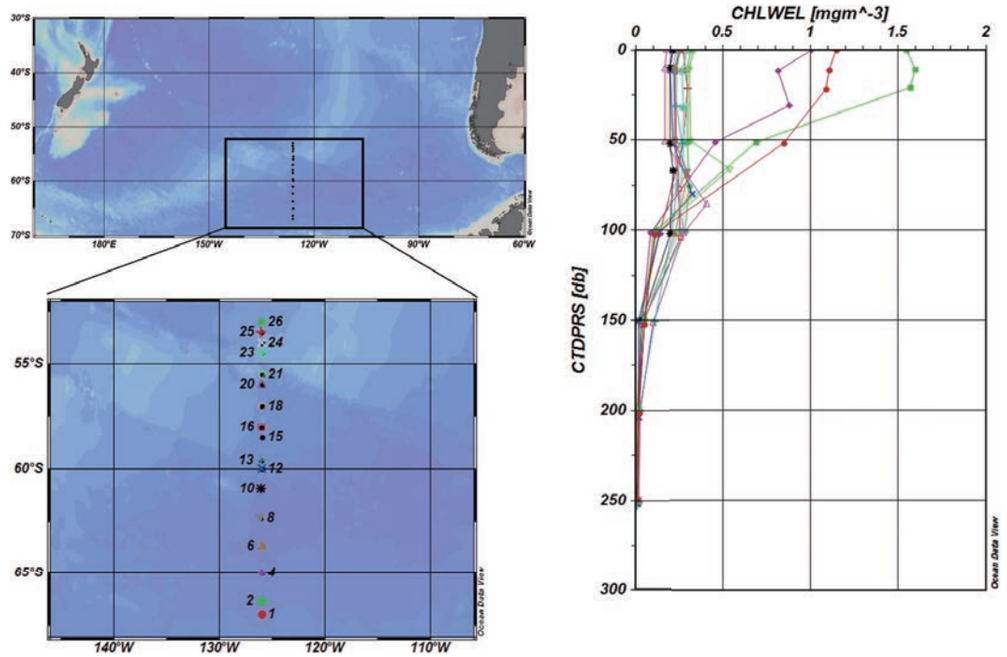

Figure 3.10.3 Vertical profiles of chlorophyll *a* concentrations along the P17E section (Leg 3) obtained from hydrographic casts.

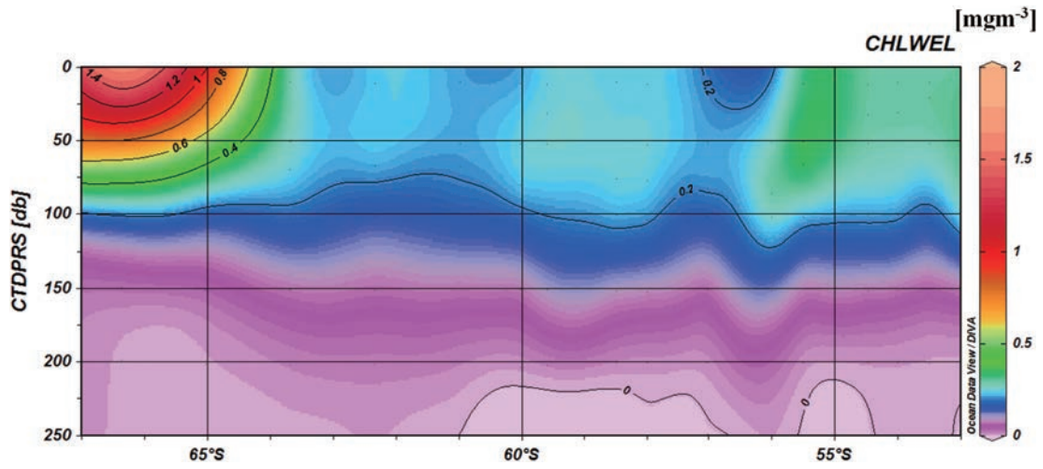

Figure 3.10.4 Cross section of chlorophyll *a* concentrations along the P17E-line (Leg 3) obtained from hydrographic casts.

3.11 Absorption Coefficients of Particulate Matter and Colored Dissolved Organic Matter (CDOM)

(1) Personnel

Kosei Sasaoka (JAMSTEC) (Leg 3)

(2) Objectives

Absorption coefficients of particulate matter (phytoplankton and non-phytoplankton particles, defined as 'detritus') and colored (chromophoric) dissolved organic matter (CDOM) play an important role in determining the optical properties of seawater. In particular, light absorption by phytoplankton is a fundamental process of photosynthesis, and their chlorophyll *a* (Chl-*a*) specific coefficient, a^*_{ph}, can be essential factors for bio-optical models to estimate primary productivities. Absorption coefficients of CDOM are also important parameters to validate and develop the bio-optical algorithms for ocean color sensors, because the absorbance spectrum of CDOM overlaps that of Chl-*a*. The global CDOM distribution appears regulated by a coupling of biological, photochemical, and physical oceanographic processes all acting on a local scale, and greater than 50% of blue light absorption is controlled by CDOM (Siegel et al., 2002). Additionally, some investigators have reported that CDOM emerges as a unique tracer for diagnosing changes in biogeochemistry and the overturning circulation, similar to dissolved oxygen (e.g., Nelson et al., 2010). The objectives of this study are to understand the North-South variability of light absorption by phytoplankton and CDOM along the P17E (126°W) section in the Southern Ocean.

(3) Methods

Seawater samples for absorption coefficient of total particulate matter ($a_p(\lambda)$) were performed using Niskin bottles and a bucket above 100m depth at 7 stations along the P17E section (Fig.3.11.1, Table 3.11.1). Samples were collected in 3000ml dark bottles and filtered (500 - 3000 ml) through 25-mm What-man GF/F glass-fiber filters under a gentle vacuum (< 0.013 MPa) on board in the dark room. After filtration, the optical density of total particulate matter on filter ($OD_{fp}(\lambda)$) between 350 and 750 nm at a rate of 1.0 nm was immediately measured by an UV-VIS recording spectrophotometer (UV-2400, Shimadzu Co.), and absorption coefficient was determined from the OD according to the quantitative filter technique (QFT) (Mitchell, 1990). A blank filter with filtered seawater was used as reference. All spectra were normalized to 0.0 at 750nm to minimize difference between sample and reference filter. To determine the optical density of non-pigment detrital particles ($OD_{fd}(\lambda)$), the filters were then soaked in methanol for a few hours and rinsed with filtered seawater to extract and remove the pigments (Kishino et al., 1985), and its absorption coefficient was measured again by UV-2400. These measured optical densities on filters ($OD_{fp}(\lambda)$ and $OD_{fd}(\lambda)$) were converted to optical densities in suspensions ($OD_{sp}(\lambda)$ and $OD_{sd}(\lambda)$) using the pathlength amplification factor of Cleveland and Weidemann (1993) as follows:

$$OD_{sp}(\lambda) = 0.378\ OD_{fp}(\lambda) + 0.523\ OD_{fp}(\lambda)^2 \text{ and}$$

$$OD_{sd}(\lambda) = 0.378\ OD_{fd}(\lambda) + 0.523\ OD_{fd}(\lambda)^2.$$

The absorption coefficient of total particles ($a_p(\lambda)$ (m^{-1})) and non-pigment detrital particles ($a_d(\lambda)$ (m^{-1})) are computed from the corrected optical densities ($OD_s(\lambda)$):

$$a_p(\lambda) = 2.303 \times OD_{sp}(\lambda) / L \quad (L = V / S), \text{ and}$$

$$a_d(\lambda) = 2.303 \times OD_{sd}(\lambda) / L \quad (L = V / S),$$

Where S is the clearance area of the filter (m^2) and V is the volume filtered (m^3). Absorption coefficient of phytoplankton ($a_{ph}(\lambda)$) was obtained by subtracting $a_d(\lambda)$ from $a_p(\lambda)$ as follows:

$$a_{ph}(\lambda) = a_p(\lambda) - a_d(\lambda).$$

Finally, we calculated chl-*a* normalized specific absorption spectra (a^*_{ph}) to divide a_{ph} by chl-*a* concentrations

obtained from same hydrographic casts.

Seawater samples for absorption coefficient of CDOM ($a_y(\lambda)$) were collected in 250ml bottles using Niskin bottles and a bucket from surface to bottom (Fig. 3.11.1, Table 3.11.1). CDOM samples were filtered using 0.2 μm Nuclepore polycarbonate filters on board. Optical densities of the CDOM ($OD_y(\lambda)$) in this filtered seawater were recorded against UV-2600 in the range from 300 to 800 nm using 10-cm pathlength quartz cells. Milli-Q water was used as a base line. A blank (Milli-Q water versus Milli-Q water) was subtracted from each wavelength of the spectrum. The absorption coefficient of CDOM ($a_y(\lambda)$ (m^{-1})) was calculated from measured optical densities ($OD_y(\lambda)$) as follows:

$$a_y(\lambda) = 2.303 \times OD_y(\lambda) / L \text{ (L is the cuvette path-length (m))}.$$

(4) Preliminary results

Chl-*a* normalized specific absorption spectra (a^*_{ph}) were shown in Fig.3.11.2. Vertical profiles and cross section of CDOM (as absorption coefficient at 325 nm, unit = m^{-1}) along the P17E section were shown in Fig. 3.11.3 and Fig.3.11.4.

(5) References

Cleveland, J.S. and Weidemann, A.D., 1993, Quantifying absorption by aquatic particles: a multiple scattering correction for glass fiber filters, Limnology and Oceanography, 38, 1321-1327.

Kishino, M., Takahashi, M., Okami, N. and Ichimura, S., 1985, Estimation of the spectral absorption coefficients of phytoplankton in the sea, Bulletin of Marine Science, 37, 634-642.

Mitchell, B.G., 1990, Algorithms for determining the absorption coefficient of aquatic particulates using the quantitative filter technique (QFT), Ocean Optics X, SPIE 1302, 137-148.

Nelson, N. B., D. A. Siegel, C. A. Carlson, and C. M. Swan, 2010, Tracing global biogeochemical cycles and meridional overturning circulation using chromophoric dissolved organic matter, Geophys. Res. Lett., 37, L03610, doi:10.1029/2009GL042325.

Siegel, D.A., Maritorena, S., Nelson, N.B., Hansell, D.A., Lorenzi-Kayser, M., 2002, Global distribution and dynamics of colored dissolved and detrital organic materials. J. Geophys. Res., 107, C12, 3228, doi:10.1029/2001JC000965.

Table 3.11.1 List of sampling stations for absorption coefficients of phytoplankton (Ap) and CDOM during MR16-09 (Leg 3).

Station	Date (UTC)	Time (UTC)	Latitude	Longitude	Sampling type	Cast No.	Sampling depth (db)	
							Particle absorbance	CDOM absorbance
1	02/16/2017	7:39	67.00 S	125.98 W	CTD + Bucket	2	0, Chlmax(20), 10, 50, 100	3797, Chlmax(20), 3000, 1000, 800, 600, 400, 200, 100, 50, 10, 0
4	02/17/2017	5:28	65.02 S	125.96 W	CTD + Bucket	1	0, Chlmax(30), 10, 50, 100	4953, Chlmax(30), 3000, 1000, 800, 600, 400, 200, 100, 50, 10, 0
8	02/18/2017	22:29	62.34 S	126.11 W	CTD + Bucket	1	0, Chlmax(65), 10, 50, 100	5143, Chlmax(65), 3080, 1070, 830, 630, 430, 200, 100, 50, 10, 0
12	02/20/2017	0:36	60.01 S	125.98 W	CTD + Bucket	1	0, Chlmax(80), 10, 50, 100	4683, Chlmax(80), 2930, 970, 770, 570, 370, 200, 100, 50, 10, 0
16	02/20/2017	20:58	58.01 S	126.00 W	CTD + Bucket	1	0, Chlmax(75), 10, 50, 100	4321, Chlmax(75), 2930, 970, 770, 570, 370, 200, 100, 50, 10, 0
21	02/21/2017	19:47	55.50 S	125.98 W	CTD + Bucket	1	0, Chlmax(65), 10, 50, 100	3576, Chlmax(65), 2930, 970, 770, 570, 370, 200, 100, 50, 10, 0
24	02/22/2017	11:19	54.01 S	125.98 W	CTD + Bucket	1	0, Chlmax(30), 10, 50, 100	3541, Chlmax(30), 2930, 970, 770, 570, 370, 200, 100, 50, 10, 0

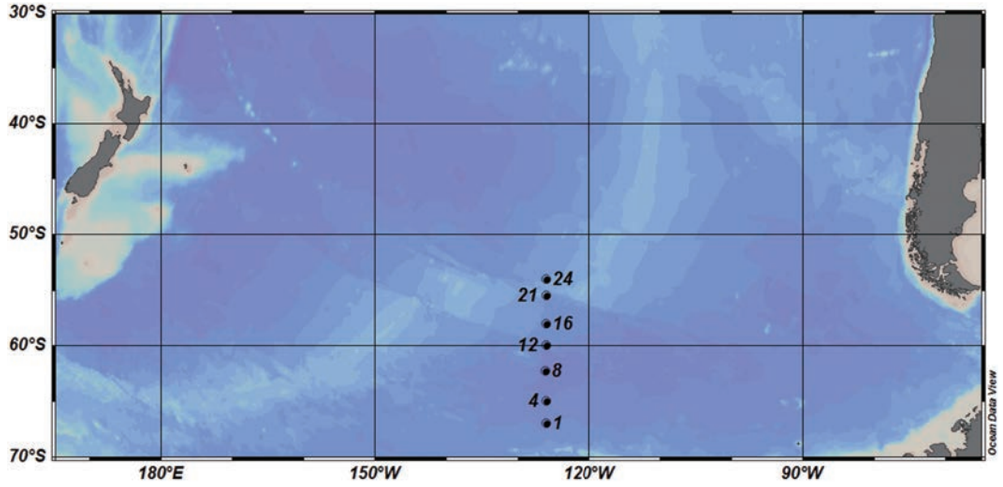

Fig. 3.11.1 Location of 7-sampling stations for absorption coefficients of phytoplankton and CDOM along the P17E section in the Southern Ocean during MR16-09 (Leg 3).

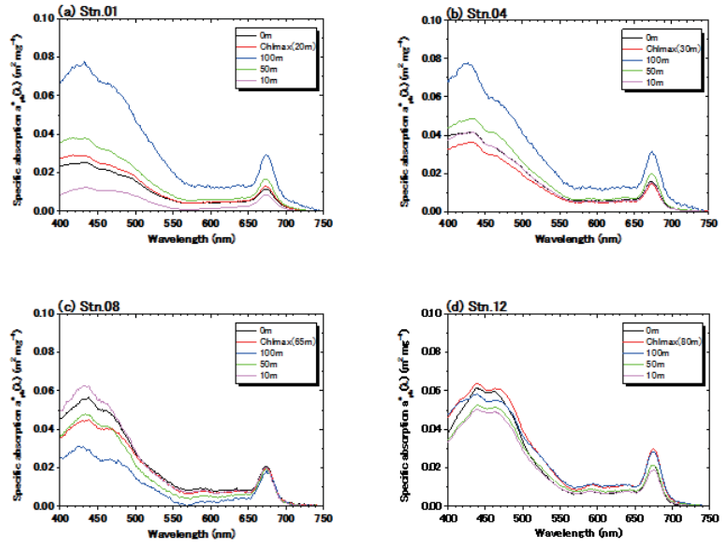

Fig. 3.11.2 Chlorophyll-specific phytoplankton absorption coefficient spectra ($a^*_{ph}(\lambda)$) at 400-750 nm. All spectra were normalized to 0.0 at 750 nm.

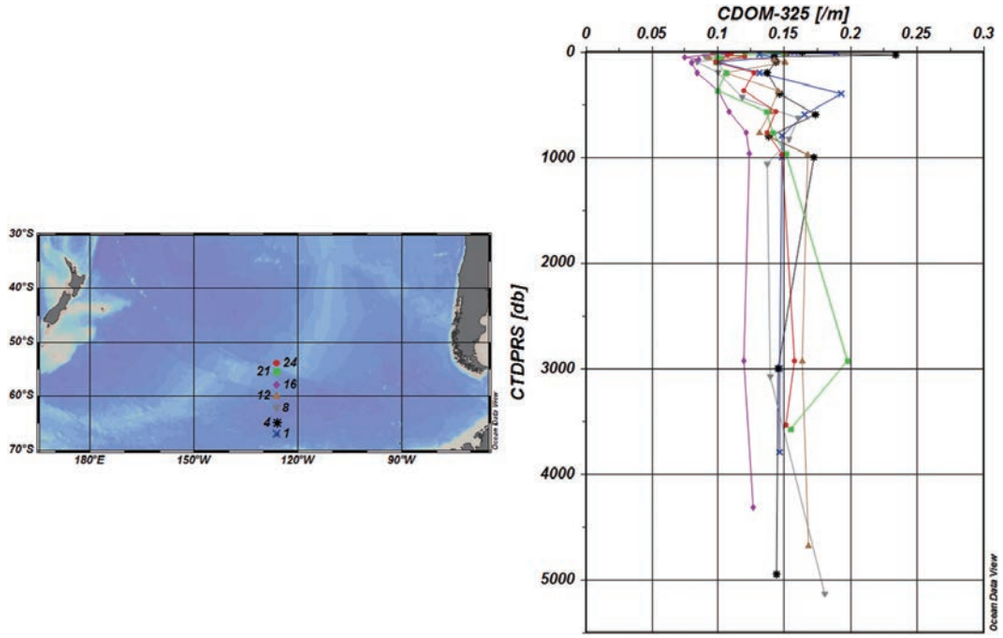

Fig. 3.11.3 Vertical profiles of CDOM (as absorption coefficient at 325 nm, unit = m^{-1}) at 7-stations along the P17E section.

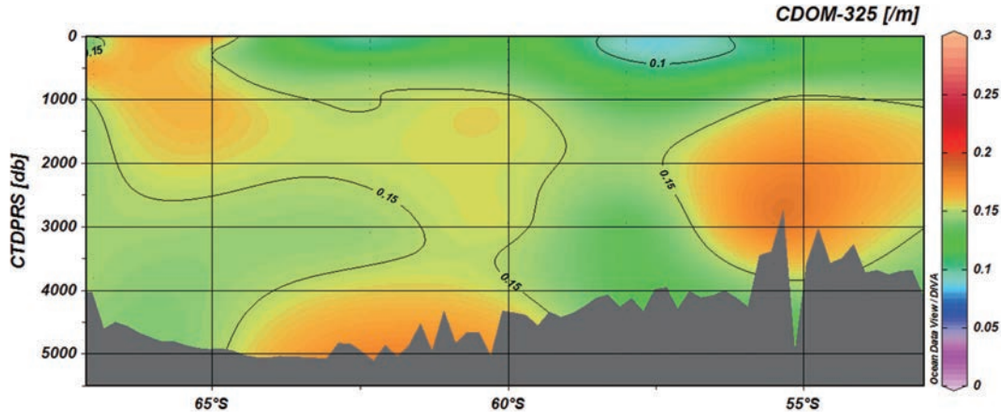

Fig. 3.11.4 Contours showing distribution of CDOM (as absorption coefficient at 325 nm, unit = m^{-1}) along the P17E section.

3.12 Lowered Acoustic Doppler Current Profiler

(1) Personnel

Shinya Kouketsu (JAMSTEC) (principal investigator)

Hiroshi Uchida (JAMSTEC)

Katsurou Katsumata (JAMSTEC)

(2) Overview of the equipment

An acoustic Doppler current profiler (ADCP) was integrated with the CTD/RMS package. The lowered ADCP (LADCP), Workhorse Monitor WHM300 (Teledyne RD Instruments, San Diego, California, USA), which has 4 downward facing transducers with 20-degree beam angles, rated to 6000 m. The LADCP makes direct current measurements at the depth of the CTD, thus providing a full profile of velocity. The LADCP was powered during the CTD casts by a 48 volts battery pack. The LADCP unit was set for recording internally prior to each cast. After each cast the internally stored observed data was uploaded to the computer on-board. By combining the measured velocity of the sea water and bottom with respect to the instrument, shipboard-ADCP velocities, and shipboard navigation data during the CTD cast, the absolute velocity profile were obtained with the method in Visbeck, 2002.

The instrument used in this cruise was as follows.

Teledyne RD Instruments, WHM300

S/N 20754 (downward looking), S/N 18324 (upward looking)

(3) Data collection

In this cruise, data were collected with the following configuration.

Bin size: 4.0 m

Number of bins: 25

Pings per ensemble: 1

Ping interval: 1.0 sec

Reference

Visbeck, M. (2002): Deep velocity profiling using Lowered Acoustic Doppler Current Profilers: Bottom track and inverse solutions. *J. Atmos. Oceanic Technol.*, **19**, 794-807.

3.13 XCTD

March 3, 2017

(1) Personnel

Hiroshi Uchida (JAMSTEC)

Shinya Okumura (NME)

Koichi Inagaki (NME)

Ryo Kimura (NME)

Masanori Murakami (NME crew)

(2) Objectives

XCTD (eXpendable Conductivity, Temperature and Depth profiler) measurements were carried out to substitute CTD casts and to evaluate the fall rate equation and the thermal bias by comparing with CTD (Conductivity, Temperature and Depth profiler) measurements.

(3) Instrument and Method

The XCTD used was XCTD-4 (Tsurumi-Seiki Co., Ltd., Yokohama, Kanagawa, Japan) with an MK-150N deck unit (Tsurumi-Seiki Co., Ltd.). The manufacturer's specifications are listed in Table 3.13.1. In this cruise, the XCTD probes were deployed by using 8-loading automatic launcher (Tsurumi-Seiki Co., Ltd.) or a hand launcher (stn. P17E_008_2). For comparison with CTD, XCTD was deployed at about 10 minutes after the beginning of the down cast of the CTD (P17E_8, 16, 22 and 23). For correction of the sound velocity profile used in the bathymetry observation, XCTD-1 was deployed near station P17E_1. Also, two XCTD-4 were deployed at CO_2 buoy deployment locations at longitude of 140°W and 160°W.

The fall-rate equation provided by the manufacturer was initially used to infer depth Z (m), $Z = at - bt^2$, where t is the elapsed time in seconds from probe entry into the water, and a (terminal velocity) and b (acceleration) are the empirical coefficients (Table 3.13.2).

(4) Data Processing and Quality Control

The XCTD data were processed and quality controlled based on a method by Uchida et al. (2011). Differences between XCTD and CTD depths were shown in Fig. 3.13.1. The terminal velocity error was estimated for the XCTD-4 (Table 3.13.2). The XCTD-4 data were corrected for the depth error by using the estimated terminal velocities. Differences of temperature on pressure surfaces were examined by using side-by-side XCTD and CTD data (Fig. 3.13.3). Average thermal bias below 900 dbar was 0.014 °C. The XCTD data were corrected for the thermal bias. Differences of salinity on reference temperature surfaces were examined by using CTD data (Fig. 3.13.4). The XCTD data were corrected for the estimated salinity bias.

(5) Results

Temperature-salinity plot using the quality controlled XCTD data is shown in Fig. 3.13.3.

(6) References

Kizu, S., H. Onishi, T. Suga, K. Hanawa, T. Watanabe, and H. Iwamiya (2008): Evaluation of the fall rates of the present and developmental XCTDs. *Deep-Sea Res I*, **55**, 571–586.

Uchida, H., K. Shimada, and T. Kawano (2011): A method for data processing to obtain high-quality XCTD data. *J. Atmos. Oceanic Technol.*, **28**, 816–826.

Uchida, H., A. Murata, and T. Doi (eds.) (2014): WHP P10 Revisit in 2011 Data Book, 179 pp., JAMSTEC.

Uchida, H., K. Katsumata, and T. Doi (eds.) (2015): WHP P14S/S04I Revisit in 2012/2013 Data Book, 187 pp., JAMSTEC.

Uchida, H and T. Doi (eds.) (2016): WHP P01 Revisit in 2014 Data Book, 149 pp., JAMSTEC, ISBN 978-4-901833-22-6.

Table 3.13.1. Manufacturer's specifications of XCTD-4.

Parameter	Range	Accuracy
Conductivity	0 ~ 60 mS cm^{-1}	±0.03 mS cm^{-1}
Temperature	–2 ~ 35 °C	±0.02 °C
Depth	0 ~ 1850 m	5 m or 2%, whichever is greater *

* Depth error is shown in Kizu et al (2008).

Table 3.13.2. Manufacturer's coefficients for the fall-rate equation.

Model	*a* (terminal velocity, m/s)	*b* (acceleration, m/s^2)	*e* (terminal velocity error, m/s)
XCTD-4	3.68081	0.00047	–0.0197

Table 3.13.3. Thermal biases of the XCTD temperature data.

Cruise	Average thermal bias (°C)	Depth range	Source
MR09-01	0.016	>= 1100 dbar	Uchida et al. (2011)
KH-02-3	0.019	>= 1100 dbar	Uchida et al. (2011)
MR11-08	0.014	>= 1100 dbar	Uchida et al. (2014)
MR12-05	0.009	>= 400 dbar	Uchida et al. (2015)
MR14-04	0.011	>= 900 dbar	Uchida et al. (2016)
MR15-05	–0.00	>= 900 dbar	Cruise report of MR15-05
MR16-09	0.014	>= 900 dbar	this report
Mean	0.011 ± 0.007		

Table 3.13.4. Salinity biases of the XCTD data.

XCTD station	Salinity bias	Reference temperature (°C)	Reference salinity	Reference CTD stations
8	–0.007	1.7	34.7306	7, 8, 9
22	0.008	2.4	34.6366	22, 23
23	0.017	2.4	34.6366	22, 23

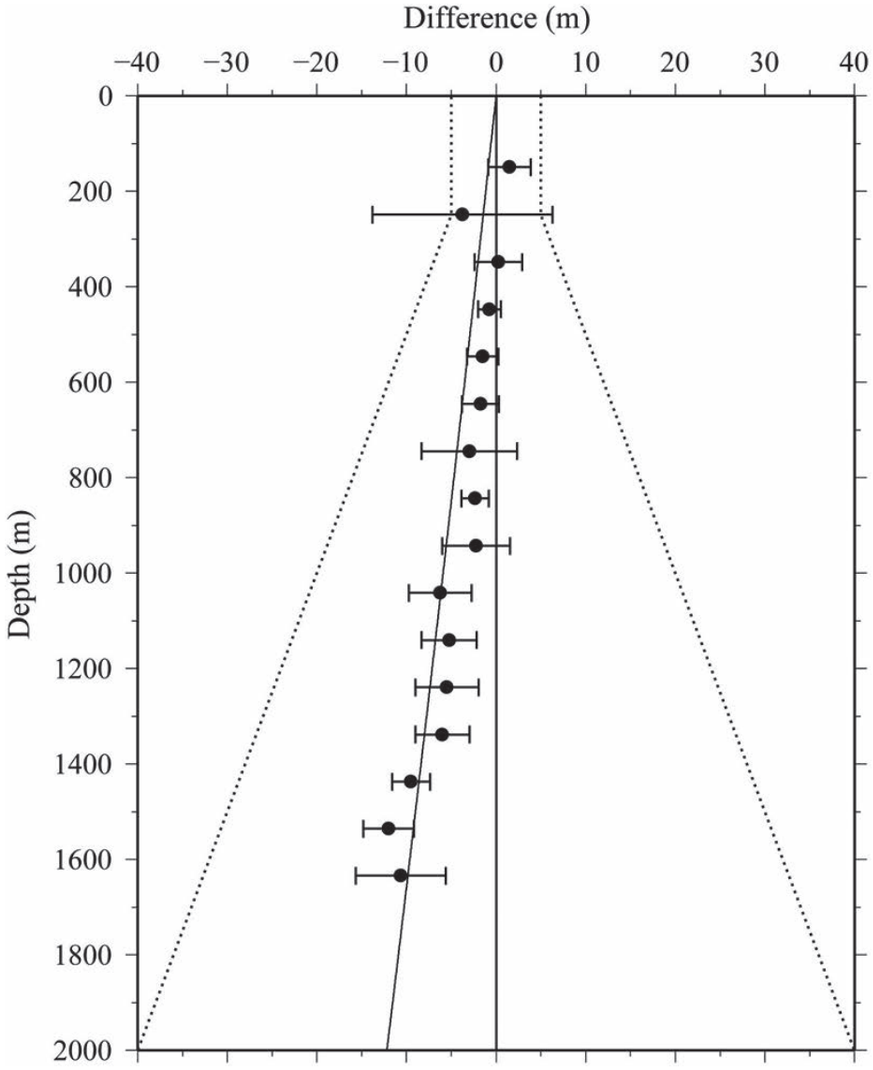

Figure 3.13.1. Differences between XCTD and CTD depths for XCTD-4. Differences were estimated with the same method as Uchida et al. (2011). Standard deviation of the estimates (horizontal bars) and the manufacturer's specification for XCTD depth error (dotted lines) are shown. The regression for the data (solid line) is also shown.

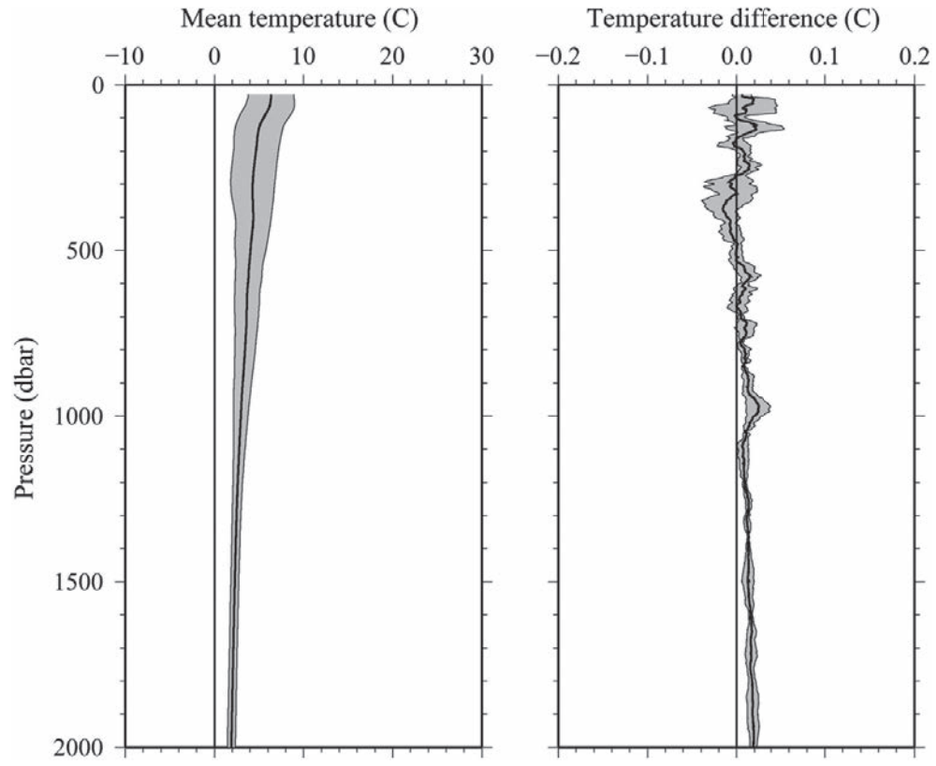

Figure 3.13.2. Comparison between XCTD and CTD temperature profiles. (a) Mean temperature of CTD profiles with standard deviation (shade) and (b) mean temperature difference with standard deviation (shade) between the XCTD and CTD. Mean profiles were low-pass filtered by a running mean with a window of 51 dbar.

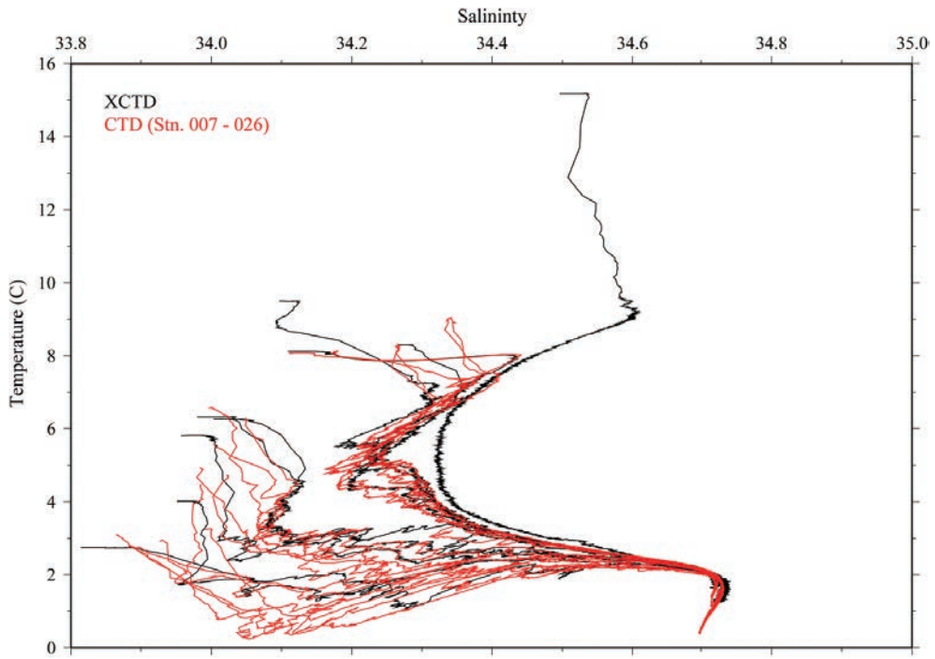

Figure 3.13.3. Comparison of temperature-salinity profiles of CTD data (red lines) used for the XCTD salinity bias estimation and salinity bias-corrected XCTD data (black lines).

3.14 Sound Velocity

May 10, 2017

(1) Personnel

Hiroshi Uchida (JAMSTEC) (Principal investigator)

Rei Ito (MWJ) (Legs 2 and 3)

Sonoka Tanihara (MWJ) (Leg 2)

Kenichi Katayama (MWJ) (Leg 3)

Shungo Oshitani (MWJ) (Leg 3)

Rio Kobayashi (MWJ) (Leg 3)

(2) Objectives

The objective of this study is to estimate Absolute Salinity (also called "density salinity") from sound velocity data with temperature and pressure data from CTD, and to evaluate an algorithm to estimate absolute salinity provided along with TEOS-10 (the International Thermodynamic Equation of Seawater 2010) (IOC et al., 2010).

(3) Materials and methods

Sound velocity profiles were measured at the CTD casts by using a velocimeter (MiniSVP, serial no. 49618, Valeport Ltd., Devon, United Kingdom). The sound velocity sensing elements are a ceramic transducer (signal sound pulse of 2.5 MHz frequency), a signal reflector, and spacer rods to control the sound path length (10 cm), providing a measurement at depths up to 6000 m. The velocimeter was attached to the CTD frame and level of the sound path of the velocimeter was same as that of the CTD temperature sensor, just next to the primary temperature sensor. Although temperature and pressure data were also measured by the velocimeter, only sound velocity data measured at a sampling rate of 8 Hz were combined with the CTD temperature and pressure data measured at a sampling rate of 24 Hz to estimate Absolute Salinity.

The sound velocity data were obtained at all CTD casts in legs 2 and 3. The sound velocity data were roughly combined with the CTD data to match the time going into and coming out of the sea water, and the combined data were interpolated at a sub-sampling rate of 16 Hz. Time difference between the sound velocity data and the CTD data were more strictly adjusted to minimize spikes of salinity data back calculated from the sound velocity, pressure and temperature data as follows. Standard deviations of difference between the back calculated salinity data and their low-pass filtered data by a running mean with a window of 161 scans (10 seconds) were calculated for a segment from 20 to 70 dbar of the down cast by advancing the sound velocity data against the CTD data from –6 scans to +6 scans at one scan intervals, and the advanced scan to minimize the standard deviation was estimated. These calculations were repeated for a segment at 50 dbar intervals from 20 dbar to 570 dbar, and a median of the estimated advanced scans was calculated as the best estimate of the advanced scan.

The estimated Absolute Salinity (S_v) were calibrated in situ referred to the Absolute Salinity measured by a density meter for water samples. The corrected Absolute Salinity were estimated as

Corrected Absolute Salinity =

$$(c_0 + c_1 \times S_v + c_2 \times T + c_3 \times P + c_4 \times S_v^2 + c_5 \times P_2 + c_6 \times T^2 + c_7 \times S_v \times P + c_8 \times S_v \times T) \times (1 + c_9 \times P)$$

where T is CTD temperature in °C, P is pressure in dbar, and $c_0 \sim c_8$ are calibration coefficients. The best fit sets of coefficients were determined by a least square technique to minimize the deviation from the Absolute Salinity measured by the density meter, except for the coefficient c_9 which was subjectively determined in advance.

The post-cruise calibrated temperature and salinity data were used for the calibration. The calibration coefficients are listed in Table 3.14.1. The results of the post-cruise calibration for the Absolute Salinity estimated from the sound velocity data are summarized in Table 3.14.2 and shown in Fig. 3.14.1. Vertical profiles of the corrected Absolute Salinity were shown in Fig. 3.14.2.

(4) Reference

IOC, SCOR and IAPSO (2010): The international thermodynamic equation of seawater – 2010: Calculation and

use of thermodynamic properties. Intergovernmental Oceanographic Commission, Manuals and Guides No. 56, United Nations Educational, Scientific and Cultural Organization (English), 196 pp.

Table 3.14.1 Calibration coefficients for Absolute Salinity estimated from the sound velocity data.

Coefficient	S/N 49618
c_0	26.70938514122043
c_1	–0.5416586809715309
c_2	–0.1354291356712744
c_3	1.401399009550316e–3
c_4	2.245731443302312e–2
c_5	5.894712917405537e–8
c_6	1.067486700100993e–3
c_7	–9.109068401397720e–5
c_8	3.551854573705933e–3
c_9	5.17e–5

Table 3.14.2 Difference between the corrected Absolute Salinity estimated from the sound velocity data and the Absolute Salinity measured by the density meter after the post-cruise calibration. Mean and standard deviation (Sdev) are calculated for the data below and above 950 dbar. Number of data used is also shown.

Serial number	Pressure ≥ 950 dbar			Pressure < 950 dbar		
	Number	Mean [g/kg]	Sdev	Number	Mean [g/kg]	Sdev
49618	227	0.0000	0.0238	227	0.0000	0.0036

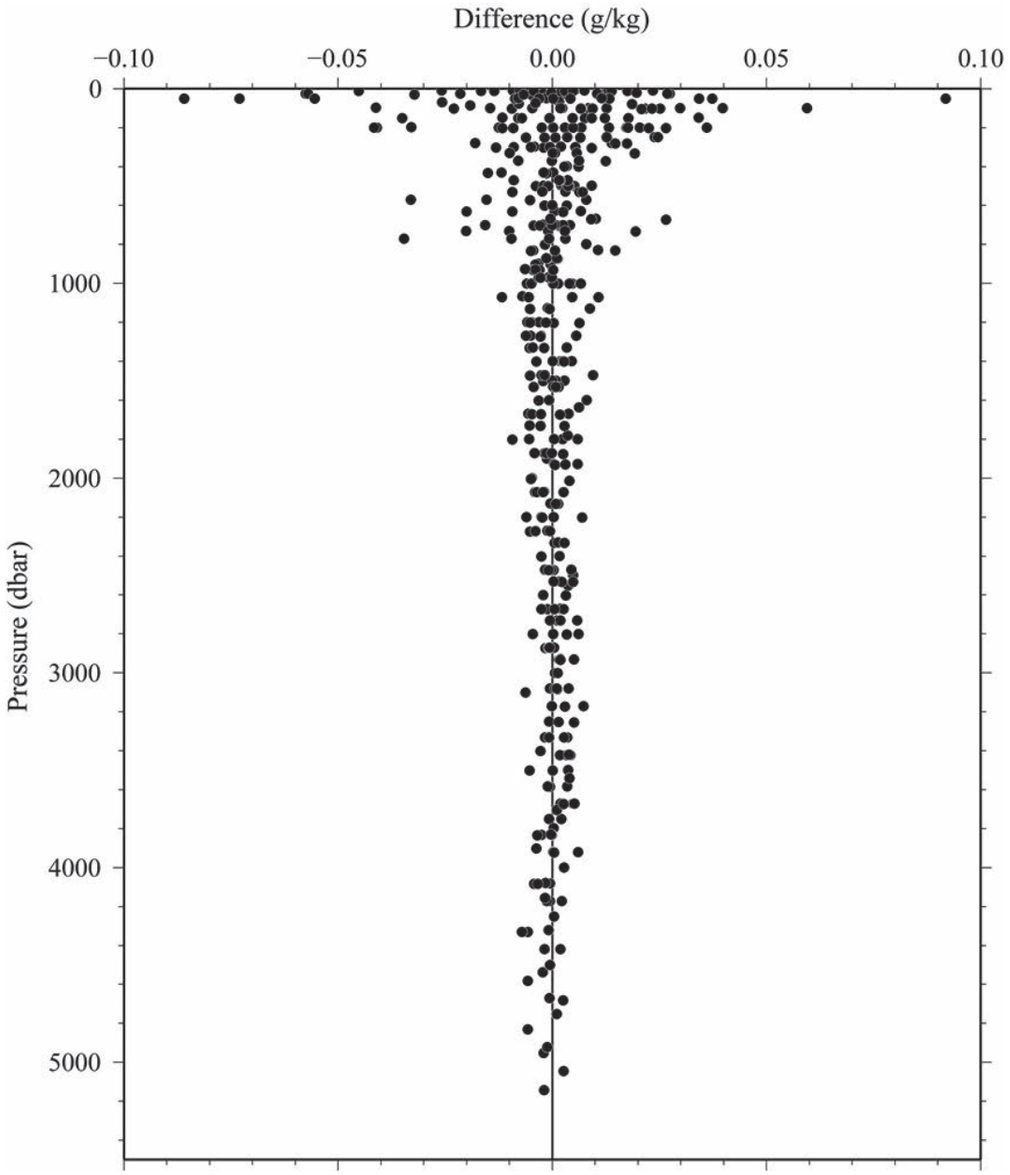

Fig. 3.14.1. Vertical distribution of differences between Absolute Salinity estimated from sound velocity data and Absolute Salinity estimated from the density meter for legs 2 and 3.

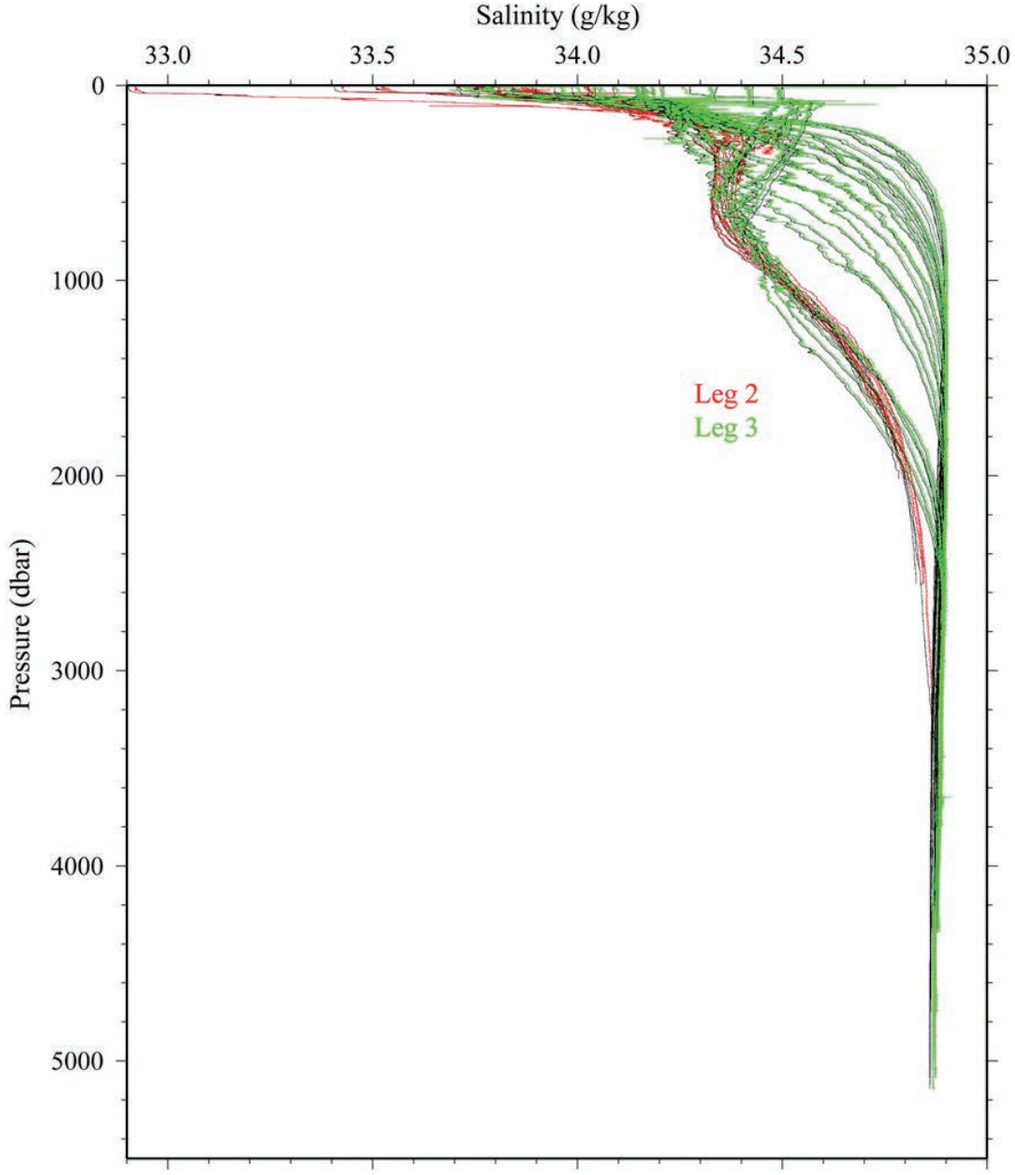

Fig. 3.14.2. Vertical profiles of Absolute Salinity estimated from sound velocity data. Black lines indicate Reference-Composition Salinity derived from CTD salinity data.

Station Summary

R/V MIRAI CRUISE MR1609 LEG1

SHIP/CRS EXPOCODE	WOCE SECT	STNNBR	CASTNO	CAST TYPE	DATE	UTC TIME	EVENT CODE	POSITION LATITUDE	POSITION LONGITUDE	NAV	UNC DEPTH	COR DEPTH	HT ABOVE BOTTOM	WIRE OUT	MAX PRESS	NO. OF BOTTLES	PARAMETERS	COMMENTS
49NZ20161227	999	101	001	DRF	010417	1920	DE	44 51.11 S	140 04.90 W	GPS	-9	5359						CO2 SURFACE BUOY S/N=16007 ARGOS=160441
49NZ20161227	999	102	001	DRF	010717	1549	DE	48 39.32 S	120 01.48 W	GPS	-9	3100						CO2 SURFACE BUOY S/N=16008 ARGOS=160442

R/V MIRAI CRUISE MR1609 LEG2

SHIP/CRS EXPOCODE	WOCE SECT	STNNBR	CASTNO	CAST TYPE	DATE	UTC TIME	EVENT CODE	POSITION LATITUDE	POSITION LONGITUDE	NAV	UNC DEPTH	COR DEPTH	HT ABOVE BOTTOM	WIRE OUT	MAX PRESS	NO. OF BOTTLES	PARAMETERS	COMMENTS
49NZ20170120	CHILE	001	001	ROS	012117	1219	BE	44 17.57 S	75 35.60 W	GPS	-9	1919						
49NZ20170120	CHILE	001	001	ROS	012117	1256	BO	44 17.72 S	75 35.53 W	GPS	-9	1920	9	1908	1930	26	1-6,23,24,34,92	
49NZ20170120	CHILE	001	001	ROS	012117	1404	EN	44 17.85 S	75 35.43 W	GPS	-9	1930						
49NZ20170120	CHILE	002	001	CTD	012217	1252	BE	46 4.36 S	75 41.28 W	GPS	-9	1541						
49NZ20170120	CHILE	002	001	CTD	012217	1304	BO	46 4.38 S	75 41.34 W	GPS	-9	1538	-9	499	506			
49NZ20170120	CHILE	002	001	CTD	012217	1313	EN	46 4.38 S	75 41.39 W	GPS	-9	1539						
49NZ20170120	CHILE	006	001	ROS	012417	0108	BE	46 10.77 S	76 17.67 W	GPS	-9	2506						
49NZ20170120	CHILE	006	001	ROS	012417	0254	EN	46 10.89 S	76 17.39 W	GPS	-9	2620	9	2520	2554	26	1-6,23,24,34,92	
49NZ20170120	CHILE	007	001	ROS	012817	0706	BE	47 47.92 S	76 1.85 W	GPS	-9	2024						
49NZ20170120	CHILE	007	001	ROS	012817	0742	BO	47 47.96 S	76 1.99 W	GPS	-9	1992	11	1993	2017	26	1-6,23,24,34,92	
49NZ20170120	CHILE	007	001	ROS	012817	0846	EN	47 47.93 S	76 2.14 W	GPS	-9	2021						
49NZ20170120	CHILE	009	001	ROS	012917	1208	BE	48 22.99 S	76 27.52 W	GPS	-9	1616						
49NZ20170120	CHILE	009	001	ROS	012917	1248	BO	48 23.16 S	76 27.77 W	GPS	-9	1639	8	1616	1639	27	1-6,23,24,34,92	
49NZ20170120	CHILE	009	001	ROS	012917	1340	EN	48 23.24 S	76 28.04 W	GPS	-9	1693						
49NZ20170120	CHILE	010	001	ROS	013117	0734	BE	50 48.33 S	79 6.84 W	GPS	-9	3853						
49NZ20170120	CHILE	010	001	ROS	013117	0744	BO	50 48.41 S	79 6.80 W	GPS	-9	3852	-9	296	301	9	1-6,23,24,34,92	
49NZ20170120	CHILE	010	001	ROS	013117	0807	EN	50 48.56 S	79 6.78 W	GPS	-9	3859						
49NZ20170120	CHILE	010	002	ROS	013117	0852	BE	50 48.37 S	79 7.06 W	GPS	-9	3852						
49NZ20170120	CHILE	010	002	ROS	013117	0954	BO	50 48.46 S	79 7.15 W	GPS	-9	3852	8	3837	3904	27	1-6,23,24,34,92	
49NZ20170120	CHILE	010	002	ROS	013117	1132	EN	50 48.52 S	79 7.09 W	GPS	-9	3855						
49NZ20170120	CHILE	12B	001	ROS	020217	0902	BE	54 20.04 S	74 38.03 W	GPS	-9	2481						
49NZ20170120	CHILE	12B	001	ROS	020217	0952	BO	54 20.20 S	74 38.03 W	GPS	-9	2462	9	2443	2474	27	1-6,23,24,34,92	
49NZ20170120	CHILE	12B	001	ROS	020217	1059	EN	54 19.90 S	74 38.39 W	GPS	-9	2518						
49NZ20170120	CHILE	11B	001	ROS	020317	0251	BE	52 59.98 S	75 29.69 W	GPS	-9	1776						
49NZ20170120	CHILE	11B	001	ROS	020317	0324	BO	53 0.08 S	75 29.35 W	GPS	-9	1767	8	1764	1783	25	1-6,23,24,34,92	
49NZ20170120	CHILE	11B	001	ROS	020317	0415	EN	53 0.15 S	75 28.82 W	GPS	-9	1758						
49NZ20170120	CHILE	11A	001	ROS	020317	1917	BE	52 19.07 S	75 56.94 W	GPS	-9	1871						
49NZ20170120	CHILE	11A	001	ROS	020317	1956	BO	52 19.08 S	75 56.71 W	GPS	-9	1822	7	1856	1878	21	1-6,23,24,34,92	
49NZ20170120	CHILE	11A	001	ROS	020317	2047	EN	52 19.15 S	75 56.39 W	GPS	-9	1701						

R/V MIRAI CRUISE MR1609 LEG3

SHIP/CRS EXPOCODE	WOCE SECT	STNNBR	CASTNO	CAST TYPE	UTC DATE	UTC TIME	EVENT CODE	POSITION LATITUDE	POSITION LONGITUDE	NAV	UNC DEPTH	COR DEPTH	HT ABOVE BOTTOM	WIRE OUT	MAX PRESS	NO. OF BOTTLES	PARAMETERS	COMMENTS
49NZ20170208	P17E	301	001	UNK	021017	1857	DE	58 54.12 S	72 47.49 W	GPS	-9	-9						CESIUM MAGNETOMETER DEPLOYED
49NZ20170208	P17E	301	001	UNK	021017	2100	BE	59 8.71 S	73 16.44 W	GPS	-9	4349						CESIUM MAGNETOMETER START
49NZ20170208	P17E	302	001	UNK	021017	2107	BE	59 9.67 S	73 18.17 W	GPS	-9	4501						MAGNETOMETER CALIBRATION
49NZ20170208	P17E	302	001	UNK	021017	2141	EN	59 9.91 S	73 17.63 W	GPS	-9	4388						MAGNETOMETER CALIBRATION
49NZ20170208	P17E	301	001	UNK	021417	2309	EN	65 57.36 S	113 21.33 W	GPS	-9	4846						CESIUM MAGNETOMETER END AND RECOVER
49NZ20170208	P17E	303	001	XCT	021617	0204	DE	66 58.73 S	125 48.26 W	GPS	-9	4351						TSK XCTD1 S/N=16027275
49NZ20170208	P17E	001	001	ROS	021617	0259	BE	67 0.23 S	125 58.86 W	GPS	-9	3783						
49NZ20170208	P17E	001	001	ROS	021617	0402	BO	67 0.10 S	125 59.00 W	GPS	-9	3737	7	3748	3814	36	118	
49NZ20170208	P17E	001	001	ROS	021617	0524	EN	67 0.07 S	125 59.13 W	GPS	-9	3681						
49NZ20170208	P17E	001	002	ROS	021617	0639	BE	67 0.15 S	125 58.61 W	GPS	-9	3779						
49NZ20170208	P17E	001	002	ROS	021617	0646	BU	67 0.14 S	125 58.66 W	GPS	-9	3764					1,3-6,20,30,31,33,34,97,98,99,101,102	0.5C
49NZ20170208	P17E	001	002	ROS	021617	0739	BO	66 59.99 S	125 58.58 W	GPS	-9	3709	7	3735	3798	35	1-8,12,13,20,23,24,27,30,31,33,34,43,82,92,93,97,98,99,101,102,106,117	
49NZ20170208	P17E	001	002	ROS	021617	0920	EN	66 59.76 S	125 58.05 W	GPS	-9	3681						
49NZ20170208	P17E	002	001	ROS	021617	1416	BE	66 21.56 S	126 2.96 W	GPS	-9	4453						
49NZ20170208	P17E	002	001	ROS	021617	1424	BU	66 21.54 S	126 3.08 W	GPS	-9	4454					1,3-6,20,30,34,40,95,97,102,119	1.0C
49NZ20170208	P17E	002	001	ROS	021617	1524	BO	66 21.56 S	126 3.77 W	GPS	-9	4470	10	4463	4538	33	1-8,20,23,24,26,27,30,34,40,92,93,95,102	
49NZ20170208	P17E	002	001	ROS	021617	1712	EN	66 21.57 S	126 5.34 W	GPS	-9	4509						
49NZ20170208	P17E	002	001	FLT	021617	1733	DE	66 21.55 S	126 1.47 W	GPS	-9	4445						SOCCOM APEX S/N=12371
49NZ20170208	P17E	003	001	ROS	021617	2133	BE	65 39.61 S	125 57.84 W	GPS	-9	4757						
49NZ20170208	P17E	003	001	ROS	021617	2143	BU	65 39.60 S	125 57.85 W	GPS	-9	4755					1,3-6,30,102	1.2C
49NZ20170208	P17E	003	001	ROS	021617	2248	BO	65 39.45 S	125 57.43 W	GPS	-9	4745	11	4740	4825	36	1-8,27,30,93,102	
49NZ20170208	P17E	004	001	ROS	021717	0414	BE	65 0.98 S	125 58.45 W	GPS	-9	4865						
49NZ20170208	P17E	004	001	ROS	021717	0421	BU	65 0.97 S	125 58.31 W	GPS	-9	4865					1,3-6,20,30,31,33,34,82,95,97,98,99,101,102,106,117	2.2C
49NZ20170208	P17E	004	001	ROS	021717	0528	BO	65 1.00 S	125 57.60 W	GPS	-9	4866	10	4866	4954	36	1-8,20,23,24,26,27,30,31,33,34,40,43,82,92,93,95,97,98,99,101,102,106,117	
49NZ20170208	P17E	004	001	ROS	021717	0727	EN	65 0.84 S	125 57.06 W	GPS	-9	4865						
49NZ20170208	P17E	004	001	FLT	021717	0742	DE	65 1.00 S	125 56.51 W	GPS	-9	4872						SOCCOM APEX S/N=12379
49NZ20170208	P17E	005	001	ROS	021717	1120	BE	64 20.75 S	126 2.00 W	GPS	-9	4882						
49NZ20170208	P17E	005	001	ROS	021717	1126	BU	64 20.77 S	126 1.97 W	GPS	-9	4879					1,3-6,30,102,119	2.5C
49NZ20170208	P17E	005	001	ROS	021717	1234	BO	64 20.81 S	126 1.84 W	GPS	-9	4891	8	4887	4984	36	1-8,27,30,93,102	
49NZ20170208	P17E	005	001	ROS	021717	1428	EN	64 20.84 S	126 1.09 W	GPS	-9	4919						
49NZ20170208	P17E	006	001	ROS	021717	1811	BE	63 40.88 S	126 0.12 W	GPS	-9	4957						
49NZ20170208	P17E	006	001	ROS	021717	1821	BU	63 40.93 S	126 0.05 W	GPS	-9	4958					1,3-6,20,30,34,97,102	2.7C
49NZ20170208	P17E	006	001	ROS	021717	1929	BO	63 41.01 S	125 59.57 W	GPS	-9	4955	9	4948	5046	36	1-8,12,13,20,23,24,27,30,34,92,93,97,102	
49NZ20170208	P17E	006	001	ROS	021717	2126	EN	63 41.14 S	125 59.20 W	GPS	-9	4954						
49NZ20170208	P17E	007	001	ROS	021817	0104	BE	63 0.83 S	126 0.73 W	GPS	-9	5015						
49NZ20170208	P17E	007	001	ROS	021817	0119	BU	63 0.91 S	126 0.58 W	GPS	-9	5005					1,3-6,30,102	3.1C
49NZ20170208	P17E	007	001	ROS	021817	0228	BO	63 1.25 S	125 59.79 W	GPS	-9	4994	11	5014	5086	36	1-8,27,30,93,102	
49NZ20170208	P17E	007	001	ROS	021817	0427	EN	63 1.87 S	125 58.18 W	GPS	-9	4986						
49NZ20170208	P17E	008	001	ROS	021817	2107	BE	62 19.76 S	126 6.77 W	GPS	-9	5049						
49NZ20170208	P17E	008	001	ROS	021817	2119	BU	62 19.85 S	126 6.79 W	GPS	-9	5049					1,3-6,20,30,31,33,34,40,82,95,97,98,99,101,102	2.7C
49NZ20170208	P17E	008	001	XCT	021817	2119	DE	62 19.85 S	126 6.80 W	GPS	-9	5049						TSK XCTD2 S/N=16070971, COND AND SAL FAILED AT 33M
49NZ20170208	P17E	008	002	XCT	021817	2132	DE	62 19.93 S	126 6.81 W	GPS	-9	5044						TSK XCTD2 S/N=16070972
49NZ20170208	P17E	008	001	ROS	021817	2229	BO	62 20.12 S	126 6.64 W	GPS	-9	5047	9	5054	5144	36	1-8,20,23,24,26,27,30,31,33,34,40,43,82,92,93,95,97,98,99,101,102	
49NZ20170208	P17E	008	001	ROS	021917	0031	EN	62 20.52 S	126 6.37 W	GPS	-9	5055						
49NZ20170208	P17E	008	001	FLT	021917	0043	DE	62 20.59 S	126 6.90 W	GPS	-9	5055						SOCCOM APEX S/N=12366
49NZ20170208	P17E	009	001	ROS	021917	0427	BE	61 39.51 S	125 59.27 W	GPS	-9	4834						

```
49NZ20170208 P17E     009    001  ROS 021917 0435    BU 61 39.60 S 125 59.41 W GPS     -9   4843                                1,3-6,30,102,119                                    2.7C
49NZ20170208 P17E     009    001  ROS 021917 0543    BO 61 39.83 S 125 59.62 W GPS     -9   4833       10      4834   4925      36 1-8,27,30,93,102
49NZ20170208 P17E     009    001  ROS 021917 0738    EN 61 40.09 S 125 59.75 W GPS     -9   4767
49NZ20170208 P17E     010    001  ROS 021917 1122    BE 60 59.11 S 126  0.69 W GPS     -9   4535
49NZ20170208 P17E     010    001  ROS 021917 1128    BU 60 59.06 S 126  0.67 W GPS     -9   4546                                1,3-6,20,30,31,33,34,82,97,101,102,106,117          2.9C
49NZ20170208 P17E     010    001  ROS 021917 1232    BO 60 58.71 S 126  0.43 W GPS     -9   4590        9      4559   4637      35 1-8,12,13,20,23,24,27,30,31,33,34,82,92,93,97,101,102,106,117
49NZ20170208 P17E     010    001  ROS 021917 1421    EN 60 58.34 S 126  0.60 W GPS     -9   4511
49NZ20170208 P17E     010    001  FLT 021917 1434    DE 60 58.14 S 126  0.26 W GPS     -9   4569                                                                    DEEP APEX S/N=17
49NZ20170208 P17E     010    001  FLT 021917 1441    DE 60 58.01 S 125 59.98 W GPS     -9   4591                                                                    DEEP NINJA S/N=20
49NZ20170208 P17E     010    001  FLT 021917 1447    DE 60 57.89 S 125 59.77 W GPS     -9   4489                                                                  ARGO (ARVOR S/N=OIN13JAP-ARL-78)
49NZ20170208 P17E     011    001  ROS 021917 1729    BE 60 28.65 S 125 59.75 W GPS     -9   4624
49NZ20170208 P17E     011    001  ROS 021917 1737    BU 60 28.64 S 125 59.66 W GPS     -9   4627                                1,3-6,30,102                                        3.2C
49NZ20170208 P17E     011    001  ROS 021917 1845    BO 60 28.63 S 125 58.51 W GPS     -9   4833       14      4797   4873      36 1-8,27,30,31,33,93,101,102
49NZ20170208 P17E     011    001  ROS 021917 2037    EN 60 28.77 S 125 55.86 W GPS     -9   4814
49NZ20170208 P17E     012    001  ROS 021917 2326    BE 60  0.73 S 125 58.71 W GPS     -9   4645
49NZ20170208 P17E     012    001  ROS 021917 2332    BU 60  0.75 S 125 58.66 W GPS     -9   4647                                1,3-6,20,30,34,98,99,102,119                        4.5C
49NZ20170208 P17E     012    001  ROS 022017 0036    BO 60  0.83 S 125 58.53 W GPS     -9   4634        9      4611   4683      33 1-8,20,23,24,27,30,31,33,34,92,93,98,99,101,102
49NZ20170208 P17E     012    001  ROS 022017 0224    EN 60  1.15 S 125 58.19 W GPS     -9   4680
49NZ20170208 P17E     012    001  DRF 022017 0233    DE 60  1.32 S 125 58.10 W GPS     -9   4689                                                                CO2 SURFACE BUOY S/N=16002 ARGOS=160444
49NZ20170208 P17E     013    001  ROS 022017 0455    BE 59 36.22 S 126  3.17 W GPS     -9   4671
49NZ20170208 P17E     013    001  ROS 022017 0502    BU 59 36.24 S 126  3.22 W GPS     -9   4643                                1,3-6,20,30,31,33,34,82,97,101,102,106,117          4.1C
49NZ20170208 P17E     013    001  ROS 022017 0610    BO 59 36.44 S 126  3.24 W GPS     -9   4637       10      4677   4747      32 1-8,12,13,20,23,24,27,30,31,33,34,43,82,93,97,101,102,106,117
49NZ20170208 P17E     013    001  ROS 022017 0801    EN 59 36.61 S 126  3.41 W GPS     -9   4697
49NZ20170208 P17E     014    001  XCT 022017 1111    DE 59  0.79 S 125 59.97 W GPS     -9   4368                                                                    TSK XCTD2 S/N=16070973
49NZ20170208 P17E     015    001  ROS 022017 1410    BE 58 29.65 S 125 59.56 W GPS     -9   4211
49NZ20170208 P17E     015    001  ROS 022017 1422    BU 58 29.73 S 125 59.38 W GPS     -9   4216                                1,3-6,20,30,31,33,34,82,101,102                     4.9C
49NZ20170208 P17E     015    001  ROS 022017 1520    BO 58 29.95 S 125 59.04 W GPS     -9   4209        8      4187   4265      36 1-8,20,23,24,27,30,31,33,34,82,93,101,102
49NZ20170208 P17E     015    001  ROS 022017 1700    EN 58 30.36 S 125 58.27 W GPS     -9   4205
49NZ20170208 P17E     016    001  ROS 022017 1949    BE 58  0.33 S 125 59.96 W GPS     -9   4233
49NZ20170208 P17E     016    001  XCT 022017 1958    DE 58  0.39 S 125 59.90 W GPS     -9   4253                                                                    TSK XCTD2 S/N=16070975
49NZ20170208 P17E     016    001  ROS 022017 1958    BU 58  0.40 S 125 59.90 W GPS     -9   4242                                1,3-6,20,30,34,97,98,99,102                         6.2C
49NZ20170208 P17E     016    001  ROS 022017 2058    BO 58  0.63 S 125 59.75 W GPS     -9   4274        8      4246   4323      33 1-8,12,13,20,23,24,27,30,34,43,92,93,97,98,99,102
49NZ20170208 P17E     016    001  ROS 022017 2241    EN 58  0.79 S 125 59.24 W GPS     -9   4256
49NZ20170208 P17E     016    001  FLT 022017 2252    DE 58  0.83 S 125 59.69 W GPS     -9   4266                                                                    ARGO (NAVIS S/N=F0415)
49NZ20170208 P17E     017    001  XCT 022117 0135    DE 57 29.52 S 126  0.07 W GPS     -9   3998                                                                    TSK XCTD2 S/N=16070976
49NZ20170208 P17E     018    001  ROS 022117 0428    BE 57  0.45 S 125 58.85 W GPS     -9   4194
49NZ20170208 P17E     018    001  ROS 022117 0435    BU 57  0.55 S 125 58.93 W GPS     -9   4195                                1,3-6,20,30,31,33,34,40,82,95,97,101,102,106,117,119  6.3C
49NZ20170208 P17E     018    001  ROS 022117 0534    BO 57  1.00 S 125 59.23 W GPS     -9   4168       10      4161   4232      36 1-8,20,23,24,27,30,31,33,34,40,43,82,93,95,97,101,102,106,117
49NZ20170208 P17E     018    001  ROS 022117 0714    EN 57  1.88 S 125 59.74 W GPS     -9   4164
49NZ20170208 P17E     018    001  FLT 022117 0726    DE 57  1.60 S 126  0.12 W GPS     -9   4115                                                                    SOCCOM APEX S/N=12386
49NZ20170208 P17E     019    001  XCT 022117 1016    DE 56 30.80 S 125 59.69 W GPS     -9   4210                                                                    TSK XCTD2 S/N=16070974
49NZ20170208 P17E     020    001  ROS 022117 1314    BE 56  0.18 S 125 58.33 W GPS     -9   4296
49NZ20170208 P17E     020    001  ROS 022117 1321    BU 56  0.24 S 125 58.14 W GPS     -9   4263                                1,3-6,20,30,34,102                                  5.5C
49NZ20170208 P17E     020    001  ROS 022117 1418    BO 56  0.65 S 125 57.34 W GPS     -9   4169        9      4106   4157      30 1-8,12,13,20,23,24,27,30,31,33,34,43,92,93,101,102
49NZ20170208 P17E     020    001  ROS 022117 1553    EN 56  1.13 S 125 55.97 W GPS     -9   4152
49NZ20170208 P17E     021    001  ROS 022117 1847    BE 55 29.89 S 125 59.62 W GPS     -9   3465
49NZ20170208 P17E     021    001  ROS 022117 1854    BU 55 29.94 S 125 59.45 W GPS     -9   3473                                1,3-6,20,30,31,33,34,82,97,98,99,101,102,119        8.0C
49NZ20170208 P17E     021    001  ROS 022117 1947    BO 55 30.21 S 125 58.63 W GPS     -9   3502        8      3536   3575      31 1-8,20,23,24,27,30,31,33,34,43,82,93,97,98,99,101,102
49NZ20170208 P17E     021    001  ROS 022117 2114    EN 55 30.68 S 125 57.07 W GPS     -9   3387
49NZ20170208 P17E     021    001  FLT 022117 2124    DE 55 30.69 S 125 57.09 W GPS     -9   3394                                                                  ARGO (ARVOR S/N=0IN13JAP-ARL-79)
49NZ20170208 P17E     021    001  DRF 022117 2127    DE 55 30.67 S 125 57.17 W GPS     -9   3378                                                                CO2 SURFACE BUOY S/N=16004 ARGOS=160438
```

```
49NZ20170208 P17E     022    001  ROS 022217 0004    BE 55  1.04 S 125 58.62 W GPS     -9   3650
49NZ20170208 P17E     022    001  XCT 022217 0012    DE 55  1.05 S 125 58.55 W GPS     -9   3651                                                                  TSK XCTD2 S/N=16070977
49NZ20170208 P17E     022    001  ROS 022217 0013    BU 55  1.05 S 125 58.55 W GPS     -9   3651                    1,3-6,30,102                                  8.1C
49NZ20170208 P17E     022    001  ROS 022217 0101    BO 55  1.09 S 125 58.60 W GPS     -9   3654       8      3647   3706      27 1-8,27,30,31,33,93,101,102
49NZ20170208 P17E     022    001  ROS 022217 0233    EN 55  1.12 S 125 58.47 W GPS     -9   3653
49NZ20170208 P17E     023    001  ROS 022217 0518    BE 54 28.47 S 125 58.89 W GPS     -9   3627
49NZ20170208 P17E     023    001  ROS 022217 0525    BU 54 28.45 S 125 58.90 W GPS     -9   3627                    1,3-6,20,30,31,33,34,82,101,102,106,117       8.0C
49NZ20170208 P17E     023    001  XCT 022217 0527    DE 54 28.44 S 125 58.89 W GPS     -9   3628                                                                  TSK XCTD2 S/N=16070978
49NZ20170208 P17E     023    001  ROS 022217 0615    BO 54 28.36 S 125 59.12 W GPS     -9   3629      10      3620   3676      33 1-8,12,13,20,23,24,27,30,31,33,34,43,82,92,93,101,102,106,117
49NZ20170208 P17E     023    001  ROS 022217 0747    EN 54 28.26 S 125 59.35 W GPS     -9   3630
49NZ20170208 P17E     024    001  ROS 022217 1024    BE 54  0.45 S 125 58.72 W GPS     -9   3486
49NZ20170208 P17E     024    001  ROS 022217 1030    BU 54  0.45 S 125 58.70 W GPS     -9   3485                    1,3-6,20,30,34,40,95,97,98,99,102             8.1C
49NZ20170208 P17E     024    001  ROS 022217 1119    BO 54  0.38 S 125 58.59 W GPS     -9   3586       9      3483   3541      33 1-8,20,23,24,26,27,30,34,40,43,92,93,95,97,98,99,102
49NZ20170208 P17E     024    001  ROS 022217 1249    EN 54  0.18 S 125 58.17 W GPS     -9   3537
49NZ20170208 P17E     024    001  FLT 022217 1301    DE 54  0.00 S 125 58.42 W GPS     -9   3543                                                                  SOCCOM APEX S/N=12542
49NZ20170208 P17E     025    001  ROS 022217 1608    BE 53 30.19 S 126  1.11 W GPS     -9   3746
49NZ20170208 P17E     025    001  ROS 022217 1615    BU 53 30.25 S 126  1.18 W GPS     -9   3745                    1,3-6,20,30,34,102,119                        9.0C
49NZ20170208 P17E     025    001  ROS 022217 1709    BO 53 30.49 S 126  1.35 W GPS     -9   3742       9      3750   3798      29 1-8,20,23,24,27,30,34,93,102
49NZ20170208 P17E     025    001  ROS 022217 1843    EN 53 31.12 S 126  1.33 W GPS     -9   3741
49NZ20170208 P17E     026    001  ROS 022217 2155    BE 53  0.30 S 125 59.99 W GPS     -9   4386
49NZ20170208 P17E     026    001  ROS 022217 2207    BU 53  0.39 S 126  0.00 W GPS     -9   4389                    1,3-6,20,30,34,102,119                        9.0C
49NZ20170208 P17E     026    001  ROS 022217 2307    BO 53  0.73 S 126  0.05 W GPS     -9   4229      11      4271   4342      30 1-8,12,13,20,23,24,27,30,34,92,93,102
49NZ20170208 P17E     026    001  ROS 022317 0050    EN 53  1.44 S 126  0.06 W GPS     -9   4073
49NZ20170208 P17E     026    001  DRF 022317 0058    DE 53  1.48 S 126  0.26 W GPS     -9   4042                                                                  CO2 SURFACE BUOY S/N=16005 ARGOS=160439
49NZ20170208 P17E     304    001  DRF 022517 0513    DE 51 54.96 S 139 59.87 W GPS     -9   4256                                                                  CO2 SURFACE BUOY S/N=16006 ARGOS=160440
49NZ20170208 P17E     305    001  XCT 022517 0519    DE 51 54.72 S 139 59.99 W GPS     -9   4350                                                                  TSK XCTD2 S/N=16070979
49NZ20170208 P17E     306    001  DRF 022817 0918    DE 46  4.97 S 159 59.92 W GPS     -9   4914                                                                  CO2 SURFACE BUOY S/N=16010 ARGOS=160443
49NZ20170208 P17E     307    001  XCT 022817 0926    DE 46  5.08 S 160  0.12 W GPS     -9   4907                                                                  TSK XCTD2 S/N=16070980
49NZ20170208 P17E     308    001  UNK 030317 0057    BE 39 46.50 S 175 19.40 W GPS     -9   4435                                                                  MAGNETOMETER CALIBRATION
49NZ20170208 P17E     308    001  UNK 030317 0117    EN 39 46.31 S 175 19.69 W GPS     -9   4444                                                                  MAGNETOMETER CALIBRATION
```

Water sample parameters:

Number	Parameter	Mnemonic	Mnemonic for expected error
1	Salinity	SALNTY	
2	Oxygen	OXYGEN	
3	Silicate	SILCAT	SILUNC *1
4	Nitrate	NITRAT	NRAUNC *1
5	Nitrite	NITRIT	NRIUNC *1
6	Phosphate	PHSPHT	PHPUNC *1
7	Freon-11	CFC-11	
8	Freon-12	CFC-12	
9	Tritium		
10	Helium		
11	He-3/He-4		
12	14Carbon	DELC14	C14ERR
13	13Carbon	DELC13	C13ERR
14	Kr-85		
15	Argon		
16	Ar-39		
17	Neon		
18	Ra-228		
19	Ra-226		
20	Ratio of O18 to O16	O18/O16	
21	Sr-90		
22	Cesium-137	CS-137	CS137ER *2
23	Total carbon	TCARBN	
24	Total alkalinity	ALKALI	
25	pCO2		
26	pH	PH	
27	Freon-113	CFC113	
28	Carbon tetrachloride	CCL4	
29	Iodate/Iodide		
30	Ammonium	NH4	
31	Methane	CH4	
32	Dissolved organic nitrogen	DON	
33	Nitrous oxide	N2O	
34	Chlorophyll-a	CHLORA	
35	Phaeophytin		
36	Halocarbons		
37	Biogenic sulfur compounds	DMS	
38	Hydrocarbons		
39	Barium		
40	Particulate organic carbon	POC	
41	Particulate organic nitrogen	PON	
42	Abundance of bacteria	BACT	
43	Dissolved organic carbon	DOC	
44	Carbon monoxide		
45	Nitrogen (gas)		
46	Total organic carbon	TOC	
47	Plutonium	PLUTO	PLUTOER *2
48	Primary productivity		
64	Incubation		
81	Particulate organic matter	POM	
82	15N-Nitrate	15NO3	
83	Particulate inorganic matter	PIM	
84	Dissolved organic phosphate		
85	Ratio of O-17 to O-16	O17/O16	
86	Flowcytometry		
87	Genetic analysis		
88	Nitrogen fixation		
89	Cesium-134	CS-134	CS134ER
90	Perfluoroalkyl substances	PFAS	
91	Iodine-129	I-129	
92	Density salinity	DNSSAL	
93	Sulfur hexafluoride	SF6	
94	Isoprene		
95	Pigment		
96	Microscope		
97	Calcium		
98	Colored dissolved organic matter	CDOM	
99	Absorption coefficients of particulate matter	AP	
100	Nitrification		
101	3C-CH4		
102	Prokaryotic abundance		
103	Fluorescence in situ hybridization		
104	Prokaryotic activity		
105	Viral production		
106	Microbial diversity		
107	N2O 15N-isotope		
108	Nitrogen fixation		
109	NH4 15N-isotope		
110	Urea		
111	NO2 15N-isotope		
112	Coenzyme F430		
113	Chlorophyll 15N-isotope		
114	Nitrogen isotope ratio of dissolved organic nitrogen	DO15N	
115	Abundance of phytoplankton		
116	Nitrogen isotope ratio of phytoplankton	15PHY	
117	Prokaryotic production		
118	Beryllium-isotope		
119	Transparent exopolymer particle	TEP	

Figure captions

Figure 1 Station locations for WHP P17E revisit in 2017 cruise with bottom topography.

Figure 2 Bathymetry (m) measured by Multi Narrow Beam Echo Sounding system.

Figure 3 Surface wind (m/s) measured at 25 m above sea level. Wind data is averaged over 6-hour.

Figure 4 (a) Sea surface temperature (°C), (b) sea surface salinity (psu), (c) sea surface oxygen (μmol/kg), and (d) sea surface chlorophyll *a* (mg/m^3) measured by the Continuous Sea Surface Water Monitoring System.

Figure 5 Difference in the partial pressure of CO_2 between the ocean and the atmosphere, ΔpCO_2 (ppmv).

Figure 6 Sea surface dissolved inorganic carbon (C_T) (μmol/kg).

Figure 7 Surface current at 100 m depth measured by shipboard acoustic Doppler current profiler (ADCP).

Figure 8 Potential temperature (°C) cross sections calculated by using CTD temperature and salinity data calibrated by bottle salinity measurements. Vertical exaggeration of the 0-6500 m section is 1000:1, and expanded section of the upper 1000 m is made with a vertical exaggeration of 2500:1.

Figure 9 CTD salinity (psu) cross sections calibrated by bottle salinity measurements. Vertical exaggeration is same as Fig. 8.

Figure 10 Absolute salinity (g/kg) cross sections calculated by using CTD salinity data. Vertical exaggeration is same as Fig. 8.

Figure 11 Density (upper: σ_0, lower: σ_4) (kg/m^3) cross sections calculated by using CTD temperature and salinity data. Vertical exaggeration of the 0-1500 m and 1500-6500 m section are 2500:1 and 1000:1, respectively. (a) EOS-80 and (b) TEOS-10 definition.

Figure 12 Neutral density (γ^n) (kg/m^3) cross sections calculated by using CTD temperature and salinity data. Vertical exaggeration is same as Fig. 8.

Figure 13 CTD oxygen (μmol/kg) cross sections. Vertical exaggeration is same as Fig. 8.

Figure 14 CTD chlorophyll *a* (mg/m^3) cross section. Vertical exaggeration of the upper 1000 m section is same as Fig. 8.

Figure 15 CTD beam attenuation coefficient (m^{-1}) cross sections. Vertical exaggeration is same as Fig. 8.

Figure 16 Bottle sampled dissolved oxygen (μmol/kg) cross sections. Data with quality flags of 2 were plotted. Vertical exaggeration is same as Fig. 8.

Figure 17 Silicate (μmol/kg) cross sections. Data with quality flags of 2 were plotted. Vertical exaggeration is same as Fig. 8.

Figure 18 Nitrate (μmol/kg) cross sections. Data with quality flags of 2 were plotted. Vertical exaggeration is same as Fig. 8.

Figure 19 Nitrite (μmol/kg) cross section. Data with quality flags of 2 were plotted. Vertical exaggeration of the upper 1000 m section is same as Fig. 8.

Figure 20 Phosphate (μmol/kg) cross sections. Data with quality flags of 2 were plotted. Vertical exaggeration is same as Fig. 8.

Figure 21 Dissolved inorganic carbon (μmol/kg) cross sections. Data with quality flags of 2 were plotted. Vertical exaggeration is same as Fig. 8.

Figure 22 Total alkalinity (μmol/kg) cross sections. Data with quality flags of 2 were plotted. Vertical exaggeration is same as Fig. 8.

Figure 23 Dissolved organic carbon (μmol/kg) cross sections. Data with quality flags of 2 were plotted. Vertical exaggeration is same as Fig. 8.

Figure 24 Calcium (mmol/kg) cross sections. Data with quality flags of 2 were plotted. Vertical exaggeration is same as Fig. 8.

Figure 25 CFC-11 (pmol/kg) cross sections. Data with quality flags of 2 were plotted. Vertical exaggeration is same as Fig. 8.

Figure 26 CFC-12 (pmol/kg) cross sections. Data with quality flags of 2 were plotted. Vertical exaggeration is same as Fig. 8.

Figure 27 CFC-113 (pmol/kg) cross sections. Data with quality flags of 2 were plotted. Vertical exaggeration is same as Fig. 8.

Figure 28 SF_6 (fmol/kg) cross sections. Data with quality flags of 2 were plotted. Vertical exaggeration is same as Fig. 8.

Figure 29 Cross sections of current velocity (cm/s) normal to the cruise track measured by LADCP (eastward or northward is positive). Vertical exaggeration is same as Fig. 8.

Figure 30 Difference in potential temperature (°C) between results from the WOCE cruise in 1992 and the revisit in 2017. Red and blue areas show areas where potential temperature increased and decreased in the revisit cruise, respectively. On white areas differences in temperature do not exceed the detection limit of 0.002 °C. Vertical exaggeration is same as Fig. 8.

Figure 31 Same as Fig. 30, but for salinity (psu). CTD salinity data with SSW batch correction[1] were used. On white areas differences in salinity do not exceed the detection limit of 0.002 psu.

Figure 32 Same as Fig. 30, but for dissolved oxygen (μmol/kg). CTD oxygen data were used. On white areas differences in dissolved oxygen do not exceed the detection limit of 2 μmol/kg.

Note

1. As for the traceability of SSW to Kawano's value (Kawano et al., 2006), the offset for the batches P120 (WOCE P17E in 1992) and P159 (WOCE P17E revisit in 2017) are −0.0009 and −0.0003, respectively. The offset values for the recent batches are listed in Table A1 (Uchida et al., in preparation).

Table A1. SSW batch to batch differences from P145 to P161 (Uchida et al., in preparation). The difference of P145 is reevaluated.

Batch no.	Production date	K15	Sp	Batch to batch difference ($\times 10^{-3}$)	
				Mantyla's standard	Kawano's standard
P145	2004/07/15	0.99981	34.9925	–2.3	–1.0
P146	2005/05/12	0.99979	34.9917	–2.8	–1.5
P147	2006/06/06	0.99982	34.9929	–1.9	–0.6
P148	2006/10/01	0.99982	34.9929	–1.3	0.0
P149	2007/10/05	0.99984	34.9937	–0.6	0.7
P150	2008/05/22	0.99978	34.9913	–0.6	0.7
P151	2009/05/20	0.99997	34.9984	–1.7	–0.4
P152	2010/05/05	0.99981	34.9926	–1.3	0.0
P153	2011/03/08	0.99979	34.9918	–0.9	0.4
P154	2011/10/20	0.99990	34.9961	–0.7	0.6
P155	2012/09/19	0.99981	34.9925	–1.2	0.1
P156	2013/07/23	0.99984	34.9937	–0.9	0.4
P157	2014/05/15	0.99985	34.9941	–2.0	–0.7
P158	2015/03/25	0.99970	34.9883	–1.5	–0.2
P159	2015/12/15	0.99988	34.9953	–1.6	–0.3
P160	2016/07/20	0.99983	34.9933	–1.3	0.0
P161	2017/05/03	0.99987	34.9949	–1.2	0.1

References

Kawano, T., M. Aoyama, T. Joyce, H. Uchida, Y. Takatsuki and M. Fukasawa (2006): The latest batch-to-batch difference table of standard seawater and its application to the WOCE onetime sections, *J. Oceanogr.*, 62, 777–792.

Figure 1
Station locations for WHP P17E revisit in 2017

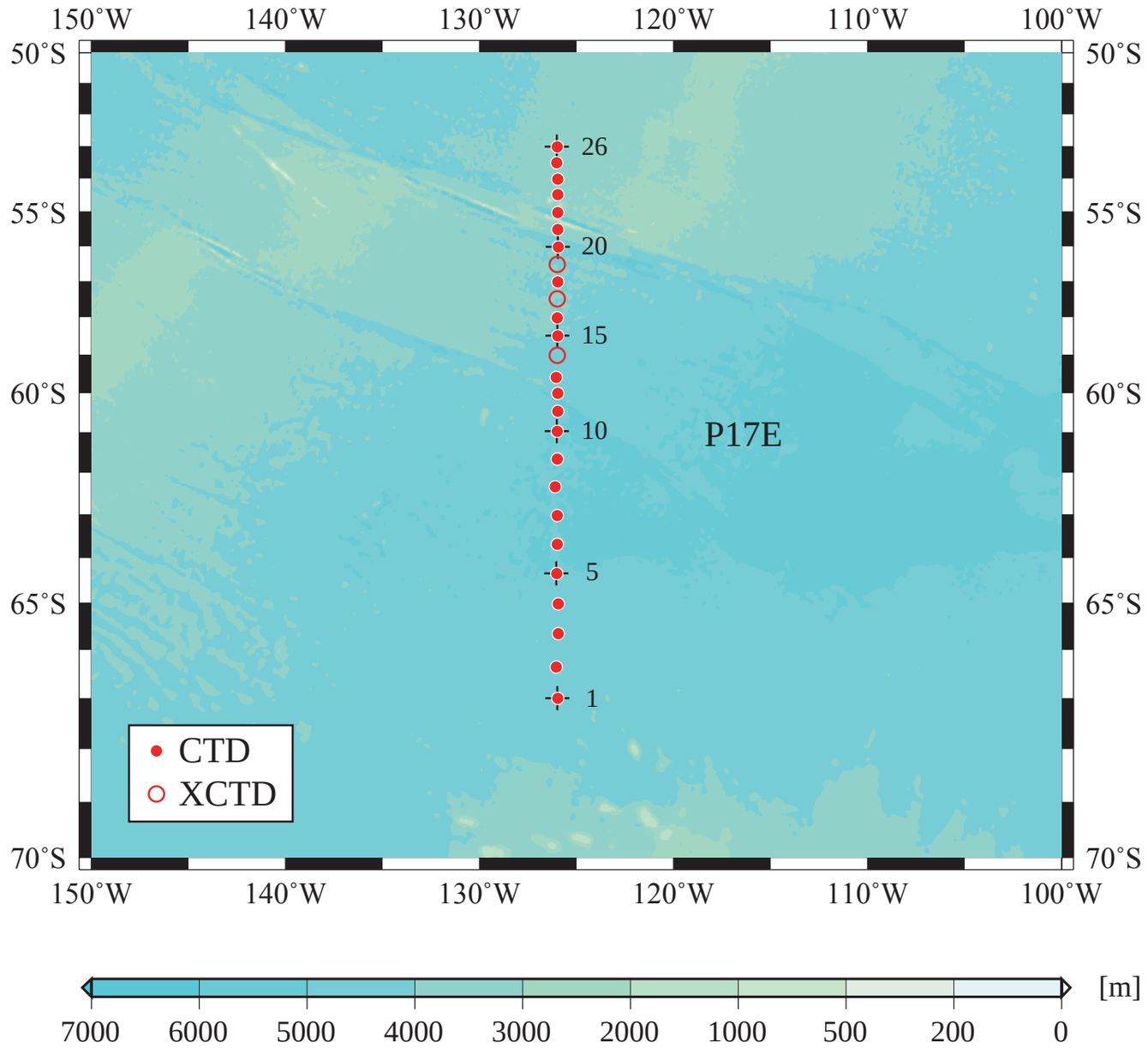

Figure 2

Bathymetry measured by Multi Narrow Beam Echo Sounding system

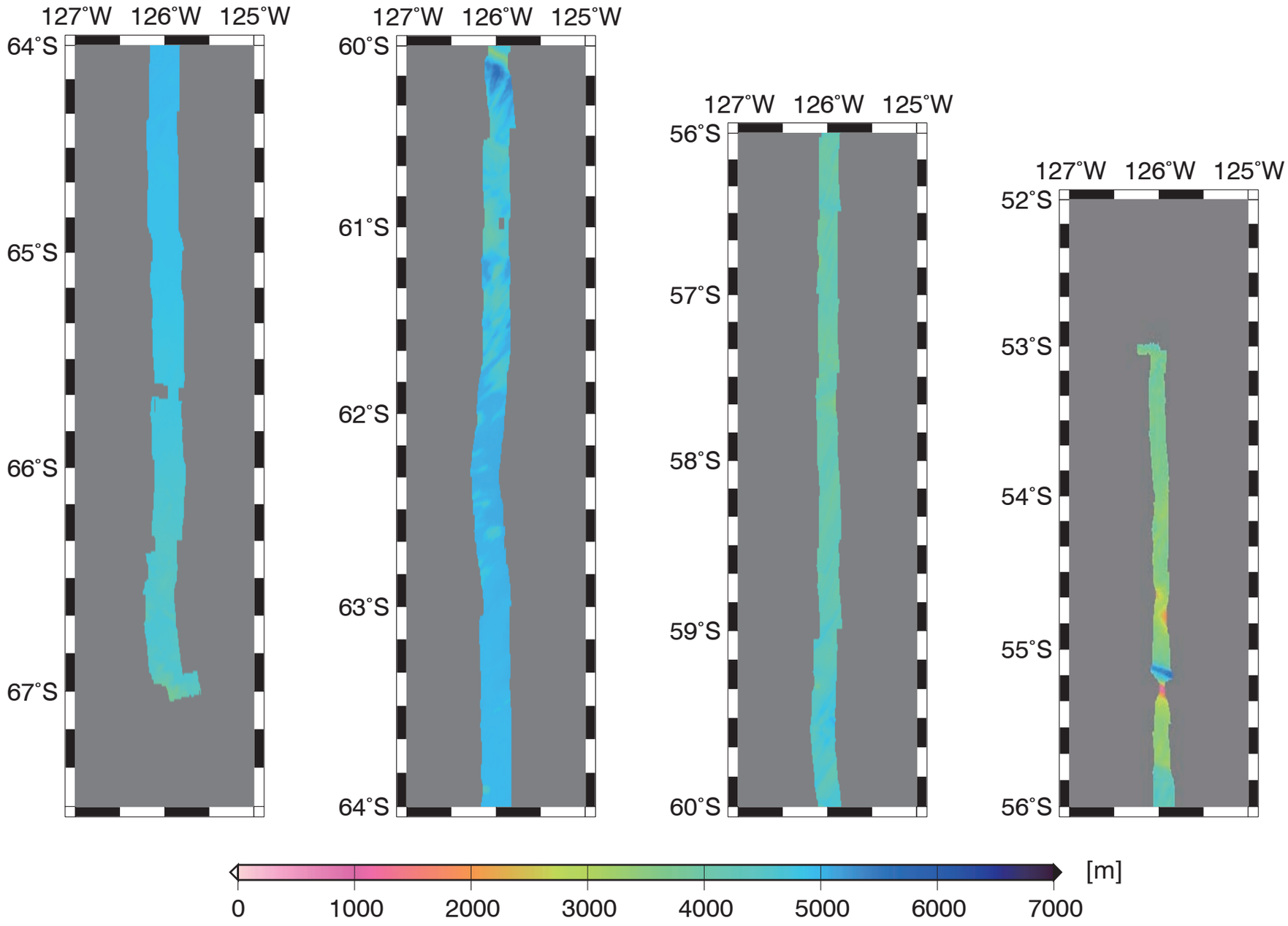

Figure 3

Surface wind measured at 25 m above sea level

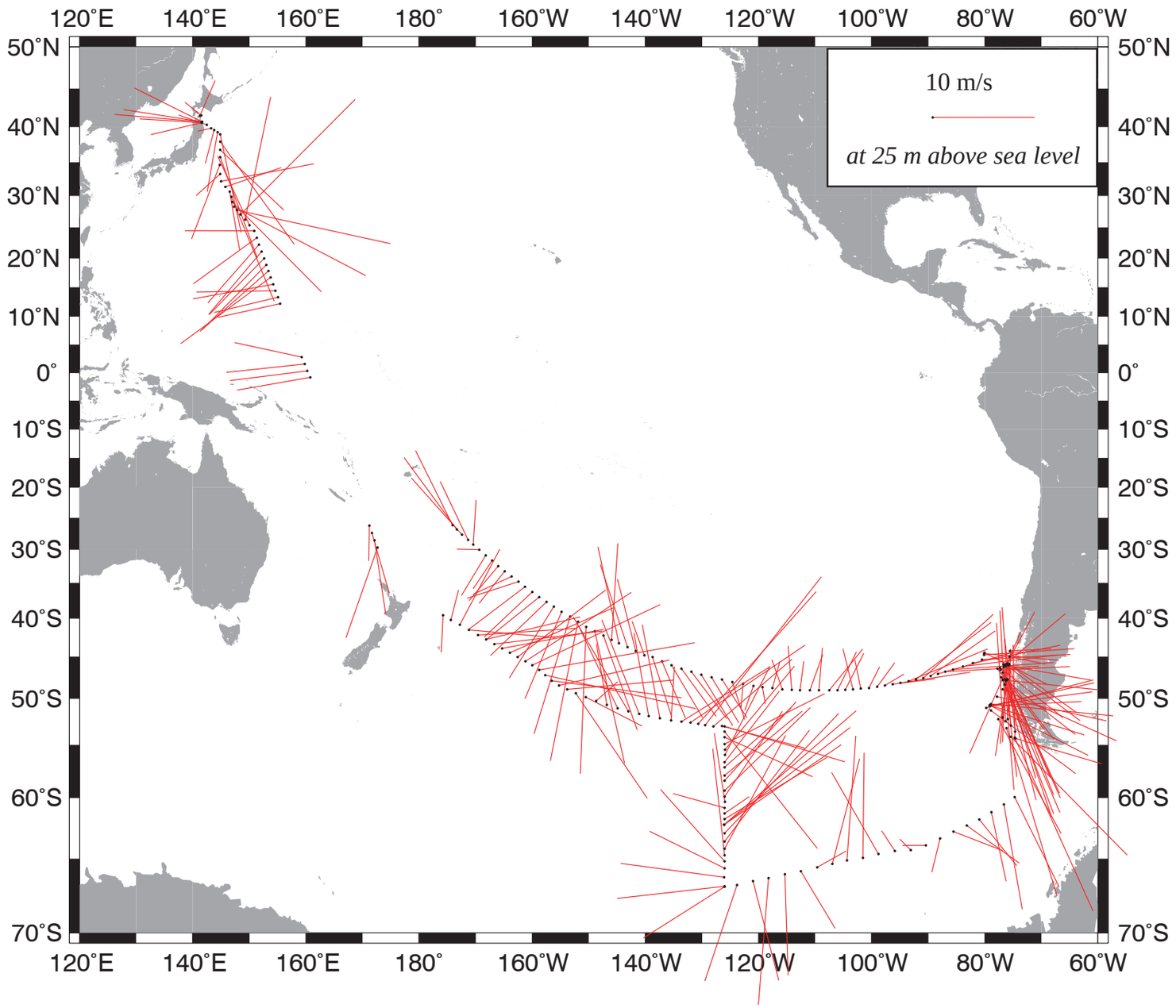

Figure 4a
Sea surface temperature (°C)

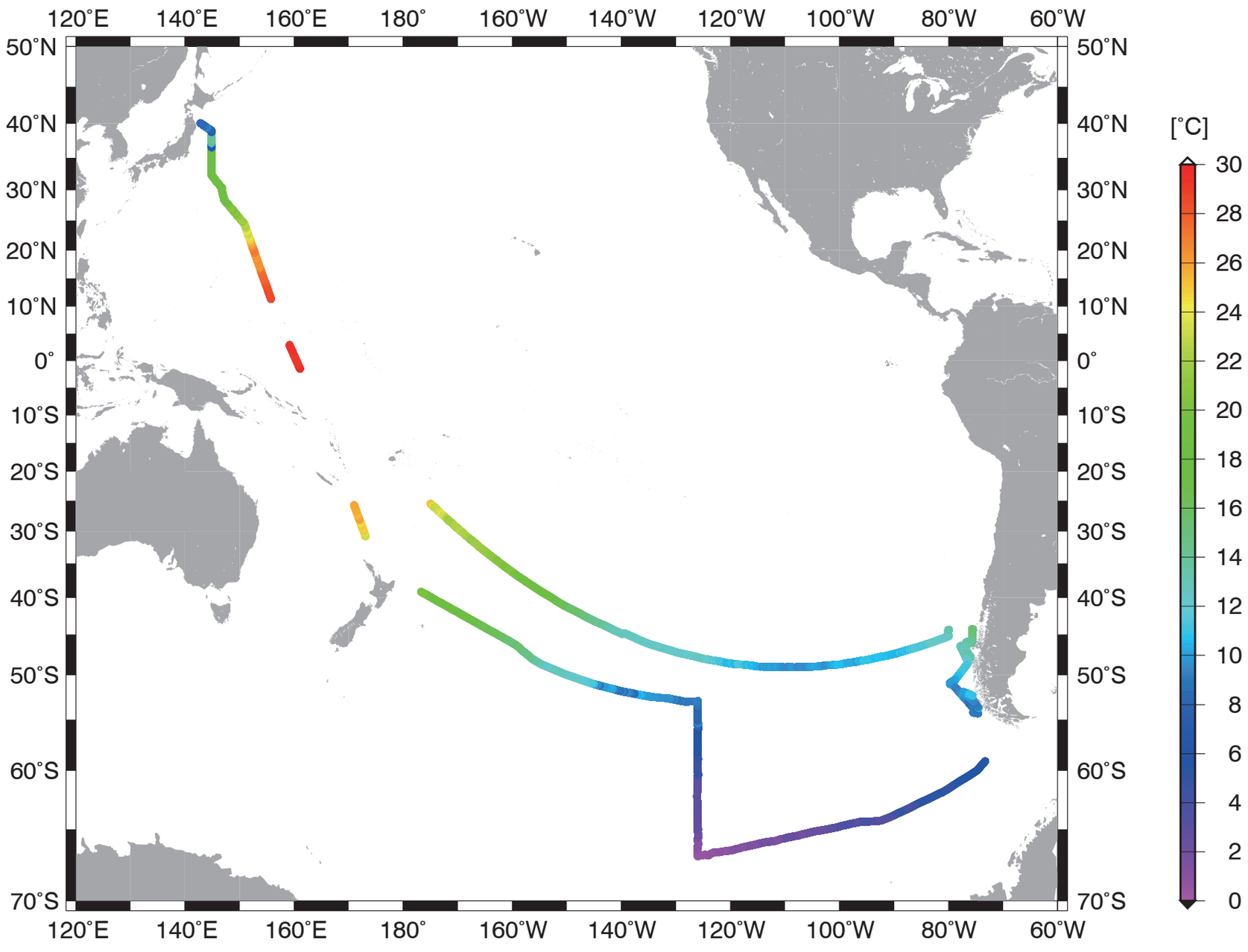

Figure 4b
Sea surface salinity (psu)

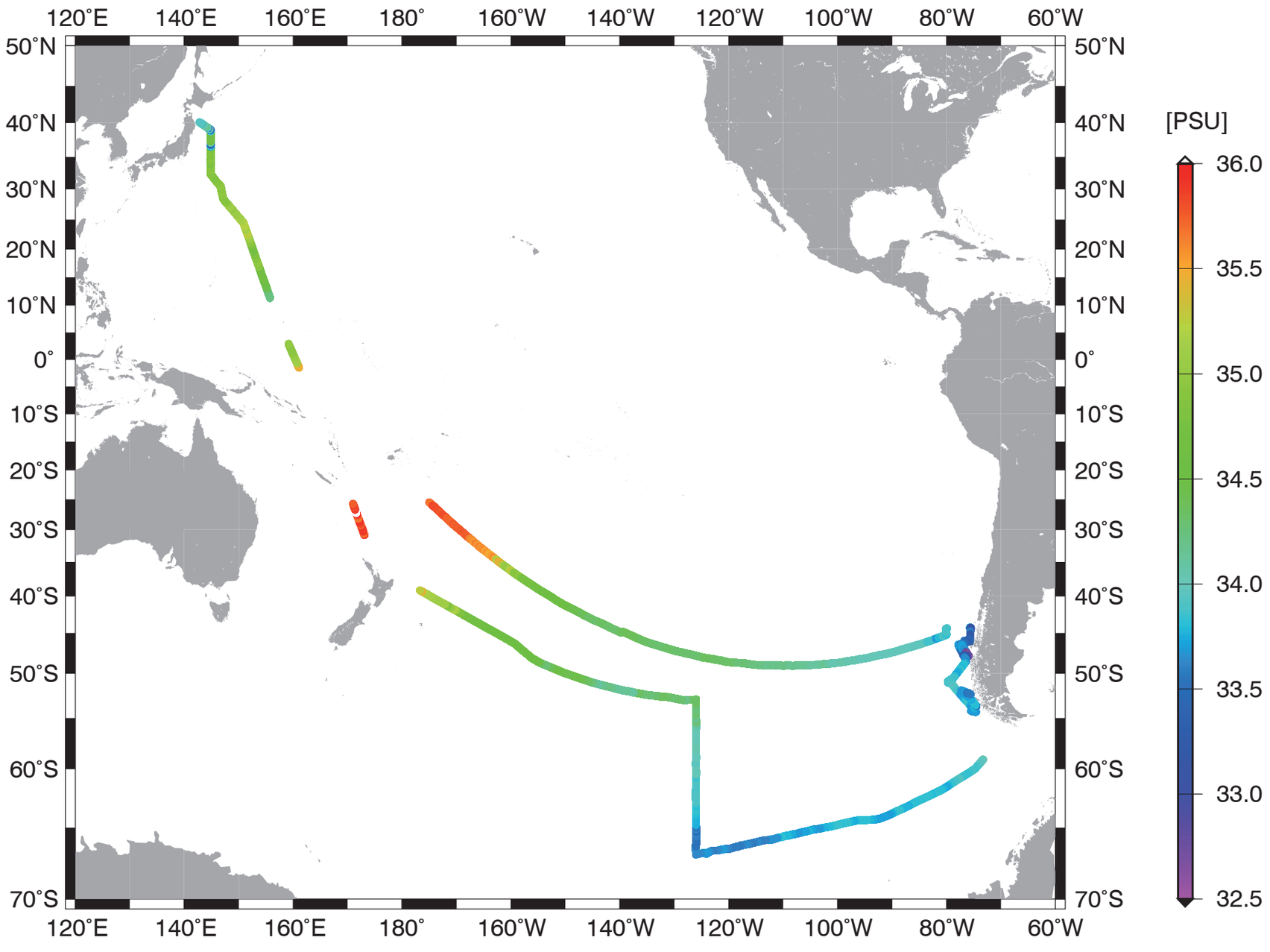

Figure 4c
Sea surface oxygen (µmol/kg)

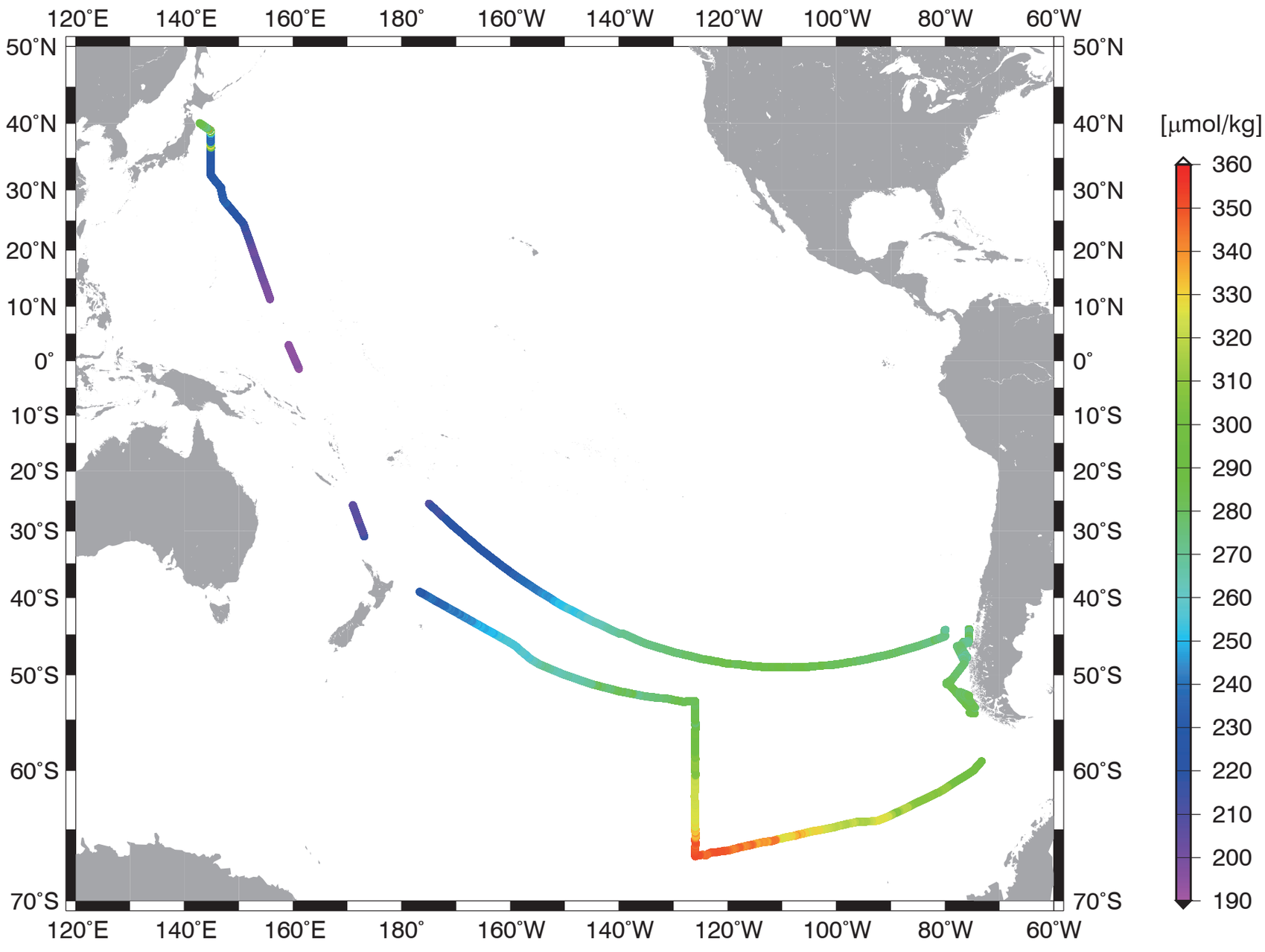

Figure 4d

Sea surface chlorophyll *a* (mg/m^3)

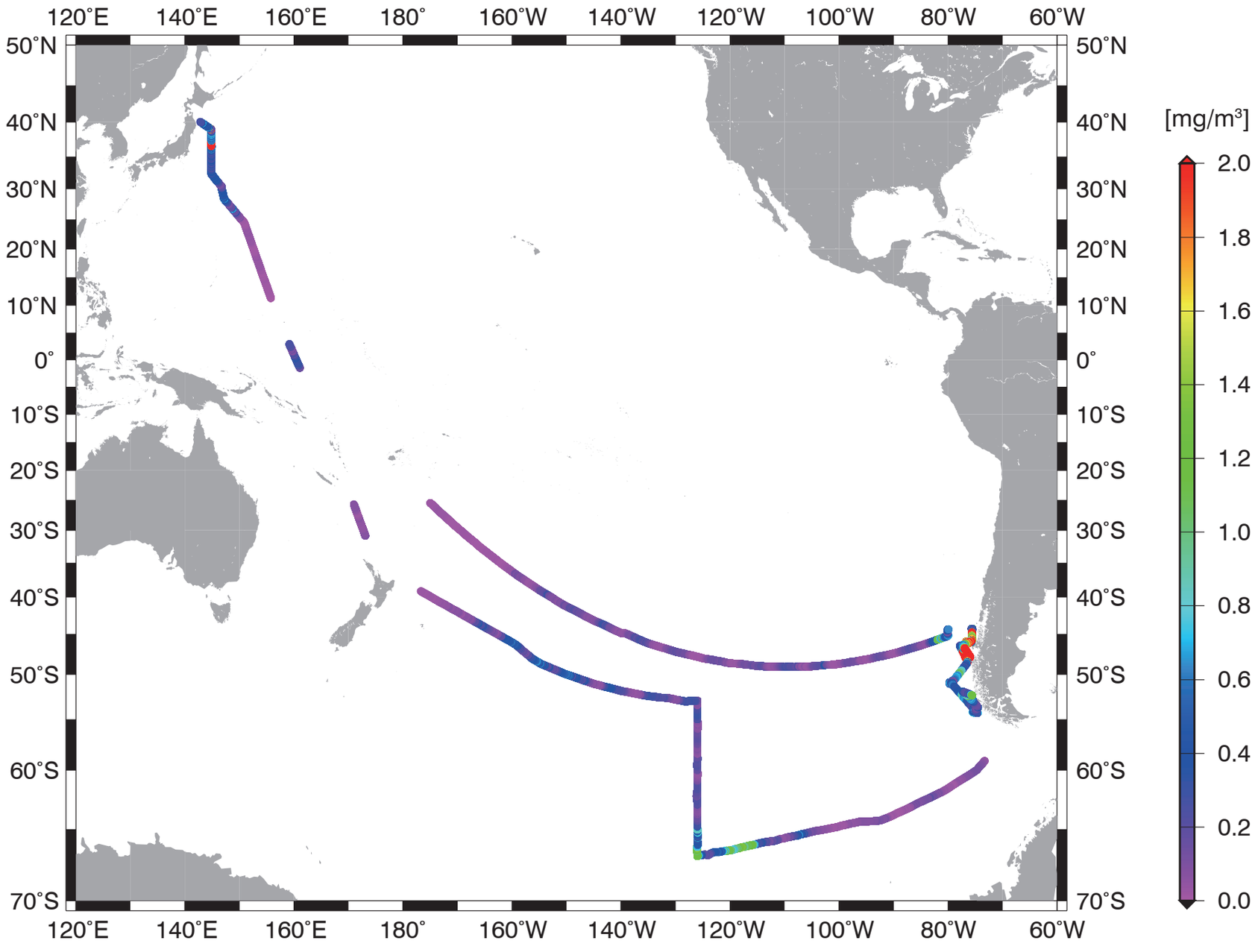

Figure 5

ΔpCO_2 (ppmv)

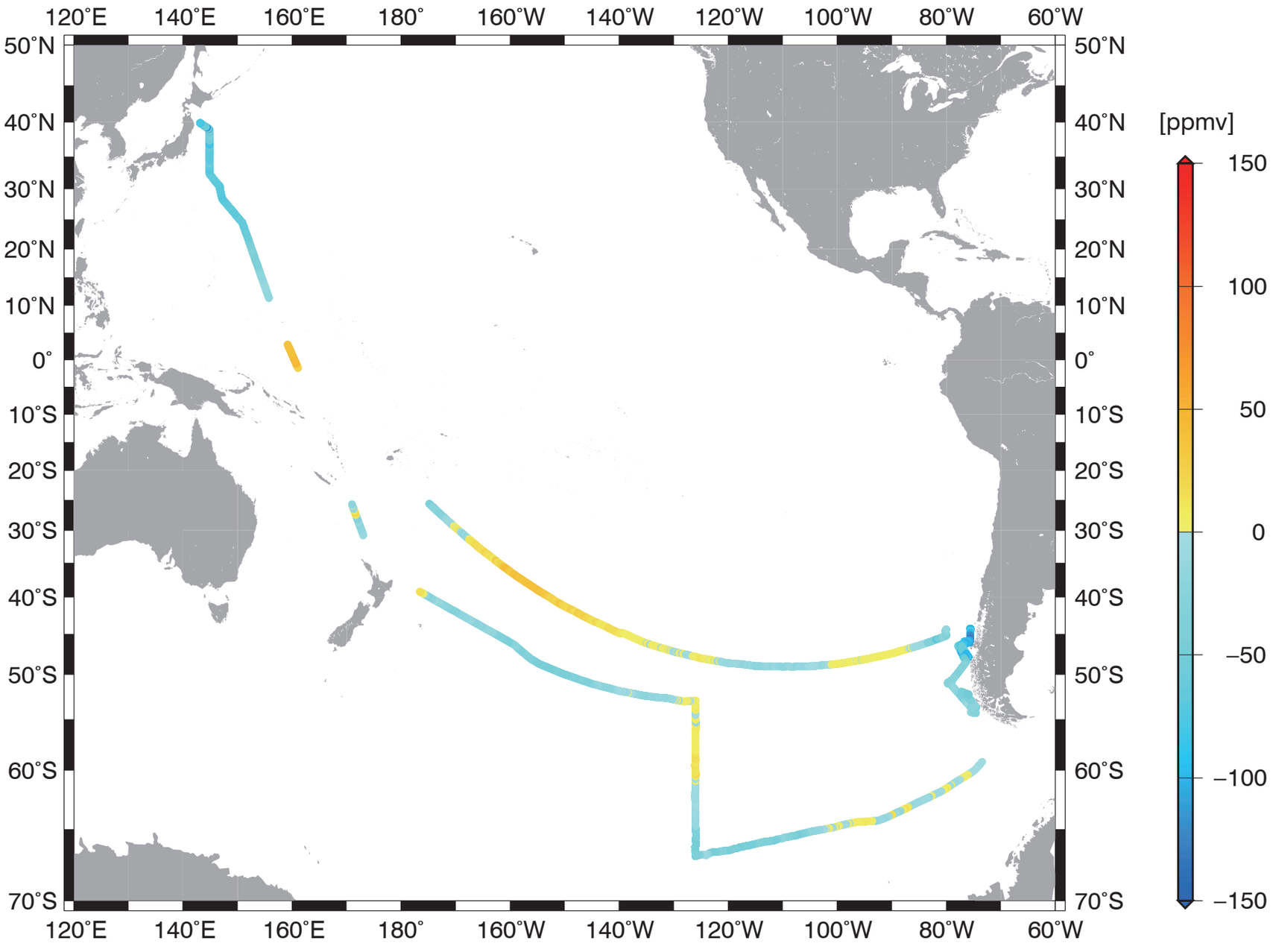

Figure 6
Sea surface C_T (µmol/kg)

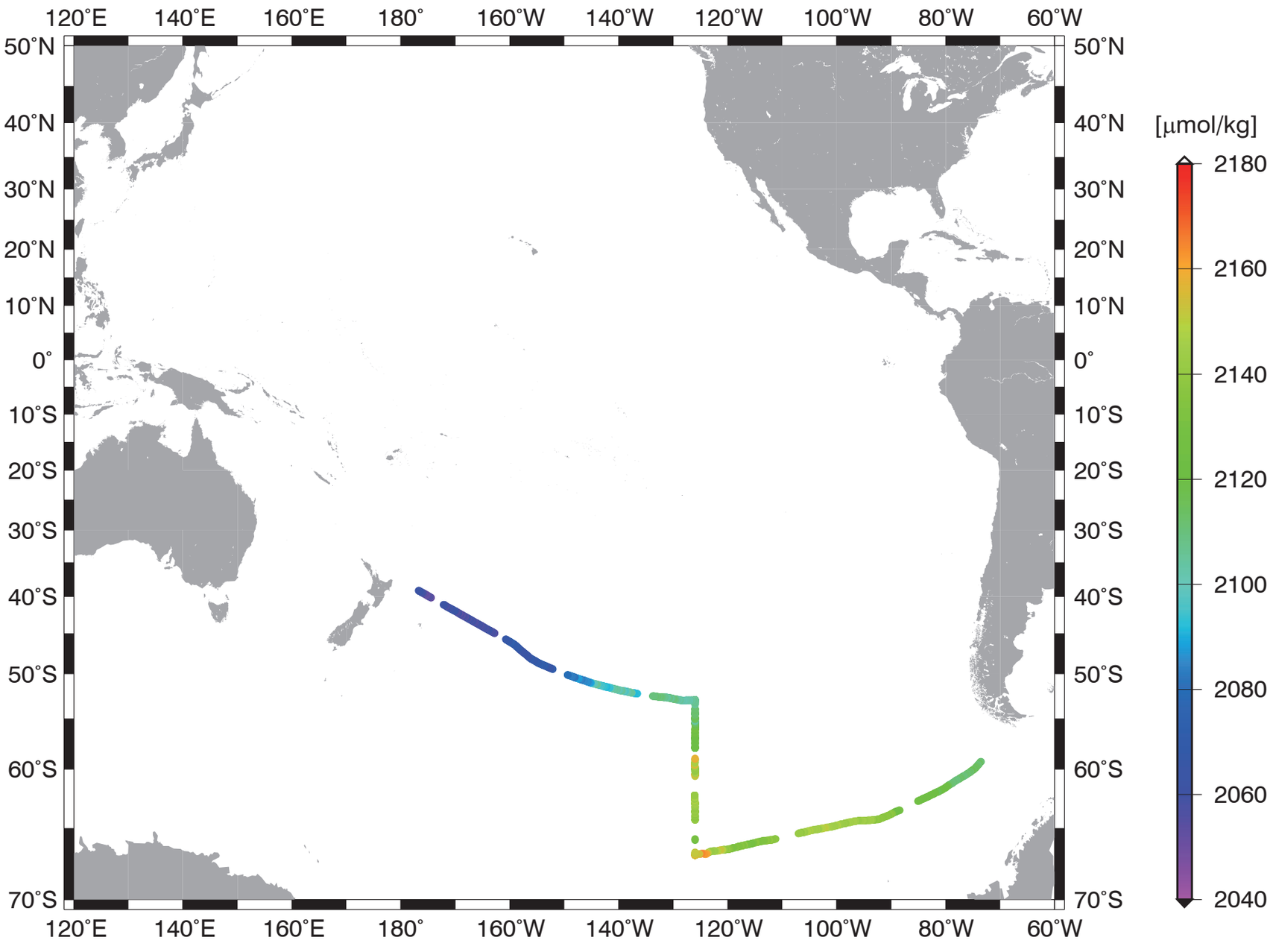

Figure 7
Surface current measured by shipboard ADCP

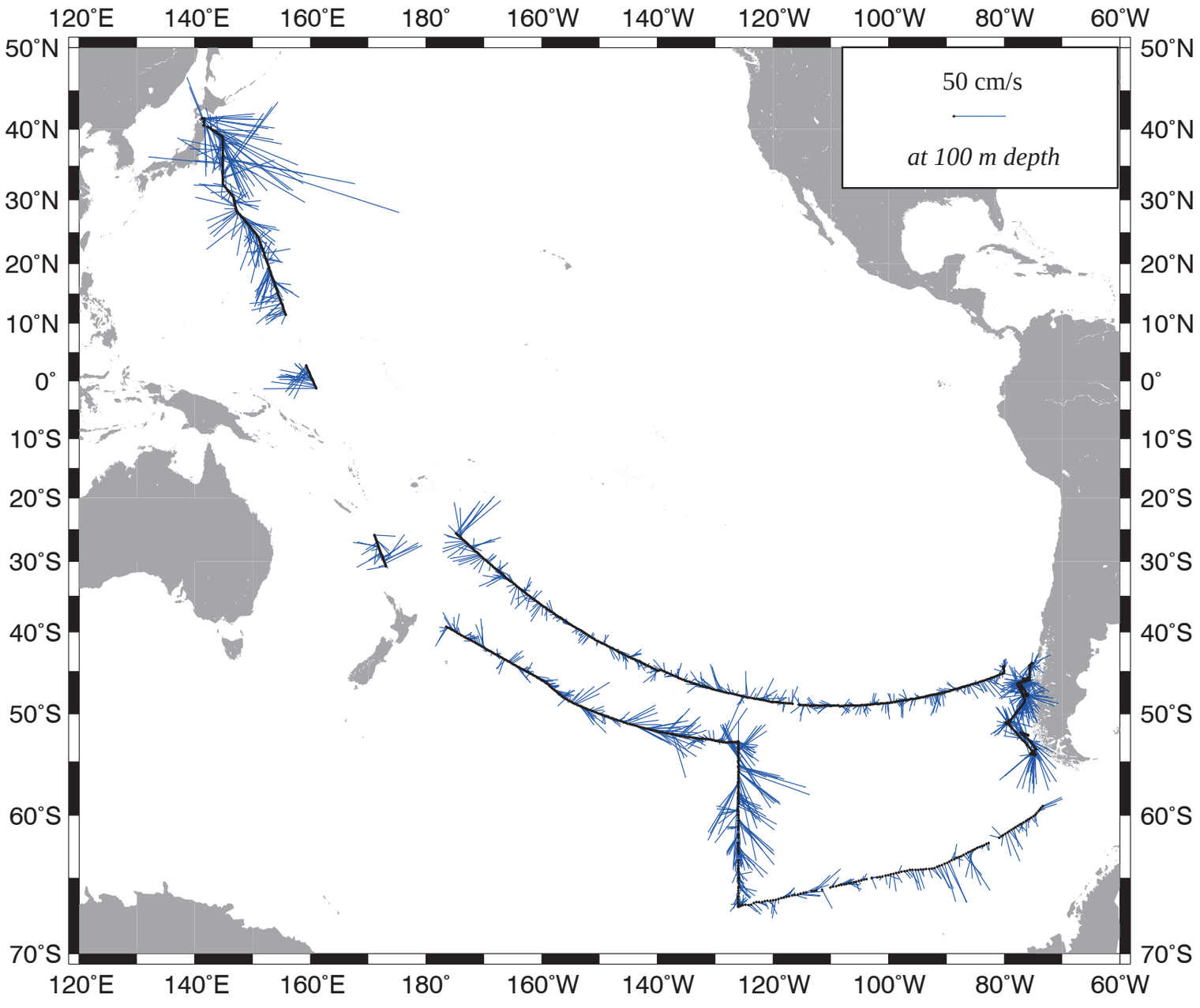

Figure 8
Potential temperature (°C)

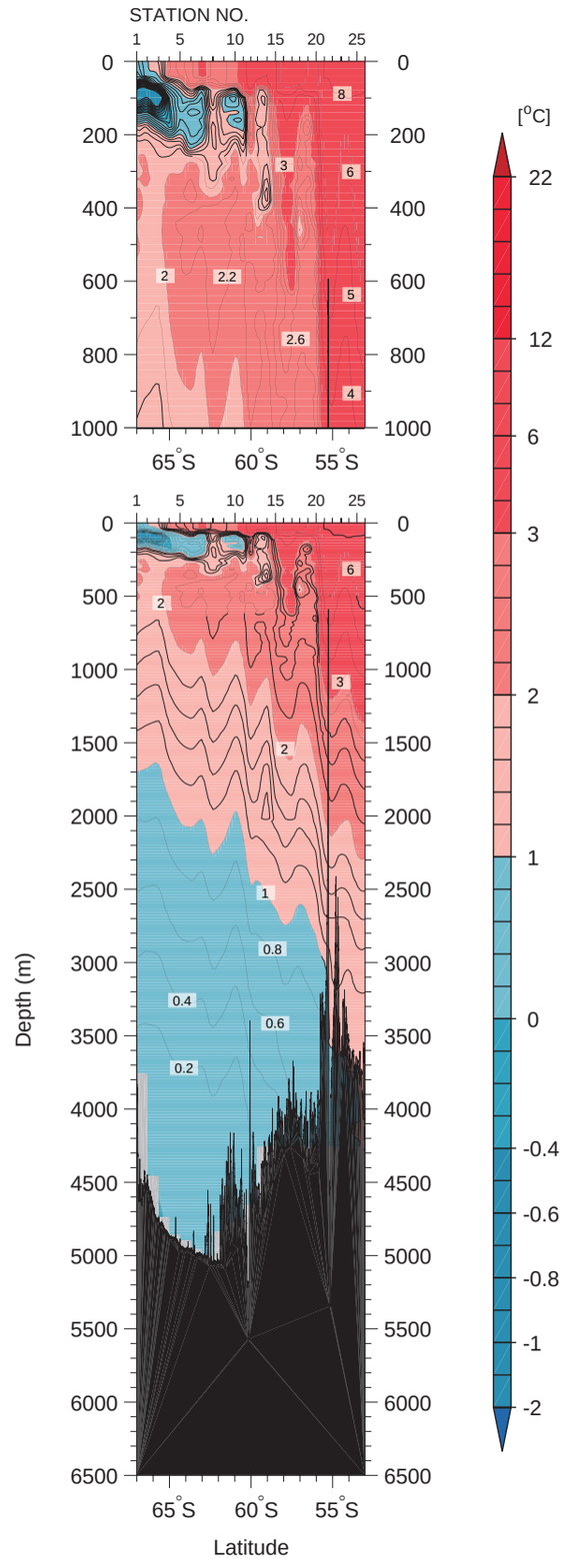

Figure 9
CTD salinity

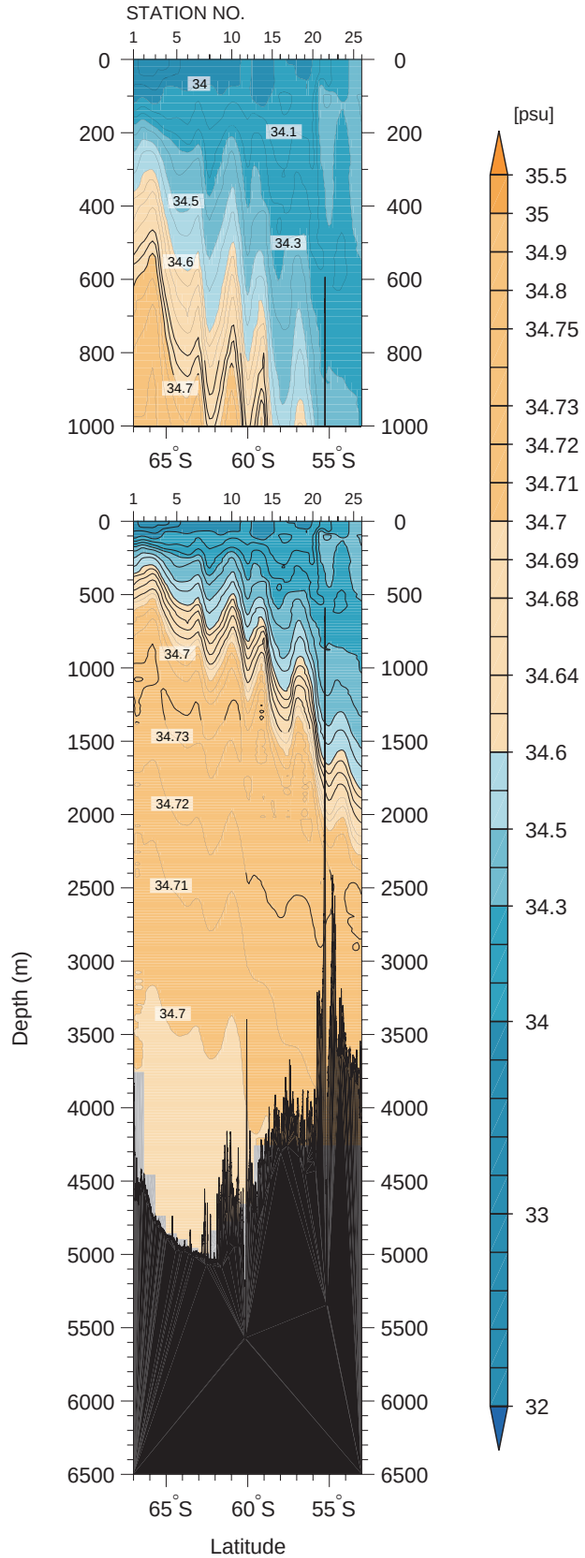

Figure 10
Absolute Salinity (g/kg)

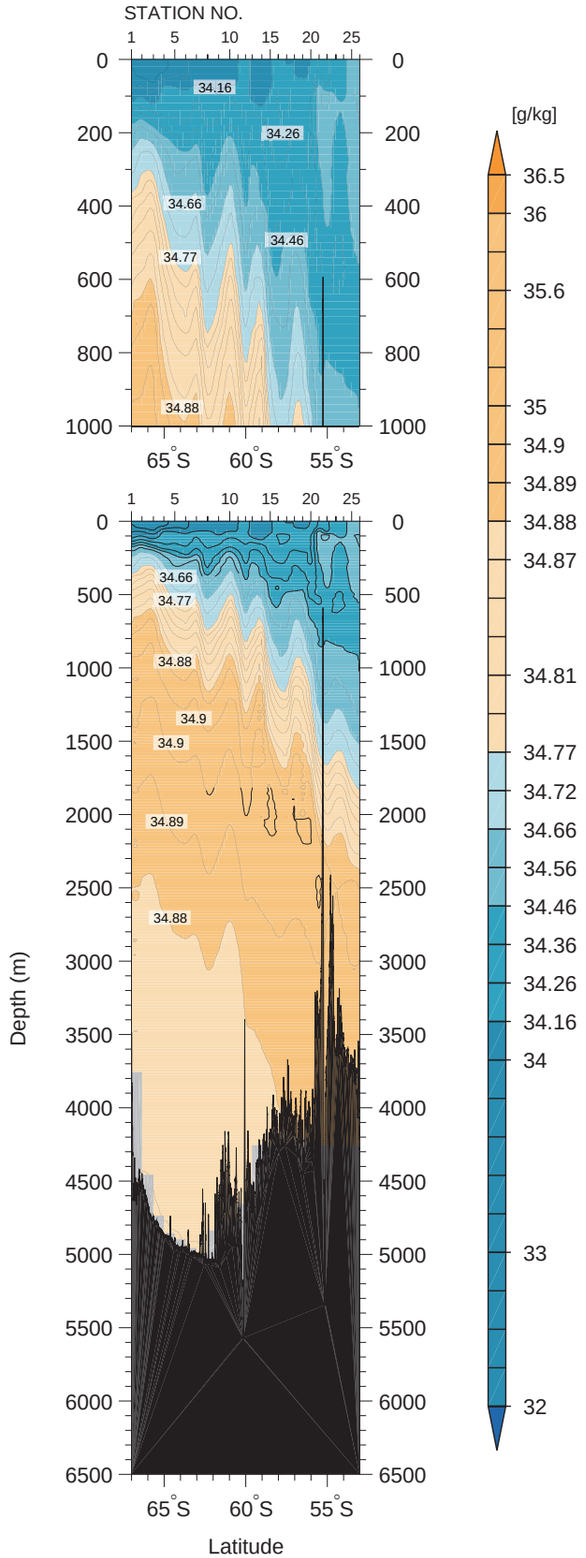

Figure 11a

Density (upper: σ_0, lower: σ_4) (kg/m^3) (EOS-80)

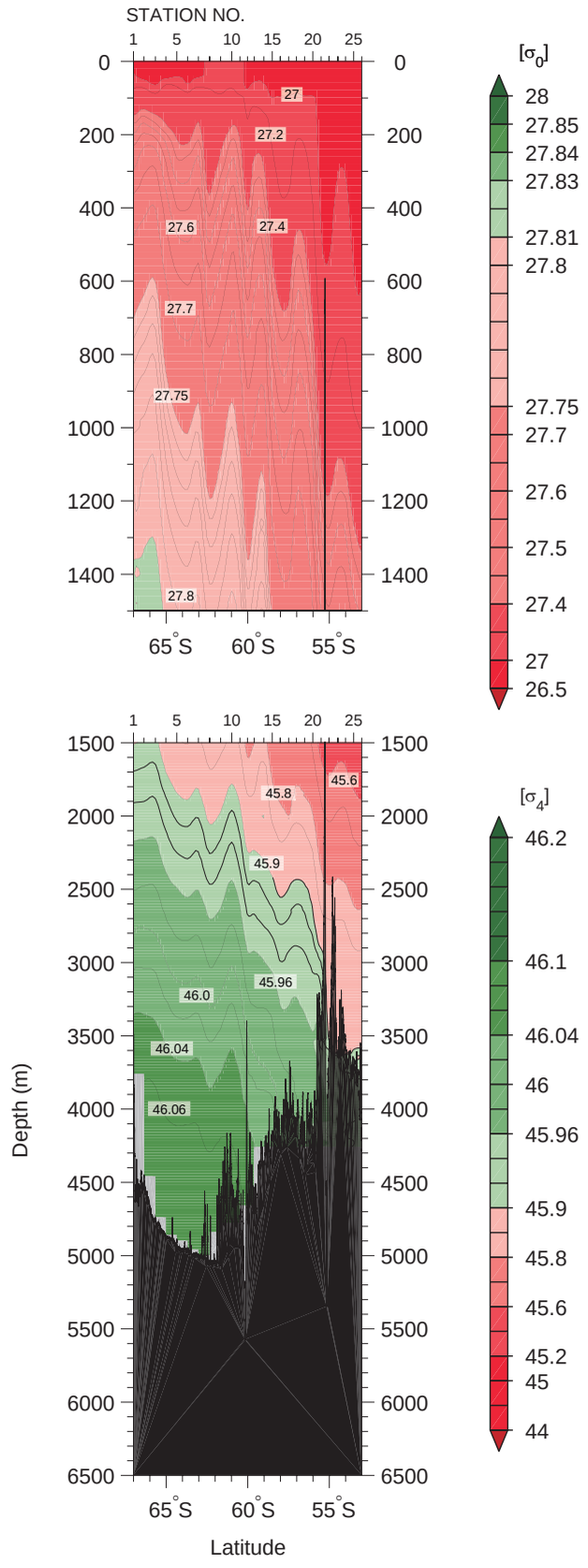

Figure 11b

Density (upper: σ_0, lower: σ_4) (kg/m^3) (TEOS-10)

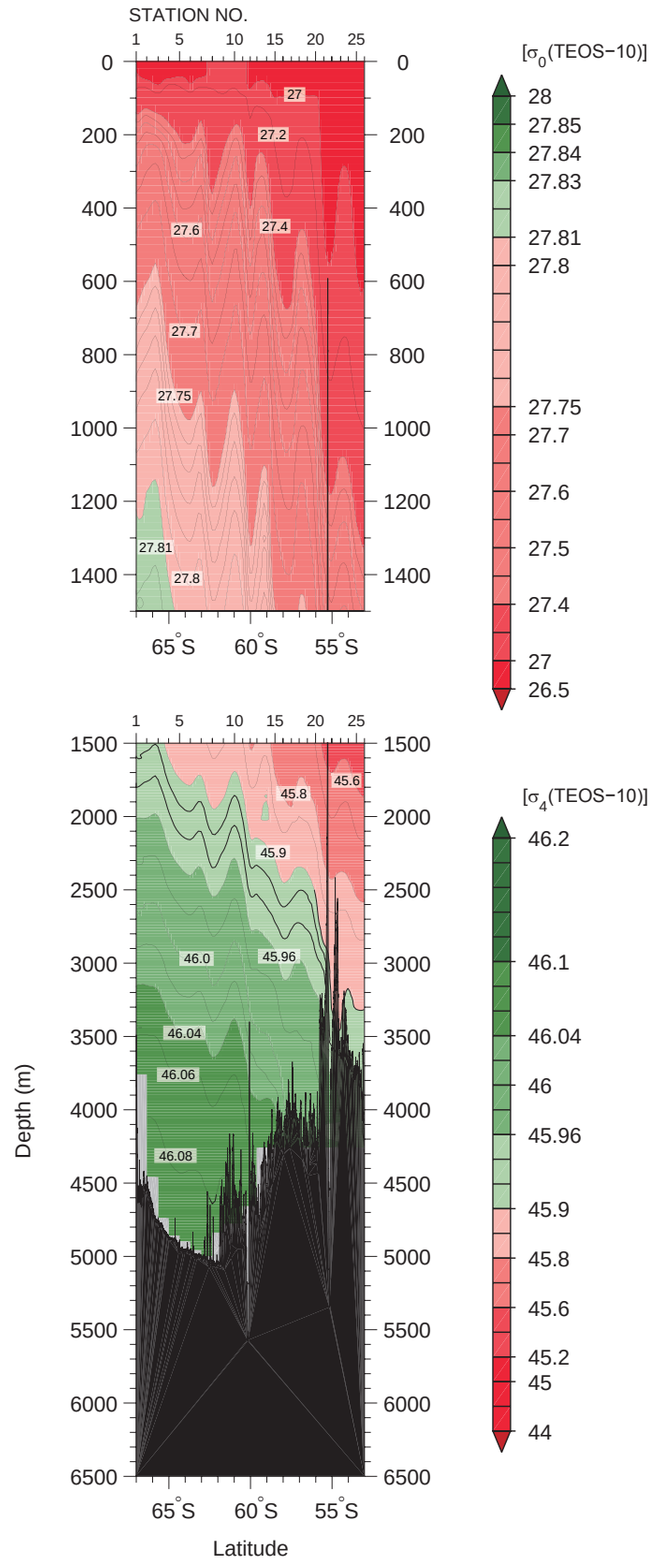

Figure 12
Neutral Density (γ^n) (kg/m^3)

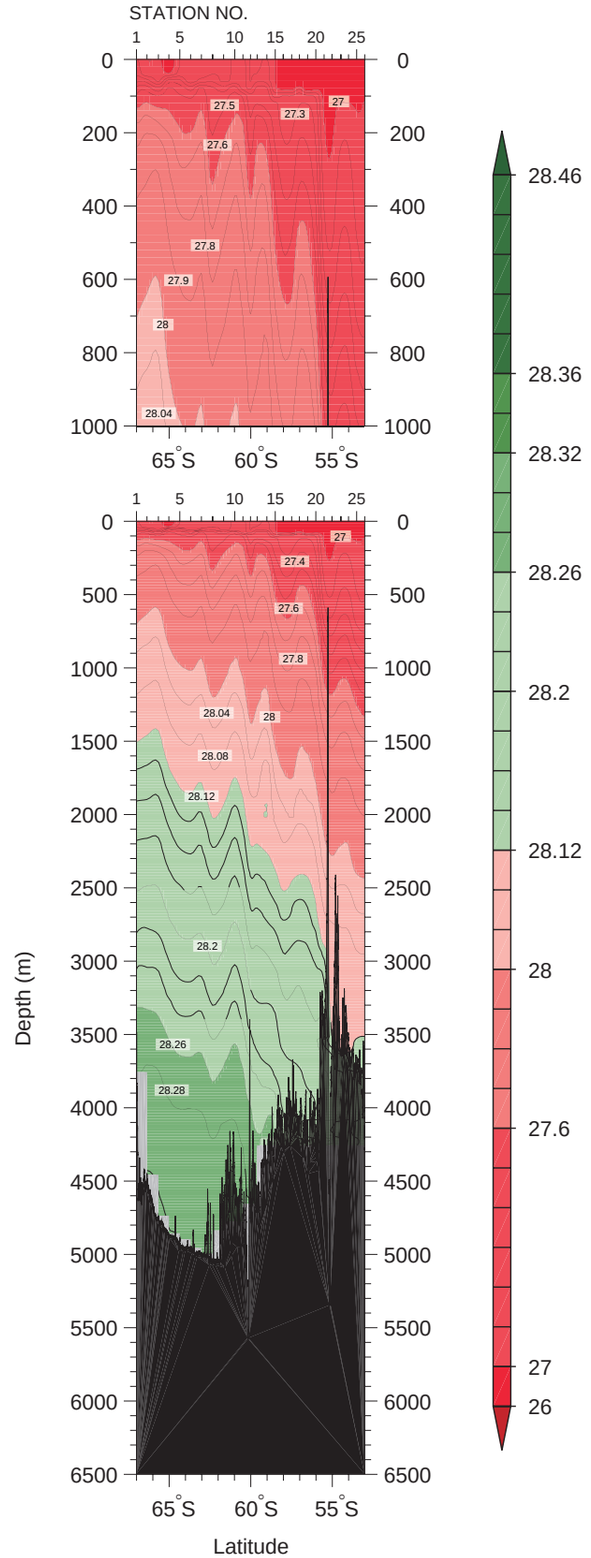

Figure 13
CTD oxygen (µmol/kg)

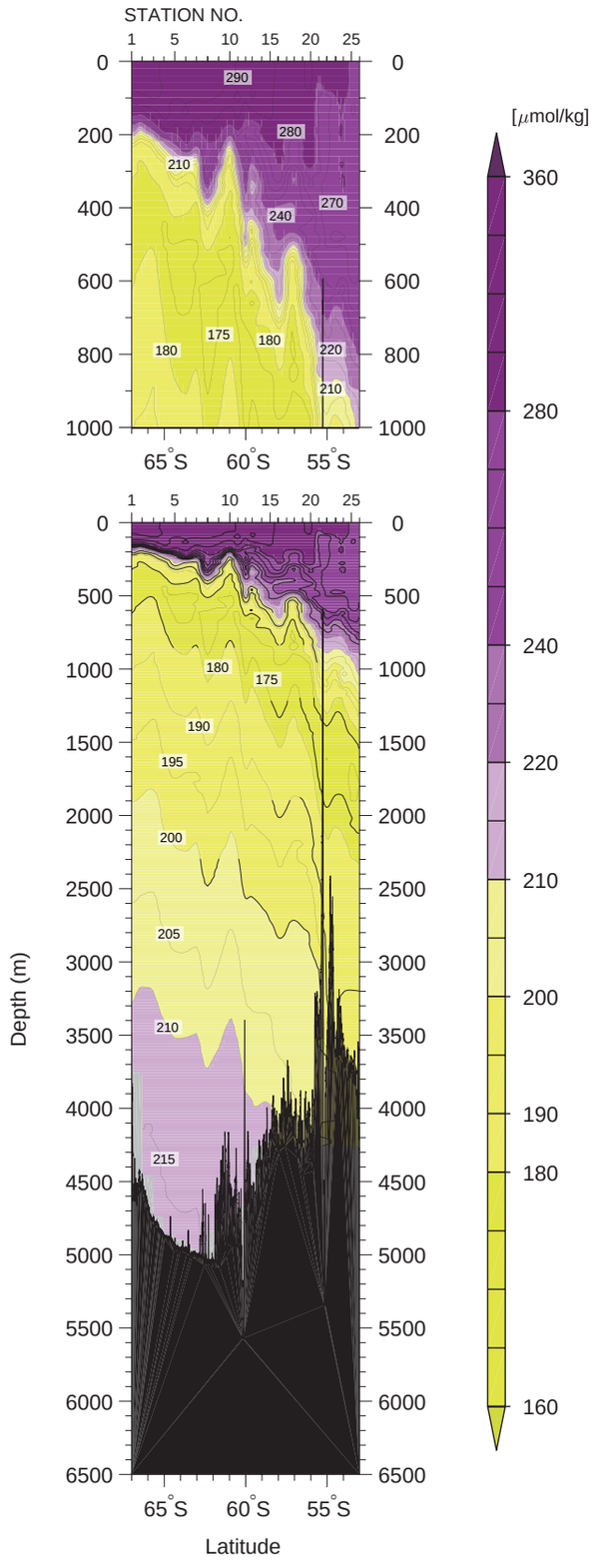

Figure 14
CTD chlorophyll *a* (mg/m^3)

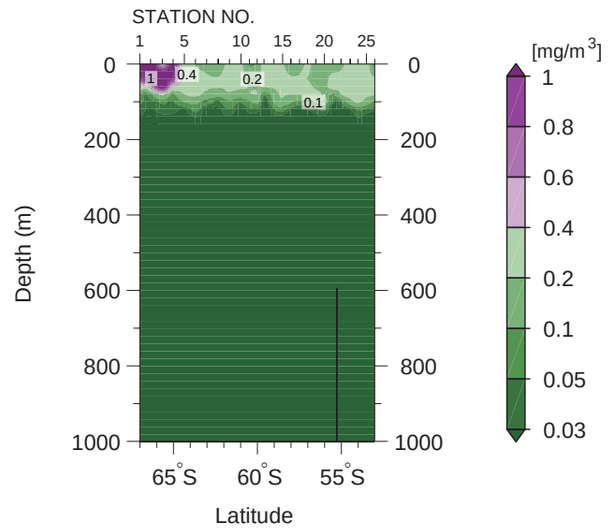

Figure 15
CTD beam attenuation coefficient (m^{-1})

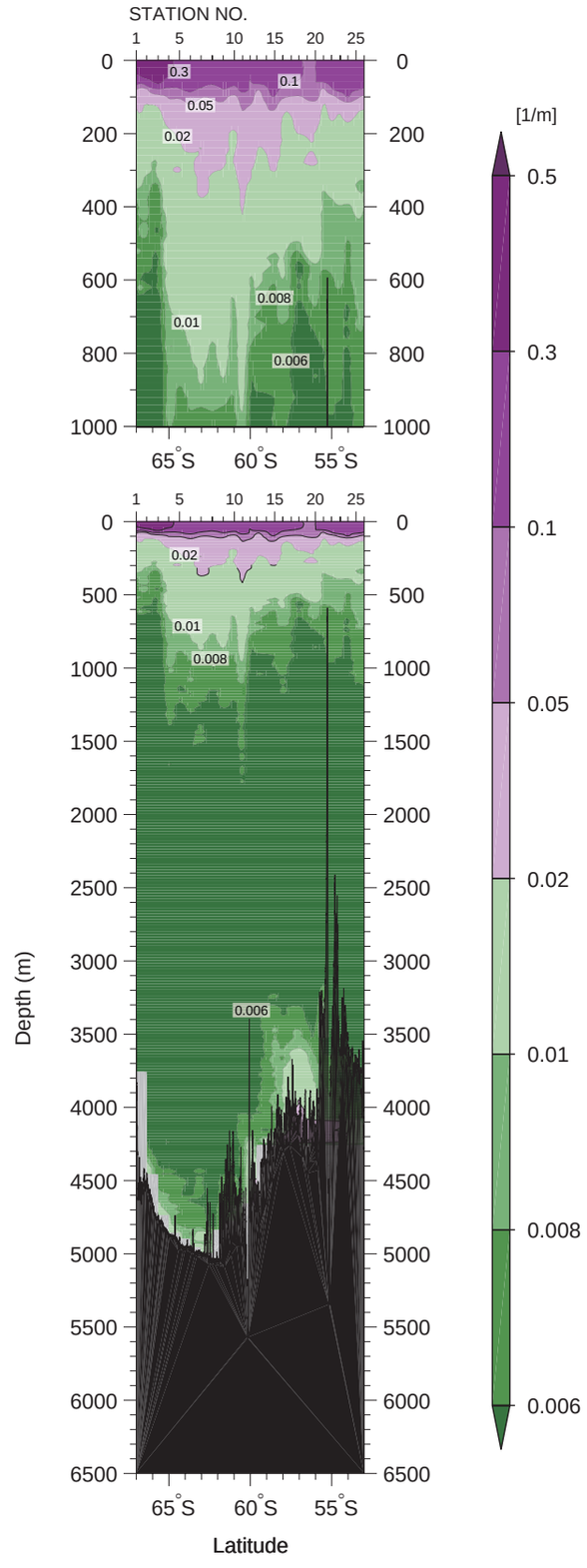

Figure 16
Bottle sampled dissolved oxygen (µmol/kg)

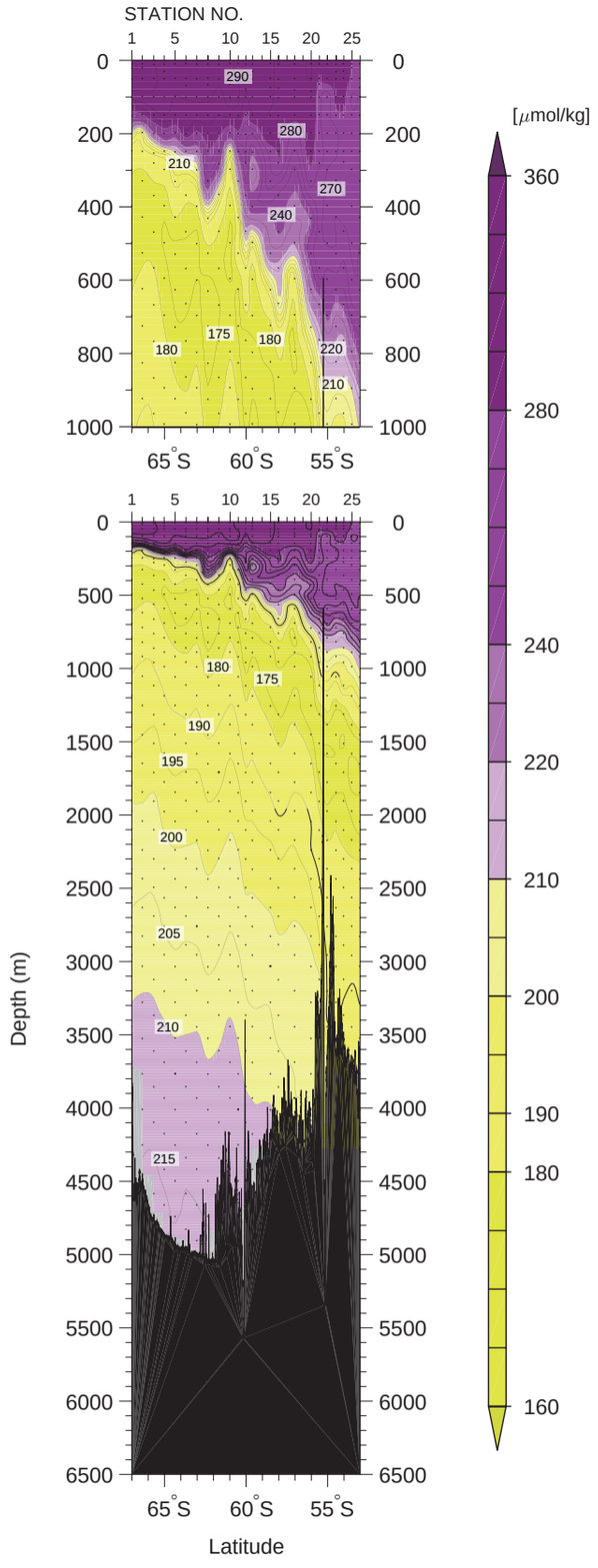

Figure 17
Silicate (µmol/kg)

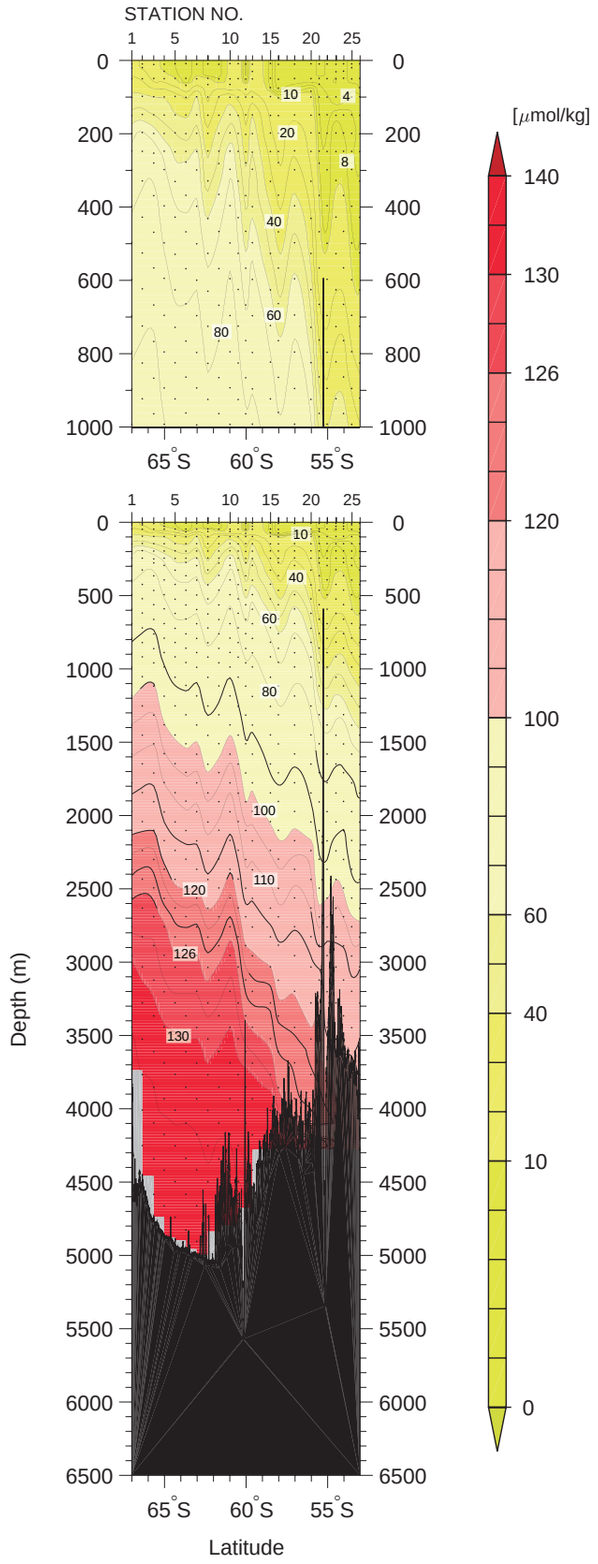

Figure 18
Nitrate (µmol/kg)

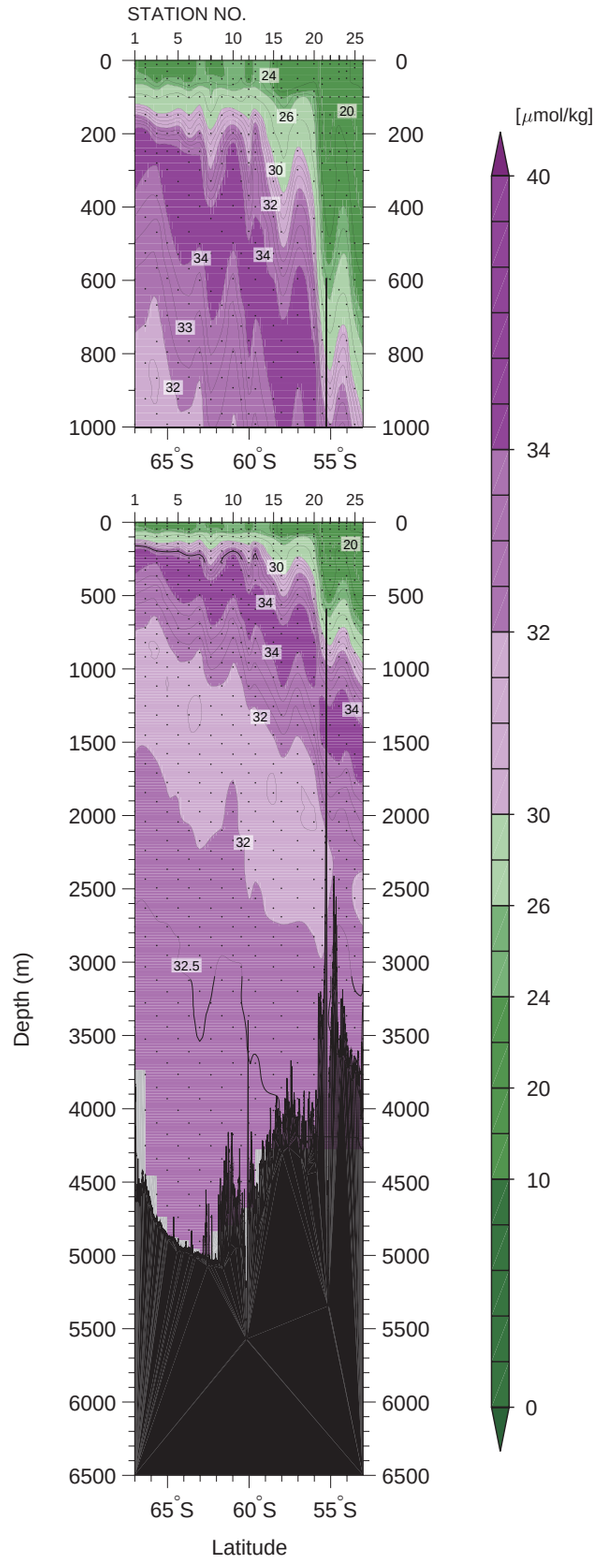

Figure 19
Nitrite (µmol/kg)

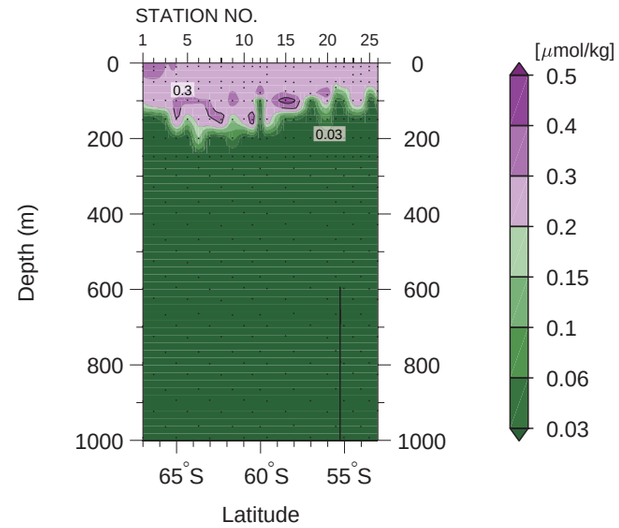

Figure 20
Phosphate (µmol/kg)

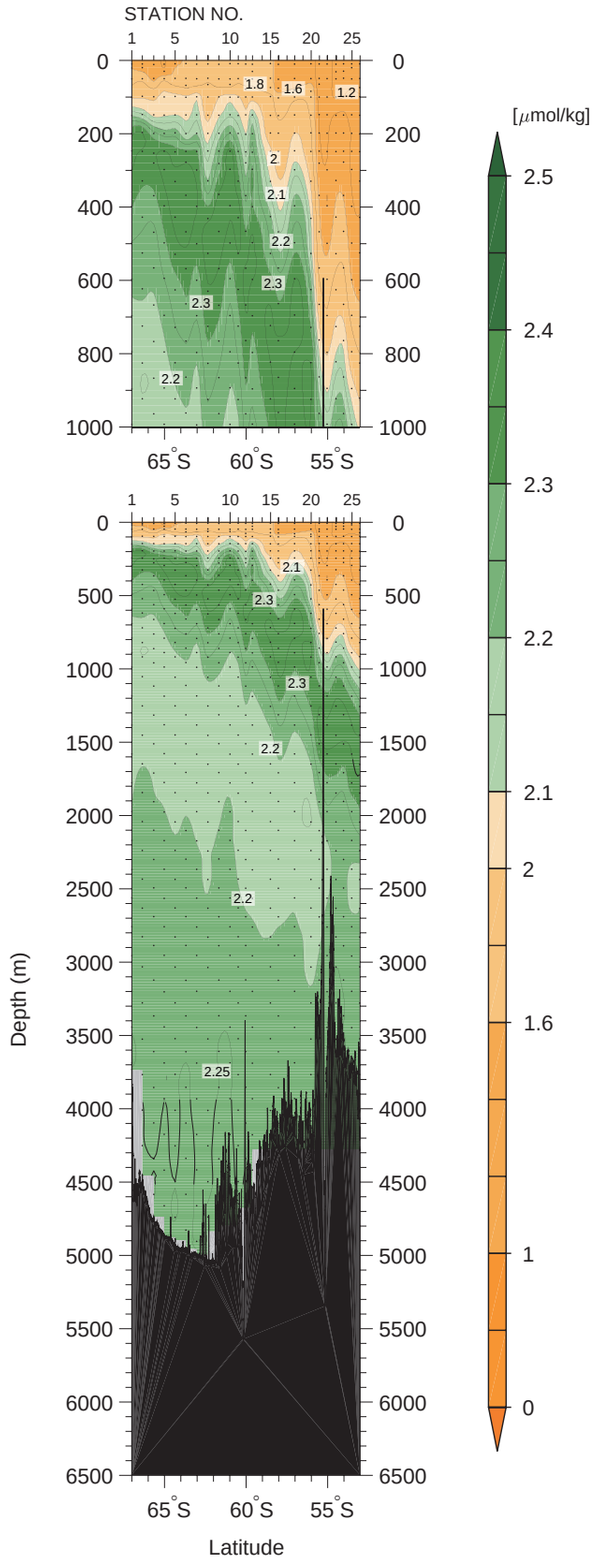

Figure 21
Dissolved inorganic carbon (C_T) (µmol/kg)

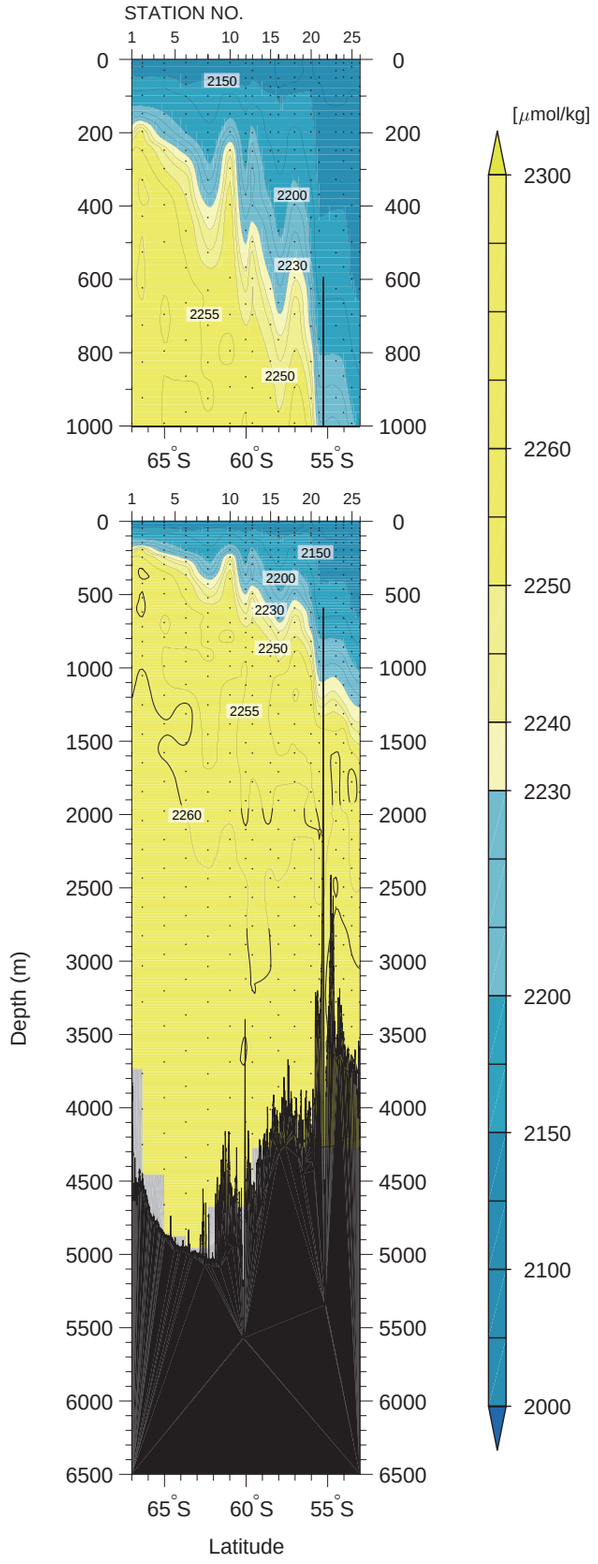

Figure 22
Total alkalinity (A_T) (µmol/kg)

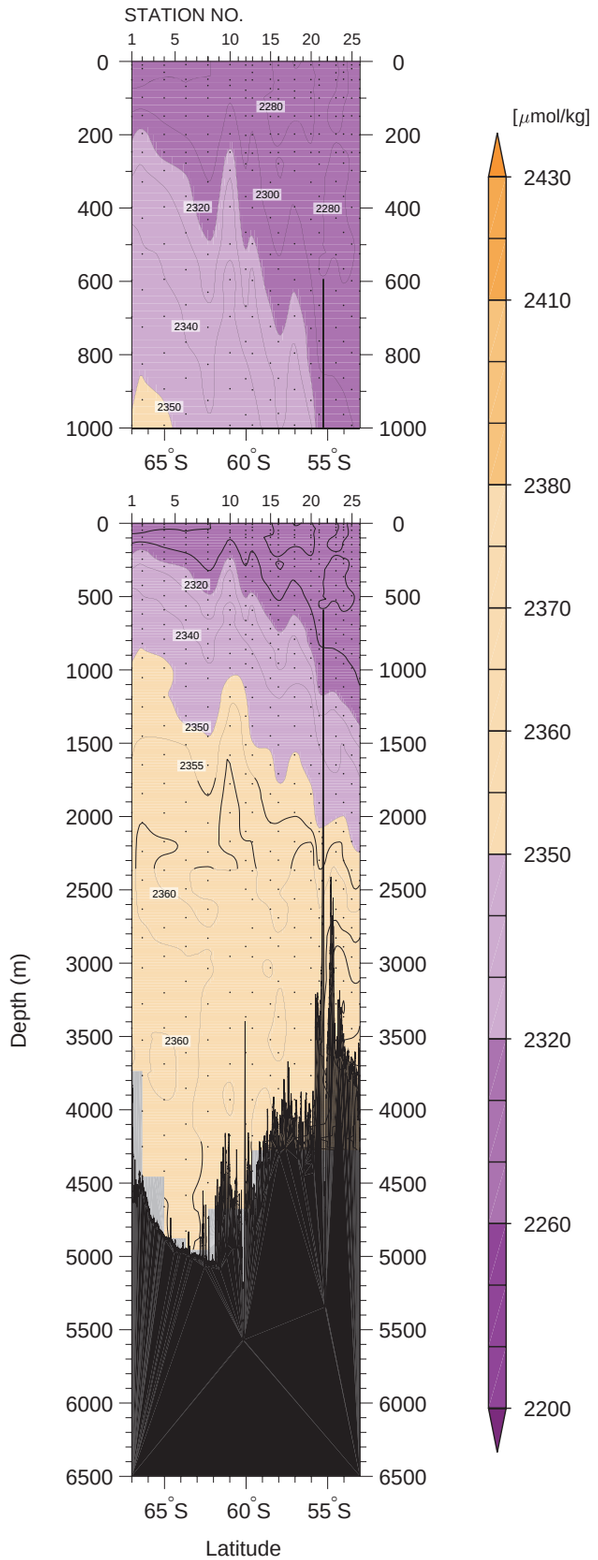

Figure 23
Dissolved organic carbon (µmol/kg)

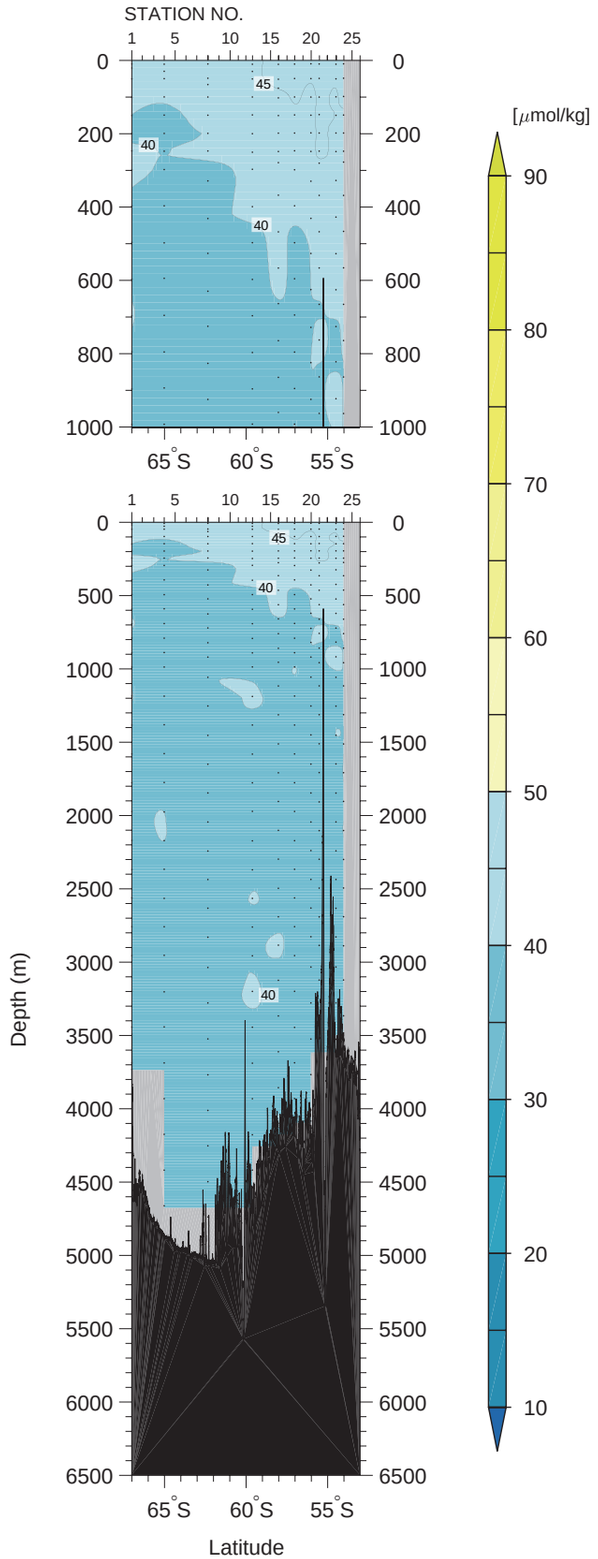

Figure 24
Calcium (mmol/kg)

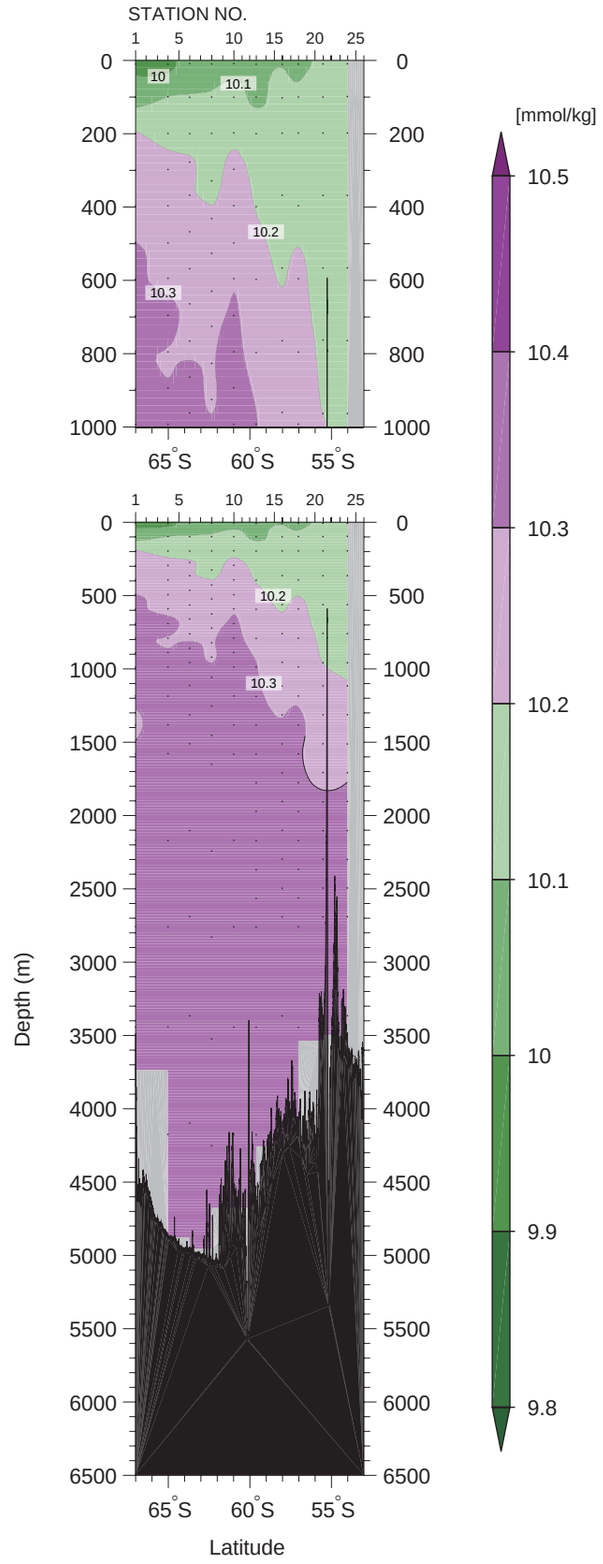

Figure 25
CFC-11 (pmol/kg)

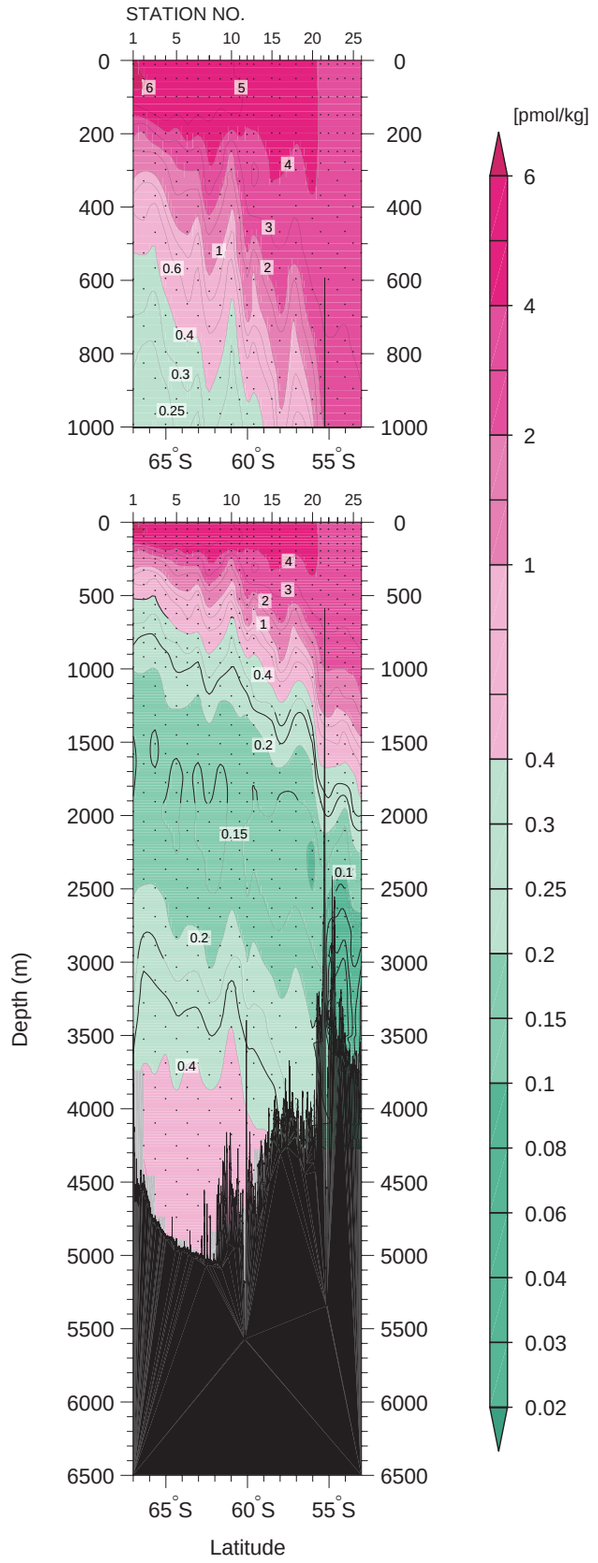

Figure 26
CFC-12 (pmol/kg)

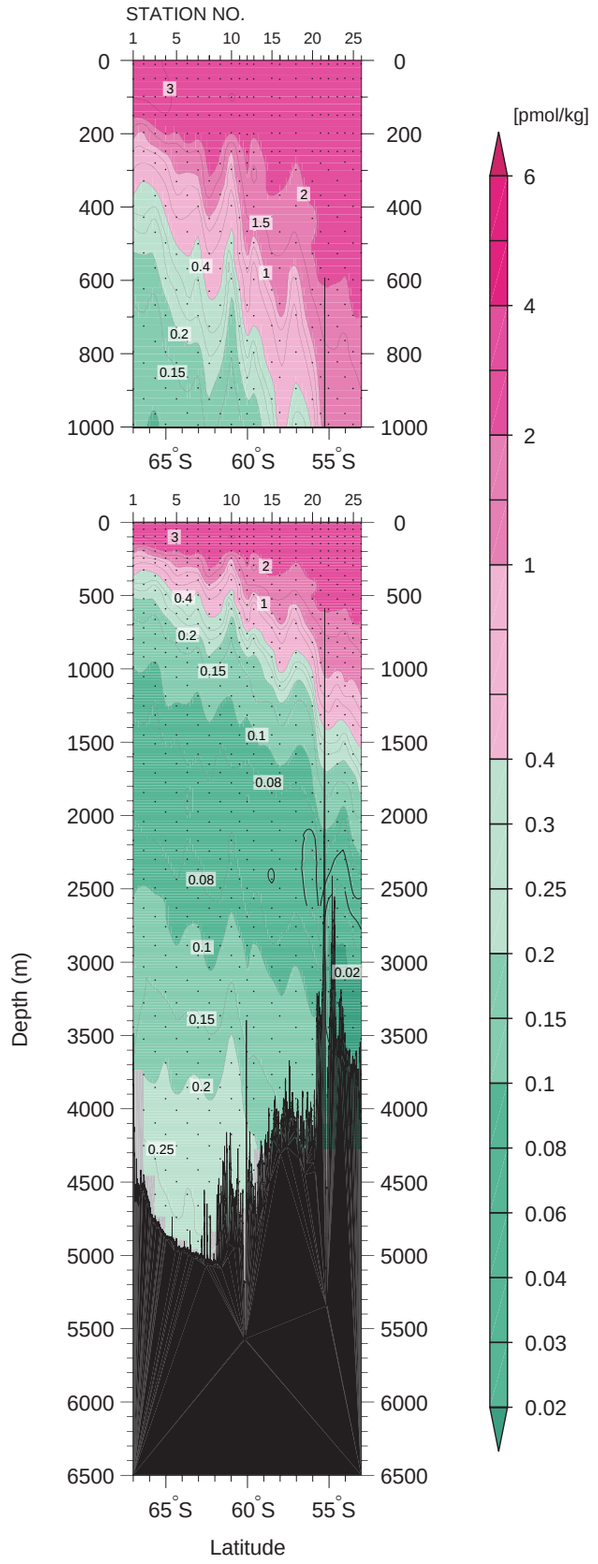

Figure 27
CFC-113 (pmol/kg)

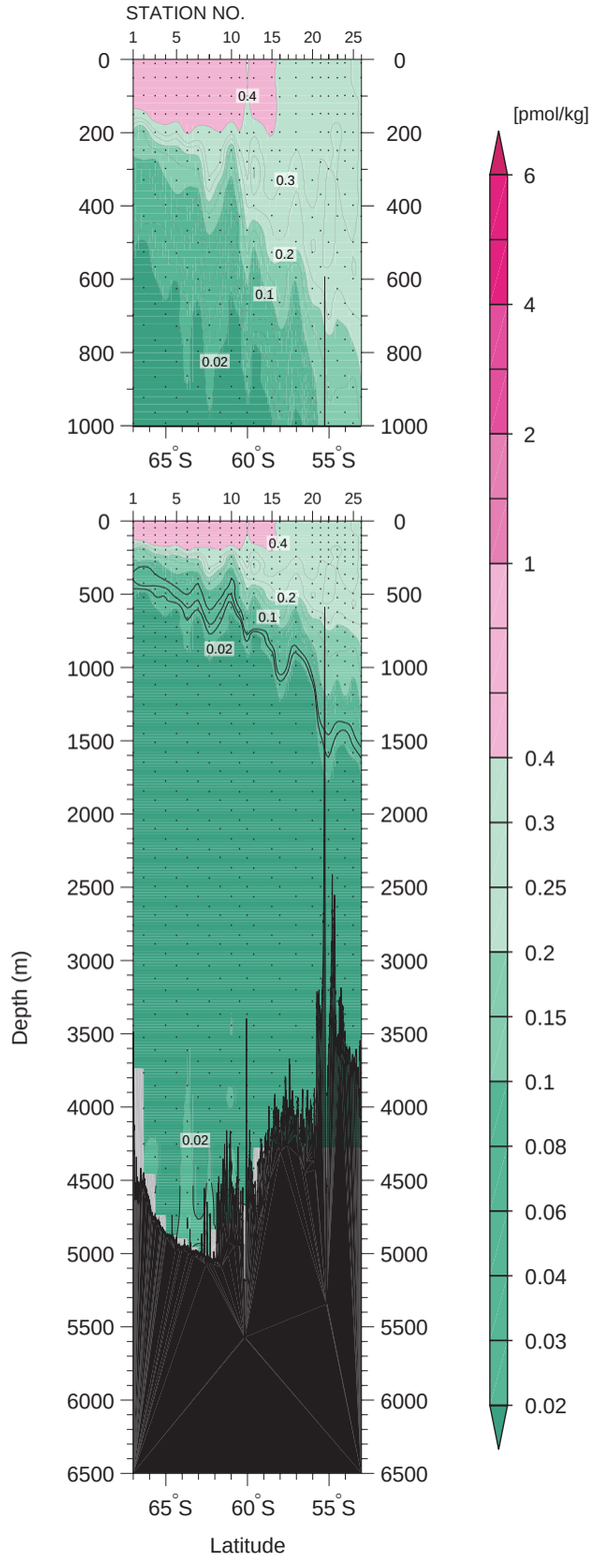

Figure 28
SF_6 (fmol/kg)

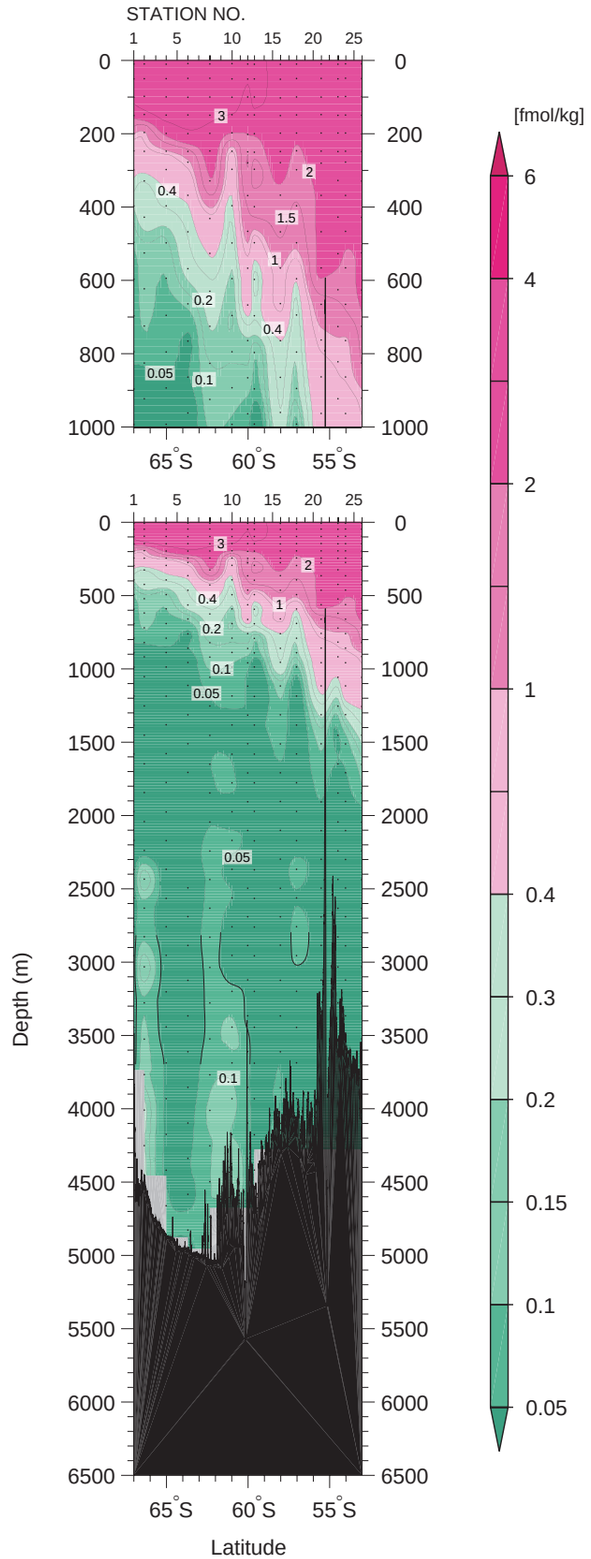

Figure 29

Current velocity (cm/s) normal to the cruise track measured By LADCP (eastward or northward is positive)

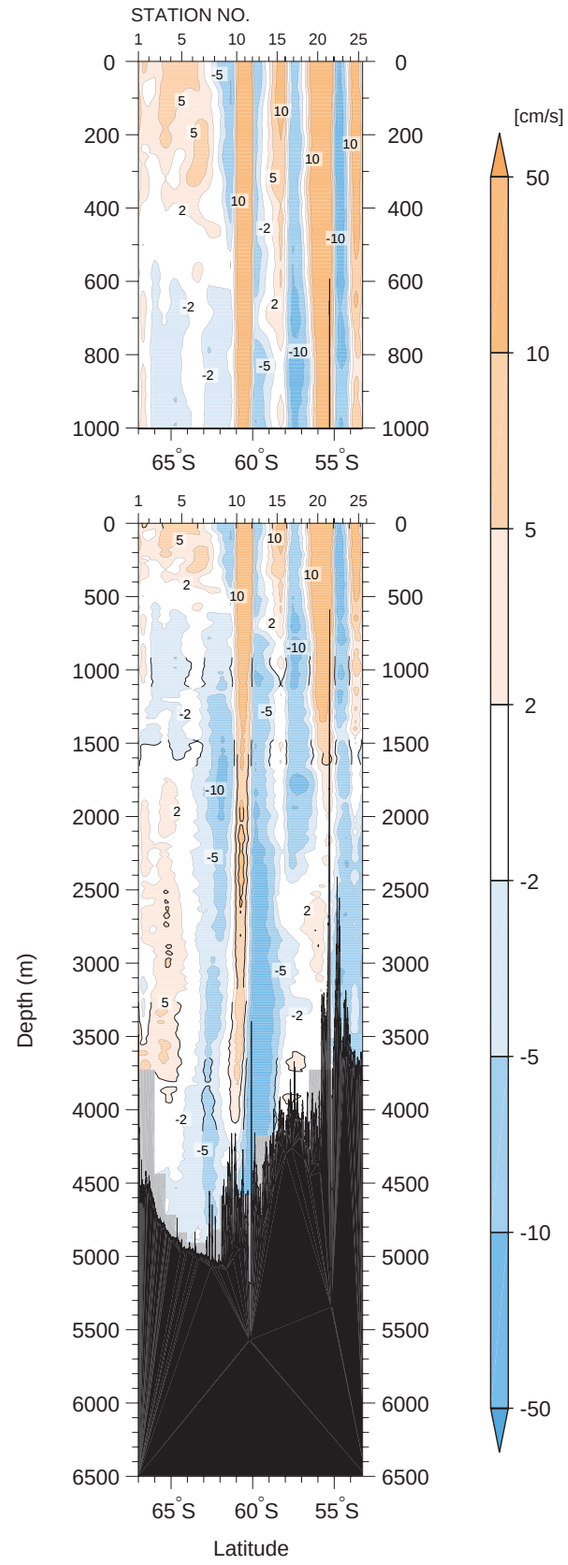

Figure 30

Difference in potential temperature (°C) between results from WHP P17E in 1992 and the revisit in 2017

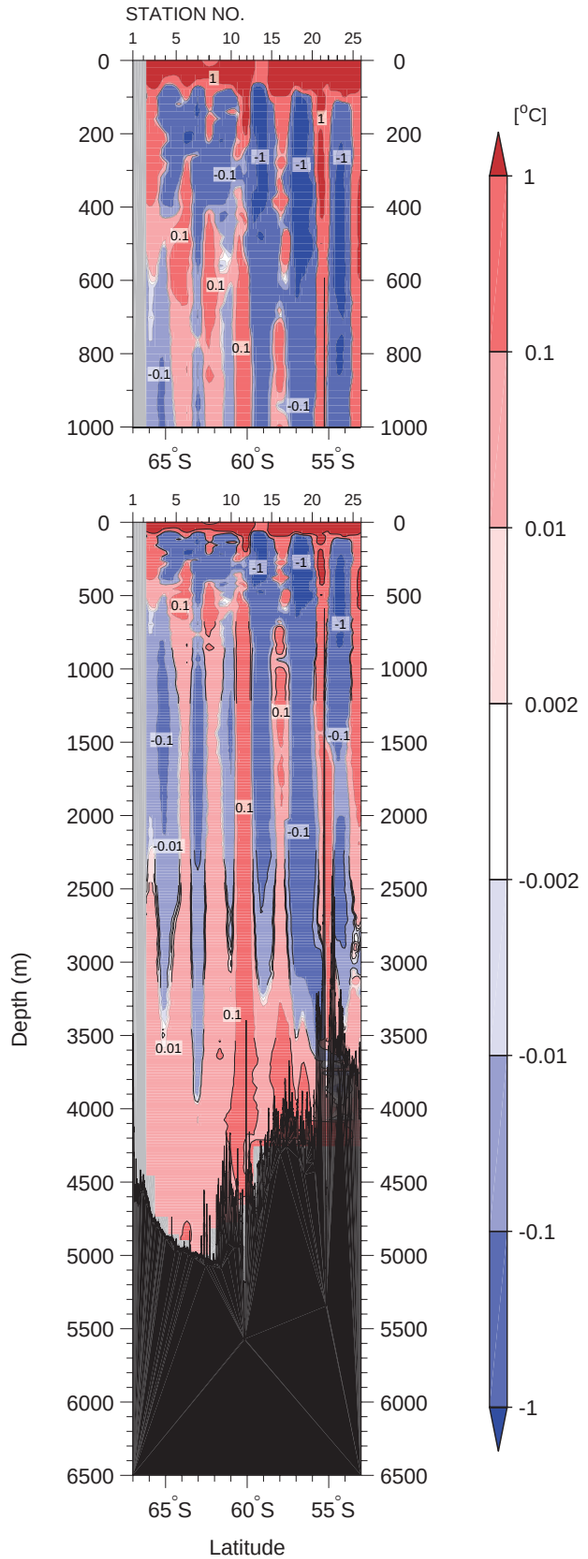

Figure 31

Difference in CTD salinity between results from WHP P17E in 1992 and the revisit in 2017

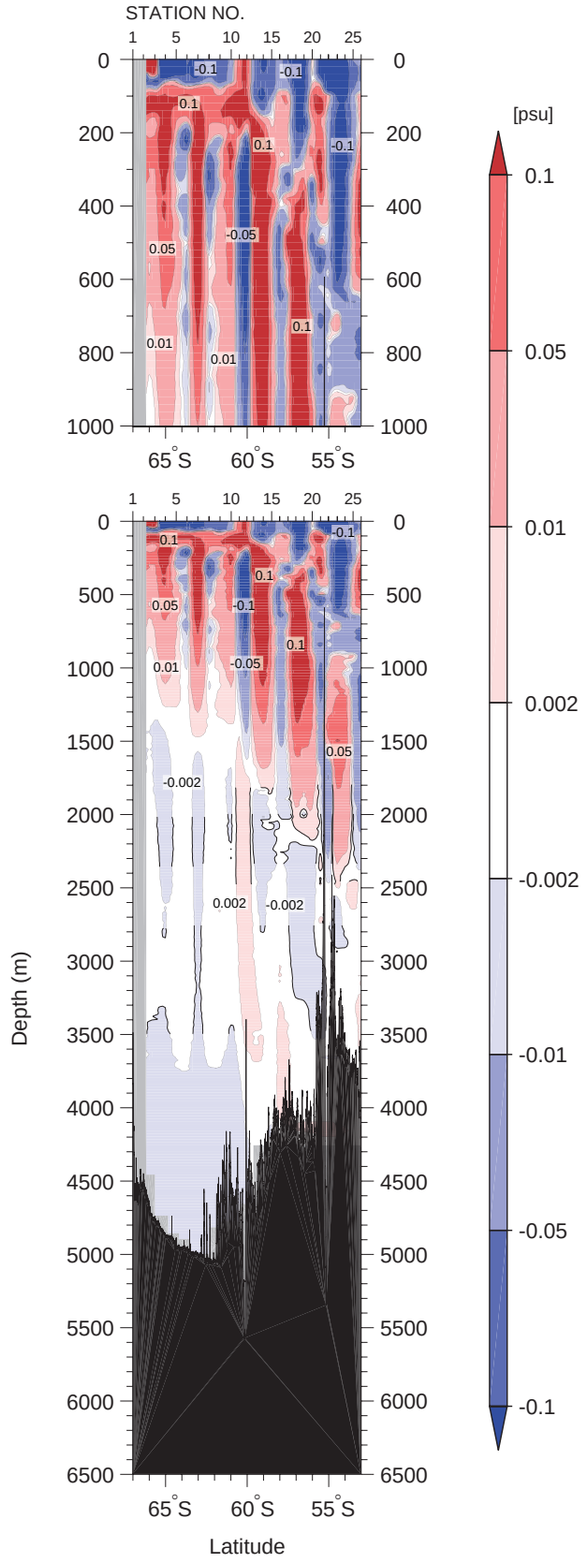

Figure 32

Difference in CTD oxygen (µmol/kg) between results from WHP P17E in 1992 and the revisit in 2017

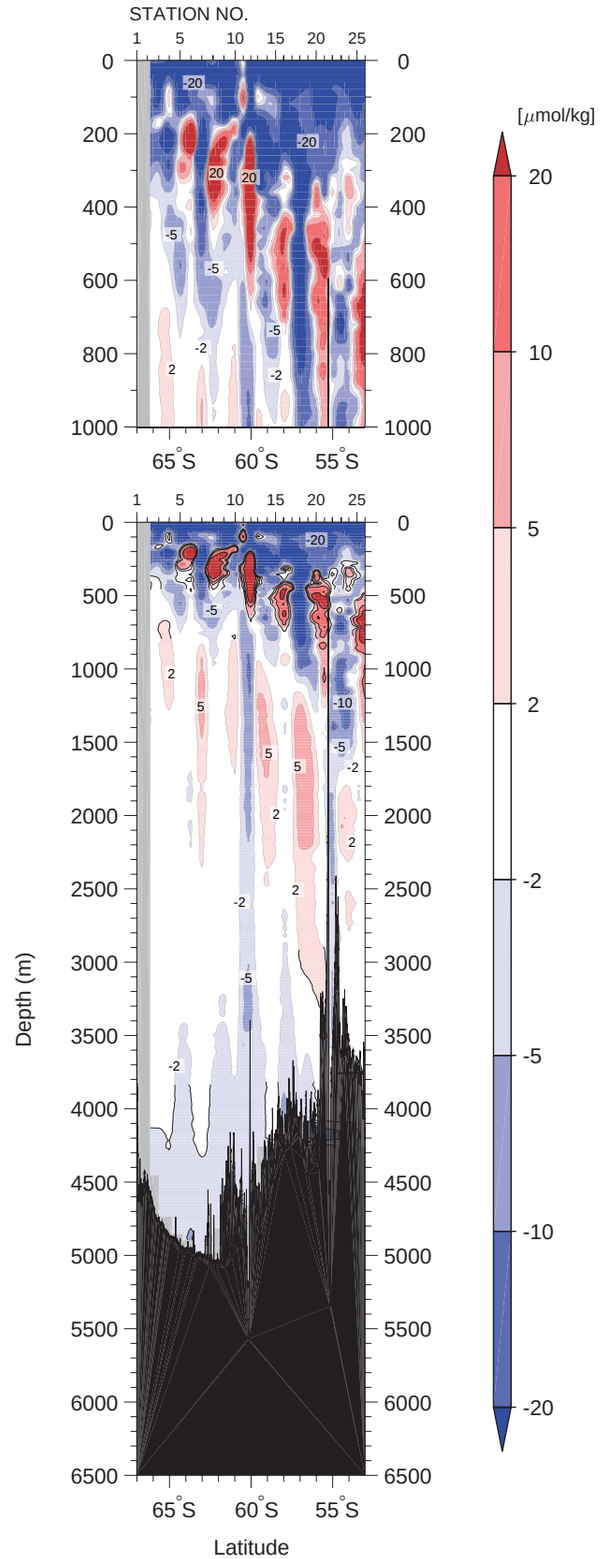

9784901833448